frontiers | Research Topics

Biological nitrogen removal from low carbon wastewater

Edited by
Chongjun Chen, Ren-Cun Jin, Wei Li, Lei Miao and Meng Zhang

Published in
Frontiers in Microbiology

ISSN 1664-8714
ISBN 978-2-83251-909-7
DOI 10.3389/978-2-83251-909-7

About Frontiers

Frontiers is more than just an open access publisher of scholarly articles: it is a pioneering approach to the world of academia, radically improving the way scholarly research is managed. The grand vision of Frontiers is a world where all people have an equal opportunity to seek, share and generate knowledge. Frontiers provides immediate and permanent online open access to all its publications, but this alone is not enough to realize our grand goals.

Frontiers journal series

The Frontiers journal series is a multi-tier and interdisciplinary set of open-access, online journals, promising a paradigm shift from the current review, selection and dissemination processes in academic publishing. All Frontiers journals are driven by researchers for researchers; therefore, they constitute a service to the scholarly community. At the same time, the *Frontiers journal series* operates on a revolutionary invention, the tiered publishing system, initially addressing specific communities of scholars, and gradually climbing up to broader public understanding, thus serving the interests of the lay society, too.

Dedication to quality

Each Frontiers article is a landmark of the highest quality, thanks to genuinely collaborative interactions between authors and review editors, who include some of the world's best academicians. Research must be certified by peers before entering a stream of knowledge that may eventually reach the public - and shape society; therefore, Frontiers only applies the most rigorous and unbiased reviews. Frontiers revolutionizes research publishing by freely delivering the most outstanding research, evaluated with no bias from both the academic and social point of view. By applying the most advanced information technologies, Frontiers is catapulting scholarly publishing into a new generation.

What are Frontiers Research Topics?

Frontiers Research Topics are very popular trademarks of the *Frontiers journals series*: they are collections of at least ten articles, all centered on a particular subject. With their unique mix of varied contributions from Original Research to Review Articles, Frontiers Research Topics unify the most influential researchers, the latest key findings and historical advances in a hot research area.

Find out more on how to host your own Frontiers Research Topic or contribute to one as an author by contacting the Frontiers editorial office: frontiersin.org/about/contact

Biological nitrogen removal from low carbon wastewater

Topic editors

Chongjun Chen — Suzhou University of Science and Technology, China
Ren-Cun Jin — Hangzhou Normal University, China
Wei Li — East China University of Science and Technology, China
Lei Miao — Huazhong University of Science and Technology, China
Meng Zhang — Zhejiang University, China

Citation

Chen, C., Jin, R.-C., Li, W., Miao, L., Zhang, M., eds. (2023). *Biological nitrogen removal from low carbon wastewater*. Lausanne: Frontiers Media SA.
doi: 10.3389/978-2-83251-909-7

Table of contents

05 Editorial: Biological nitrogen removal from low carbon wastewater
Chongjun Chen, Rencun Jin, Wei Li, Lei Miao and Meng Zhang

08 Achieving Partial Nitritation by Treating Sludge With Free Nitrous Acid: The Potential Role of Quorum Sensing
Cancan Jiang, Xu Wang, Huacai Wang, Shengjun Xu, Wei Zhang, Qingjie Meng and Xuliang Zhuang

18 Autotrophic Fe-Driven Biological Nitrogen Removal Technologies for Sustainable Wastewater Treatment
Suyan Pang, Ning Li, Huan Luo, Xiaonan Luo, Tong Shen, Yanan Yang and Jin Jiang

35 *Pseudomonas oligotrophica* sp. nov., a Novel Denitrifying Bacterium Possessing Nitrogen Removal Capability Under Low Carbon–Nitrogen Ratio Condition
Mingxia Zhang, Anzhang Li, Qing Yao, Botao Xiao and Honghui Zhu

48 Morphological and Spatial Heterogeneity of Microbial Communities in Pilot-Scale Autotrophic Integrated Fixed-Film Activated Sludge System Treating Coal to Ethylene Glycol Wastewater
Fangxu Jia, Jiayi Chen, Xingcheng Zhao, Chenyu Liu, Yiran Li, Jinyuan Ma, Anming Yang and Hong Yao

59 Nitrogen Removal From Nitrate-Containing Wastewaters in Hydrogen-Based Membrane Biofilm Reactors *via* Hydrogen Autotrophic Denitrification: Biofilm Structure, Microbial Community and Optimization Strategies
Kun Dong, Xinghui Feng, Yi Yao, Zongqiang Zhu, Hua Lin, Xuehong Zhang, Dunqiu Wang and Haixiang Li

72 Integration of Zeolite Membrane Bioreactor With Granular Sludge-Based Anammox in High-Efficiency Nitrogen Removal From Iron Oxide Red Wastewater
Xing-Hui Feng, Xiao-Jun Wang, Hai-Xiang Li, Hai-Ya Zhang, Zong-Qiang Zhu, Yan-Peng Liang, Kun Dong and Hong-Hu Zeng

82 Denitrification Performance in Packed-Bed Reactors Using Novel Carbon-Sulfur-Based Composite Filters for Treatment of Synthetic Wastewater and Anaerobic Ammonia Oxidation Effluent
Yao Wang, Baorui Liang, Fei Kang, Youzhao Wang, Zhihong Yuan, Zhenning Lyu, Tong Zhu and Zhijun Zhang

94 An efficient anoxic/aerobic/aerobic/anoxic process for domestic sewage treatment: From feasibility to application
Yao Wang, Baorui Liang, Fei Kang, Youzhao Wang, Chaoyue Zhao, Zhenning Lyu, Tong Zhu and Zhijun Zhang

106 Screening and characteristics of ammonia nitrogen removal bacteria under alkaline environments
Rui Zhang, Liang Luo, Shihui Wang, Kun Guo, Wei Xu and Zhigang Zhao

117 Biological nitrogen removal from low carbon wastewater
Kiprotich Kosgey, Phumza Vuyokazi Zungu, Faizal Bux and Sheena Kumari

frontiers | Frontiers in Microbiology

TYPE Editorial
PUBLISHED 28 February 2023
DOI 10.3389/fmicb.2023.1137125

OPEN ACCESS

EDITED AND REVIEWED BY
Eric Altermann,
Massey University, New Zealand

*CORRESPONDENCE
Chongjun Chen
✉ chongjunchen@163.com
Meng Zhang
✉ zhang.meng@ntu.edu.sg

SPECIALTY SECTION
This article was submitted to Microbiotechnology, a section of the journal Frontiers in Microbiology

RECEIVED 04 January 2023
ACCEPTED 14 February 2023
PUBLISHED 28 February 2023

CITATION
Chen C, Jin R, Li W, Miao L and Zhang M (2023) Editorial: Biological nitrogen removal from low carbon wastewater.
Front. Microbiol. 14:1137125.
doi: 10.3389/fmicb.2023.1137125

Editorial: Biological nitrogen removal from low carbon wastewater

Chongjun Chen[1,2]*, Rencun Jin[3], Wei Li[4], Lei Miao[5] and Meng Zhang[6,7]*

[1]School of Environmental Science and Engineering, Suzhou University of Science and Technology, Suzhou, China, [2]Jiangsu Collaborative Innovation Center of Technology and Material of Water Treatment, Suzhou University of Science and Technology, Suzhou, China, [3]Laboratory of Water Pollution Remediation, School of Engineering, Hangzhou Normal University, Hangzhou, China, [4]School of Resources and Environmental Engineering, East China University of Science and Technology, Shanghai, China, [5]School of Environmental Science and Engineering, Huazhong University of Science and Technology, Wuhan, China, [6]College of Environmental and Resource Sciences, Zhejiang University, Hangzhou, China, [7]Advanced Environmental Biotechnology Centre, Nanyang Environment & Water Research Institute, Nanyang Technological University, Singapore, Singapore

KEYWORDS

biological nitrogen removal, low carbon wastewater, anammox, autotrophic Fe-driven process, wastewater treatment

Editorial on the Research Topic
Biological nitrogen removal from low carbon wastewater

In conventional nitrogen removal process, the deep nitrogen removal was realized by nitrification and denitrification for low carbon wastewater with external organic carbon addition, which would lead to higher cost, excessive sludge production and also greenhouse gas emission (Li et al., 2022). Carbon neutrality is an unprecedented challenge for the world, it is particularly necessary to invent innovative and economic process for nitrogen removal from low carbon wastewater (Bae and Kim, 2021; Rui and Peng, 2021). Recently, the relevant research is developing rapidly, including the carbon sources utilization, autotrophic nitrogen removal, novel microorganisms, and so on (Xie et al., 2022). For example, the Strass sewage plant in Austria (Nowak et al., 2015), the Changi sewage plant in Singapore (Trinh et al., 2021), and the new concept sewage plant in Yixing, China were all tried to achieve high-quality nitrogen removal from low carbon wastewater in the field.

The Frontiers Research Topic—Biological nitrogen removal from low carbon wastewater—invited contributions in the following areas: (a) low carbon wastewater treatment; (b) Biological nitrogen removal; (c) autotrophic nitrogen removal; (d) anaerobic ammonia oxidation (anammox); (e) innovative nitrogen removal biotechnology; (f) energy-carbon nexus analysis. In this Research Topic combined the total of 10 articles in this e-book to emphasis on the new findings and recent advances in various aspects of low carbon wastewater treatment.

In this topic, Jiang et al. systematically reviewed the potential ability of quorum sensing (QS) in the partial nitritation process using the control of free nitrous acid (FNA). Meanwhile, the QS would regulate the microbial community structure and function of sludge in sewage treatment systems. However, the metabolic network relationship, the molecular types of QS signals and the regulation of FNA on physiological functions of AOB and NOB should be needed for future study.

Kosgey et al. summarized the principles and advantages of several main nitrogen removal processes for low carbon wastewater, such as the partial nitrification/anammox (PN/A), autotrophic denitrification, nitritation-denitritation, and bioelectrochemical processes. In addition, the process kinetics, large-scale applicability and process configuration of the process were provided. However, the anammox-mediated processes were identified as the best alternative for nitrogen removal in low- or high-strength wastewaters treatment.

Pang et al. systematically summarizes abiotic and biotic nitrogen conversion process involving Fe, including nitrate/nitrite-dependent anaerobic Fe(II) oxidation (NDAFO) and anaerobic ammonium oxidation coupled with Fe(III) reduction (Feammox), and reviewed the biodiversity and microbial community structure of iron-oxidizing or -reducing microorganisms for nitrate/nitrite reduction or ammonium oxidation, respectively. In addition, the effects of pH, redox potential, Fe species, extracellular electron shuttles and natural organic matter were analyzed on the FeBNR reaction efficiency.

Wang et al. utilized the anoxic/aerobic/aerobic/anoxic (AOOA) process with fixed biofilms to improve nitrogen removal, and indicated the optimized running parameters including the volume ratio and dissolved oxygen (DO) concentration in the aerobic zone. In addition, the effluent could meet the discharge standard even in lower temperature and hydraulic retention time (HRT) for real domestic sewage treatment. This issue found that the main nitrogen removal pathway was elemental-sulfur-based autotrophic denitrification (ESAD), and proposed a new heoretical basis and research findings.

Wang et al. indicated the different filter (with different elemental sulfur powder, shell powder, and peanut hull powder) could achieve the differential operation effect for nitrate removal rate (NRR) using novel solid-phase carbon-sulfur-based composite filters. However, the research identified the HRT would considerably impact effluent quality after combined solid-phase-based mixotrophic denitrification process (SMDP) and anammox process. Meanwhile, the concentration of suspended solids (SS) of anammox effluent would also affect the performance of filters with the autotrophs and heterotrophs.

Feng et al. developed the zeolite membrane biological reactor (ZMBR) to enhance the PN process for iron oxide red wastewater (IORW) treatment. The results indicated the ZMBR could dramatically tolerate higher influent nitrogen loading rate (NLR) and nitrite production rate (NPR) than the traditional MBR. After the analysis found that the *Candidatus Kuenenia stuttgartiensis* was the main microorganism in the granular sludge, which would provide more proteins and lipids for better settle ability. The issue paper showed that zeolite addition remarkably enhanced the NLR and NPR, changed the composition and role of bacterial communities to increase capacity for nitrogen removal.

Jia et al. used a pilot-scale integrated fixed-film activated sludge (IFAS) reactor with one-stage partial nitritation/anammox (PN/A) process for real coal to ethylene glycol (CtEG) wastewater treatment, and better treatment effect was obtained. The authors found that the ammonia-oxidizing bacteria (AOB) and anammox bacteria (AnAOB) were co-action in flocs and biofilms respectively. Moreover, the issue paper found that the niche differentiation caused by morphological (DO) and spatial heterogeneity (gradient distribution of nutrients and toxins) maybe the main reason for the distribution of dominant microorganism. This issue paper provides support for enhancing microbial distribution and improving nitrogen removal efficiency.

Dong et al. indicated that the hydrogen pressure, pH, and biofilm thickness would dramatically influence the removal flux of NO_3^--N, and obtained for the optimal control parameters. At the same time, the chemical and microbial mechanisms regulating the removal efficiency of MBfR surface biofilms were preliminarily identified through scanning and composition analysis of MBFR surface biofilms, combined with microbial community structure analysis. This issue paper provided a reference for the application and theoretical analysis of MBfR process.

Zhang M. et al. isolated a denitrifying bacterium named JM10B5aT (*Pseudomonas oligotrophica* sp. nov.) from the *juvenile Litopenaeus vannamei* aquaculture pond, and revealed that the sodium acetate was the optimum carbon source for denitrification process. In addition, the strain JM10B5aT could achieve complete nitrate removal with low C/N ratio. This issue paper indicated the main functional genes for JM10B5aT by genomic analyses, which provided the basis for the analysis of how the JM10B5aT participated in the complete denitrification process. However, how to promote the application of the strain in the actual wastewater engineering remained to be studied.

Zhang R. et al. indicated three ammonia nitrogen (AN) removal strains, designated as *Bacillusidriensis* CT-WN-B3, *Bacillus australimaris* CT-WL5-10, and *Pseudomonas oleovorans* CT-WL5-6 under alkaline conditions. At the same time, the AN removal efficiency of three strains under different pH, salinity and alkalinity was studied. The results of this paper were of great significance for understanding the physiological conditions of AN removal strains. However, the effects of multiple environmental factors need further study.

In general, this Research Topic not only reviewed the latest research progress of biological nitrogen removal from low carbon wastewater, but also developed a variety of suitable treatment processes in combination with laboratory tests and preliminarily explain of microbial mechanism. However, at present, there is a lack of pilot and engineering practice in biological nitrogen removal from low carbon wastewater. In the future, laboratory research and practical engineering application should be combined to promote engineering application with theoretical research.

Author contributions

CC: supervision, funding acquisition, writing—review, and editing. RJ, WL, LM, and MZ: writing—review and editing. All authors contributed to the article and approved the submitted version.

Funding

This work was financially supported by the National Natural Science Foundation of China (No. 51508366), Natural Science Foundation of Jiangsu Province (No. BK20201450), and Jiangsu Qing Lan Project.

Conflict of interest

The authors declare that the research was conducted in the absence of any commercial or financial relationships that could be construed as a potential conflict of interest.

Publisher's note

References

Bae, S., and Kim, Y. M. (2021). Carbon-neutrality in wastewater treatment plants: advanced technologies for efficient operation and energy/resource recovery. *Energies* 14, 8514. doi: 10.3390/en14248514

Li, J. M., Zeng, W., Liu, H., Zhan M. J., and Miao, H. H. (2022). Achieving deep autotrophic nitrogen removal in aerated biofilter driven by sponge iron: performance and mechanism. *Environ. Res.* 213, 113653 doi: 10.1016/j.envres.2022.113653

Nowak, O., Enderle, P., and Varbanov, P. (2015). Ways to optimize the energy balance of municipal wastewater systems: lessons learned from Austrian applications. *J. Clean. Prod.* 88, 125–131. doi: 10.1016/j.jclepro.2014.08.068

Rui, D. U., and Peng, Y. Z. (2021). Technical revolution of biological nitrogen removal from municipal wastewater: recent advances in Anammox research and application. *Sci. Sin. Technol.* 52, 389–402. doi: 10.1360/SST-2020-0407

Trinh, H. P., Lee, S. H., Jeong, G., Yoon, H., and Park, H. D. (2021). Recent developments of the mainstream anammox processes: challenges and opportunities. *J. Environ. Chem. Eng.* 9, 105583. doi: 10.1016/j.jece.2021.105583

Xie, J. X., Guo, M. L., Xie, J. W., Chang, Y. F., Mabruk, A., Zhang, T. C., et al. (2022). COD inhibition alleviation and anammox granular sludge stability improvement by biochar addition. *J. Clean. Prod.* 345, 131167. doi: 10.1016/j.jclepro.2022.131167

frontiers | Frontiers in Microbiology

REVIEW
published: 27 April 2022
doi: 10.3389/fmicb.2022.897566

Achieving Partial Nitritation by Treating Sludge With Free Nitrous Acid: The Potential Role of Quorum Sensing

*Cancan Jiang[1,2], Xu Wang[1,2], Huacai Wang[1,3], Shengjun Xu[1,2], Wei Zhang[4], Qingjie Meng[4] and Xuliang Zhuang[1,2,5]**

[1]Research Center for Eco-Environmental Sciences, Chinese Academy of Sciences, Beijing, China, [2]College of Resources and Environment, University of Chinese Academy of Sciences, Beijing, China, [3]The Institute of International Rivers and Eco-Security, Yunnan University, Kunming, China, [4]Shenzhen Shenshui Water Resources Consulting Co., Ltd., Shenzhen, China, [5]Institute of Tibetan Plateau Research, Chinese Academy of Sciences, Beijing, China

OPEN ACCESS

Edited by:
Lei Miao,
Huazhong University of Science and Technology, China

Reviewed by:
Haoran Duan,
The University of Queensland, Australia
Xiaoling Li,
Chang'an University, China
Dong Wei,
University of Jinan, China

***Correspondence:**
Xuliang Zhuang
xlzhuang@rcees.ac.cn

Specialty section:
This article was submitted to Microbiotechnology, a section of the journal Frontiers in Microbiology

Received: *16 March 2022*
Accepted: *08 April 2022*
Published: *27 April 2022*

Citation:
Jiang C, Wang X, Wang H, Xu S, Zhang W, Meng Q and Zhuang X (2022) Achieving Partial Nitritation by Treating Sludge With Free Nitrous Acid: The Potential Role of Quorum Sensing. Front. Microbiol. 13:897566. doi: 10.3389/fmicb.2022.897566

Partial nitritation is increasingly regarded as a promising biological nitrogen removal process owing to lower energy consumption and better nitrogen removal performance compared to the traditional nitrification process, especially for the treatment of low carbon wastewater. Regulating microbial community structure and function in sewage treatment systems, which are mainly determined by quorum sensing (QS), by free nitrous acid (FNA) to establish a partial nitritation process is an efficient and stable method. Plenty of research papers reported that QS systems ubiquitously existed in ammonia oxidizing bacteria (AOB) and nitrite oxidizing bacteria (NOB), and various novel nitrogen removal processes based on partial nitritation were successfully established using FNA. Although the probability that partial nitritation process might be achieved by the regulation of FNA on microbial community structure and function through the QS system was widely recognized and discussed, the potential role of QS in partial nitritation achievement by FNA and the regulation mechanism of FNA on QS system have not been reviewed. This article systematically reviewed the potential role of QS in the establishment of partial nitritation using FNA to regulate activated sludge flora based on the summary and analysis of the published literature for the first time, and future research directions were also proposed.

Keywords: low carbon wastewater, partial nitritation, free nitrous acid, acid oxidizing bacteria, quorum sensing

INTRODUCTION

Nitrogen pollution is recognized as a serious environmental problem all over the world. Among the sources of nitrogen pollution in water bodies, the effluent of wastewater treatment plants (WWTPs) has always been an easily overlooked but very important source of pollution (Sun et al., 2016; Zhang et al., 2016). The lower carbon–nitrogen ratio in the influent of WWTP is one of the main reasons for the high concentration of total nitrogen in the effluent (Sinha and Annachhatre, 2006; Hao et al., 2015). This is because the removal of nitrogen in most

WWPTs at this stage is mainly dependent on the traditional activated sludge process which generally includes two processes: nitrification and denitrification (**Figure 1A**; Peng and Zhu, 2006). The nitrification process mainly includes two steps: ammonia oxidation and nitrite oxidation. The ammonia oxidation process is completed by ammonia oxidizing bacteria (AOB), which convert ammonia into nitrite under aerobic conditions. Nitrite oxidation is accomplished by nitrite oxidizing bacteria (NOB), which oxidize nitrite to nitrate. The successful progress of these two steps requires the electron acceptor (O_2) to be provided by a large amount of aeration. In the denitrification process, denitrifying bacteria (DNB) use carbon sources in the sewage as electron donors to reduce nitrogen from nitrate to nitrite and then further reduce it to nitrogen gas (N_2) to achieve final nitrogen removal (**Figure 1A**; Sun et al., 2021). Under such process conditions, an insufficient carbon source in the influent will lead to insufficient denitrification, resulting in an excessively high concentration of total nitrogen (nitrate nitrogen) in the effluent (Rahimi et al., 2020). In order to solve the problems of high energy consumption, carbon source shortage, and low nitrogen removal efficiency faced by traditional nitrogen removal processes, novel processes based on partial nitritation have gradually developed in recent years, such as the partial nitritation and denitrification process (PN/D) and the partial nitritation and anaerobic ammonia oxidation process (PN/A; Duan et al., 2020; Li et al., 2020, 2021; Qiu et al., 2020; Yao et al., 2021). Different from the traditional nitrification and denitrification process, nitrogen removal processes based on partial nitritation only oxidizes ammonia to nitrite, and then directly enters the subsequent nitrogen removal stage, which greatly saves oxygen consumption and carbon source demand, while reducing excess sludge production and greenhouse gas emissions (Sinha and Annachhatre, 2006). For example, compared to the traditional nitrification and denitrification process, the PN/D process has the following advantages: (1) saving 20% oxygen consumption in the nitrification stage; (2) saving 40% carbon demand in the denitrification stage; (3) reducing carbon dioxide production by 20%; (4) reducing excess sludge production by 35 and 55% in the nitrification stage and denitrification stage, respectively (**Figure 1B**; Jiang et al., 2019). When partial nitritation and anaerobic ammonia oxidation processes are combined, i.e., PN/A process, NH_4^+ and NO_2^- produced by partial nitritation can be converted into N_2 by autotrophic anammox bacteria. Therefore, compared to traditional nitrification and denitrification, PN/A can save 25% oxygen consumption and 100% carbon source demand, greatly reduce process energy consumption and excess sludge production, and at the same time improve the denitrification efficiency of wastewater (**Figure 1C**; Kang et al., 2020; Adams et al., 2022). At present, many novel nitrogen removal processes based on partial nitritation have been successfully established and applied in engineering, such as SHARON process and CANON process (Ye et al., 2020; Xu et al., 2021).

Stable accumulation of nitrite is the prerequisite and necessary condition for the successful establishment of a novel nitrogen removal process based on PN, which is achieved mainly by suppressing NOB while retaining AOB (Jiang et al., 2018). A variety of regulation methods have been reported to achieve effective NOB inhibition, such as low dissolved oxygen, intermittent aeration, shortening sludge residence time, inhibitor addition, etc. (Liu et al., 2017; Yang et al., 2017; Zhang et al., 2018a; Zhou et al., 2018). In recent years, the method of selective inhibition of NOB by free nitrous acid (FNA) to establish PN has attracted a lot of attention and is considered a very promising technology (Kinh et al., 2017; Pedrouso et al., 2017). FNA is an efficient bacterial inhibitor, but the growth of NOB is more sensitive to FNA than the growth of AOB. The most commonly used methods of FNA to establish PN in laboratory research and practical applications are sidestream treatment of activated sludge by FNA and *in-situ* selective inhibition of NOB by FNA (Zhou et al., 2011; Duan et al., 2020; Ren et al., 2021). In the former method, a part of the mainline activated sludge ~30% was transported to a side-stream treatment unit to be exposed to high levels of FNA

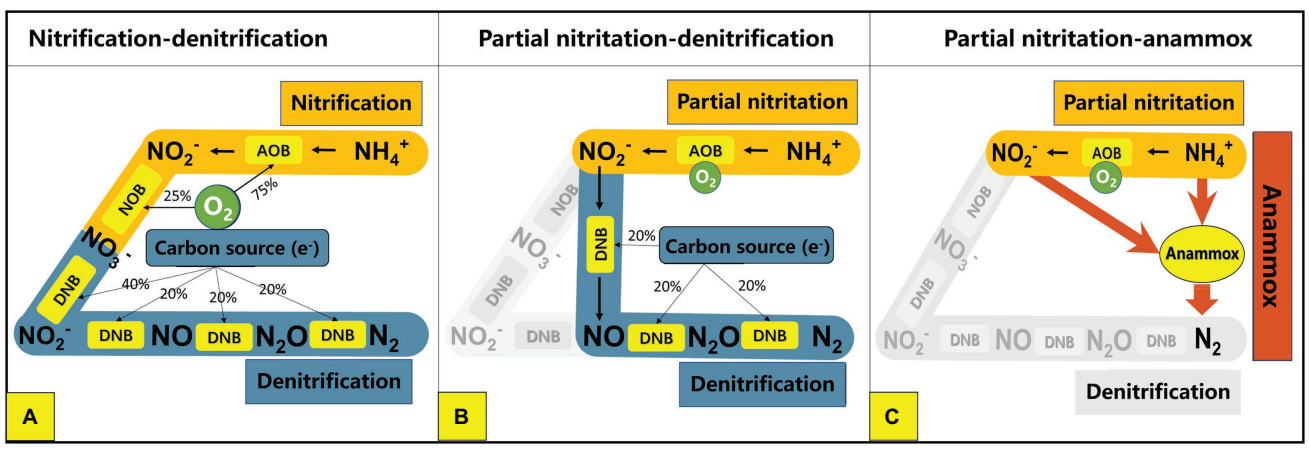

FIGURE 1 | Pathways of different biological nitrogen removal processes: **(A)** traditional nitrification denitrification process; **(B)** partial nitritation denitrification process; **(C)** partial nitritation anammox process. AOB, ammonia oxidizing bacteria; NOB, nitrite oxidizing bacteria; DNB, denitrifying bacteria.

in order to inactivate the NOB present in the activated sludge. This approach is generally used to establish the PN process during the treatment of municipal wastewater with low ammonia nitrogen concentration (Wang et al., 2014). A previous study found that after activated sludge was treated with 1.2 mg/l FNA for 18 h, the activity of NOB could be completely inhibited, while the activity of AOB remained above 57% (Jiang et al., 2018, 2019). Other researchers have reported similar results, but with differences in FNA concentrations and treatment times due to diversity in sludge properties and microbial community structure and composition (Duan et al., 2020). For example, Wang et al. (2014) reported that AOB activity could still be maintained at approximately 50% after activated sludge was treated with 1.35 mg/l of FNA for 24 h, while NOB completely lost its activity, while treatment conditions that can completely inactivate NOB while retaining 47% of AOB's activity are: A FNA concentration of 0.25 mg/l and a treatment time of 18 h was proposed (Wang et al., 2019). Taking advantage of the selective inhibition of NOB by FNA, researchers successfully established PN process in various types of reactors. Wang et al. (2021b) achieved PN by treating 22% of the activated sludge in a sequencing batch reactor (SBR) every day with simulated wastewater as influent, and the accumulation rate of nitrite could reach more than 80% in PN stage (Wang et al., 2021b). In our previous work, a stable PN/D process was successfully established in the continuous flow reactor A^2O by treating 30% of the sludge daily in the side flow FNA treatment unit. The accumulation rate of nitrite nitrogen could be maintained at more than 78% in PN stage, and the removal efficiency of total nitrogen was increased by 20% compared with the control group (Jiang et al., 2019). Some researchers also used this technology to achieve PN/A process, and the accumulation rate of nitrite could be maintained at 60%∼80% in PN stage (Wang et al., 2019). In order to achieve green and low-cost acquisition of FNA, researchers have developed a technology to produce FNA using sludge digested liquid rich in high-concentration ammonia, which could reduce 14% of the total cost and did not lead to a higher N_2O emission by avoiding external chemicals addition in comparison with commercial supply (Law et al., 2015). In the treatment of high-strength ammonia-nitrogen wastewater, the method of *in-situ* selective inhibition of NOB by FNA is commonly used to construct a PN process. When compared to sidestream inhibition, this method saves space and cost as both the sludge treatment with FNA and the nitritation reaction simultaneously take place in a single reactor and therefore a side-stream sludge treatment unit is not required. Moreover, external NO_2^- and acid are also not required to obtain the required FNA concentrations. Ren et al. (2021) achieved a sustained nitrite accumulation rate above 90% in PN stage when treating mature landfill leachate. To sum up, using FNA to selectively inhibit NOB to establish PN process is a green, efficient, low-cost and highly applicable technology. Understanding how FNA regulates specific microorganisms and their metabolism in the process of PN biological nitrogen removal can further develop its potential and maximize its effectiveness. Although there have been a lot of studies on the establishment of PN by FNA and the underlying mechanisms, they have not been systematic reviewed from the perspective of community mechanisms. Many researches showed that the regulation of activated sludge flora by FNA played an important role in establishing PN process (Zhang et al., 2020; Hu et al., 2021; Luo et al., 2021). And meanwhile, the community structure and functions of activated sludge flora were under the regulation of quorum sensing (QS) and quorum quenching (QQ) which were the molecular communication systems employed by bacteria to regulate their density and organize their collective behavior. Thus, this paper systematically reviewed the function of FNA and QS/QQ systems on PN establishment based on the summary and analysis of the published literatures, and then the potential role of QS/QQ systems in the establishment of PN using FNA to regulate activated sludge flora were discussed, and future research directions were also proposed.

FUNCTION OF FNA ON PN ESTABLISHMENT: BACTERICIDAL EFFECT AT SINGLE-BACTERIA LEVEL

Bactericidal Mechanisms of FNA

Research on bactericidal effects of FNA on microorganisms at single-bacteria level mainly focuses on its impacts on bacterial metabolism, transmembrane transport of substrates, oxygen acquisition, and oxidative phosphorylation (Laloo et al., 2018; Zheng et al., 2021). FNA can act as a proton uncoupling agent, which is a reagent that stimulates electron transfer, ATP hydrolysis, and inhibits ATP synthesis, ATPase catalysis, and other exchange reactions (Almeida et al., 1995). As a proton carrier, FNA can increase the ability of protons to penetrate cells. Therefore, to maintain the balance of intracellular and intracellular potentials, cells need to expel excess free protons from the intracellular to the extracellular. This process will consume additional ATP, resulting in insufficient ATP to maintain normal metabolism of cells and inhibit cell survival (Anthonisen et al., 1976; Sijbesma et al., 1996; Gao et al., 2016). However, Vadivelu et al. (2006a) found that FNA does not inhibit the ATP production and metabolism of all microorganisms, and the uncoupling effect of FNA alone may not be the only mechanism for FNA inhibition (Vadivelu et al., 2006a,b). In addition, another major action pathway of FNA is to inhibit the growth of bacterial cells by affecting various enzymes in bacterial metabolism. These mainly include enzymes related to nitrogen form conversion, transcription and translation, and decomposition and anabolism (Fang, 1997).

Differential Impacts of FNA on AOB and NOB

Previous reports suggested that the difference in the inhibitory effect of FNA on AOB and NOB activity may be due to their different regulation ability on the above-mentioned pathways. In terms of the removal of the toxic substrate (FNA), both AOB and NOB have nitrite reductase (*nirK*), a nitrite detoxification gene, which can convert nitrite into non-toxic

nitric oxide (NO). However, NOB has two additional nitrite scavenging pathways than AOB, including the nitrite reductase (*nirB/D*) pathway that can convert nitrite into ammonia and nitrite oxidoreductase (*norA/B*) pathway that can convert nitrite into nitrate (Cantera and Stein, 2007). The paradox that AOB has fewer detoxification pathways but higher FNA tolerance has not been definitively concluded in previous studies. Some researchers have explained the mechanism of AOB tolerance to FNA by means of metagenomic and proteomic methods. When *N. eutropha* is treated with FNA, in order to maintain the homeostasis in the bacteria, oxidative stress repair enzymes, denitrification-related enzymes, DNA and protein repair enzymes were up-regulated, and energy production and ion transmembrane transport were strengthened. In addition, β-lactam hydrolase-like proteins and alginate transporters associated with biofilm formation increased in AOB after FNA exposure, suggesting that FNA may promote AOB biofilm formation. However, due to the low detection of NOB-related proteins in the experiment, the molecular biological response mechanism of NOB after FNA treatment has not been fully explained, and the comparison of the regulatory effects of FNA on the same or similar metabolic pathways in AOB and NOB cannot be fully explained (Laloo et al., 2018). Moreover, many studies have reported that under FNA treatment, although the activity of NOB in activated sludge was almost completely inhibited, the survival of NOB was still detected. After applying FNA over an extended period of time the activity and abundance of NOB gradually increased because of NOB adaptation and community shift, resulting in the destruction of PN (Wang et al., 2021a). This indicates the inhibitory effect of FNA on NOB activity is reversible at the community level after prolonged application. Therefore, it might be that FNA affects the structure of the bacterial community by affecting the interaction between AOB, NOB, and the entire activated sludge flora, thus forming a structure of the bacterial community conducive to the growth and reproduction of AOB and at the same time greatly inhibiting the activity of NOB, thus establishing PN.

FUNCTION OF QS/QQ SYSTEMS DURING PN ESTABLISHMENT

QS Systems in PN Process

As single-celled organisms, the interaction between microorganisms is mainly achieved through quorum sensing (QS; Shrout and Nerenberg, 2012). QS is one of the most important ways of communication between microorganisms in the colony gathering area, and signal molecules are the main molecular substances to realize QS regulation (Huang et al., 2016). Microorganisms synthesize and secrete signal molecules with specific chemical structures through QS system. With the growth and reproduction of microorganisms, the concentration of signal molecules increases continuously. When the density of microorganisms and the concentration of signal molecules reach a certain threshold, the transcription expression of downstream target genes will be regulated. By sensing the expression and secretion of signal molecules, QS system coordinates the physiological behavior and regulates the ecological relationship of the flora, and ultimately determines the bacterial community structure, thus showing the physiological functions and regulatory mechanisms that a single individual bacterium cannot achieve, such as bioluminescence, antibiotic synthesis, biofilm formation, and pathogenic toxicity (Hu et al., 2021). N-acyl homoserine lactones (AHL), oligopeptides, furanborate diesters, quinolones, and γ-butyrolactones are the most common and consistent with the principle of QS signaling molecules in bacteria. AHLs, produced by gram-negative bacteria, are the widely studied signal molecule (Juretschko et al., 2002; Chain et al., 2003; Norton et al., 2008; Gao et al., 2014). It has been reported that more than 100 kinds of *Proteobacteria* can produce AHL signal molecules (Yates et al., 2002). AHL-mediated QS system mainly includes AHL signaling molecules, AHL synthase and AHL receptor. When the concentration of AHLs reaches a certain threshold, it will bind to its receptors and activate the transcription of target genes controlled by the QS system to realize the regulation of QS (Burton et al., 2005; Chen et al., 2018; Maddela et al., 2019). The AHL-mediated QS system is ubiquitous in the nitrification process of activated sludge bacteria (Rice et al., 2016; Shen et al., 2016). AOB and NOB can be regulated by various AHLs with different carbon chain lengths (**Table 1**). The synthesis and recognition of AHL in nitrifying bacteria are regulated by genes on LuxI/LuxR. LuxI-AHL synthetase catalyzes the condensation reaction between S-adenosylmethionine and acylated acyl carrier protein to generate AHL molecules with homoserine lactone ring as the main body, connecting fatty acyl chains of different lengths and degrees of saturation (Fuqua et al., 2001). When the AHL concentration reaches the threshold concentration, it will combine with the LuxR receptor in the cytoplasm to form the transcriptional regulatory complex LuxR-AHL, and then combine with the specific promoter sequence to regulate the expression of the QS system, thus showing changes in community-level characteristics (**Figure 2**; Waters and Bassler, 2005; Churchill and Chen, 2011). Recent studies have shown that not only AOB and NOB can produce signal molecules to participate in QS regulation, but different signal molecules can produce different regulatory results when acting on specific nitrifying bacteria (**Table 1**). Mellbye et al. (2015) reported that the QS regulatory effect of NOB can not only affect the production and consumption of various nitrogen oxides (such as NO, NO_2, and N_2O), but also regulate the nitrification completed by AOB (Mellbye et al., 2015, 2016, 2017a,b). Sun et al. (2018) also found that C4-HSL was correlated with the activity of AOB; however, C6-HSL and C8-HSL facilitated the activity of NOB (Sun et al., 2018). A similar result found that C4-HSL promoted nitrite accumulation, while C8-HSL could inhibit AOB activity (Feng et al., 2019). To sum up, these findings indicated that QS played crucial roles in regulating the balance between AOB and NOB, and thus affecting the performance of partial nitritation systems.

QQ Systems in PN Process

At bacterial community level, nitrification process is not only regulated by QS, but may also be affected by the interfering or destroying of QS system, i.e., quorum quenching (QQ), which

TABLE 1 | QS systems related to partial nitritation.

Bacteria type	Bacteria species	Signal type	Functions	References
AOB	*Nitrosomonas europaea*	C6-HSL C8-HSL C10-HSL	Resistance against starvation Recovery of starved Nitrosomonas europaea biofilm;	Juretschko et al., 2002; Chain et al., 2003; Burton et al., 2005
	Nitrosospira multiformis	C10-HSL C14-HSL 3OC14-HSL	Discovery of a functional AHL synthase in Nitrosospira multiformis	Norton et al., 2008; Gao et al., 2014; Mellbye et al., 2017a,b
	Nitrosospira briensis	3-OH-C14-HSL	Unknown	Rice et al., 2016; Mellbye et al., 2017b
	Nitrococcus mobilis	Genome contains QS genes and AHLs are not detected	Unknown	Feng et al., 2019
NOB	*Nitrobacter winogradskyi*	C7-HSL C8-HSL C9-HSL, C10-HSL C10:1-HSL	Regulation of possible nitrogen oxide flux and nitrification; Nitrite oxidation, nitrogen oxides metabolism	Mellbye et al., 2016; Shen et al., 2016
	Nitrobacter vulgaris	C10:1-HSL	Nitrogen oxides metabolism	Mellbye et al., 2017a,b
	Nitrospira moscoviensis	C8-HSL	Unknown	Mellbye et al., 2017b
	Nitrobacter hamburgensis	Genome contains QS genes and AHLs are not detected	Unknown	Feng et al., 2019

could block the information exchange between cells, and lead to failure of microbial community regulation (Grandclement et al., 2016). The main ways to achieve QQ, as shown in **Figure 3**, include: (1) inhibiting the synthesis of signal molecules. Blocking the QS system by inhibiting AHL production seems to be a theoretically easy strategy. However, there are just a few experiments targeting the LuxI-type synthase protein that have been published. LuxI-type synthases catalyze the formation of AHL from acyl-ACP and SAM (Geske et al., 2008). Because SAM is an essential and unique step for AHL synthesis, most research on inhibiting AHL synthesis has focused on the use of different analogues of SAM. Thus, damaging AHL synthase and using different intermediate analogues of SAM become the two most commonly reported methods to inhibit AHL synthesis. (2) destructing signal molecules. Chemical, metabolic and enzymatic destruction were the three main types of AHLs destruction (Kalia, 2013). H^+/OH^- were reported to be the primarily chemicals that could destruct AHL structure. There are four main types of AHL degrading enzymes: lactase that breaks the homoserine lactone ring, acylation amide enzyme that cleaves the amide bond and releases fatty acids and homoserine lactones, reductase that converts 3-oxo-AHL to 3-OH-AHL, and cytochrome oxidase that catalyzes acyl chain oxidation. Bacteria are the primary source of the above-mentioned AHL degrading enzymes (Huang et al., 2016; Mellbye et al., 2016). (3) hindering the binding of signal molecules to receptors. The ways of intervening in the binding of signal molecules to receptors mainly include the competition of signal molecule analogs. Those QQ approaches interfere with and disrupt AHL-based QS system, and then inhibit gene expression mediating bacterial desired phenotypes (Chen et al., 2011). Bacteria and chemicals with QQ ability, including *Pseudomonas* sp. 1A1, *Rhodococcus* sp. BH4, paraoxonase, azithromycin, and TiO2, etc., were widely detected in nitrification systems in activated sludge (Kalia, 2013; Kim et al., 2014; Oh and Lee, 2018; Yu et al., 2018). Apparently, FNA can also greatly affect AHL-based QS and QQ systems of microorganisms in activated sludge, and regulate their behaviors and functions at the microbial community level.

FUNCTION OF FNA ON PN ESTABLISHMENT

Potential QS mechanisms as FNA is able to passively pass through bacterial cytoplasmic membranes and interact with enzymes that contain thiols, heme groups, iron sulfur clusters, phenolic or aromatic amino acid residues, tyrosyl radicals, and amines (Zhou et al., 2008; Gao et al., 2019), the activity of AHL synthase can be easily inhibited, thus influencing the synthesis of AHL. Similar effects might occur on LuxR and receptor protein of AHL, therefore, hinder the regulation of QS on nitrifying bacteria community. Proton permeability of bacterial membranes could increase as FNA diffuse across cell membranes, which might cause the transmembrane electrochemical proton motive force (pmf) to dissipate. The collapse of pmf would limit ATP generation, which further impeded the active transportation of AHL the extracellular and influenced its exudation (Zhou et al., 2007). Moreover, FNA may accumulate inside cells in its anionic form as a result of the near-neutral intracellular pH. This release of protons within the cells would decrease the intracellular pH, which might influence QS and QQ systems during PN establishment (Brul and Coote, 1999; Byers et al., 2002; Vadivelu et al., 2006b). According to Byers et al. (2002), alkaline pH causes the lactone ring to open, resulting in the loss of AHL signal activity. At acidic pH, however, the lactone ring re-cyclizes, and the activity

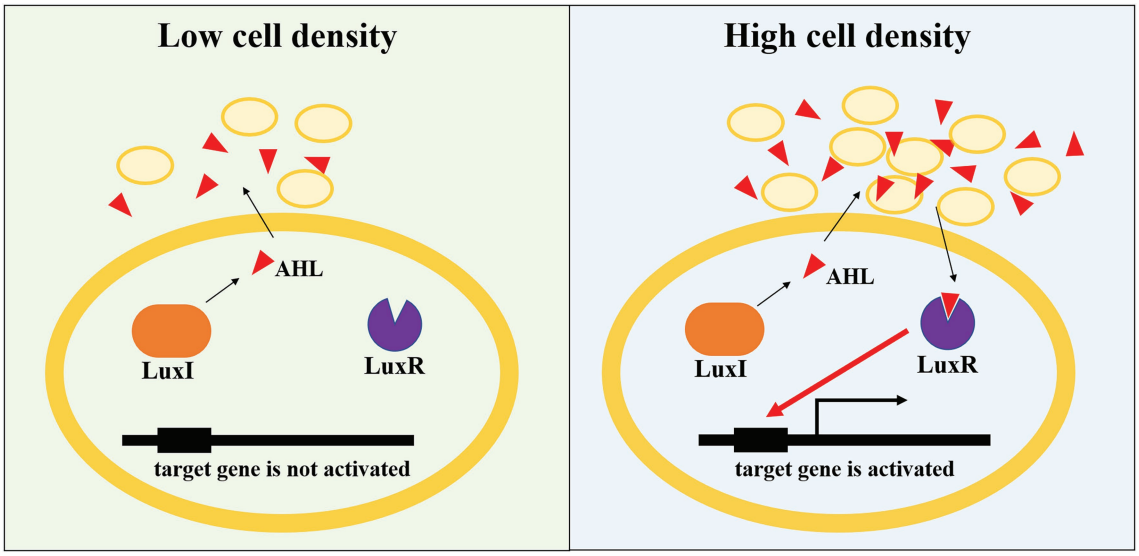

FIGURE 2 | Schematic of AHL-mediated QS in gene express regulation.

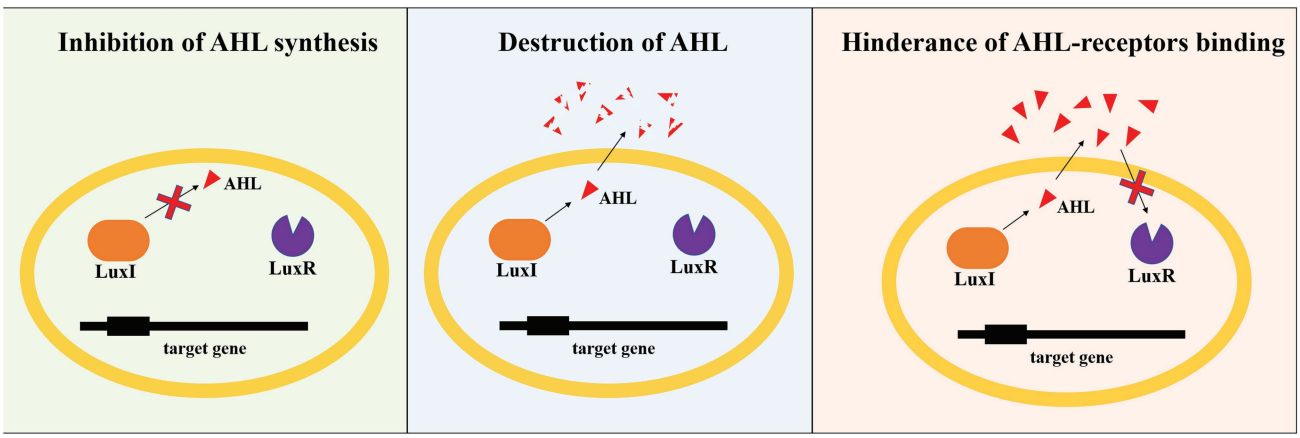

FIGURE 3 | There major types of AHL-mediated quorum quenching.

of the AHL signal is reversed. In addition, AHL synthesis has also been discovered to be inhibited by some antibiotics, and nitrite (FNA) has long been known to have antimicrobial properties, which might also contribute to the QQ ability of FNA (Pierson and Smoot, 1982; Rao et al., 2006; **Figure 4**).

FNA treatment may also result in uneven distribution of signal molecules in extracellular polymeric substances (EPS) in activated sludge (Tan et al., 2014; Ding et al., 2015). EPS is a kind of macromolecular polymer secreted by microorganisms, which is the framework of activated sludge flocculation structure. EPS has the functions of aggregation of microorganisms, enrichment and degradation of organic matter, so it plays a vital role in the distribution of signal molecules in activated sludge (Ding et al., 2015). The structure of EPS from inside to outside is the tightly bound layer (TB), the loose bound layer (LB), and the mucus layer (S), where the tightly bound layer directly contacts the internal microbial cell aggregates. The hierarchical and limited spatial structure of EPS is conducive to the continuous enrichment of signal molecule concentration and reaching the level required for QS regulation (Zhang et al., 2020). Therefore, EPS structure may be the main site of QS regulation in activated sludge. EPS components include proteins, polysaccharides, humus and extracellular DNA, among which proteins and polysaccharides are the main components. Previous studies have shown that the protein and polysaccharide content of LB layer is much higher than that of TB and S layer, but the protein/polysaccharide ratio of TB layer is higher than that of LB layer, indicating that LB layer may be the main area for adsorption of organic matter, but the adsorption of organic matter on TB layer is stronger, and the signal molecules produced by internal bacterial micelles are likely to be firmly adsorbed by TB layer to continuously enrich and reach the

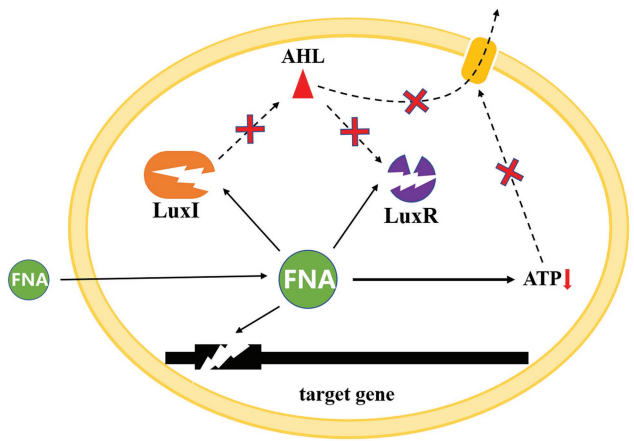

FIGURE 4 | Potential mechanisms of FNA effect on QS system.

QS regulation level (Zhang et al., 2018b; Liu et al., 2021; Zhao et al., 2021; Zheng et al., 2021). Therefore, in order to better explain the QS regulation pathway in activated sludge, it is necessary to further analyze the influence of FNA on the distribution of signal molecules in EPS.

CONCLUSION AND PROSPECTS

FNA can selectively inhibit NOB, affect the expression of various synthetases in the metabolic processes of AOB and NOB, and cause the up-regulation of the expression of proteins related to the formation of AOB biofilm. The formation and structure of microbial biofilm and EPS are closely related to the synthesis and expression of QS signaling molecules. The regulatory effect of FNA on the structure and function of activated sludge flora is likely to be achieved by regulating the metabolic process directly related to QS in the system, including regulating the synthesis of QS signaling molecules. The spatial distribution of QS signal molecules in activated sludge bacterial micelles was further affected. Regulation of FNA in AOB and NOB can cause secondary regulation of QS in the system. The biological functions of QS signaling molecule synthase directly or indirectly related to QS, EPS synthesis, biofilm formation, nutrient transport and absorption, and nitrogen transformation are further cascade regulated.

Therefore, it is necessary to further reveal the microbial ecology and molecular biology mechanism of FNA that regulates QS in the partial nitritation process from two aspects: (1) changes in the structure and function of the microbial community, the metabolic network relationship, the molecular types of QS signals; (2) the regulation of FNA on physiological functions of AOB and NOB, molecular synthesis of QS signaling, and related metabolic pathways at the cellular and molecular levels. The revelations of these questions will enhance the understanding of FNA regulating the partial nitritation of activated sludge, and provide theoretical guidance for the future application of FNA technology in practice, and lay the foundation for further study of activated sludge ecological system at the molecular level.

AUTHOR CONTRIBUTIONS

CJ conceived and wrote the manuscript. XW and HW refined the manuscript. SX, WZ, and QM reviewed the manuscript. XZ supervised the project. All authors have read the final manuscript and approved it.

FUNDING

This research was supported by the National Natural Science Foundation of China (Nos. 42177099, 91951108, and 21976197), the Knowledge Innovation Program of Shenzhen (JSGG20191129112812329), and the CAS International Partnership Program (No. 121311KYSB20200017).

REFERENCES

Adams, M., Xie, J., Kabore, A. W. J., Chang, Y., Xie, J., Guo, M., et al. (2022). Research advances in anammox granular sludge: A review. *Crit. Rev. Environ. Sci. Technol.* 52, 631–674. doi: 10.1080/10643389.2020.1831358

Almeida, J. S., Julio, S. M., Reis, M. A. M., and Carrondo, M. J. T. (1995). Nitrite inhibition of denitrification by Pseudomonas fluorescens. *Biotechnol. Bioeng.* 46, 194–201. doi: 10.1002/bit.260460303

Anthonisen, A. C., Loehr, R. C., Prakasam, T. B. S., and Srinath, E. G. (1976). Inhibition of nitrification by ammonia and nitrous acid. *J. Water Pollution Control Federation* 48, 835–852. PMID: 948105

Brul, S., and Coote, P. (1999). Preservative agents in foods - mode of action and microbial resistance mechanisms. *Int. J. Food Microbiol.* 50, 1–17. doi: 10.1016/s0168-1605(99)00072-0

Burton, E. O., Read, H. W., Pellitteri, M. C., and Hickey, W. J. (2005). Identification of acyl-homoserine lactone signal molecules produced by Nitrosomonas europaea strain Schmidt. *Appl. Environ. Microbiol.* 71, 4906–4909. doi: 10.1128/AEM.71.8.4906-4909.2005

Byers, J. T., Lucas, C., Salmond, G. P., and Welch, M. (2002). Nonenzymatic turnover of an Erwinia carotovora quorum-sensing signaling molecule. *J. Bacteriol.* 184, 1163–1171. doi: 10.1128/jb.184.4.1163-1171.2002

Cantera, J. J., and Stein, L. Y. (2007). Molecular diversity of nitrite reductase genes (nirK) in nitrifying bacteria. *Environ. Microbiol.* 9, 765–776. doi: 10.1111/j.1462-2920.2006.01198.x

Chain, P., Lamerdin, J., Larimer, F., Regala, W., Lao, V., Land, M., et al. (2003). Complete genome sequence of the ammonia-oxidizing bacterium and obligate chemolithoautotroph *Nitrosomonas europaea*. *J. Bacteriol.* 185, 2759–2773. doi: 10.1128/JB.185.9.2759-2773.2003

Chen, H., Li, A., Cui, D., Wang, Q., Wu, D., Cui, C., et al. (2018). N-acyl-homoserine lactones and autoinducer-2-mediated quorum sensing during wastewater treatment. *Appl. Microbiol. Biotechnol.* 102, 1119–1130. doi: 10.1007/s00253-017-8697-3

Chen, G., Swem, L. R., Swem, D. L., Stauff, D. L., O'Loughlin, C. T., Jeffrey, P. D., et al. (2011). A strategy for antagonizing quorum sensing. *Mol. Cell* 42, 199–209. doi: 10.1016/j.molcel.2011.04.003

Churchill, M. E. A., and Chen, L. (2011). Structural basis of acyl-homoserine lactone-dependent signaling. *Chem. Rev.* 111, 68–85. doi: 10.1021/cr1000817

Ding, Z., Bourven, I., Guibaud, G., van Hullebusch, E. D., Panico, A., Pirozzi, F., et al. (2015). Role of extracellular polymeric substances (EPS) production in bio-aggregation: application to wastewater treatment. *Appl. Microbiol. Biotechnol.* 99, 9883–9905. doi: 10.1007/s00253-015-6964-8

Duan, H., Gao, S., Li, X., Ab Hamid, N. H., Jiang, G., Zheng, M., et al. (2020). Improving wastewater management using free nitrous acid (FNA). *Water Res.* 171:115382. doi: 10.1016/j.watres.2019.115382

Fang, F. C. (1997). Mechanisms of nitric oxide-related antimicrobial activity. *J. Clin. Investig.* 99, 2818–2825. doi: 10.1172/jci119473

Feng, Z., Sun, Y., Li, T., Meng, F., and Wu, G. (2019). Operational pattern affects nitritation, microbial community and quorum sensing in nitrifying wastewater treatment systems. *Sci. Total Environ.* 677, 456–465. doi: 10.1016/j.scitotenv.2019.04.371

Fuqua, C., Parsek, M. R., and Greenberg, E. P. (2001). Regulation of gene expression by cell-to-cell communication: acyl-homoserine lactone quorum sensing. *Annu. Rev. Genet.* 35, 439–468. doi: 10.1146/annurev.genet.35.102401.090913

Gao, S.-H., Ho, J. Y., Fan, L., Nouwens, A., Hoelzle, R. D., Schulz, B., et al. (2019). A comparative proteomic analysis of Desulfovibrio vulgaris Hildenborough in response to the antimicrobial agent free nitrous acid. *Sci. Total Environ.* 672, 625–633. doi: 10.1016/j.scitotenv.2019.03.442

Gao, S.-H., Ho, J. Y., Fan, L., Richardson, D. J., Yuan, Z., and Bond, P. L. (2016). Antimicrobial effects of free nitrous acid on Desulfovibrio vulgaris: implications for sulfide-induced corrosion of concrete. *Appl. Environ. Microbiol.* 82, 5563–5575. doi: 10.1128/aem.01655-16

Gao, J., Ma, A., Zhuang, X., and Zhuang, G. (2014). An N-acyl Homoserine lactone synthase in the ammonia-oxidizing bacterium *Nitrosospira multiformis*. *Appl. Environ. Microbiol.* 80, 951–958. doi: 10.1128/aem.03361-13

Geske, G. D., O'Neill, J. C., and Blackwell, H. E. (2008). Expanding dialogues: from natural autoinducers to non-natural analogues that modulate quorum sensing in gram-negative bacteria. *Chem. Soc. Rev.* 37, 1432–1447. doi: 10.1039/b703021p

Grandclement, C., Tannieres, M., Morera, S., Dessaux, Y., and Faure, D. (2016). Quorum quenching: role in nature and applied developments. *FEMS Microbiol. Rev.* 40, 86–116. doi: 10.1093/femsre/fuv038

Hao, X., Liu, R., and Huang, X. (2015). Evaluation of the potential for operating carbon neutral WWTPs in China. *Water Res.* 87, 424–431. doi: 10.1016/j.watres.2015.05.050

Hu, H., Luo, F., Liu, Y., and Zeng, X. (2021). Function of quorum sensing and cell signaling in wastewater treatment systems. *Water Sci. Technol.* 83, 515–531. doi: 10.2166/wst.2020.601

Huang, J., Shi, Y., Zeng, G., Gu, Y., Chen, G., Shi, L., et al. (2016). Acyl-homoserine lactone-based quorum sensing and quorum quenching hold promise to determine the performance of biological wastewater treatments: An overview. *Chemosphere* 157, 137–151. doi: 10.1016/j.chemosphere.2016.05.032

Jiang, C., Xu, S., Wang, R., Feng, S., Zhou, S., Wu, S., et al. (2019). Achieving efficient nitrogen removal from real sewage via nitrite pathway in a continuous nitrogen removal process by combining free nitrous acid sludge treatment and DO control. *Water Res.* 161, 590–600. doi: 10.1016/j.watres.2019.06.040

Jiang, C., Xu, S., Wang, R., Zhou, S., Wu, S., Zeng, X., et al. (2018). Comprehensive assessment of free nitrous acid-based technology to establish partial nitrification. *Environ. Sci. Water Res. Technol.* 4, 2113–2124. doi: 10.1039/c8ew00637g

Juretschko, S., Loy, A., Lehner, A., and Wagner, M. (2002). The microbial community composition of a nitrifying-denitrifying activated sludge from an industrial sewage treatment plant analyzed by the full-cycle rRNA approach. *Syst. Appl. Microbiol.* 25, 84–99. doi: 10.1078/0723-2020-00093

Kalia, V. C. (2013). Quorum sensing inhibitors: an overview. *Biotechnol. Adv.* 31, 224–245. doi: 10.1016/j.biotechadv.2012.10.004

Kang, D., Li, Y., Xu, D., Li, W., Li, W., Ding, A., et al. (2020). Deciphering correlation between chromaticity and activity of anammox sludge. *Water Res.* 185:116184. doi: 10.1016/j.watres.2020.116184

Kim, A. L., Park, S. Y., Lee, C. H., Lee, C. H., and Lee, J. K. (2014). Quorum quenching bacteria isolated from the sludge of a wastewater treatment plant and their application for controlling biofilm formation. *J. Microbiol. Biotechnol.* 24, 1574–1582. doi: 10.4014/jmb.1407.07009

Kinh, C. T., Ahn, J., Suenaga, T., Sittivorakulpong, N., Noophan, P., Hori, T., et al. (2017). Free nitrous acid and pH determine the predominant ammonia-oxidizing bacteria and amount of N2O in a partial nitrifying reactor. *Appl. Environ. Microbiol.* 101, 1673–1683. doi: 10.1007/s00253-016-7961-2

Laloo, A. E., Wei, J., Wang, D., Narayanasamy, S., Vanwonterghem, I., Waite, D., et al. (2018). Mechanisms of persistence of the ammonia-oxidizing bacteria Nitrosomonas to the biocide free nitrous acid. *Environ. Sci. Technol.* 52, 5386–5397. doi: 10.1021/acs.est.7b04273

Law, Y., Ye, L., Wang, Q., Hu, S., Pijuan, M., and Yuan, Z. (2015). Producing free nitrous acid - A green and renewable biocidal agent - From anaerobic digester liquor. *Chem. Eng. J.* 259, 62–69. doi: 10.1016/j.cej.2014.07.138

Li, Z., Wei, C., Chen, Y., Chen, B., Qiu, G., Wan, J., et al. (2021). Achieving nitritation in an aerobic fluidized reactor for coking wastewater treatment: operation stability, mechanisms and model analysis. *Environ. Sci. Technol.* 406:126816. doi: 10.1016/j.cej.2020.126816

Li, J., Xu, K., Liu, T., Bai, G., Liu, Y., Wang, C., et al. (2020). Achieving stable partial Nitritation in an acidic nitrifying bioreactor. *Environ. Sci. Technol.* 54, 456–463. doi: 10.1021/acs.est.9b04400

Liu, W., Yang, Q., Ma, B., Li, J., Ma, L., Wang, S., et al. (2017). Rapid achievement of Nitritation using aerobic starvation. *Environ. Sci. Technol.* 51, 4001–4008. doi: 10.1021/acs.est.6b04598

Liu, Z., Zhou, A., Wang, S., Cheng, S., Yin, X., and Yue, X. (2021). Quorum sensing shaped microbial consortia and enhanced hydrogen recovery from waste activated sludge electro-fermentation on basis of free nitrous acid treatment. *Sci. Total Environ.* 766:144348. doi: 10.1016/j.scitotenv.2020.144348

Luo, F., Hu, H., and Liu, Y. (2021). Function and potential application of quorum sensing in nitrogen-removing functional bacteria: a review. *Desalin. Water Treat.* 229, 104–115. doi: 10.5004/dwt.2021.27373

Maddela, N. R., Sheng, B., Yuan, S., Zhou, Z., Villamar-Torres, R., and Meng, F. (2019). Roles of quorum sensing in biological wastewater treatment: A critical review. *Chemosphere* 221, 616–629. doi: 10.1016/j.chemosphere.2019.01.064

Mellbye, B. L., Bottomley, P. J., and Sayavedra-Soto, L. A. (2015). Nitrite-oxidizing bacterium Nitrobacter winogradskyi produces N-acyl-Homoserine lactone autoinducers. *Appl. Environ. Microbiol.* 81, 5917–5926. doi: 10.1128/aem.01103-15

Mellbye, B. L., Davis, E. W. II, Spieck, E., Chang, J. H., Bottomley, P. J., and Sayavedra-Soto, L. A. (2017a). Draft genome sequence of Nitrobacter vulgaris strain Ab(1), a nitrite-oxidizing bacterium. *Microbiol. Res. Announcements* 5:e0290-17. doi: 10.1128/genomeA.00290-17

Mellbye, B. L., Giguere, A. T., Bottomley, P. J., and Sayavedra-Soto, L. A. (2016). Quorum quenching of Nitrobacter winogradskyi suggests that quorum sensing regulates fluxes of nitrogen oxide(s) during nitrification. *MBio* 7:e01753-16. doi: 10.1128/mBio.01753-16

Mellbye, B. L., Spieck, E., Bottomley, P. J., and Sayavedra-Soto, L. A. (2017b). Acyl-Homoserine lactone production in nitrifying bacteria of the genera Nitrosospira, Nitrobacter, and Nitrospira identified via a survey of putative quorum-sensing genes. *Appl. Environ. Microbiol.* 83:e01540-17. doi: 10.1128/aem.01540-17

Norton, J. M., Klotz, M. G., Stein, L. Y., Arp, D. J., Bottomley, P. J., Chain, P. S. G., et al. (2008). Complete genome sequence of Nitrosospira multiformis, an ammonia-oxidizing bacterium from the soil environment. *Appl. Environ. Microbiol.* 74, 3559–3572. doi: 10.1128/aem.02722-07

Oh, H.-S., and Lee, C.-H. (2018). Origin and evolution of quorum quenching technology for biofouling control in MBRs for wastewater treatment. *J. Membr. Sci.* 554, 331–345. doi: 10.1016/j.memsci.2018.03.019

Pedrouso, A., Val del Río, Á., Morales, N., Vázquez-Padín, J. R., Campos, J. L., Méndez, R., et al. (2017). Nitrite oxidizing bacteria suppression based on in-situ free nitrous acid production at mainstream conditions. *Sep. Purif. Technol.* 186, 55–62. doi: 10.1016/j.seppur.2017.05.043

Peng, Y., and Zhu, G. (2006). Biological nitrogen removal with nitrification and denitrification via nitrite pathway. *Appl. Microbiol. Biotechnol.* 73, 15–26. doi: 10.1007/s00253-006-0534-z

Pierson, M. D., and Smoot, L. A. (1982). Nitrite, nitrite alternatives, and the control of clostridium botulinum in cured meats. *Crit. Rev. Food Sci. Nutr.* 17, 141–187. doi: 10.1080/10408398209527346

Qiu, S., Li, Z., Hu, Y., Shi, L., Liu, R., Shi, L., et al. (2020). What's the best way to achieve successful mainstream partial nitritation-anammox application? *Crit. Rev. Environ. Sci. Technol.* 51, 1045–1077. doi: 10.1080/10643389.2020.1745015

Rahimi, S., Modin, O., and Mijakovic, I. (2020). Technologies for biological removal and recovery of nitrogen from wastewater. *Biotechnol. Adv.* 43:107570. doi: 10.1016/j.biotechadv.2020.107570

Rao, A., Jump, R. L. P., Pultz, N. J., Pultz, M. J., and Donskey, C. J. (2006). In vitro killing of nosocomial pathogens by acid and acidified nitrite. *Antimicrob. Agents Chemother.* 50, 3901–3904. doi: 10.1128/aac.01506-05

Ren, S., Wang, Z., Jiang, H., Qiu, J., Li, X., Zhang, Q., et al. (2021). Stable nitritation of mature landfill leachate via in-situ selective inhibition by free nitrous acid. *Bioresour. Technol.* 340:125647. doi: 10.1016/j.biortech.2021.125647

Rice, M. C., Norton, J. M., Valois, F., Bollmann, A., Bottomley, P. J., Klotz, M. G., et al. (2016). Complete genome of Nitrosospira briensis C-128, an ammonia-oxidizing bacterium from agricultural soil. *Stand. Genomic Sci.* 11:46. doi: 10.1186/s40793-016-0168-4

Shen, Q., Gao, J., Liu, J., Liu, S., Liu, Z., Wang, Y., et al. (2016). A new acyl-homoserine lactone molecule generated by Nitrobacter winogradskyi. *Sci. Rep.* 6:22903. doi: 10.1038/srep22903

Shrout, J. D., and Nerenberg, R. (2012). Monitoring bacterial twitter: does quorum sensing determine the behavior of water and wastewater treatment biofilms? *Environ. Sci. Technol.* 46, 1995–2005. doi: 10.1021/es203933h

Sijbesma, W. F. H., Almeida, J. S., Reis, M. A. M., and Santos, H. (1996). Uncoupling effect of nitrite during denitrification by Pseudomonas fluorescens: An in vivo P-31-NMR study. *Biotechnol. Bioeng.* 52, 176–182. doi: 10.1002/(sici)1097-0290(19961005)52:1<176::Aid-bit18>3.0.Co;2-m

Sinha, B., and Annachhatre, A. P. (2006). Partial nitrification—operational parameters and microorganisms involved. *Rev. Environ. Sci. Biotechnol.* 6, 285–313. doi: 10.1007/s11157-006-9116-x

Sun, Y., Chen, Z., Wu, G., Wu, Q., Zhang, F., Niu, Z., et al. (2016). Characteristics of water quality of municipal wastewater treatment plants in China: implications for resources utilization and management. *J. Clean. Prod.* 131, 1–9. doi: 10.1016/j.jclepro.2016.05.068

Sun, Y., Guan, Y., Wang, D., Liang, K., and Wu, G. (2018). Potential roles of acyl homoserine lactone based quorum sensing in sequencing batch nitrifying biofilm reactors with or without the addition of organic carbon. *Bioresour. Technol.* 259, 136–145. doi: 10.1016/j.biortech.2018.03.025

Sun, C., Zhang, B., Ning, D., Zhang, Y., Dai, T., Wu, L., et al. (2021). Seasonal dynamics of the microbial community in two full-scale wastewater treatment plants: diversity, composition, phylogenetic group based assembly and co-occurrence pattern. *Water Res.* 200:117295. doi: 10.1016/j.watres.2021.117295

Tan, C. H., Koh, K. S., Xie, C., Tay, M., Zhou, Y., Williams, R., et al. (2014). The role of quorum sensing signalling in EPS production and the assembly of a sludge community into aerobic granules. *ISME J.* 8, 1186–1197. doi: 10.1038/ismej.2013.240

Vadivelu, V. M., Keller, J., and Yuan, Z. (2006a). Effect of free ammonia and free nitrous acid concentration on the anabolic and catabolic processes of an enriched Nitrosomonas culture. *Biotechnol. Bioeng.* 95, 830–839. doi: 10.1002/bit.21018

Vadivelu, V. M., Yuan, Z., Fux, C., and Keller, J. (2006b). The inhibitory effects of free nitrous acid on the energy generation and growth processes of an enriched Nitrobacter culture. *Environ. Sci. Technol.* 40, 4442–4448. doi: 10.1021/es051694k

Wang, Z., Wang, B., Gong, X., Qiao, X., and Peng, Y. (2019). Free nitrous acid pretreatment of sludge to achieve nitritation: The effect of sludge concentration. *Bioresour. Technol.* 285:121358. doi: 10.1016/j.biortech.2019.121358

Wang, Q., Ye, L., Jiang, G., Hu, S., and Yuan, Z. (2014). Side-stream sludge treatment using free nitrous acid selectively eliminates nitrite oxidizing bacteria and achieves the nitrite pathway. *Water Res.* 55, 245–255. doi: 10.1016/j.watres.2014.02.029

Wang, Z., Zheng, M., Hu, Z., Duan, H., De Clippeleir, H., Al-Omari, A., et al. (2021a). Unravelling adaptation of nitrite-oxidizing bacteria in mainstream PN/A process: mechanisms and counter-strategies. *Water Res.* 200:117239. doi: 10.1016/j.watres.2021.117239

Wang, Z., Zheng, M., Meng, J., Hu, Z., Ni, G., Guerrero Calderon, A., et al. (2021b). Robust Nitritation sustained by acid-tolerant ammonia-oxidizing bacteria. *Environ. Sci. Technol.* 55, 2048–2056. doi: 10.1021/acs.est.0c05181

Waters, C. M., and Bassler, B. L. (2005). "Quorum sensing: cell-to-cell communication in bacteria," in *Annual Review of Cell and Developmental Biology*; November 10, 2005, 319–346.

Xu, D., Fan, J., Pan, C., Kang, D., Li, W., Chen, W., et al. (2021). Dimension effect of anammox granule: potential vs performance. *Sci. Total Environ.* 795:148681. doi: 10.1016/j.scitotenv.2021.148681

Yang, Y., Zhang, L., Cheng, J., Zhang, S., Li, B., and Peng, Y. (2017). Achieve efficient nitrogen removal from real sewage in a plug-flow integrated fixed-film activated sludge (IFAS) reactor via partial nitritation/anammox pathway. *Bioresour. Technol.* 239, 294–301. doi: 10.1016/j.biortech.2017.05.041

Yao, Y., Wang, Z., and Criddle, C. S. (2021). Robust Nitritation of anaerobic digester Centrate using dual stressors and timed alkali additions. *Environ. Sci. Technol.* 55, 2016–2026. doi: 10.1021/acs.est.0c04613

Yates, E. A., Philipp, B., Buckley, C., Atkinson, S., Chhabra, S. R., Sockett, R. E., et al. (2002). N-acylhomoserine lactones undergo lactonolysis in a pH-, temperature-, and acyl chain length-dependent manner during growth of Yersinia pseudotuberculosis and Pseudomonas aeruginosa. *Inf. Immun.* 70, 5635–5646. doi: 10.1128/IAI.70.10.5635-5646.2002

Ye, J., Liu, J., Ye, M., Ma, X., and Li, Y.-Y. (2020). Towards advanced nitrogen removal and optimal energy recovery from leachate: A critical review of anammox-based processes. *Crit. Rev. Environ. Sci. Technol.* 50, 612–653. doi: 10.1080/10643389.2019.1631989

Yu, H., Qu, F., Zhang, X., Wang, P., Li, G., and Liang, H. (2018). Effect of quorum quenching on biofouling and ammonia removal in membrane bioreactor under stressful conditions. *Chemosphere* 199, 114–121. doi: 10.1016/j.chemosphere.2018.02.022

Zhang, Q., Fan, N.-S., Fu, J.-J., Huang, B.-C., and Jin, R.-C. (2020). Role and application of quorum sensing in anaerobic ammonium oxidation (anammox) process: A review. *Crit. Rev. Environ. Sci. Technol.* 51, 626–648. doi: 10.1080/10643389.2020.1738166

Zhang, Y., Gao, J., Wang, L., Liu, S., Bai, Z., Zhuang, X., et al. (2018b). Environmental adaptability and quorum sensing: iron uptake regulation during biofilm formation by Paracoccus denitrificans. *Appl. Environ. Microbiol.* 84:e00865-18. doi: 10.1128/aem.00865-18

Zhang, T., Wang, B., Li, X., Zhang, Q., Wu, L., He, Y., et al. (2018a). Achieving partial nitrification in a continuous post-denitrification reactor treating low C/N sewage. *Environ. Sci. Technol.* 335, 330–337. doi: 10.1016/j.cej.2017.09.188

Zhang, Q. H., Yang, W. N., Ngo, H. H., Guo, W. S., Jin, P. K., Dzakpasu, M., et al. (2016). Current status of urban wastewater treatment plants in China. *Environ. Int.* 93, 11–22. doi: 10.1016/j.envint.2016.03.024

Zhao, Z. C., Xie, G. J., Liu, B. F., Xing, D. F., Ding, J., Han, H. J., et al. (2021). A review of quorum sensing improving partial nitritation-anammox process: functions, mechanisms and prospects. *Sci. Total Environ.* 765:142703. doi: 10.1016/j.scitotenv.2020.142703

Zheng, M., Wang, Z., Meng, J., Hu, Z., Liu, Y., Yuan, Z., et al. (2021). Inactivation kinetics of nitrite-oxidizing bacteria by free nitrous acid. *Sci. Total Environ.* 752:141876. doi: 10.1016/j.scitotenv.2020.141876

Zhou, X., Liu, X., Huang, S., Cui, B., Liu, Z., and Yang, Q. (2018). Total inorganic nitrogen removal during the partial/complete nitrification for treating domestic wastewater: removal pathways and main influencing factors. *Bioresour. Technol.* 256, 285–294. doi: 10.1016/j.biortech.2018.01.131

Zhou, Y., Oehmen, A., Lim, M., Vadivelu, V., and Ng, W. J. (2011). The role of nitrite and free nitrous acid (FNA) in wastewater treatment plants. *Water Res.* 45, 4672–4682. doi: 10.1016/j.watres.2011.06.025

Zhou, Y., Pijuan, M., and Yuan, Z. (2007). Free nitrous acid inhibition on anoxic phosphorus uptake and denitrification by poly-phosphate accumulating organisms. *Biotechnol. Bioeng.* 98, 903–912. doi: 10.1002/bit.21458

Zhou, Y., Pijuan, M., Zeng, R. J., and Yuan, Z. (2008). Free nitrous acid inhibition on nitrous oxide reduction by a denitrifying-enhanced biological phosphorus removal sludge. *Environ. Sci. Technol.* 42, 8260–8265. doi: 10.1021/es800650j

Conflict of Interest: WZ and QM are employed by Shenzhen Shenshui Water Resources Consulting Co., Ltd.

The remaining authors declare that the research was conducted in the absence of any commercial or financial relationships that could be construed as a potential conflict of interest.

be evaluated in this article, or claim that may be made by its manufacturer, is not guaranteed or endorsed by the publisher.

frontiers | Frontiers in Microbiology

REVIEW
published: 29 April 2022
doi: 10.3389/fmicb.2022.895409

Autotrophic Fe-Driven Biological Nitrogen Removal Technologies for Sustainable Wastewater Treatment

Suyan Pang[1], Ning Li[2,3,4], Huan Luo[4], Xiaonan Luo[2,3], Tong Shen[2,3], Yanan Yang[4] and Jin Jiang[2,3]*

[1]Key Laboratory of Songliao Aquatic Environment, School of Municipal and Environmental Engineering, Ministry of Education, Jilin Jianzhu University, Changchun, China, [2]Key Laboratory for City Cluster Environmental Safety and Green Development of the Ministry of Education, School of Ecology, Environment and Resources, Guangdong University of Technology, Guangzhou, China, [3]Southern Marine Science and Engineering Guangdong Laboratory (Guangzhou), Guangzhou, China, [4]Guangdong Provincial Engineering Technology Research Center for Life and Health of River & Lake, Pearl River Water Resources Research Institute, Pearl River Water Resources Commission of the Ministry of Water Resources, Guangzhou, China

Fe-driven biological nitrogen removal (FeBNR) has become one of the main technologies in water pollution remediation due to its economy, safety and mild reaction conditions. This paper systematically summarizes abiotic and biotic reactions in the Fe and N cycles, including nitrate/nitrite-dependent anaerobic Fe(II) oxidation (NDAFO) and anaerobic ammonium oxidation coupled with Fe(III) reduction (Feammox). The biodiversity of iron-oxidizing microorganisms for nitrate/nitrite reduction and iron-reducing microorganisms for ammonium oxidation are reviewed. The effects of environmental factors, e.g., pH, redox potential, Fe species, extracellular electron shuttles and natural organic matter, on the FeBNR reaction rate are analyzed. Current application advances in natural and artificial wastewater treatment are introduced with some typical experimental and application cases. Autotrophic FeBNR can treat low-C/N wastewater and greatly benefit the sustainable development of environmentally friendly biotechnologies for advanced nitrogen control.

Keywords: biological nitrogen removal, Feammox, nitrate-dependent anaerobic Fe(II) oxidation, iron-reducing microorganisms, iron-oxidizing microorganisms

OPEN ACCESS

Edited by:
Lei Miao,
Huazhong University of Science and Technology, China

Reviewed by:
Fangxu Jia,
Beijing Jiaotong University, China
Xiaoxia Wang,
Qingdao University, China

***Correspondence:**
Ning Li
lining_10@163.com;
lining_10@gdut.edu.cn

Specialty section:
This article was submitted to Microbiotechnology, a section of the journal Frontiers in Microbiology

Received: *13 March 2022*
Accepted: *08 April 2022*
Published: *29 April 2022*

Citation:
Pang S, Li N, Luo H, Luo X, Shen T, Yang Y and Jiang J (2022) Autotrophic Fe-Driven Biological Nitrogen Removal Technologies for Sustainable Wastewater Treatment. Front. Microbiol. 13:895409. doi: 10.3389/fmicb.2022.895409

INTRODUCTION

Nitrogen-containing wastewater has negative effects on human health and aquatic ecosystems. Biological nitrogen removal (BNR) is a low-cost and efficient way to control nitrogen pollution. However, conventional denitrification requires large amounts of carbon-containing compounds, such as methanol, sodium acetate and glucose, causing enormous resource waste, and secondary pollution (Tian and Yu, 2020). Autotrophic denitrification provides multiple alternative methods that adopt inorganic sulfur, hydrogen, and iron as electron donors to reduce nitrate (NO_3^-) or nitrite (NO_2^-), especially for treating low C/N wastewater (Di Capua et al., 2019). Therefore, the development of autotrophic denitrification techniques has attracted considerable attention in biological wastewater treatment.

Anammox-based techniques have been developed for decades as a representative autotrophic process, but the requisite substrate NO_2^- heavily relies on short-cut nitrification or denitrification processes (Sheng et al., 2020b). Sulfur-driven autotrophic denitrification utilizes reduced sulfate (S^{2-}, S^0, $S_2O_3^{2-}$) as an electron donor to reduce NO_3^-, but the acidic environment erodes municipal pipes, leading to billions of dollars in expense per year in Australia (Pikaar et al., 2014). Hydrogen-driven denitrification still has several unaddressed issues, such as safety concerns, high costs, and complex equipment. Although these technologies provide useful solutions to treat low C/N sewage, it is still necessary to explore more efficient and safer autotrophic denitrification technologies.

Fe-driven biological nitrogen removal (FeBNR) consists of two processes, i.e., anaerobic ammonium (NH_4^+) oxidation coupled with Fe(III) reduction (Feammox) and nitrate/nitrite-dependent anaerobic Fe(II) oxidation (NDAFO). In the Feammox process, NH_4^+ is oxidized to N_2, NO_2^- and NO_3^- by iron-reducing microorganisms (IRM) in paddy soils, estuary regions, and riparian zones (Ding et al., 2017; Yi et al., 2019). It was estimated that a nitrogen loss of 8.3–17.8 kg-N/(ha·yr) was associated with Feammox in Taihu estuary soils (Ding et al., 2019). In the NDAFO process, NO_x^- is reduced to N_2 by iron-oxidizing microorganisms (IOM) using zero-valent iron (ZVI) or Fe(II) as electron donors (Kiskira et al., 2017). Moreover, an Anammox-like process involving the integration of Feammox and NDAFO was used to remove NH_4^+ using NO_x^- as a terminal electron acceptor through the Fe(III)/Fe(II) cycle (Yang et al., 2020). Since Fe(III)/Fe(II) easily form solid iron compounds in neutral aquatic environments, a single Feammox or NDAFO process is challenging to operate for a long time and easy to produce large amounts of iron sludge (Li et al., 2021b). Ideally, FeBNR can effectively solve the above problem of sludge mineralization and constantly consume NH_4^+ and NO_3^-. The environmentally friendly characteristics, abundance of its constituent species and wide distribution make FeBNR an emerging technique to remediate environmental pollution. The biotic and abiotic reactions between Fe and N are ubiquitous and complex, and a systematic review should be provided for an in-depth understanding of the application of FeBNR to wastewater treatment.

The low reaction rate and the long incubation time of functional microorganisms still hinder FeBNR applications in practical sewage treatment. Unlike conventional heterotrophic denitrification using soluble organic carbon as an electron donor, FeBNR adopts insoluble Fe(III)/Fe(II) minerals to transfer electrons specifically during microbial extracellular respiration. The solubility and bioavailability of solid iron minerals limit the nitrogen removal efficiency. Therefore, the iron metabolizing microorganism and the effect of environmental factors on nitrogen removal efficiency should be summarized. Moreover, various abiotic iron reactions occur extensively in anaerobic environments, increasing the diversity of nitrogen transformation pathways. The underlying mechanisms of nitrogen transformation pathways, including biotic or abiotic processes, should be further identified and discussed.

The purpose of this paper is to review (1) the abiotic and biotic reactions between Fe and N species, elucidating the important effect of the iron cycle on nitrogen transformation; (2) the environmental factors affecting FeBNR efficiency, providing technical references for controlling nitrogen pollution; and (3) the current wastewater treatment processes based on Feammox and NDAFO. On this basis, potential development and application trends of FeBNR technology are proposed.

ABIOTIC AND BIOTIC MECHANISMS UNDERLYING THE INTERACTION OF THE Fe AND N CYCLES

Abiotic Fe Element Reactions

Zero-Valent Iron

zero-valent iron is an effective and abundant reducing agent with a standard redox potential of −0.44 V for NO_x^- removal from groundwater and wastewater. According to the particle size, ZVI can be classified as nanoscale ZVI (nZVI) and microscale ZVI (mZVI), and nZVI generally has a higher reductive capacity than mZVI due to its greater specific surface area. The mechanisms of the ZVI reaction with NO_x^- mainly involve (1) direct electron transfer from ZVI to NO_3^- to form lower-valence nitrogen species, as shown in Eq. 1–3 (Jeong et al., 2012) in **Table 1**; (2) indirect reduction of NO_2^- by the produced Fe(II), as in Eq. 4–5 (Liu and Wang, 2019); and (3) removal of NO_3^- *via* the H_2 secondarily generated by hydrogenotrophic nitrate-respiring bacteria, as in Eq. 6–8 (Kim and Cha, 2021). In addition, NO_3^- can be transformed to NH_4^+ by adding both ZVI and Fe(II) with strong reducibility (Eq. 9). Fe(II)EDTA generally has a high adsorption capacity for NO, and the ZVI added in the reactor could convert Fe(II) EDTA-NO to NH_4^+, providing substrates for Anammox and decreasing the toxicity of NO in activated sludge (Eq. 10; Zhang et al., 2019a).

Although ZVI has been adopted to remediate nitrate-containing wastewater pollution, the shell of the iron oxides formed on the surface of ZVI and the agglomeration of ZVI particles significantly affect the nitrate reduction efficiency. Hence, physical and chemical strategies have been developed to enhance the transformation efficiency and iron corrosion. ZVI composites are prepared to increase the adsorption capacity for NO_3^- as well as to increase the number of active sites for electron transfer to NO_3^-, mainly through (1) doping ZVI with metal or inorganic components such as Cu, Pt, Al and activated carbon (AC); (2) supporting ZVI composites with matrixes such as calcium alginate and AC; and (3) adding reducing-state additives such as sulfur to ZVI. Meng et al. (2020) encapsulated mZVI and AC into porous calcium alginate to achieve good dispersion of mZVI particles and enhance the iron-carbon galvanic cell effect. An acid mine drainage-based nZVI was synthesized to couple NO_3^- reduction and norfloxacin oxidation with ultrasound irradiation to overcome passivation (Diao et al., 2019).

TABLE 1 | Abiotic and biotic reactions of ZVI, Fe(II) and Fe(III) with nitrogen species.

Iron species	Reactions	Types	Comments	Eq.	References
ZVI	$4Fe^0 + 2NO_3^- + 10H^+ \rightarrow 4Fe^{2+} + NH_4^+ + 3H_2O$	Abiotic	ZVI directly reacts with nitrate.	(1)	Jeong et al., 2012
	$5Fe^0 + 2NO_3^- + 12H^+ \rightarrow 5Fe^{2+} + N_2 + 6H_2O$	Abiotic		(2)	
	$Fe^0 + 2NO_3^- + 4H^+ \rightarrow Fe^{2+} + 2NO_2^- + 2H_2O$	Abiotic		(3)	
	$Fe^0 \rightarrow Fe^{2+} + 2e^-$ $6Fe^{2+} + NO_2^- + 8H^+ \rightarrow 6Fe^{3+} + NH_4^+ + 2H_2O$	Abiotic	The formed Fe(II) reacts with nitrite.	(4)	Liu and Wang, 2019
		Abiotic		(5)	
	$Fe^0 + 2H_2O \rightarrow H_2 + Fe^{2+} + 2OH^-$	Abiotic	The produced H_2 reacts with nitrate.	(6)	Kim and Cha, 2021
	$Fe^0 + 2H^+ \rightarrow Fe^{2+} + H_2$ (acidic conditions)	Abiotic		(7)	
	$5H_2 + 2NO_3^- \rightarrow N_2 + 4H_2O + 2OH^-$	Biotic		(8)	
	$2.82Fe^0 + 0.75Fe^{2+} + NO_3^- + 2.25H_2O \rightarrow 1.19Fe_3O_4 + NH_4^+ + 0.5OH^-$	Abiotic	The other transformations of iron species occur.	(9)	Zhang et al., 2019a
	$5Fe^0 + 2Fe^{2+}EDTA - NO^{2-} + 12H^+ \rightarrow 2Fe^{2+}EDTA^{2-} + 5Fe^{2+} + 2NH_4^+ + 2H_2O$	Abiotic		(10)	
Fe(II)	$Fe^{2+}EDTA^{2-}(aq) + NO(aq) \leftrightarrow Fe^{2+}EDTA^{2-} - NO(aq)$	Abiotic	The Fe(II)-EDTA absorption combines Anammox.	(11)	
	$6Fe^{2+}EDTA - NO^{2-}(aq) + 4NH_4^+ \rightarrow 5N_2 + 6H_2O + 4H^+ + 6Fe^{2+}EDTA^{2-}(aq)$	Biotic		(12)	
	$4Fe^{2+} + 2NO_2^- + 9H_2O \rightarrow 4Fe(OH)_3 + N_2O + 6H^+$	Abiotic	Nitrite chemically reacts with ferrous ion.	(13)	Jones et al., 2015
	$4Fe^{2+} + 2NO_2^- + 5H_2O \rightarrow 4FeOOH + N_2O + 6H^+$	Abiotic		(14)	
	$4Fe^{2+} + 2HNO_2 + 4H^+ \rightarrow 4Fe^{3+} + N_2O + 3H_2O$	Abiotic	Intermediates of nitritation abiotically react with ferrous ion.	(15)	Yang et al., 2018
	$10Fe^{2+} + 2NO_3^- + 24H_2O \rightarrow 10Fe(OH)_3 + N_2 + 18H^+$	Biotic	Nitrate reacts with ferrous ion *via* autotrophic denitrifying bacteria.	(16)	Tian et al., 2020
	$10Fe^{2+} + 2NO_3^- + 14H_2O \rightarrow 10FeOOH + N_2 + 18H^+$	Biotic		(17)	
	$15Fe^{2+} + 2NO_3^- + 14H_2O \rightarrow 54Fe_3O_4 + N_2 + 28H^+$	Biotic		(18)	
Fe(III)	$4Fe^{3+} + 2NH_2OH \rightarrow 4Fe^{2+} + N_2O + H_2O + 4H^+$	Abiotic	Intermediates of nitritation abiotically react with ferric ion.	(19)	Yang et al., 2018
	$3Fe(OH)_3 + 5H^+ + NH_4^+ \rightarrow 3Fe^{2+} + 9H_2O + 0.5N_2$	Biotic	Ammonium reacts with ferric ion *via* Feammox.	(20)	Tan et al., 2021
	$6Fe(OH)_3 + 10H^+ + NH_4^+ \rightarrow 6Fe^{2+} + 16H_2O + NO_2^-$	Biotic		(21)	
	$8Fe(OH)_3 + 14H^+ + NH_4^+ \rightarrow 8Fe^{2+} + 21H_2O + NO_3^-$	Biotic		(22)	

Fe(II)

In early 1966, Chao and Kroontje (1966) studied the feasibility and intermediates of inorganic NO_3^- transformation through Fe(II) oxidation. Only under acidic and high-temperature conditions, can Fe(II) be chemically oxidized by NO_3^-. Even Fe(II) can theoretically react with NO_3^- in a thermodynamically favored reaction at near-neutral pH and environmental temperature, but the kinetic rate is extremely low. Although the redox potential of the Fe(III)/Fe(II) couple (−314–14 mV) is lower than that of all nitrogen couples (NO_3^- / NO_2^-, +430 mV; NO_2^-/NO, +350 mV; NO/N_2O, +1,180 mV; N_2O/N_2, +1,350 mV) in denitrification, Fe(II) oxidation coupled with NO_3^- reduction cannot proceed smoothly without a catalyst. The common catalysts are Cu^{2+}, iron (hydr)oxides and even cell surface enzymes. For example, under anoxic conditions in soils and sediments, the dissimilatory reduction of nitrate to ammonia has been observed in the presence of green rust compounds [$Fe^{II}_4Fe^{III}_2(OH)_{12}SO_4 \bullet yH_2O$; Hansen et al., 1996], representing the occurrence of chemical denitrification or chemodenitrification. The unique structure of green rust may self-catalyze this reaction.

In addition, Fe(II)-EDTA could promote the adoption of aqueous NO and provide a substrate for the production of N_2 by Anammox bacteria (Eq. 11–12). N_2O is a natural product primarily derived from biotic denitrification, but chemodenitrification processes also contribute to N_2O release to the atmosphere. Among them, NO_2^- can be reduced by Fe(II) to produce N_2O along with Fe(III; hydr)oxides as byproducts (Eq. 13–14; Jones et al., 2015). In the intermediate step of nitritation, the produced HNO_2 could be chemically reduced by Fe(II) to release N_2O, as shown in Eq. 15 (Yang et al., 2018). Nitrite can rapidly be absorbed on goethite at low pH, and surface Fe(II)-goethite complexes show variable reactivity with NO_2^- to produce N_2O (Dhakal et al., 2021).

Fe(III)

Hydroxylamine (NH_2OH) is an intermediate in short-cut nitrification and can abiotically react with Fe(III) to produce nitrous oxide (N_2O), as shown in Eq. 19, and this process is greatly affected by pH. Generally, abiotic reactions play an essential role in the production of total N_2O at pH values less than 5. To prevent excessive greenhouse gas emissions, short-cut nitrification reactors usually control pH at near-neutral conditions to reduce the release of N_2O from abiotic reactions (Hikino et al., 2021).

Microbially Mediated ZVI/Fe(II) Oxidation

Iron and nitrogen cycles are tightly coupled under natural anoxic conditions due to the co-occurrence iron minerals and nitrate in soils, sediments and groundwater. NDAFO is a widely reported biogeochemical process using aqueous or solid-state Fe(II) as electron donors for nitrate/nitrite reduction under circumneutral conditions, as shown in Eq. 16–18 (Tian et al., 2020). ZVI-based autotrophic denitrification utilizes elemental iron substances as electron donors to reduce NO_x^-.

Nitrate/Nitrite-Dependent IOM

IOM are widely distributed in the bacterial and archaeal domains (as shown in **Table 2**). Moreover, IOM are mainly classified into Proteobacteria, Actinobacteria (Zhang et al., 2016a), Firmicutes (Li and Pan, 2019) and Euryarchaeota (Hafenbradl

TABLE 2 | ZVI/Fe(II)-oxidizing microorganisms for NO_2^- / NO_3^- reduction.

Phylum	Species	Sample sites	Electron donors	Electron acceptors	Products	Nutrition type	References
Actinobacteria	*Thermoleophilia* sp.	Cultivated sludge	$FeSO_4·7H_2O$	NO_3^-	N_2	Mixotrophic	Zhang et al., 2016a
Firmicutes	*Clostridium* sp. strain PXL2	Anoxic activated sludge	$FeCl_2·4H_2O$	NO_3^-	N_2	Mixotrophic	Li and Pan, 2019
Euryarchaeota	*Ferroglobus placidus*	Shallow beach	FeS	NO_3^-	N_2	Autotrophic	Hafenbradl et al., 1996
α-Proteobacteria	*Hoeflea siderophila* sp.	River sediments	FeS	NO_3^- , N_2O	N_2	Mixotrophic	Sorokina et al., 2012
	Paracoccus denitrificans	Lab-scale bioreactor	$FeCl_2$	NO_3^- / NO_2^-	N_2	Mixotrophic	Park et al., 2018
	Paracoccus ferrooxidans BDN-1	Denitrifying bioreactor	$[Fe(II)EDTA]^{2-}$	NO_3^-	N_2	Mixotrophic	Kumaraswamy et al., 2006
	Paracoccus sp.	Lab-scale serum bottles	nZVI	NO_3^-	N_2	Mixotrophic	Jiang et al., 2015
β-Proteobacteria	*Acidovorax* sp. strain BoFeN1	Lake littoral sediments	$FeCl_2·6H_2O$	NO_3^-	NO_2^- , N_2O, N_2	Mixotrophic	Liu et al., 2019b
	Alcaligenes eutrophus	Anoxic flask	ZVI	NO_3^-	N_2	Mixotrophic	Zhang et al., 2019c
	Aquabacterium parvum B6	Upflow bioreactor	$FeCl_2·4H_2O$	NO_3^-	N_2	Mixotrophic	Zhang et al., 2016b
	Azospira	Lab-scale UCT-A/MBR	$FeSO_4·7H_2O$	NO_3^-	N_2	Mixotrophic	Zhang et al., 2020a
	Dechloromonas sp. strain UWNR4	River sediments	Fe(II)-EDTA	NO_3^-	N_2	Mixotrophic	Anirban and Flynn, 2013
	Pseudogulbenkiania sp. strain 2002	Freshwater sediments	$FeSO_4·7H_2O$	NO_3^-	N_2O, N_2	Mixotrophic	Chen et al., 2020a
	Rhodopseudom onas	CWs	Iron scraps	NO_3^-	N_2	Mixotrophic	Ma et al., 2020
	Thiobacillus sp.	Black odorous sediment	Fe(II)	NO_3^-	NO_2^-	Autotrophic	Mai et al., 2021
	Zoogloea sp. L2	River sediments	Fe–C powder	NO_3^-	N_2	Mixotrophic	Xu et al., 2021
γ-Proteobacteria	*Citrobacter freundii* strain PXL1	Anoxic activated sludge	$FeCl_2·4H_2O$	NO_3^-	N_2	Mixotrophic	Li et al., 2015
	Klebsiella mobilis	Lab stock	$FeSO_4·7H_2O$,	NO_3^-	NO_2^-	Mixotrophic	Etique et al., 2014
	Pseudomonas stutzeri LS-2	Paddy soil	$FeCl_2·4H_2O$	NO_3^- / NO_2^-	N_2O, N_2	Mixotrophic	Li et al., 2018a
	Thermomonas sp.	River surface sediments	Fe(II)	NO_3^- / NO_2^-	N_2	Mixotrophic	He et al., 2017
δ-Proteobacteria	*Desulfovibrio* sp. CMX	Lab-scale anaerobic vial	ZVI	NO_3^- / NO_2^-	NH_4^+	Mixotrophic	Su et al., 2020

et al., 1996). In 1991, Brons et al. (1991) reported that the nitrate-reducing bacteria *Escherichia coli* reduced NO_3^- to NO and N_2O in the presence of Fe(II) and L-lactic acid under anaerobic conditions. In 1996, Straub et al. (1996) enriched and isolated three strains of gram-negative bacteria, which can use Fe(II) as an electron donor for NO_3^- reduction. Subsequently, NDAFO IOM were found in river and lake sediments, paddy soils, water treatment reactors and constructed wetlands (CWs) and were mainly categorized as α-Proteobacteria (Kumaraswamy et al., 2006; Sorokina et al., 2012; Jiang et al., 2015; Park et al., 2018), β-Proteobacteria (Anirban and Flynn, 2013; Zhang et al., 2016b, 2019c, 2020a; Liu et al., 2019b; Chen et al., 2020a; Ma et al., 2020; Mai et al., 2021; Xu et al., 2021), γ-Proteobacteria (Etique et al., 2014; Li et al., 2015, 2018a; He et al., 2017) and δ-Proteobacteria (Su et al., 2020), which play important roles in Fe(II) reduction coupled with NO_x^- oxidation.

Nitrate/nitrite-dependent IOM can be divided into autotrophic and mixotrophic microorganisms in terms of metabolic types. Autotrophic IOM do not require organic carbon and use only Fe(II) as an electron donor to generate energy and fix carbon dioxide. However, such bacteria are rarely reported or distributed in wild environments. In contrast, mixotrophic IOM require organic carbon as a common reducing substrate with Fe(II). At present, it has been observed that 90% of nitrate-reducing bacteria can oxidize Fe(II) in the presence of organic matter. In other words, many heterotrophic denitrifying bacteria are also IOM in nature and are mostly heterotrophic or mixotrophic. These facts indicate great possibilities for the application of NDAFO with abundant and readily available functional microorganisms sources.

Electron Transfer Mechanism for NDAFO

Currently, the precise electron transfer mechanism of enzyme-catalyzed NDAFO is not well understood. According to existing studies, electrons supplied by Fe(II) are transferred to NO_3^- and intermediate nitrogen species during denitrification by iron oxidoreductase, the quinone pool, NAR, cytochrome bc_1 complex, etc., coupled with the conventional heterotrophic electron transfer chain (**Figure 1**). Although no specific enzyme has been identified to accept an electron from extracellular Fe(II), it has been reported that cytochrome *c* (*c*-Cyts) is likely involved in the electron transfer between Fe(II) and IOM; however, more direct evidence is needed for verification, and other enzyme proteins need to be evaluated (Liu et al., 2019a). In addition, Fe(II) can penetrate the outer membrane into the

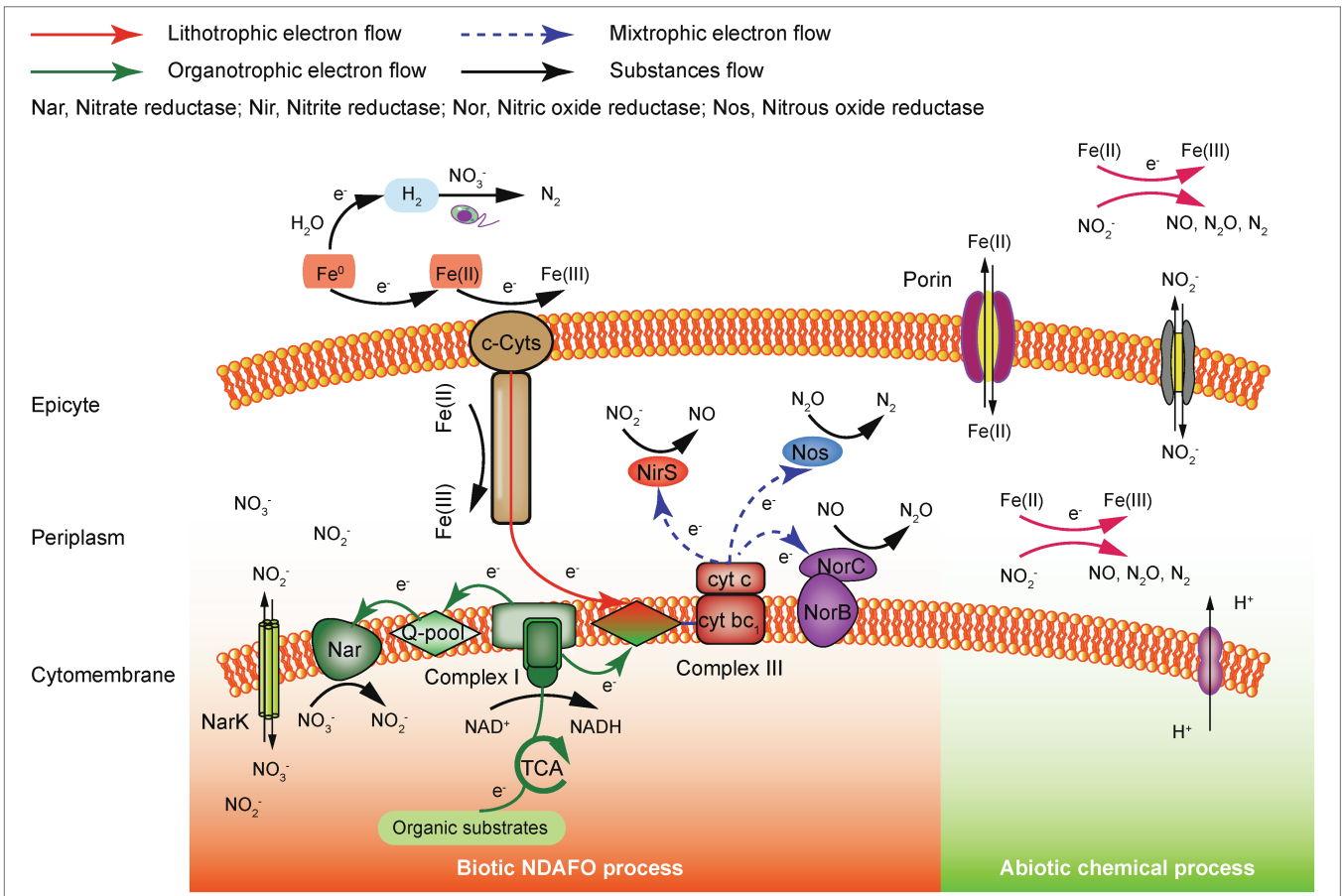

FIGURE 1 | Electron transfer mechanism of the ZVI/Fe(II)-supported NDAFO process (Zhang et al., 2020b).

periplasm through porin-containing proteases and chemically react with NO_2^- to produce gaseous NO, N_2O and N_2.

Microbial-Mediated Fe(III) Reduction

IRM for Feammox

Feammox plays an important role in nitrogen cycling globally, especially in Fe(III)-rich soils or wetlands. IRM are the dominant microorganisms in the Feammox process, which oxidizes NH_4^+ to NO_2^-, NO_3^- and N_2 to produce bioenergy for cell growth (Eq. 20–22; Tan et al., 2021). In 1993, Lovley et al. (1993) first reported that *Geobacter metallireducens* could use Fe(III) as the sole electron acceptor to oxidize short-chain fatty acids, alcohols and monoaromatic compounds, which proved the existence of IRM. In 2005, Clément et al. (2005) accidentally detected the production of NO_2^- and Fe(II) in riparian wetland soils for the first time and observed dissimilar iron reduction by ammonium oxidation under anaerobic conditions. In 2006, Sawayama (2006) observed that NH_4^+ was oxidized to NO_2^- in an anaerobic fixed-bed reactor supplemented with Fe(III)-EDTA and named the process "Feammox" (ferric ammonium oxidation). *Exiguobacterium* sp. was found to be the dominant IRM from high-throughput sequencing targeting the 16S rRNA gene. Subsequently, many different IRM have been observed to participate in the Feammox process, including Proteobacteria (Benaiges-Fernandez et al., 2019; Li et al., 2019; Ding et al., 2020a,b; Wang et al., 2021; Yang et al., 2021a), Actinobacteria (Shuai and Jaffé, 2019; Ma et al., 2021) and Firmicutes (Sawayama, 2006; Qin et al., 2019; Yang et al., 2019; Yao et al., 2020; **Table 3**). Among them, *Geobacteraceae* sp. and *Shewanella* sp. have been widely reported and studied. Although 16S rRNA high-through sequencing is promising to identify more IRM in recent studies, pure strain isolation in enrichment cultures is still needed to explore the mechanisms underlying Feammox.

Electron Transfer Mechanism for Feammox

Many IRM rely on a series of redox-sensitive proteins or multiple heme cytochromes to transfer extracellular electrons by direct contact with ion minerals, which form an extracellular electron transfer (EET) pathway that binds the cell's internal respiratory chain to external solid Fe(III) minerals. *Shewanella* sp. and *Geobacter* sp. often use *c*-Cyts to transfer electrons, exploiting the many solvent-exposed hemes as electron transfer centers, as heme comprises iron atoms and porphyrin rings.

Shewanella oneidensis has 39 genes that encode *c*-Cyts, which are considered to be electron transport mediators, including CymA in the cytoplasmic membrane, Fcc3 and STC in the periplasm, and MtrCBA in the outer membrane (**Figure 2A**). CymA is a dehydrogenase that oxidizes quinols to release electrons and then transfers electrons directly or indirectly *via* Fcc3 and STC to MtrA. For the MtrCBA structure, MtrA is inserted into the porin-like protein MtrB and then interconnects with MtrC in the outer membrane, which finally forms a ternary trans-outer membrane complex. In addition, *Shewanella* sp. can also secrete small molecules, such as flavin and quinones, as electron shuttles (ESs) to achieve long-distance EET (Shi et al., 2016).

Regarding *Geobacter* sp., *G. sulfurreducens* has 111 genes encoding these *c*-Cyts, which can be divided into three categories (**Figure 2B**): (1) ImcH and CbcL first oxidize quinols to release electrons in the cytoplasmic membrane; (2) PpcA and PpcD receive and transfer electrons in the periplasm; and (3) Omas (B and C) and Omcs (B, C or Z) form trans-outer membrane protein complexes, which combine with porin-like proteins OmbB and OmbC to eventually transfer electrons to the extracellular space (Liu et al., 2018). Overall, electrons are derived from quinols in the cell's inner membrane through periplasm transport and outer membrane emission to the final electron acceptor outside the cell.

TABLE 3 | Fe(III)-reducing microorganisms for NH_4^+ oxidation in Feammox.

Phylum	Species	Sample sites	Electron donors	Electron acceptors	Products	References
β-Proteobacteria	*Thiobacillus* sp.	Farmland soils	NH_4^+	Fe(III)	N_2	Ding et al., 2020a
γ-Proteobacteria	*Pseudomonas* sp.	Paddy soil	NH_4^+	Fe(III)	N_2	Li et al., 2019
	Shewanella lohica	Marine sediment	NH_4^+	Fe(III) oxides	N_2	Benaiges-Fernandez et al., 2019
δ-Proteobacteria	*Anaeromyxobacter* sp.	Paddy soil	NH_4^+	Fe(III)	N_2	Wang et al., 2021
	Geobacteraceae	Ecosystem habitats	NH_4^+	Fe(III)	NO_3^-, NO_2^-, N_2	Ding et al., 2020b
	Geobacter sp.	Anaerobic bottles	NH_4^+	Fe(III) coagulants	N_2	Yang et al., 2021a
Actinobacteria	*Acidimicrobiaceae* sp. A6	CWs	NH_4^+	2-Line ferrihydrite	NO_2^-	Shuai and Jaffé, 2019
	Geothrix sp.	CWs	NH_4^+	Oxidized iron scraps	NO_2^-	Ma et al., 2021
Firmicutes	*Bacillus* sp.	Wheat-rice rotation area	NH_4^+	Fe(III)	N_2	Qin et al., 2019
	Desulfosporosinus sp.	Anaerobic vials	NH_4^+	Fe_2O_3	N_2	Yang et al., 2019
	Exiguobacterium sp.	Fixed-bed reactor	NH_4^+	Fe(III)-EDTA	N_2	Sawayama, 2006
	Fervidicella sp.	Biofilm reactor	NH_4^+	Oxidized sponge iron	NO_3^-, N_2	Yao et al., 2020

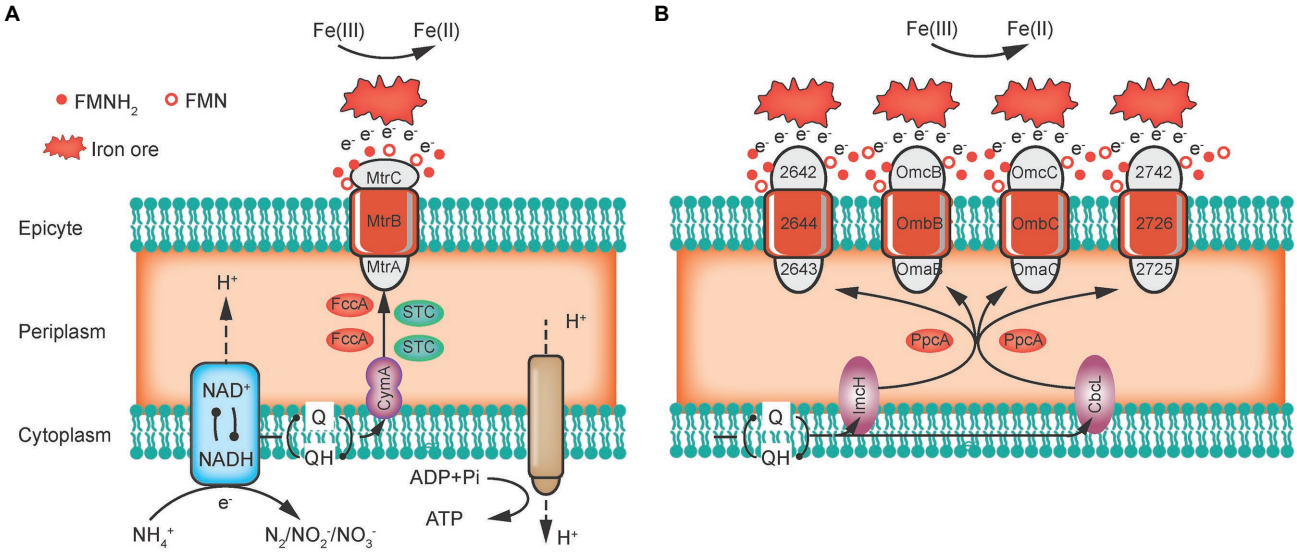

FIGURE 2 | Extracellular electron transfer pathways of *Geobacter sulfurreducens* **(A)** and *Shewanella oneidensis* (**B**; Liu et al., 2018).

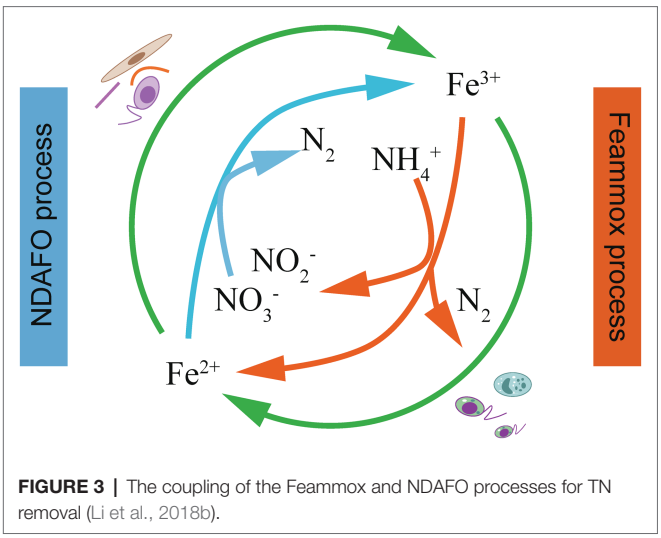

FIGURE 3 | The coupling of the Feammox and NDAFO processes for TN removal (Li et al., 2018b).

The Integration of Fe Oxidation and Reduction

The Coupling of Biotic and Abiotic Reactions

The reduction of NO_3^- to NO_2^- is the first step of microbial denitrification, which is catalyzed by membrane-bound nitrate reductase (NAR) or nitrate reductase in the periplasm (NAP). Depending on environmental conditions, such as the temperature, concentration of organics, pH, and aeration time, NO_2^- can accumulate to mM concentrations in the partial nitrification process. Microbially produced NO_2^- can be reduced by Fe(II) to gaseous NO, N_2O, and N_2 *via* chemodenitrification. In anoxic iron-containing environments, this process results from integrating biotic and abiotic processes, which jointly promote total nitrogen (TN) removal in the aqueous phase. This coupling provides a solution to the problem where Fe(II) does not react with NO_3^- in certain environments. However, accurate contribution ratios for the biotic and abiotic pathways should be quantitatively determined for an in-depth understanding of the denitrification process.

The Coupling of Microbial Fe(II) Oxidation and Fe(III) Reduction

Some Fe(III) minerals, as electron acceptors, could biotically oxidize NH_4^+ in IRM-mediated Fe(III) reduction, and the Fe(II; hydr)oxides produced in the above process might be utilized as electron donors and react with NO_x^- in anaerobic conditions (**Figure 3**). The biotic enzymatic Fe(III) reduction and Fe(II) oxidation rates are generally higher than those of abiotic chemical reactions in nitrogen-rich conditions (Lovley, 1997). This integration has important implications for microbial ecology since specific bacteria can gain chemical energy for growth from the two energy generation processes. Although the IRM and IOM might be spatially or temporally separated, a syntrophic relationship is formed in which iron-bearing minerals mutually support the growth of each group (Zhao et al., 2015). Yang et al. (2020) developed an Anammox-like process to treat sludge digest effluent with high-concentration NH_4^+ using NO_3^- as a terminal electron acceptor in the Fe(III)/Fe(II) cycle, in which NH_4^+ was mainly oxidized by Fe(III) to N_2 through Feammox. The produced Fe(II) triggered NDAFO to reduce NO_x^- to achieve effective TN removal. The coupled processes provide a safe and efficient method to treat NH_4^+ and NO_3^- wastewater simultaneously.

ENVIRONMENTAL FACTORS

pH

The environmental pH generally has an important effect on iron speciation. At extremely low pH, Fe(II) is oxidized to

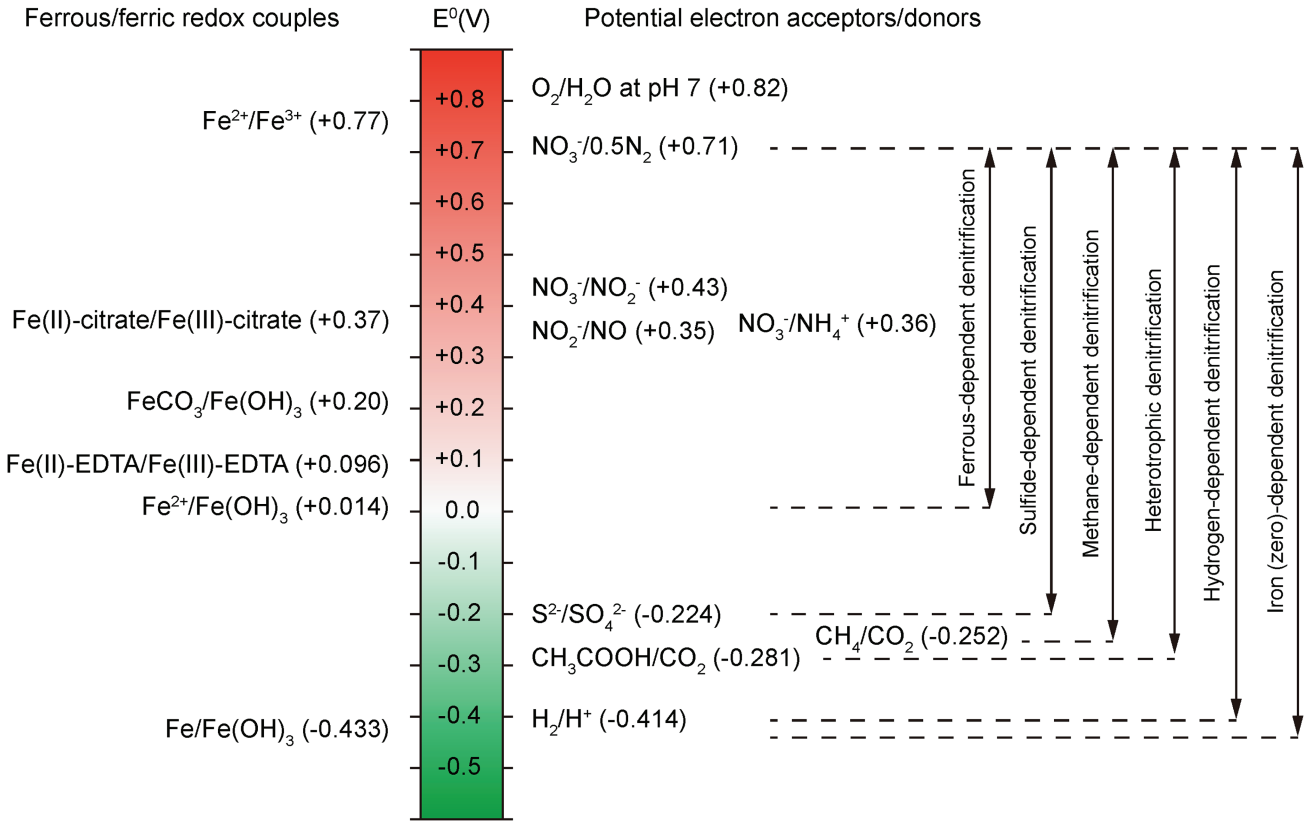

FIGURE 4 | Redox potential of Fe and N species couples in NDAFO; the double-headed arrows refer to the ΔORP between different denitrification processes (Hedrich et al., 2011).

Fe(III), which exists in the form of free ions or iron complexes under aerobic conditions. When the pH is over 4, aqueous Fe(II) is easily transformed to structural Fe(III) that precipitates as poorly crystalline iron minerals (Johnson et al., 2012). For example, at low pH, reduced nontronite containing structural Fe(II) can be oxidized to aqueous Fe(III), but the high pH is not favorable for this electron transfer process due to the precipitation of aqueous Fe(III; Guo et al., 2020). Thus, pH has a significant impact on the form and availability of iron.

Furthermore, microbial iron-associated metabolism also has significant implications for controlling the environmental pH of the microbial habit. For example, pH is the critical control parameter for maintaining sustainable fermentation, but pH could constantly decrease as organic substrates (e.g., glucose or pyruvate) are consumed. Fermentative iron reducers, such as *Orenia metallireducens* strain Z6, enhanced the degradation of fermentable substrates in the presence of hematite and effectively generated alkalinity that balances acid production, providing favorable buffering conditions for microbial fermentation (Dong et al., 2017). Similarly, ZVI can consume protons in the solution, thus increasing the pH in the reaction system (Eq. 7). In summary, the presence of iron minerals can affect environmental pH indirectly or directly.

Oxidation–Reduction Potential

ORP is another crucial parameter that affects the removal of nitrogen in an anaerobic BNR system. As shown in **Figure 4**, at neutral pH, the ORP of $Fe(II)/Fe(OH)_3$ is +0.014 V, which is lower than that for any denitrifying nitrogen intermediate couple of $NO_3^-/0.5N_2$ (+0.71 V), NO_3^-/NO_2^- (+0.43 V) and NO_3^-/NO (+0.35 V). Different NO_3^- reduction products are associated with different ORPs, resulting in different bioenergies obtained by IOM. In addition, microbes get different energy from different types of denitrification processes due to the ORP difference (ΔORP). Note that the ΔORP of ferrous-dependent denitrification is smaller than that of sulfide-, methane-, heterotrophic- and hydrogen-dependent denitrification, which means NDAFO microorganisms may derive less energy from a sole Fe(II) oxidation process. It is reported that a few IOM strains were found to survive under autotrophic conditions just using Fe(II) as electron donor, and most NDAFO microorganisms are mixotrophic to simultaneously obtain energy from organic matter (Liu et al., 2019a). Furthermore, ZVI-dependent denitrification has a larger ΔORP than the other denitrification pathways, providing an efficient potential for NO_3^- reduction.

Some anaerobic microbes can create low-redox-potential conditions for growth and preservation by reducing a range

of oxidized compounds into products with a rather low reduction potential. *Methanosarcina barkeri* utilizes hydrogen gas (H_2) as an electron donor and ferredoxin ($E^{0'} = -500$ mV) and coenzyme F_{420} ($E^{0'} = -360$ mV) as electron carriers to reduce Fe(III) to Fe(II), such as FeOOH(am) → Fe(II), $E^{0'} = -50$ mV, or ZVI, such as Fe(III) + $3e^-$ → Fe(0), $E^{0'} = -37$ mV (Shang et al., 2020). Additionally, the increase in Fe(II) concentration can remarkably decrease the redox potential and favor denitrification by microorganisms. A high TN removal efficiency was observed with external addition of 50 mg/l Fe(II) in a horizontal subsurface flow CW (Zhang et al., 2019d). Thus, the relatively low ORP environment created by the microorganism itself or artificial measures contributes to the Feammox or NDAFO process.

Fe Species

Fe mineralogical properties such as crystallinity have an important role in IOM and IRM bioavailability, affecting the rate and extent of Fe reduction and oxidation. The metabolic rate is generally inversely proportional to mineral crystallinity. For example, Fe(II) in clay minerals contains structural sites, Fe(II)-complexed surface hydroxyl group (edge) sites and basal/interlayer sites, and only structural and edge Fe(II) sites are highly reactive toward NO_3^- reduction (Zhang et al., 2019b). Low-crystallinity Fe(III; hydr)oxides, such as ferrihydrite, for microbial Fe(III) reduction were found earlier than crystalline Fe(III) minerals, such as goethite, lepidocrocite and magnetite. In microbial Fe(III) reduction, although the mineral type is the same, goethite with more defects could produce more reduced atoms (ferrous iron ions) than goethite with fewer defects (Notini et al., 2019).

Moreover, microbial metabolism and environmental conditions can also bring about the evolution of Fe species. Mejia et al. (2016) compared the transformation of lepidocrocite and ferrihydrite with soil microbial communities at the interface of anaerobic/anoxic environments during redox cycling, and magnetite was observed as the same main product of both mineral reductions. Additionally, subsequent Fe(II) oxidation by O_2 promoted the production of ferrihydrite and lepidocrocite, which are accessible to IRM for redox cycling but formed nonstoichiometric and low-bioavailability magnetite during the NO_3^- reduction periods.

Fe(II)

In the Fe(II)-driven denitrification system, biogenic Fe(III; hydr) oxides largely depend on different inoculated denitrifiers. A *Thiobacillus*-dominated mixed culture converted poorly crystalline ferrihydrite to crystalline akaganeite, while *T. denitrificans* and *Pseudogulbenkiania* strain 2002 preferentially produced maghemite and hematite (Kiskira et al., 2019). This in-depth understanding of microbial factors is critical to predicting the fate and recovery of Fe species in natural or engineered conditions.

Fe(III)

Ferrihydrite is a thermodynamically metastable iron (hydr) oxide that can be gradually transformed to crystalline goethite and hematite. (Bi)carbonate levels that are elevated (pCO_2, ~2%) compared to atmospheric CO_2 levels (~0.04%), a critical geochemical parameter in sediments, could increase the occurrence of hematite through olation, ligand exchange, and rearrangement (Li et al., 2020b). Under suboxic conditions, aqueous Fe(II) can catalyze ferrihydrite transformation to more stable lepidocrocite (Lp) and goethite (Gt), and citrate greatly affects the ratio of Lp to Gt (Sheng et al., 2020a).

Extracellular Electron Transfer

The primary sources of Fe(III)/Fe(II) oxides that microorganisms can access are highly insoluble in natural environments. Thus, the dissolution of solid iron phases becomes a key process affecting the bioavailability of iron minerals. Through extracellular respiration, bacteria directly contact or link with iron oxides through specific physiological nanowires to transfer electrons, generally at a low rate that is highly dependent on the species. Indirect electron transfer between microbes and ore can be achieved with ligands, ESs and other microbial Fe acquisition strategies (**Figure 5**).

Fe(II)

Ligand and ESs have been reported to facilitate electron transfer between Fe(II) and IOM, enhancing microbial Fe(II) oxidation in wastewater treatment. *c*-Cyts is a key protein involved in IOM extracellular electron transfer. Organic ligands were detected with a rapid stopped-flow spectrometer and found to significantly accelerate the reaction between *c*-Cyts and Fe(II), with a reaction rate order of EDTA > citric acid > ammonia triacetate > malonic acid > glycine amino acid > control (Wang et al., 2019b). In addition, Fe(II) can be oxidized by ESs, e.g., oxidized riboflavin, flavin mononucleotide (FMN) and quinone, providing bioreinforcement strategies for the reduction of redox-sensitive nitrogen species (Zhang et al., 2020c). Thus, ESs are demonstrated a feasible and efficient strategy to promote NDAFO process.

Fe(III)

The addition of iron ligands, such as nitrilotriacetic acid (NTA), ethylenediaminetetraacetic acid (EDTA), *N*-methyliminodiacetic acid (MIDA) and polyphosphate significantly accelerated Fe(III) reduction coupled to ammonium oxidation. Synergetic effects of submicromolar Fe(II) addition and ligands catalyzed the dissolution of lepidocrocite due to interfacial electron transfer of Fe(III)/Fe(II) and detachment of Fe ligands (Biswakarma et al., 2020). The extent of Feammox and the reduction of ferrihydrite were enhanced when amended with the ES AQDS (Zhou et al., 2016). Biochar facilitated long-term microbial reduction of hematite at a two fold higher rate than that in the control since the semiquinone groups on biochar likely participated in the redox reactions (Xu et al., 2016). Hence, ES-mediated Feammox could lead to greater N loss and a promoted reaction rate in wastewater.

Natural Organic Matter

ZVI/Fe(II)

NOM is abundant in aquatic environments and has a critical impact on FeBNR. In a ZVI-oxidizing supported autotrophic

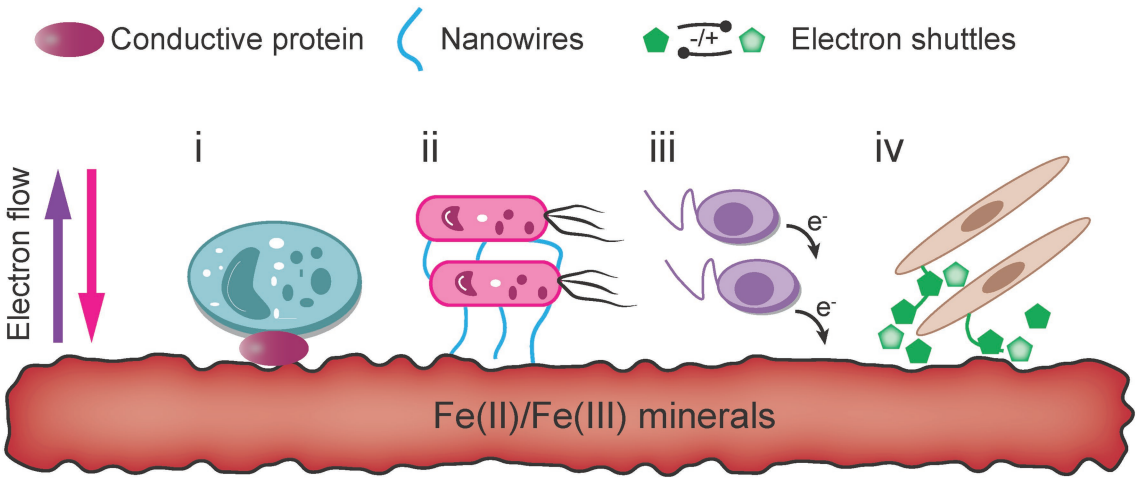

FIGURE 5 | Mechanisms of extracellular electron transfer for iron-metabolizing extracellular respiratory bacteria (Li et al., 2021a).

denitrification process based on iron-carbon microelectrolysis and iron scraps (ME-ISs-AD), an optimum dosage of 1.0 mg-COD/mg-TN can significantly increase the denitrification load from 0.19 to 0.44 kg-N/(m^3·d) and reduce the accumulation of N_2O/NO_2^-. The study demonstrated that organic carbon simulated the bioconversion of iron compounds and enhanced ZVI passivation, increasing the production of H_2 and Fe(II) and promoting autotrophic denitrification (Deng et al., 2020). NOM has positive and negative influences on the NDAFO process. On the one hand, NOM can behave as an electron donor to enrich mixotrophic IOM and increase bacterial activity. On the other hand, Fe(II)-NOM complexes cannot enter the periplasm to participate in electron transport chains. Aqueous Fe(II) may react enzymatically or abiotically with NO_2^- in the periplasm or at the surface of cells. The inhibition of denitrification by Fe(II)-OM was observed due to the large size and negative charge of such complexes (Peng et al., 2018).

Fe(III)

Under anaerobic conditions with ferric ions as the sole electron acceptor, NOM can compete with NH_4^+ as the electron donor for Feammox. Therefore, NH_4^+ is preferentially utilized in the absence of organic carbon. In wild environments, such as saline-alkaline paddy soils, NH_4^+ is generally uncorrelated or negatively related to NOM under Fe(III)-dominant reducing conditions (Liu et al., 2021). However, recent studies showed that NOM was favorable for Feammox because (1) organic carbon can promote the release of structural Fe in clay minerals, supporting the release of amorphous Fe and promoting the bioavailability of Fe minerals (Glodowska et al., 2020); (2) some organic carbon, such as a humic substances, can act as electron donors and ESs to link insoluble Fe(III) and IRM (Stern et al., 2018); and (3) the degradation of organic carbon can release protons, which leads to a decrease in pH and directly provides H^+ to the Feammox process. Although organic carbon is not required for Feammox metabolism, it does play a key role in mediating and enhancing Feammox rates.

PROCESSES AND APPLICATIONS

Natural Water Systems and Wetlands

Groundwater

Nitrogen pollution in groundwater is a pervasive and increasing global issue mainly due to the intense application of nitrogen fertilizers, affecting human health if exposure is long-term. Nitrate is usually reduced to N_2 by denitrifying bacteria and removed from drinking water, but this process consumes extensive amounts of organic carbon and possibly causes secondary pollution. Techniques utilizing Fe minerals provide alternative cost-effective solutions to remediate nitrogen-polluted groundwater.

ZVI/Fe(II)

The nanosized Fe(II)-containing mineral magnetite was proven to reduce NO_3^- to N_2 in a batch environment with groundwater and sediments derived from wells located in Barcelona, Spain, to simulate aquifer conditions (Jiang et al., 2019). A similar study reported that magnetite nanoparticles could complete NO_3^- reduction to NO_2^- coupled to biological Fe(II) oxidation, and dissolved Fe(II) mainly contributed to abiotic NO_2^- reduction (Margalef-Marti et al., 2020). Li et al. (2015) adopted a single anaerobic nitrate-reducing Fe(II)-oxidizing *Citrobacter freundii* strain PXL1 for the simultaneous removal of arsenic and NO_3^- from groundwater. As an economical and available material, ZVI is widely used in remediating NO_3^--contaminated groundwater, but iron passivation has always been a complex problem to be solved effectively. More long-term methods to prevent passion or keep the activity of ZVI are the subject of future research.

Fe(III)

Fe(III; hydr)oxides, functional IRM and ESs could be injected into groundwater aquifers to remove NH_4^+ by constructing injection wells, permeable reactive barriers (PRBs) or Kariz

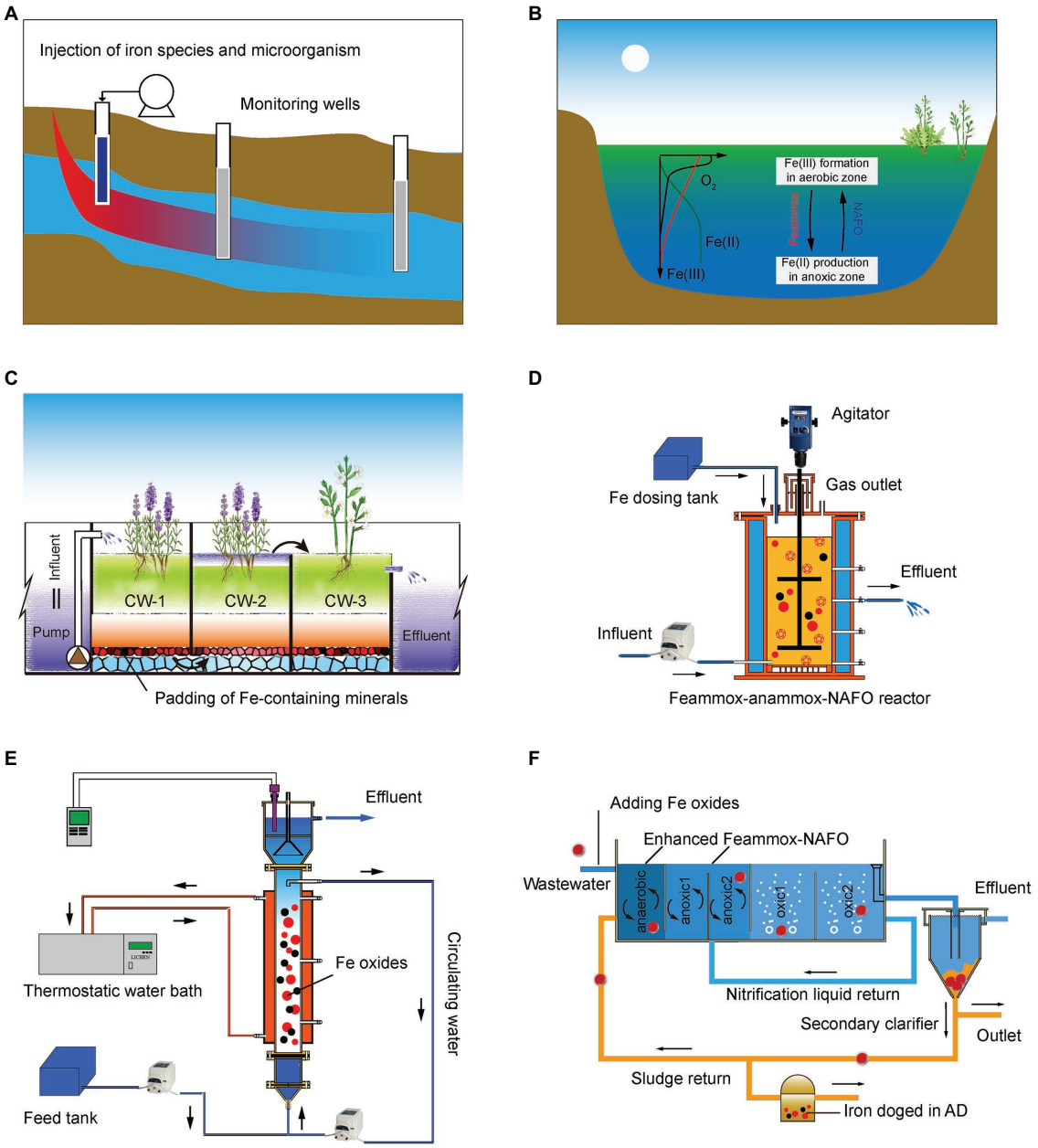

FIGURE 6 | Application scenarios for FeBNR in wastewater treatment processes for groundwater **(A)**; lake and river water **(B)**; CWs **(C)**; sequencing biological reactor **(D)**; continuous-flow reactor **(E)** and mainstream waste water treatment plants (WWTPs) process (**F**; Zhao et al., 2016).

systems (also known as canals), as shown in **Figure 6** (Jiang et al., 2019). Spearman analysis between the geochemical parameters and microbial community in the western Hetao Basin of China indicated a widespread occurrence of Feammox in groundwater systems (Xiu et al., 2020).

Surface Water Ecosystems

ZVI/Fe(II)

Nitrogen biotransformation regulated by FeBNR has been observed in ecosystem habitats, rivers and natural wetlands. Urbanization has increased the nitrogen pollution in sediments of urban river networks, and Pearson correlation analysis showed that Fe(II) had a significant influence on the NO_3^- reduction process, contributing to TN loss in an investigated river network in Shanghai, China (Zhang et al., 2019d). In the freshwater lake Almind (Silkeborg, Denmark), the addition of Fe(II) simulated nitrate reduction to N_2 (Robertson and Thamdrup, 2017). The occurrences of NDAFO provide a potential nitrogen mitigation pathway to purify surface water.

Fe(III)

Agricultural fertilizer is a great producer and emitter of nitrogen into surrounding water bodies, and Feammox in agricultural drainage ditches was reported to mitigate nitrogen pollution in the Jiuli River, Taihu Lake Basin (Chen et al., 2020b). A further field investigation in these watersheds in China indicated that the potential Feammox rates varied from 2.4 to 22.5 kg-N/(ha·yr) both seasonally and spatially within the investigated farmland, riparian land and sediment (Ding et al., 2020b). An ^{15}N-labeled isotopic tracing technique indicated that a loss of 12.33 t-N/y was associated with Feammox, accounting for 6.4–6.7% of TN loss through N_2, in the Jiulong River estuary, China (Guan et al., 2018). Thus, more reports demonstrated that Feammox is a vital biochemical nitrogen cycle in aquatic ecosystems.

Constructed Wetlands

A CW could be designed and built on an *in situ* polluted site to control nitrogen transformation, decrease transportation fees, and avoid excessive interference with the local environment. However, nitrogen removal is always limited by the absence of electron donors in CWs. Autotrophic denitrification, especially with iron supplements, has become a practical alternative method to enhance nitrogen removal. The complicated interactions between environmental parameters, substrates, and microorganisms significantly affect nitrogen transformation in iron-based CWs and have been the focus of many studies.

ZVI/Fe(II)

Regarding iron as an electron donor, iron-containing materials, such as iron scraps, iron ore and steel slag, can be chosen as supporting substrates for autotrophic denitrification. The coupling in ferric-carbon microelectrolysis enhanced the TN removal efficiency to 90.5% from 31.4% in ordinary subsurface-flow CWs (Shen et al., 2019). The production of H_2/[H] on the cathode and Fe(II) from ZVI on the anode facilitated the enrichment of facultative autotrophic denitrifiers, leading to further NO_3^- reduction. For example, with nZVI as a cosubstrate, modified agricultural wastes as solid carbon sources (SCSs) further enhanced the NO_3^- removal efficiency (75.3–91.9%) compared with that in SCSs-CW alone (63.3–65.5%; Zhao et al., 2019). In addition, microelectrolysis transforms macromolecular organic matter into micromolecular organic matter, which is a suitable biodegraded carbon source for biological denitrification. Various Fe(II)-containing minerals, such as siderite, pyrite, pyrrhotite, and biotite, have been added to CWs to enhance denitrification.

Fe(III)

Fe(III)-containing materials, such as ferrihydrite, goethite and lepidocrocite, have been applied to anaerobic ammonium oxidation. Feammox was enhanced in a CW by incubating with functional *Acidimicrobiaceae* sp. A6 and increasing the content of ferrihydrite (Shuai and Jaffé, 2019). Yang et al. (2021b) developed an integrated CW-microbial fuel cell system (CW-MFCs) with pyrrhotite as one of the supported substances, and Feammox and pyrrhotite-based autotrophic denitrification co-occurred, increasing the NH_4^+ removal efficiency by 87%. The addition of iron minerals can improve the contribution of autotrophic nitrogen removal in CW, and further research should focus on new composites and operating conditions for applications.

Artificial Water Treatment System

Sequencing Batch Reactor

ZVI/Fe(II)

The SBR is characterized by simplicity, low cost and flexibility of operation, which are good advantages for cultivating slow-growing bacteria enriched in a reactor. In an SBR treating digested effluent, the addition of ZVI provided electrons for denitrification, and the produced Fe(II) was favorable for Anammox enrichment (Wang et al., 2018). A nZVI–supported denitrifying bacteria, *Alcaligenes eutrophus*, was cultivated in a cylindrical culture tank, and the results of this study demonstrated that ferrous iron [Fe(II)(ad)] adsorbed on ferric oxides is likely an effective electron donor for NO_3^- removal (Xu et al., 2018).

Fe(III)

Feng et al. (2020) chose SBR to enrich both marine Anammox bacteria (MAB) and autotrophic Feammox bacteria to treat nitrogen-laden saline wastewater with Fe(III) addition, achieving a maximal substrate conversion rate of 2.97–3.47 kg/(m^3·d). Even under low-temperature and high-salinity conditions, Fe(III) addition still greatly improved the NH_4^+ removal rate and had no adverse effect on MAB activity (Li et al., 2020a). Simultaneous nitrification and denitrification coupled with Fe redox cycling were achieved in SBR, treating domestic sewage and integrating the internal recycling of nanostructured Fe oxyhydroxides (FeOOH). The NH_4^+ removal reached 73.1 ± 17.4 mg/l/d when associated with biogenic Fe(III) reduction (Desireddy et al., 2020). According to the stoichiometric amount of Fe(III) in the Feammox process, it is required to continuously or intermittently supply Fe(III) to maintain a continuous nitrogen removal but obviously uneconomical in practical application. The intermittent addition of NO_3^- or aeration might be an appropriate strategy to oxidize Fe(II) to produce secondary Fe(III) for the next round of Feammox.

Continuous-Flow Reactor

ZVI

ZVI-supported autotrophic denitrification has been developed for decades due to the well-documented characteristics of ZVI-based materials. Various continuous-flow processes are conducted for nitrate-contaminated wastewater treatment, including iron-(activated carbon) microelectrolysis-based carrier (IA-MEC) reactors and anoxic fluidized-bed membrane bioreactors (AnFB-MBRs; Peng et al., 2020). Generally, the

products of nitrate reduction by ZVI are NH_4^+ as the main product and little NO_2^- (the intermediate product) and N_2; then, the corresponding ZVI is converted to ferrous or ferric oxides. On the basis of these traits Khalil et al. (2018) designed a laboratory-scale continuous-flow system (LSCFS) using reactor-settler-polisher techniques. The reagents nZVI, bimetallic nZVI-Cu and $CuCl_2$-added nZVI were dosed into the reactor to transform NO_3^- with a nitrogen removal efficiency above 90%. A coupling of Anammox and ZVI/Fe(II) reduction was achieved in a continuous-flow expanded granular sludge blanket (EGSB) to enhance autotrophic nitrogen removal, in which iron-dependent dissimilatory nitrate reduction to nitrite or ammonia positively supported the Anammox process (Bi et al., 2019).

Fe(II)

Fe(II)-driven autotrophic denitrification has been achieved in upflow packed bed reactors (PBRs) and ferrous iron-based chemoautotrophic denitrification (Fe-CAD) reactors (Wang et al., 2017; Kiskira et al., 2020). NO has low solubility in aqueous solution and is generally harder to degrade with conventional biological techniques, but Fe(II)-EDTA exhibits strong complexation and high adsorption on it. Hence, Zhang et al. (2019a) developed an autotrophic upflow bioreactor with a sponge iron bed to combine NO adsorption and Anammox process for greater nitrogen removal, and the NDAFO rate was also increased. The autotrophic sulfur-based denitrification process has been widely adopted for NO_3^- removal to avoid the external addition of organic carbon. However, the produced acid is unfavorable to microbial growth and necessitates continual adjustment of the pH by limestone, NaOH solution, etc. Zhu et al. (2019) proposed a sulfur coupled with iron(II) carbonate-driven autotrophic denitrification (SICAD) system, in which siderite ($FeCO_3$) was leached from the ore and promoted the NDAFO process. Similar NO_3^- and phosphate removal rates were achieved in a sulfur-siderite autotrophic denitrification (SSAD) system showing the feasibility of the pilot experiments using columns and pilot biofilters (SSAD-PB; Wang et al., 2019a).

Fe(III)

In 2015, Huang and Jaffé (2015) operated a continuous-flow membrane Feammox reactor with added ferrihydrite and NH_4^+. After 180 days of incubation, uncultured *Acidimicrobiaceae* bacterium A6 was enriched in this reactor. Despite the fact that Feammox has recently received considerable attention, large-scale applications for mainstream WWTPs have rarely been reported. Feammox technology can be combined with other BNR processes (Zhu et al., 2021). For example, in a conventional A^2/O process, even though nitrification must occur in an aerobic tank, external NH_4^+ can be oxidized in an anaerobic or anoxic tank to increase the NH_4^+ removal efficiency. The products of NO_2^- can be coupled with Anammox in an anoxic environment to increase the contribution of autotrophic BNR. Feammox can be similarly applied in a sidestream AD system with a higher NH_4^+ load.

PERSPECTIVES ON FeBNR

In the past 30 years, nitrogen control and remediation methods for eutrophic lakes have mainly included chemical methods (addition of $CuSO_4$ or herbicides to control algae blooms), physical methods (dilution and flushing, deep aeration, sediment dredging) and biological methods (microbial remediation, aquatic phytoremediation). FeBNR provide alternative or enhanced methods to integrate with the above techniques. For example, (1) covering sediments with of iron minerals *in situ* could hinder the release of NH_4^+ from contaminated bottom sediments and absorb and biodegrade the NH_4^+ *via* Feammox process in these sediments; (2) a combination of aquatic ecological floating beds and FeBNR on the mat not only mitigates the seasonal impact on and the treatment efficiency due to plant growth period but also notably improves the water purification; (3) in field remediation, since the landform and water depth determine the species and fates of nitrogen in lakes (Qin et al., 2020), the selected Fe(II) or Fe(III)-containing substrates and their addition amount should be based on the corresponding conditions; (4) if the iron mineral source is rich in some local or nearby sites, water transfer projects might be investigated and designed to utilize these Fe minerals to reduce N pollution. For Fe-poor conditions, iron supplementation with an *in situ* covering technique could be considered for further N removal in shallow or deep lakes. Fe and N cycles are tightly coupled as important biogeochemical processes, enabling multiple remediation techniques for nitrogen control in aquatic and terrestrial systems. Although the integration of Feammox and NDAFO is an emerging method to reduce TN, further studies should focus on the following:

(1) The accurate stoichiometry between the Fe and N loads. In treating wastewater with high concentrations of NH_4^+ using Feammox, the produced Fe(II) is generally inadequately oxidized to Fe(III) due to the absence of oxidizers, i.e., NO_3^- or NO_2^-, hindering the next round of Feammox. Thus, the moderate N loads and proportion should match the well-balanced Fe(III)/Fe(II);
(2) The identification and bioavailability of secondary biogenic minerals. Fe speciation and properties have significant influences on the rate and extent of ore bioavailability, and the optimal selectivity of Fe species could be favourable to enrich iron oxidizers or reducers, and operational parameters affecting Fe species transformation should be optimized to benefit the nitrogen removal efficiency;
(3) The distinction of nitrogen transformation pathways. The complex substances in actual wastewater determine the diversity of nitrogen loss pathways, and heterotrophic denitrification, Anammox, Feammox and NDAFO might coexist in the same environment. Quantitatively differentiating the contributions of each pathway could help to determine proper control strategies;
(4) FeBNR provides an effective method for eliminating nitrogen contaminants, and the rate limitation of FeBNR could

be relieved by ESs. Biochar, as ES, is easy to prepare and widely used in practical projects. Hence, optimizing the key parameters of biochar production and catalysis for the FeBNR process deserves further study. The redox properties of biochar could be improved by adjusting the hydrothermal temperature or surface modifications, etc.

CONCLUSION

Autotrophic FeBNR, coupling NDAFO with the Feammox process, has excellent potential to mitigate total nitrogen pollution with low C/N wastewater. This paper systematically summarized the recent advances in FeBNR technologies, especially mechanisms, microorganisms, and environmental factors that affect its reactive rate in natural habitats and engineered systems. The nitrogen conversion rate is generally low due to multiple environmental factors, and ESs provides an emerging strategy to facilitate the iron cycle by accelerating extracellular electron transfer. Furthermore, nitrogen transformation pathways between abiotic and biotic reactions should be accurately distinguished, and the effects of secondary minerals on the FeBNR process might be investigated in future studies. The novel FeBNR process is conducive to reducing organic carbon sources and energy consumption for future sustainable wastewater treatment.

AUTHOR CONTRIBUTIONS

SP: project administration, funding acquisition, writing—review and editing, and supervision. NL: conceptualization, writing—original draft, and investigation. HL: validation and writing—review and editing. XL: writing—original draft and visualization preparation. TS: visualization preparation and data curation. YY: validation and data curation. JJ: investigation, resources, and data curation. All authors contributed to the article and approved the submitted version.

FUNDING

This work was supported by the National Natural Science Foundation of China (42077160, 52000039, and 52100004) and Jilin Province Natural Science Funds (20200201041JC).

ACKNOWLEDGMENTS

We express our deep gratitude to Hanping Pan, Jie Cao, and Yingbin Hu from the School of Ecology, Environment and Resources, Guangdong University of Technology for their constructive comments on this article.

REFERENCES

Anirban, C., and Flynn, P. (2013). Induction of nitrate-dependent Fe(II) oxidation by Fe(II) in Dechloromonas sp. strain UWNR4 and Acidovorax sp. strain 2AN. *Appl. Environ. Microbiol.* 79, 748–752. doi: 10.1128/AEM.02709-12

Benaiges-Fernandez, R., Palau, J., Offeddu, F. G., Cama, J., Urmeneta, J., Soler, J. M., et al. (2019). Dissimilatory bioreduction of iron(III) oxides by Shewanella loihica under marine sediment conditions. *Mar. Environ. Res.* 151:104782. doi: 10.1016/j.marenvres.2019.104782

Bi, Z., Zhang, W., Song, G., and Huang, Y. (2019). Iron-dependent nitrate reduction by anammox consortia in continuous-flow reactors: A novel prospective scheme for autotrophic nitrogen removal. *Sci. Total Environ.* 692, 582–588. doi: 10.1016/j.scitotenv.2019.07.078

Biswakarma, J., Kang, K., Schenkeveld, W. D. C., Kraemer, S. M., Hering, J. G., and Hug, S. J. (2020). Linking isotope exchange with Fe(II)-catalyzed dissolution of iron(hydr)oxides in the presence of the bacterial Siderophore Desferrioxamine-B. *Environ. Sci. Technol.* 54, 768–777. doi: 10.1021/acs.est.9b04235

Brons, H. J., Hagen, W. R., and Zehnder, A. J. B. (1991). Micrnbiology in nitrate reducing cultures of Escherichia coli. *Arch. Microbiol.* 155, 341–347. doi: 10.1007/BF00243453

Chao, T.-T., and Kroontje, W. (1966). Inorganic nitrogen transformations through the oxidation and reduction of iron. *Soil Sci. Soc. Am. J.* 30, 193–196. doi: 10.2136/sssaj1966.03615995003000020016x

Chen, G., Chen, D., Li, F., Liu, T., Zhao, Z., and Cao, F. (2020a). Dual nitrogen-oxygen isotopic analysis and kinetic model for enzymatic nitrate reduction coupled with Fe(II) oxidation by Pseudogulbenkiania sp. strain 2002. *Chem. Geol.* 534:119456. doi: 10.1016/j.chemgeo.2019.119456

Chen, S., Ding, B., Qin, Y., Chen, Z., and Li, Z. (2020b). Nitrogen loss through anaerobic ammonium oxidation mediated by Mn(IV)-oxide reduction from agricultural drainage ditches into Jiuli River Taihu Lake Basin. *Sci. Total Environ.* 700:134512. doi: 10.1016/j.scitotenv.2019.134512

Clément, J.-C., Shrestha, J., Ehrenfeld, J. G., and Jaffé, P. R. (2005). Ammonium oxidation coupled to dissimilatory reduction of iron under anaerobic conditions in wetland soils. *Soil Biol. Biochem.* 37, 2323–2328. doi: 10.1016/j.soilbio.2005.03.027

Deng, S., Peng, S., Xie, B., Yang, X., Sun, S., Yao, H., et al. (2020). Influence characteristics and mechanism of organic carbon on denitrification, N_2O emission and NO_2^- accumulation in the iron [Fe(0)]-oxidizing supported autotrophic denitrification process. *Chem. Eng. J.* 393:124736. doi: 10.1016/j.cej.2020.124736

Desireddy, S., Sabumon, P. C., and Maliyekkal, S. (2020). Anoxic ammonia removal using granulated nanostructured Fe oxyhydroxides and the effect of pH, temperature and potential inhibitors on the process. *J. Water Process Eng.* 33:101066. doi: 10.1016/j.jwpe.2019.101066

Dhakal, P., Coyne, M. S., McNear, D. H., Wendroth, O. O., Vandiviere, M. M., D'Angelo, E. M., et al. (2021). Reactions of nitrite with goethite and surface Fe(II)-goethite complexes. *Sci. Total Environ.* 782:146406. doi: 10.1016/j.scitotenv.2021.146406

Di Capua, F., Pirozzi, F., Lens, P. N. L., and Esposito, G. (2019). Electron donors for autotrophic denitrification. *Chem. Eng. J.* 362, 922–937. doi: 10.1016/j.cej.2019.01.069

Diao, Z. H., Qian, W., Lei, Z. X., Kong, L. J., Du, J. J., Liu, H., et al. (2019). Insights on the nitrate reduction and norfloxacin oxidation over a novel nanoscale zero valent iron particle: reactivity, products, and mechanism. *Sci. Total Environ.* 660, 541–549. doi: 10.1016/j.scitotenv.2019.01.037

Ding, B., Chen, Z., Li, Z., Qin, Y., and Chen, S. (2019). Nitrogen loss through anaerobic ammonium oxidation coupled to iron reduction from ecosystem habitats in the Taihu estuary region. *Sci. Total Environ.* 662, 600–606. doi: 10.1016/j.scitotenv.2019.01.231

Ding, B., Li, Z., and Qin, Y. (2017). Nitrogen loss from anaerobic ammonium oxidation coupled to iron(III) reduction in a riparian zone. *Environ. Pollut.* 231, 379–386. doi: 10.1016/j.envpol.2017.08.027

Ding, B., Luo, W., Qin, Y., and Li, Z. (2020a). Effects of the addition of nitrogen and phosphorus on anaerobic ammonium oxidation coupled with iron reduction (Feammox) in the farmland soils. *Sci. Total Environ.* 737:139849. doi: 10.1016/j.scitotenv.2020.139849

Ding, B., Qin, Y., Luo, W., and Li, Z. (2020b). Spatial and seasonal distributions of Feammox from ecosystem habitats in the Wanshan region of the Taihu watershed China. *Chemosphere* 239:4742. doi: 10.1016/j.chemosphere.2019.124742

Dong, Y., Sanford, R. A., Chang, Y. J., McInerney, M. J., and Fouke, B. W. (2017). Hematite reduction buffers acid generation and enhances nutrient

uptake by a fermentative iron reducing bacterium, Orenia metallireducens strain Z6. *Environ. Sci. Technol.* 51, 232–242. doi: 10.1021/acs.est.6b04126

Etique, M., Jorand, F. P. A., Zegeye, A., Grégoire, B., Despas, C., and Ruby, C. (2014). Abiotic process for Fe(II) oxidation and green rust mineralization driven by a heterotrophic nitrate reducing bacteria (Klebsiella mobilis). *Environ. Sci. Technol.* 48, 3742–3751. doi: 10.1021/es403358v

Feng, L., Li, J., Ma, H., and Chen, G. (2020). Effect of Fe(II) on simultaneous marine anammox and Feammox treating nitrogen-laden saline wastewater under low temperature: enhanced performance and kinetics. *Desalination* 478:114287. doi: 10.1016/j.desal.2019.114287

Glodowska, M., Stopelli, E., Schneider, M., Lightfoot, A., Rathi, B., Straub, D., et al. (2020). Role of in situ natural organic matter in mobilizing as during microbial reduction of FeIII-mineral-bearing aquifer sediments from Hanoi (Vietnam). *Environ. Sci. Technol.* 54, 4149–4159. doi: 10.1021/acs.est.9b07183

Guan, Q. S., Cao, W. Z., Wang, M., Wu, G. J., Wang, F. F., Jiang, C., et al. (2018). Nitrogen loss through anaerobic ammonium oxidation coupled with iron reduction in a mangrove wetland. *Eur. J. Soil Sci.* 69, 732–741. doi: 10.1111/ejss.12552

Guo, J., Zhang, X., Hu, Q., and Gao, X. (2020). Applied clay science roles of aqueous Fe (III) in oxidation of partially reduced nontronite under sub-acidic conditions. *Appl. Clay Sci.* 195:105689. doi: 10.1016/j.clay.2020.105689

Hafenbradl, D., Keller, M., Dirmeier, R., Rachel, R., Roßnagel, P., Burggraf, S., et al. (1996). Ferroglobus placidus gen. Nov., sp. nov., a novel hyperthermophilic archaeum that oxidizes Fe^{2+} at neutral pH under anoxic conditions. *Arch. Microbiol.* 166, 308–314. doi: 10.1007/s002030050388

Hansen, H. C. B., Koch, C. B., Nancke-Krogh, H., Borggaard, O. K., and Sørensen, J. (1996). Abiotic nitrate reduction to ammonium: key role of green rust. *Environ. Sci. Technol.* 30, 2053–2056. doi: 10.1021/es950844w

He, Z., Long, X., Li, L., Yu, G., Chong, Y., Xing, W., et al. (2017). Temperature response of sulfide/ferrous oxidation and microbial community in anoxic sediments treated with calcium nitrate addition. *J. Environ. Manag.* 191, 209–218. doi: 10.1016/j.jenvman.2017.01.008

Hedrich, S., Schlömann, M., and Johnson, D. B. (2011). The iron-oxidizing proteobacteria. *Microbiology* 157, 1551–1564. doi: 10.1099/mic.0.045344-0

Hikino, A., Sugahara, S., Kato, T., Senga, Y., Egawa, M., Park, J. Y., et al. (2021). Sensitive gas chromatography detection of nanomolar hydroxylamine in environmental water by Fe(III) oxidation. *Anal. Sci.* 37, 347–351. doi: 10.2116/analsci.20P254

Huang, S., and Jaffé, P. R. (2015). Characterization of incubation experiments and development of an enrichment culture capable of ammonium oxidation under iron-reducing conditions. *Biogeosciences* 12, 769–779. doi: 10.5194/bg-12-769-2015

Jeong, J.-Y., Kim, H.-K., Kim, J.-H., and Park, J.-Y. (2012). Electrochemical removal of nitrate using ZVI packed bed bipolar electrolytic cell. *Chemosphere* 89, 172–178. doi: 10.1016/j.chemosphere.2012.05.104

Jiang, Y., Xi, B., Li, R., Li, M., Xu, Z., Yang, Y., et al. (2019). Advances in Fe(III) bioreduction and its application prospect for groundwater remediation: A review. *Front. Environ. Sci. Eng.* 13:173. doi: 10.1007/s11783-019-1173-9

Jiang, C., Xu, X., Megharaj, M., Naidu, R., and Chen, Z. (2015). Inhibition or promotion of biodegradation of nitrate by Paracoccus sp. in the presence of nanoscale zero-valent iron. *Sci. Total Environ.* 530-531, 241–246. doi: 10.1016/j.scitotenv.2015.05.044

Johnson, D. B., Kanao, T., and Hedrich, S. (2012). Redox transformations of iron at extremely low pH: fundamental and applied aspects. *Front. Microbiol.* 3:96. doi: 10.3389/fmicb.2012.00096

Jones, L. C., Peters, B., Lezama Pacheco, J. S., Casciotti, K. L., and Fendorf, S. (2015). Stable isotopes and iron oxide mineral products as markers of chemodenitrification. *Environ. Sci. Technol.* 49, 3444–3452. doi: 10.1021/es504862x

Khalil, A. M. E., Eljamal, O., Saha, B. B., and Matsunaga, N. (2018). Performance of nanoscale zero-valent iron in nitrate reduction from water using a laboratory-scale continuous-flow system. *Chemosphere* 197, 502–512. doi: 10.1016/j.chemosphere.2018.01.084

Kim, I., and Cha, D. K. (2021). Effect of low temperature on abiotic and biotic nitrate reduction by zero-valent iron. *Sci. Total Environ.* 754:142410. doi: 10.1016/j.scitotenv.2020.142410

Kiskira, K., Papirio, S., Mascolo, M. C., Fourdrin, C., Pechaud, Y., van Hullebusch, E. D., et al. (2019). Mineral characterization of the biogenic Fe(III)(hydr)oxides produced during Fe(II)-driven denitrification with cu. *Ni and Zn. Sci. Total Environ.* 687, 401–412. doi: 10.1016/j.scitotenv.2019.06.107

Kiskira, K., Papirio, S., Pechaud, Y., Matassa, S., van Hullebusch, E. D., and Esposito, G. (2020). Evaluation of Fe(II)-driven autotrophic denitrification in packed-bed reactors at different nitrate loading rates. *Process. Saf. Environ. Prot.* 142, 317–324. doi: 10.1016/j.psep.2020.05.049

Kiskira, K., Papirio, S., van Hullebusch, E. D., and Esposito, G. (2017). Fe(II)-mediated autotrophic denitrification: A new bioprocess for iron bioprecipitation/biorecovery and simultaneous treatment of nitrate-containing wastewaters. *Int. Biodeterior. Biodegrad.* 119, 631–648. doi: 10.1016/j.ibiod.2016.09.020

Kumaraswamy, R., Sjollema, K., Kuenen, G., van Loosdrecht, M., and Muyzer, G. (2006). Nitrate-dependent $[Fe(II)EDTA]^{2-}$ oxidation by Paracoccus ferrooxidans sp. nov., isolated from a denitrifying bioreactor. *Syst. Appl. Microbiol.* 29, 276–286. doi: 10.1016/j.syapm.2005.08.001

Li, J., Feng, L., Biswal, B. K., Chen, G., and Wu, D. (2020a). Bioaugmentation of marine anammox bacteria (MAB)-based anaerobic ammonia oxidation by adding Fe(III) in saline wastewater treatment under low temperature. *Bioresour. Technol.* 295:122292. doi: 10.1016/j.biortech.2019.122292

Li, N., Jiang, J., Xu, Y., Pan, H., Luo, X., Hu, Y., et al. (2021a). Insoluble carbonaceous materials as electron shuttles enhance the anaerobic/anoxic bioremediation of redox pollutants: recent advances. *Chinese Chem. Lett.* 33, 71–79. doi: 10.1016/j.cclet.2021.06.064

Li, S., Li, X., and Li, F. (2018a). Fe(II) oxidation and nitrate reduction by a denitrifying bacterium, pseudomonas stutzeri LS-2, isolated from paddy soil. *J. Soils Sediments* 18, 1668–1678. doi: 10.1007/s11368-017-1883-1

Li, B. H., and Pan, X. L. (2019). Effect of temperature on clostridium sp. strain pxl2 and removal of arsenic and nitrate from groundwater. *Appl. Ecol. Environ. Res.* 17, 6201–6211. doi: 10.15666/aeer/1703_62016211

Li, B., Pan, X., Zhang, D., Lee, D.-J., Al-Misned, F. A., and Mortuza, M. G. (2015). Anaerobic nitrate reduction with oxidation of Fe(II) by Citrobacter Freundii strain PXL1 – a potential candidate for simultaneous removal of As and nitrate from groundwater. *Ecol. Eng.* 77, 196–201. doi: 10.1016/j.ecoleng.2015.01.027

Li, H., Su, J. Q., Yang, X. R., Zhou, G. W., Lassen, S. B., and Zhu, Y. G. (2019). RNA stable isotope probing of potential Feammox population in paddy soil. *Environ. Sci. Technol.* 53, 4841–4849. doi: 10.1021/acs.est.8b05016

Li, Y., Yang, M., Pentrak, M., He, H., and Arai, Y. (2020b). Carbonate-enhanced transformation of ferrihydrite to hematite. *Environ. Sci. Technol.* 54, 13701–13708. doi: 10.1021/acs.est.0c04043

Li, X., Yuan, Y., and Huang, Y. (2021b). Enhancing the nitrogen removal efficiency of a new autotrophic biological nitrogen-removal process based on the iron cycle: feasibility, progress, and existing problems. *J. Clean. Prod.* 317, 128499–128498. doi: 10.1016/j.jclepro.2021.128499

Li, X., Yuan, Y., Huang, Y., Liu, H., Bi, Z., Yuan, Y., et al. (2018b). A novel method of simultaneous NH4+ and NO3− removal using Fe cycling as a catalyst: Feammox coupled with NAFO. *Sci. Total Environ.* 631-632, 153–157. doi: 10.1016/j.scitotenv.2018.03.018

Liu, T., Chen, D., Li, X., and Li, F. (2019a). Microbially mediated coupling of nitrate reduction and Fe(II) oxidation under anoxic conditions. *FEMS Microbiol. Ecol.* 95:30. doi: 10.1093/femsec/fiz030

Liu, T., Chen, D., Luo, X., Li, X., and Li, F. (2019b). Microbially mediated nitrate-reducing Fe(II) oxidation: quantification of chemodenitrification and biological reactions. *Geochim. Cosmochim. Acta* 256, 97–115. doi: 10.1016/j.gca.2018.06.040

Liu, X., Shi, L., and Gu, J.-D. (2018). Microbial electrocatalysis: redox mediators responsible for extracellular electron transfer. *Biotechnol. Adv.* 36, 1815–1827. doi: 10.1016/j.biotechadv.2018.07.001

Liu, Y., and Wang, J. (2019). Reduction of nitrate by zero valent iron (ZVI)-based materials: A review. *Sci. Total Environ.* 671, 388–403. doi: 10.1016/j.scitotenv.2019.03.317

Liu, D., Zhang, S., Fei, C., and Ding, X. (2021). Impacts of straw returning and N application on NH_4^+ reducible Fe(III) and bacterial community composition in saline-alkaline paddy soils. *Appl. Soil Ecol.* 168:104115. doi: 10.1016/j.apsoil.2021.104115

Lovley, D. R. (1997). Microbial Fe(III) reduction in subsurface environments. *FEMS Microbiol. Rev.* 20, 305–313. doi: 10.1016/S0168-6445(97)00013-2

Lovley, D. R., Giovannoni, S. J., White, D. C., Champine, J. E., Phillips, E. J. P., Gorby, Y. A., et al. (1993). Geobacter metallireducens gen. Nov. sp. nov., a microorganism capable of coupling the complete oxidation of organic

compounds to the reduction of iron and other metals. *Arch. Microbiol.* 159, 336–344. doi: 10.1007/BF00290916

Ma, Y., Dai, W., Zheng, P., Zheng, X., He, S., and Zhao, M. (2020). Iron scraps enhance simultaneous nitrogen and phosphorus removal in subsurface flow constructed wetlands. *J. Hazard. Mater.* 395:122612. doi: 10.1016/j.jhazmat.2020.122612

Ma, Y., Zheng, X., He, S., and Zhao, M. (2021). Nitrification, denitrification and anammox process coupled to iron redox in wetlands for domestic wastewater treatment. *J. Clean. Prod.* 300:126953. doi: 10.1016/j.jclepro.2021.126953

Mai, Y., Liang, Y., Cheng, M., He, Z., and Yu, G. (2021). Coupling oxidation of acid volatile sulfide, ferrous iron, and ammonia nitrogen from black-odorous sediment via autotrophic denitrification-anammox by nitrate addition. *Sci. Total Environ.* 790:147972. doi: 10.1016/j.scitotenv.2021.147972

Margalef-Marti, R., Carrey, R., Benito, J. A., Marti, V., Soler, A., and Otero, N. (2020). Nitrate and nitrite reduction by ferrous iron minerals in polluted groundwater: isotopic characterization of batch experiments. *Chem. Geol.* 548:119691. doi: 10.1016/j.chemgeo.2020.119691

Mejia, J., Roden, E. E., and Ginder-Vogel, M. (2016). Influence of oxygen and nitrate on Fe (hydr)oxide mineral transformation and soil microbial communities during redox cycling. *Environ. Sci. Technol.* 50, 3580–3588. doi: 10.1021/acs.est.5b05519

Meng, F., Li, M., Wang, H., Xin, L., Wu, X., and Liu, X. (2020). Encapsulating microscale zero valent iron-activated carbon into porous calcium alginate for the improvement on the nitrate removal rate and Fe^0 utilization factor. *Microporous Mesoporous Mater.* 307:110522. doi: 10.1016/j.micromeso.2020.110522

Notini, L., Byrne, J. M., Tomaszewski, E. J., Latta, D. E., Zhou, Z., Scherer, M. M., et al. (2019). Mineral defects enhance bioavailability of goethite toward microbial Fe(III) reduction. *Environ. Sci. Technol.* 53, 8883–8891. doi: 10.1021/acs.est.9b03208

Park, S., Lee, J.-H., Shin, T. J., Hur, H.-G., and Kim, M. G. (2018). Adsorption and incorporation of arsenic to biogenic Lepidocrocite formed in the presence of ferrous iron during denitrification by Paracoccus denitrificans. *Environ. Sci. Technol.* 52, 9983–9991. doi: 10.1021/acs.est.8b02101

Peng, S., Kong, Q., Deng, S., Xie, B., Yang, X., Li, D., et al. (2020). Application potential of simultaneous nitrification/Fe^0-supported autotrophic denitrification (SNAD) based on iron-scraps and micro-electrolysis. *Sci. Total Environ.* 711:135087. doi: 10.1016/j.scitotenv.2019.135087

Peng, C., Sundman, A., Bryce, C., Catrouillet, C., Borch, T., and Kappler, A. (2018). Oxidation of Fe(II)-organic matter complexes in the presence of the mixotrophic nitrate-reducing Fe(II)-oxidizing bacterium Acidovorax sp. BoFeN1. *Environ. Sci. Technol.* 52, 5753–5763. doi: 10.1021/acs.est.8b00953

Pikaar, I., Sharma, K. R., Hu, S., Gernjak, W., Keller, J., and Yuan, Z. (2014). Reducing sewer corrosion through integrated urban water management. *Science* 345, 812–814. doi: 10.1126/science.1251418

Qin, Y., Ding, B., Li, Z., and Chen, S. (2019). Variation of Feammox following ammonium fertilizer migration in a wheat-rice rotation area, Taihu Lake China. *Environ. Pollut.* 252, 119–127. doi: 10.1016/j.envpol.2019.05.055

Qin, B., Zhou, J., Elser, J. J., Gardner, W. S., Deng, J., and Brookes, J. D. (2020). Water depth underpins the relative roles and fates of nitrogen and phosphorus in lakes. *Environ. Sci. Technol.* 54, 3191–3198. doi: 10.1021/acs.est.9b05858

Robertson, E. K., and Thamdrup, B. (2017). The fate of nitrogen is linked to iron(II) availability in a freshwater lake sediment. *Geochim. Cosmochim. Acta* 205, 84–99. doi: 10.1016/j.gca.2017.02.014

Sawayama, S. (2006). Possibility of anoxic ferric ammonium oxidation. *J. Biosci. Bioeng.* 101, 70–72. doi: 10.1263/jbb.101.70

Shang, H., Daye, M., Sivan, O., Borlina, C. S., Tamura, N., Weiss, B. P., et al. (2020). Formation of zerovalent iron in iron-reducing cultures of Methanosarcina barkeri. *Environ. Sci. Technol.* 54, 7354–7365. doi: 10.1021/acs.est.0c01595

Shen, Y., Zhuang, L., Zhang, J., Fan, J., Yang, T., and Sun, S. (2019). A study of ferric-carbon micro-electrolysis process to enhance nitrogen and phosphorus removal efficiency in subsurface flow constructed wetlands. *Chem. Eng. J.* 359, 706–712. doi: 10.1016/j.cej.2018.11.152

Sheng, L., Lei, Z., Dzakpasu, M., Li, Y.-Y., Li, Q., and Chen, R. (2020b). Application of the anammox-based process for nitrogen removal from anaerobic digestion effluent: A review of treatment performance, biochemical reactions, and impact factors. *J. Water Process Eng.* 38:101595. doi: 10.1016/j.jwpe.2020.101595

Sheng, A., Li, X., Arai, Y., Ding, Y., Rosso, K. M., and Liu, J. (2020a). Citrate controls Fe(II)-catalyzed transformation of ferrihydrite by complexation of the labile Fe(III) intermediate. *Environ. Sci. Technol.* 54, 7309–7319. doi: 10.1021/acs.est.0c00996

Shi, L., Dong, H., Reguera, G., Beyenal, H., Lu, A., Liu, J., et al. (2016). Extracellular electron transfer mechanisms between microorganisms and minerals. *Nat. Rev. Microbiol.* 14, 651–662. doi: 10.1038/nrmicro.2016.93

Shuai, W., and Jaffé, P. R. (2019). Anaerobic ammonium oxidation coupled to iron reduction in constructed wetland mesocosms. *Sci. Total Environ.* 648, 984–992. doi: 10.1016/j.scitotenv.2018.08.189

Sorokina, A. Y., Chernousova, E. Y., and Dubinina, G. A. (2012). Hoeflea siderophila sp. nov., a new neutrophilic iron-oxidizing bacterium. *Microbiology* 81, 59–66. doi: 10.1134/S0026261712010146

Stern, N., Mejia, J., He, S., Yang, Y., Ginder-Vogel, M., and Roden, E. E. (2018). Dual role of humic substances as electron donor and shuttle for dissimilatory iron reduction. *Environ. Sci. Technol.* 52, 5691–5699. doi: 10.1021/acs.est.7b06574

Straub, K. L., Benz, M., Schink, B., and Widdel, F. (1996). Anaerobic, nitrate-dependent microbial oxidation of ferrous iron. *Appl. Environ. Microbiol.* 62, 1458–1460. doi: 10.1128/aem.62.4.1458-1460.1996

Su, Z., Zhang, Y., Jia, X., Xiang, X., and Zhou, J. (2020). Research on enhancement of zero-valent iron on dissimilatory nitrate/nitrite reduction to ammonium of Desulfovibrio sp. *CMX. Sci. Total Environ.* 746:141126. doi: 10.1016/j.scitotenv.2020.141126

Tan, X., Xie, G.-J., Nie, W.-B., Xing, D.-F., Liu, B.-F., Ding, J., et al. (2021). Fe(III)-mediated anaerobic ammonium oxidation: A novel microbial nitrogen cycle pathway and potential applications. *Crit. Rev. Environ. Sci. Technol.* 1–33, 1–33. doi: 10.1080/10643389.2021.1903788

Tian, T., and Yu, H.-Q. (2020). Denitrification with non-organic electron donor for treating low C/N ratio wastewaters. *Bioresour. Technol.* 299:122686. doi: 10.1016/j.biortech.2019.122686

Tian, T., Zhou, K., Xuan, L., Zhang, J. X., Li, Y. S., Liu, D. F., et al. (2020). Exclusive microbially driven autotrophic iron-dependent denitrification in a reactor inoculated with activated sludge. *Water Res.* 170:115300. doi: 10.1016/j.watres.2019.115300

Wang, C., Huang, Y., Zhang, C., Zhang, Y., Yuan, K., Xue, W., et al. (2021). Inhibition effects of long-term calcium-magnesia phosphate fertilizer application on cd uptake in rice: regulation of the iron-nitrogen coupling cycle driven by the soil microbial community. *J. Hazard. Mater.* 416:125916. doi: 10.1016/j.jhazmat.2021.125916

Wang, W., Wei, D., Li, F., Zhang, Y., and Li, R. (2019a). Sulfur-siderite autotrophic denitrification system for simultaneous nitrate and phosphate removal: From feasibility to pilot experiments. *Water Res.* 160, 52–59. doi: 10.1016/j.watres.2019.05.054

Wang, R., Yang, C., Zhang, M., Xu, S. Y., Dai, C. L., Liang, L. Y., et al. (2017). Chemoautotrophic denitrification based on ferrous iron oxidation: reactor performance and sludge characteristics. *Chem. Eng. J.* 313, 693–701. doi: 10.1016/j.cej.2016.12.052

Wang, Y., Yuan, X., Li, X., Li, F., and Liu, T. (2019b). Ligand mediated reduction of c-type cytochromes by Fe(II): kinetic and mechanistic insights. *Chem. Geol.* 513, 23–31. doi: 10.1016/j.chemgeo.2019.03.006

Wang, S., Zheng, D., Wang, S., Wang, L., Lei, Y., Xu, Z., et al. (2018). Remedying acidification and deterioration of aerobic post-treatment of digested effluent by using zero-valent iron. *Bioresour. Technol.* 247, 477–485. doi: 10.1016/j.biortech.2017.09.078

Xiu, W., Lloyd, J., Guo, H., Dai, W., Nixon, S., Bassil, N. M., et al. (2020). Linking microbial community composition to hydrogeochemistry in the western Hetao Basin: potential importance of ammonium as an electron donor during arsenic mobilization. *Environ. Int.* 136:105489. doi: 10.1016/j.envint.2020.105489

Xu, S., Adhikari, D., Huang, R., Zhang, H., Tang, Y., Roden, E., et al. (2016). Biochar-facilitated microbial reduction of hematite. *Environ. Sci. Technol.* 50, 2389–2395. doi: 10.1021/acs.est.5b05517

Xu, L., Ali, A., Su, J., Huang, T., Wang, Z., and Yang, Y. (2021). Denitrification potential of sodium alginate gel beads immobilized iron–carbon, Zoogloea

sp. L2, and riboflavin: performance optimization and mechanism. *Bioresour. Technol.* 336:125326. doi: 10.1016/j.biortech.2021.125326

Xu, C., Wang, X., An, Y., Yue, J., and Zhang, R. (2018). Potential electron donor for nanoiron supported hydrogenotrophic denitrification: H_2 gas, Fe^0, ferrous oxides, Fe^{2+}(aq), or Fe^{2+}(ad)? *Chemosphere* 202, 644–650. doi: 10.1016/j.chemosphere.2018.03.148

Yang, Y., Jin, Z., Quan, X., and Zhang, Y. (2018). Transformation of nitrogen and iron species during nitrogen removal from wastewater via Feammox by adding ferrihydrite. *ACS Sustain. Chem. Eng.* 6, 14394–14402. doi: 10.1021/acssuschemeng.8b03083

Yang, Y., Peng, H., Niu, J., Zhao, Z., and Zhang, Y. (2019). Promoting nitrogen removal during Fe(III) reduction coupled to anaerobic ammonium oxidation (Feammox) by adding anthraquinone-2,6-disulfonate (AQDS). *Environ. Pollut.* 247, 973–979. doi: 10.1016/j.envpol.2019.02.008

Yang, Y., Xiao, C., Lu, J., and Zhang, Y. (2020). Fe(III)/Fe(II) forwarding a new anammox-like process to remove high-concentration ammonium using nitrate as terminal electron acceptor. *Water Res.* 172:115528. doi: 10.1016/j.watres.2020.115528

Yang, Y., Xiao, C., Yu, Q., Zhao, Z., and Zhang, Y. (2021a). Using Fe(II)/Fe(III) as catalyst to drive a novel anammox process with no need of anammox bacteria. *Water Res.* 189:116626. doi: 10.1016/j.watres.2020.116626

Yang, Y., Zhao, Y., Tang, C., Mao, Y., Chen, T., and Hu, Y. (2021b). Novel pyrrhotite and alum sludge as substrates in a two-tiered constructed wetland-microbial fuel cell. *J. Clean. Prod.* 293:126087. doi: 10.1016/j.jclepro.2021.126087

Yao, Z., Wang, C., Song, N., Wang, C., and Jiang, H. (2020). Oxidation of ammonium in aerobic wastewater by anoxic ferric iron-dependent ammonium oxidation (Feammox) in a biofilm reactor. *Desalin. Water Treat.* 173, 197–206. doi: 10.5004/dwt.2020.24822

Yi, B., Wang, H., Zhang, Q., Jin, H., Abbas, T., Li, Y., et al. (2019). Alteration of gaseous nitrogen losses via anaerobic ammonium oxidation coupled with ferric reduction from paddy soils in southern China. *Sci. Total Environ.* 652, 1139–1147. doi: 10.1016/j.scitotenv.2018.10.195

Zhang, L., Dong, H., Kukkadapu, R. K., Jin, Q., and Kovarik, L. (2019b). Electron transfer between sorbed Fe(II) and structural Fe(III) in smectites and its effect on nitrate-dependent iron oxidation by Pseudogulbenkiania sp. strain 2002. *Geochim. Cosmochim. Acta* 265, 132–147. doi: 10.1016/j.gca.2019.08.042

Zhang, Y., Douglas, G. B., Kaksonen, A. H., Cui, L., and Ye, Z. (2019c). Microbial reduction of nitrate in the presence of zero-valent iron. *Sci. Total Environ.* 646, 1195–1203. doi: 10.1016/j.scitotenv.2018.07.112

Zhang, X., Li, A., Szewzyk, U., and Ma, F. (2016b). Improvement of biological nitrogen removal with nitrate-dependent Fe(II) oxidation bacterium Aquabacterium parvum B6 in an up-flow bioreactor for wastewater treatment. *Bioresour. Technol.* 219, 624–631. doi: 10.1016/j.biortech.2016.08.041

Zhang, Y., Liu, X., Fu, C., Li, X., Yan, B., and Shi, T. (2019d). Effect of Fe^{2+} addition on chemical oxygen demand and nitrogen removal in horizontal subsurface flow constructed wetlands. *Chemosphere* 220, 259–265. doi: 10.1016/j.chemosphere.2018.12.144

Zhang, J., Qu, Y., Qi, Q., Zhang, P., Zhang, Y., Tong, Y. W., et al. (2020b). The bio-chemical cycle of iron and the function induced by ZVI addition in anaerobic digestion: A review. *Water Res.* 186:116405. doi: 10.1016/j.watres.2020.116405

Zhang, J., Ren, L., Zhang, D., Li, J., Peng, S., Han, X., et al. (2019a). Reduction of NO to N_2 in an autotrophic up-flow bioreactor with sponge iron bed based Fe(II)EDTA complexation. *Fuel* 254:115631. doi: 10.1016/j.fuel.2019.115631

Zhang, P., Van Cappellen, P., Pi, K., and Yuan, S. (2020c). Oxidation of Fe(II) by flavins under anoxic conditions. *Environ. Sci. Technol.* 54, 11622–11630. doi: 10.1021/acs.est.0c02916

Zhang, C., Xu, X., Yuan, L., Mao, Z., and Li, W. (2020a). Performance enhancement by adding ferrous to a combined modified University of Cape Town and post-anoxic/aerobic-membrane bioreactor. *Chemosphere* 243:125300. doi: 10.1016/j.chemosphere.2019.125300

Zhang, M., Zheng, P., Zeng, Z., Wang, R., Shan, X., He, Z., et al. (2016a). Physicochemical characteristics and microbial community of cultivated sludge for nitrate-dependent anaerobic ferrous-oxidizing (NAFO) process. *Sep. Purif. Technol.* 169, 296–303. doi: 10.1016/j.seppur.2016.05.048

Zhao, L., Dong, H., Kukkadapu, R. K., Zeng, Q., Edelmann, R. E., Pentrák, M., et al. (2015). Biological redox cycling of iron in nontronite and its potential application in nitrate removal. *Environ. Sci. Technol.* 49, 5493–5501. doi: 10.1021/acs.est.5b00131

Zhao, X., Liu, W., Cai, Z., Han, B., Qian, T., and Zhao, D. (2016). An overview of preparation and applications of stabilized zero-valent iron nanoparticles for soil and groundwater remediation. *Water Res.* 100, 245–266. doi: 10.1016/j.watres.2016.05.019

Zhao, Y., Song, X., Cao, X., Wang, Y., Zhao, Z., Si, Z., et al. (2019). Modified solid carbon sources with nitrate adsorption capability combined with nZVI improve the denitrification performance of constructed wetlands. *Bioresour. Technol.* 294:122189. doi: 10.1016/j.biortech.2019.122189

Zhou, G. W., Yang, X. R., Li, H., Marshall, C. W., Zheng, B. X., Yan, Y., et al. (2016). Electron shuttles enhance anaerobic ammonium oxidation coupled to iron(III) reduction. *Environ. Sci. Technol.* 50, 9298–9307. doi: 10.1021/acs.est.6b02077

Zhu, T. T., Cheng, H. Y., Yang, L. H., Su, S. G., Wang, H. C., Wang, S. S., et al. (2019). Coupled sulfur and iron(II) carbonate-driven autotrophic denitrification for significantly enhanced nitrate removal. *Environ. Sci. Technol.* 53, 1545–1554. doi: 10.1021/acs.est.8b06865

Zhu, J., Li, T., Liao, C., Li, N., and Wang, X. (2021). A promising destiny for Feammox: From biogeochemical ammonium oxidation to wastewater treatment. *Sci. Total Environ.* 790:148038. doi: 10.1016/j.scitotenv.2021.148038

Conflict of Interest: The authors declare that the research was conducted in the absence of any commercial or financial relationships that could be construed as a potential conflict of interest.

frontiers | Frontiers in Microbiology

ORIGINAL RESEARCH
published: 20 May 2022
doi: 10.3389/fmicb.2022.882890

Pseudomonas oligotrophica sp. nov., a Novel Denitrifying Bacterium Possessing Nitrogen Removal Capability Under Low Carbon–Nitrogen Ratio Condition

Mingxia Zhang[1,2], *Anzhang Li*[2,3], *Qing Yao*[4], *Botao Xiao*[1*] and *Honghui Zhu*[2*]

[1] Guangdong Provincial Key Laboratory of Fermentation and Enzyme Engineering, School Biology and Biological Engineering, South China University of Technology, Guangzhou, China, [2] Guangdong Provincial Key Laboratory of Microbial Culture Collection and Application, Key Laboratory of Agricultural Microbiomics and Precision Application, Ministry of Agriculture and Rural Affairs, State Key Laboratory of Applied Microbiology Southern China, Guangdong Microbial Culture Collection Center, Institute of Microbiology, Guangdong Academy of Sciences, Guangzhou, China, [3] Guangdong BOWOTE BioSciTech, Co., Ltd., Zhaoqing, China, [4] Guangdong Province Key Laboratory of Microbial Signals and Disease Control, College of Horticulture, South China Agricultural University, Guangzhou, China

OPEN ACCESS

Edited by:
Chongjun Chen,
Suzhou University of Science and Technology, China

Reviewed by:
Shihai Deng,
Xi'an Jiaotong University, China
Xiaomei Su,
Zhejiang Normal University, China

***Correspondence:**
Honghui Zhu
zhuhh_gdim@163.com
Botao Xiao
xiaob@scut.edu.cn

Specialty section:
This article was submitted to Microbiotechnology, a section of the journal Frontiers in Microbiology

Received: 24 February 2022
Accepted: 25 April 2022
Published: 20 May 2022

Citation:
Zhang M, Li A, Yao Q, Xiao B and Zhu H (2022) Pseudomonas oligotrophica sp. nov., a Novel Denitrifying Bacterium Possessing Nitrogen Removal Capability Under Low Carbon–Nitrogen Ratio Condition. Front. Microbiol. 13:882890. doi: 10.3389/fmicb.2022.882890

Pseudomonas is a large and diverse genus within the *Gammaproteobacteria* known for its important ecological role in the environment. These bacteria exhibit versatile features of which the ability of heterotrophic nitrification and aerobic denitrification can be applied for nitrogen removal from the wastewater. A novel denitrifying bacterium, designated JM10B5a^T, was isolated from the pond water for juvenile *Litopenaeus vannamei*. The phylogenetic, genomic, physiological, and biochemical analyses illustrated that strain JM10B5a^T represented a novel species of the genus *Pseudomonas*, for which the name *Pseudomonas oligotrophica* sp. nov. was proposed. The effects of carbon sources and C/N ratios on denitrification performance of strain JM10B5a^T were investigated. In addition, the results revealed that sodium acetate was selected as the optimum carbon source for denitrification of this strain. Besides, strain JM10B5a^T could exhibit complete nitrate removal at the low C/N ratio of 3. Genomic analyses revealed that JM10B5a^T possessed the functional genes including *napA*, *narG*, *nirS*, *norB,* and *nosZ*, which might participate in the complete denitrification process. Comparative genomic analyses indicated that many genes related to aggregation, utilization of alkylphosphonate and tricarballylate, biosynthesis of cofactors, and vitamins were contained in the genome of strain JM10B5a^T. These genomic features were indicative of its adaption to various niches. Moreover, strain JM10B5a^T harbored the complete operons required for the biosynthesis of vibrioferrin, a siderophore, which might be conducive to the high denitrification efficiency of denitrifying bacterium at low C/N ratio. Our findings demonstrated that the strain JM10B5a^T could be a promising candidate for treating wastewater with a low C/N ratio.

Keywords: *Pseudomonas*, 16S rRNA gene, phylogenetic analysis, genomic analysis, denitrifying bacteria, low carbon–nitrogen ratio

INTRODUCTION

Pseudomonas is widely distributed in various natural environments including water, soil, sediment, plants, animals, and clinical samples, and this genus contains a large number of species (Zou et al., 2019; Li et al., 2020; Mamtimin et al., 2021). The genus *Pseudomonas* was first proposed with the description of *P. aeruginosa* JCM 5962^T by Migula (1894) and belongs to the family *Pseudomonadaceae* within the class *Gammaproteobacteria*. Recently, Lalucat et al. (2021) proposed the division of *Pseudomonas* into five new genera: "*Halopseudomonas,*" "*Linyingimonas,*" "*Stutzerimonas,*" "*Alcaligenimonas,*" and "*Ubiquimonas*" based on the phylogenetic and phylogenomic analyses, and the genus *Halopseudomonas* published by Rudra and Gupta (2021) has been validated. *Pseudomonas* strains displayed some potential roles, such as the high biodegradation capability of polycyclic aromatic hydrocarbons, sulfide oxidation, phosphate accumulation, and denitrification (Xie et al., 2016, 2021; Sun et al., 2019; Zhang R. C. et al., 2020). For example, a denitrifying phosphorus-accumulating bacterium *P. stutzeri* ADP-19 could remove 96.9% of nitrate and 73.3% of phosphorus under aerobic conditions (Li et al., 2021); a heterotrophic nitrifying–aerobic denitrifying bacterium *P. bauzanensis* DN13-1 could remove 98.8, 98.9, and 65.9% of nitrite (NO_2^--N), nitrate (NO_3^--N), and ammonium (NH_4^+-N), respectively (Zhang M. et al., 2020). Although the 16S rRNA gene is the basic tool for current bacterial classification, it cannot be used availably to differentiate closely related species of *Pseudomonas* (Wang et al., 2020). Thus, the taxonomy of *Pseudomonas* strains has evolved with the available methodologies. Up-to-date Bacterial Core Gene set (UBCG, 92 bacterial core gene sets commonly present in all bacterial genomes which are shown on the website of EZBioCloud[1]) together with a phylogenomic pipeline could provide the accurate phylogenomic trees for the taxonomic purpose (Na et al., 2018).

Nitrogen pollution mainly comes from the excessive use of fertilizers, poultry production, domestic sewage, industrial manufacture, and aquaculture wastewater (Rezvani et al., 2019). Excess nitrite and nitrate accumulation can cause eutrophication and pose threat to aquatic animals and human health. For instance, excess nitrate could cause the regressive, circulatory, and inflammatory damages in the post-larvae and juvenile of *Macrobrachium amazonicum* (Dutra et al., 2020). Among the nitrate-contaminated wastewaters, the low organic carbon-to-nitrogen (C/N) ratio wastewater is a common type such as the polluted groundwater, industrial wastewater, rural sewage, and effluent from wastewater treatment plants (Deng et al., 2016; Hong et al., 2019; Gao et al., 2020).

Biological denitrification is an effective and general method for reducing nitrate to nitrogen gas due to its high efficiency, low cost, and environmental friendliness (Pang and Wang, 2021). Heterotrophic denitrification, which utilizes the organic carbon sources as electron donors, has a higher denitrification rate compared with autotrophic denitrification (Yang et al., 2020). However, the deficiency of available carbon source is an intractable problem for heterotrophic denitrification in the treatment of wastewater with low C/N ratio. To ensure sufficient electron donors for the denitrification process, the conventional solution is to add external organic carbon (often methanol, ethanol, glucose, and acetic acid) into the wastewater with low C/N ratio (Wang et al., 2018). Nevertheless, the addition of external organic carbon may result in the risk of secondary contamination and a high cost (Ling et al., 2021). Therefore, effective and sustainable strategies to enhance heterotrophic denitrification in the treatment of wastewater with a low C/N ratio are needed.

Accumulating approaches have been developed for the nitrate removal from the low C/N ratio wastewater, such as the system coupled with iron-based chemical reduction and autotrophic denitrification (Liu et al., 2020), the heterotrophic denitrification system amended with redox-active biochar (Wu et al., 2019), the fungal pellets immobilized bacterial bioreactor (Zheng et al., 2021), and the utilization of biodegradable and inert carriers in the sequencing batch reactors (Huang et al., 2020). These approaches are focused on generating more electron donors to enhance nitrate removal capability or providing carriers for microorganisms to create a suitable environment. In addition, some heterotrophic denitrifying bacteria that can achieve efficient denitrification at low C/N ratio have been reported, such as *Acinetobacter* sp., *Comamonas* sp., and *Pseudomonas* sp. (Zhang S. et al., 2020; Chen et al., 2021; Fan et al., 2021). Compared with the abovementioned approaches, these denitrifying bacteria can not only effectively and readily remove nitrate from low C/N ratio wastewater without the utilization of complex engineering but also provide the functional microorganisms possessing excellent nitrate removal ability for the wastewater treatment systems. Among the denitrifying bacteria, *Pseudomonas* is the dominant bacterial genus in activated sludge and biofilm reactors (Deng et al., 2018; Zhang et al., 2019). Moreover, several *Pseudomonas* strains possess the denitrification ability and other functions, such as phosphorus removal ability and polyhydroxybutyrate-degrading ability (Di et al., 2019; Li et al., 2021). Therefore, *Pseudomonas* strains would outcompete other bacteria in the practical application.

In this study, a novel denitrifying bacterium, designated JM10B5a^T, was isolated from the pond water for juvenile *Litopenaeus vannamei*. The phylogenetic, genomic, physiological, and biochemical analyses illustrated that strain JM10B5a^T represented a novel species of the genus *Pseudomonas*, for which the name *Pseudomonas oligotrophica* sp. nov. was proposed. This strain performed excellent capability for denitrification under the low C/N ratio condition. Genomic information revealed that the functional genes of *napA*, *narG*, *nirS*, *norB,* and *nosZ*

Abbreviations: ANI, average nucleotide identity; CCUG, Culture Collection University of Gothenburg; CDS, protein-coding sequences; CGMCC, China General Microbiological Culture Collection Center; dDDH, digital DNA–DNA hybridization; DPG, diphosphatidylglycerol; DSM, denitrification screening medium; GDMCC, Guangdong Microbial Culture Collection Center; JCM, Japan Collection of Microorganisms; ML, maximum likelihood; NA, nutrient broth agar medium; NB, nutrient broth medium; OGRIs, overall genome relatedness indices; PE, phosphatidylethanolamine; PG, phosphatidylglycerol; RAST, Rapid Annotation using Subsystem Technology; TLC, thin-layer chromatography; UBCG, up-to-date bacterial core gene.

[1]https://help.ezbiocloud.net/ubcg-gene-set/

encoding the enzymatic repertoire for completely denitrification were identified in strain JM10B5a^T. Our findings demonstrated that strain JM10B5a^T could be a promising candidate for treating wastewater with a low C/N ratio.

MATERIALS AND METHODS

Bacterial Strains

Strain JM10B5a^T was isolated from pond water for juvenile *Litopenaeus vannamei* collected from Jiangmen city, Guangdong Province, P. R. China (N 21° 56' 31"; E 112° 46' 16"). To isolate the aerobic denitrifying bacteria, the denitrification screening medium (DSM) was utilized. DSM was formulated as follows (per liter): sodium succinate 0.25 g, sodium citrate dihydrate 0.25 g, Na_2HPO_4 1.0 g, KH_2PO_4 1.0 g, $NaNO_2$ 0.069 g, KNO_3 0.1 g, $(NH_4)_2SO_4$ 0.066 g, $MgSO_4{\cdot}7H_2O$ 0.2 g, 2.0 ml of trace element solution (TES) and 1.0 ml of mixed carbon source solution (CSS), pH 7.3, and the solid plate contained the DSM supplemented with 15.0 g/L agar. $MgSO_4{\cdot}7H_2O$, TES, and CSS were all added to the autoclaved DSM after filtering using 0.22-μm filter membrane. The TES contained (per liter) EDTA-Na 10.0 g, $ZnSO_4{\cdot}7H_2O$ 0.5 g, $MnCl_2{\cdot}4H_2O$ 0.4 g, $CoCl_2{\cdot}2H_2O$ 0.5 g, $CuSO_4{\cdot}5H_2O$ 0.2 g, $CaCl_2$ 5.5 g, $FeSO_4{\cdot}7H_2O$ 1.1 g, and $NaMoO_4{\cdot}2H_2O$ 0.4 g. The CSS was described in the previous work (Zhang M. et al., 2020) and contained (per liter) D-glucose 13.8 g, D-fructose 13.8 g, D-lactose 13.8 g, sodium acetate 19.0 g, 90% lactic acid 12.8 ml, mannitol 14.0 g, ethyl alcohol 14.0 ml, glycerin 12.6 ml, sodium benzoate 9.6 g, and salicylic acid 9.2 g. Serial dilutions of 10^{-1} to 10^{-4} of pond water were made, and 0.1 ml of the 10^{-2}, 10^{-3}, and 10^{-4} dilutions was spread on DSM agar plates, respectively. Then, these plates were incubated at 30°C for 5 days. Strain JM10B5a^T was isolated and stored at −80°C in the nutrient broth medium (NB) supplemented with 20% (v/v) glycerol.

P. stutzeri CGMCC 1.1803^T and *P. balearica* CCUG 44487^T were obtained from China General Microbiological Culture Collection Center (CGMCC) and Culture Collection University of Gothenburg (CCUG), respectively. These two type strains were used as the related strains for phenotypic, chemotaxonomic, and genetic analyses.

Phylogenetic Analysis

Genomic DNA of strains JM10B5a^T was extracted from fresh cells, and the 16S rRNA gene sequence was amplified using the universal primers (27F/1492R) as described previously (Zhang et al., 2021). Sequencing was performed by GENEWIZ, Inc. (Suzhou, China). The BLAST algorithm[2] and EzBioCloud database[3] were used to search for similar sequences (Yoon et al., 2017). Pairwise identities of 16S rRNA gene sequences were calculated using the software DNAMAN version 8. Multiple alignments of the 16S rRNA sequences were performed using the software MAFFT version 7.037 under the L-INS-i iterative refinement (Katoh and Standley, 2014). The phylogenetic tree was reconstructed using the software IQ-TREE version 2.1.2 with the maximum likelihood (ML) method under the TN+F+I+G4 nucleotide substitution model (Felsenstein, 1981; Kalyaanamoorthy et al., 2017; Minh et al., 2020). Support for the inferred ML tree was inferred by the ultrafast bootstrapping with 1,000 replicates (Diep Thi et al., 2018). The visualization and annotation of the resulting phylogenetic tree were performed using the software MEGA version X (Kumar et al., 2018).

Morphological Observations and Analyses of Physiological Characteristics

Cells and colonies of strain JM10B5a^T cultivated on the nutrient broth agar medium (NA) at 30°C for 48 h were observed by a transmission electron microscope (H7650, Hitachi) and naked eyes, respectively. Oxidase activity was determined using oxidase testing strips (HKM), and catalase activity was detected by bubble production after the addition of 3.0% H_2O_2 (v/v) solution. Growth under an anaerobic environment was determined after 5 days of incubation on NA at 30°C in an anaerobic pouch (MGC, Mitsubishi). Hydrolysis of casein, starch, tyrosine, and Tweens 20, 40, and 80 was investigated according to the protocols described by Lanyi (1987) and Tindall et al. (2007). Cellular motility was examined using the hanging-drop method (Bernardet et al., 2002).

The temperature range for growth was measured on NA at 4, 10, 15, 20, 25, 30, 37, 40, 45, and 50°C, respectively. The pH range for growth was determined after incubation at 30°C and 180 rpm in the modified NB medium with appropriate biological buffers (50 mM): sodium citrate buffer (pH 5.0, 5.5, and 6.0), HEPES buffer (pH 6.5, 7.0, and 7.5), Tris buffer (pH 8.0, 8.5, and 9.0), and Na_2CO_3/$NaHCO_3$ (pH 9.5, 10.0, 11.0, and 12.0). The pH of the medium was adjusted by adding 1.0 M HCl or 1.0 M NaOH before autoclaving. The NaCl tolerance for growth was examined in the modified NB medium (without NaCl) with different NaCl concentrations (w/v, 0, 0.5, 1.0, 2.0, 3.0, 4.0, 5.0, 6.0, 7.0, 8.0, 9.0, and 10.0 %) at 30°C and 180 rpm. After incubation for 72 h, the bacterial growth was estimated by the spectrophotometric measurement of cell density (OD_{600}).

Additional biochemical characteristics such as the enzyme activities, acid production by fermentation, and utilization of carbon sources were carried out using API ZYM and 20NE kits (bioMérieux) and Biolog GEN III MicroPlate (Biolog) according to the manufacturers' instructions. The API strips and Biolog results were recorded every 24 h after incubation at 30°C until all reactions were steady. All API and Biolog tests were performed in duplicate under the consistent condition.

Analyses of Chemotaxonomic Characteristics

For fatty acid composition assay, the exponentially growing cells of strain JM10B5a^T were harvested. Fatty acids were saponified, methylated, and extracted using the standard protocol of the Sherlock Microbial Identification System (MIDI). The prepared fatty acids were analyzed by gas chromatography (model 7890A; Agilent) using the Microbial Identification software package with the Sherlock MIDI 6.1 system and the Sherlock Aerobic Bacterial Database (TSBA 6.1).

[2]https://blast.ncbi.nlm.nih.gov/Blast.cgi
[3]https://www.ezbiocloud.net/

Polar lipids were extracted using the chloroform/methanol system and separated by two-dimensional thin-layer chromatography (TLC, Silica gel 60 F254, Merck) (Minnikin et al., 1984). The plates dotted with samples were subjected to two-dimensional development with the first solvent of chloroform–methanol–water (65:25:4, v/v) and the second solvent of chloroform–methanol–acetic acid–water (80:12:15:4, v/v). Total lipids and specific functional groups were detected using the different spray staining reagents on separate TLC plates: 10% ethanolic molybdophosphoric acid, ninhydrin, molybdenum blue, and α-naphthol–sulfuric acid. The quinone was extracted from the freeze-dried cells and determined using high-performance liquid chromatography (Agilent 1200; ODS 250 × 4.6 mm × 5.0 μm; flowing phase, methanol–isopropanol, 2:1; 1.0 ml/min) according to the methods described by Collins and Jones (1981).

Genome Sequencing and Function Analysis

The genomic DNA of strain JM10B5a^T was extracted using the HiPure Bacterial DNA Kit (Magen Biotech, Guangzhou) according to the manufacturer's instruction. The genome was sequenced using the Illumina NovaSeq PE150 platform in Shanghai Majorbio Bio-Pharm Technology Co., Ltd. (Shanghai, China). Raw reads were filtered and then *de novo* assembled using the software SPAdes version 3.14.1 under "–careful" mode and with a k-mer value of 127 (Bankevich et al., 2012). Available genomes of the related type strains *P. stutzeri* CGMCC 1.1803^T and *P. balearica* CCUG 44487^T were obtained from the GenBank database with the numbers CP002881 and CP007511, respectively. The genome of strain JM10B5a^T was in draft status and was quality-checked using the software CheckM version 1.1.2 (Parks et al., 2015). Overall genome relatedness indices (OGRIs) including digital DNA–DNA hybridization values (dDDH) and average nucleotide identity values (ANI) were estimated using the genome-to-genome distance calculator version 2.1 online service with the recommended formula 2[4] and the software FastANI version 1.31, respectively (Meier-Kolthoff et al., 2013; Jain et al., 2018). The UBCG pipeline which could provide an accurate phylogenomic tree for the taxonomic purpose was used (Chun et al., 2018; Na et al., 2018). The genomes of strain JM10B5a^T and the related type strains were annotated using the software Prokka version 1.13 (Seemann, 2014) and Rapid using Subsystem Technology (RAST) version 2.0 with the default parameters (Overbeek et al., 2014).

Assessment of Nitrogen Removal Characteristics

The results of the API 20NE test preliminarily indicated that strain JM10B5a^T was capable of reducing nitrate and nitrite. Furthermore, the genome annotation revealed that strain JM10B5a^T possessed the functional genes including *napA*, *narG*, *nirS*, *norB,* and *nosZ* that participated in the denitrification process. These results suggested that strain JM10B5a^T had the potential capability of complete denitrification. To investigate the optimum carbon source of denitrification for strain JM10B5a^T, the carbon source was replaced in the DSM-1 (DSM with KNO_3 0.36 g/L as the sole nitrogen source) or DSM-2 (DSM with $NaNO_2$ 0.25 g/L as the sole nitrogen source) by sodium acetate, sodium succinate, sodium citrate, glucose, sucrose, and starch, respectively, with the C/N ratio of 10 (the molar mass of carbon to the molar mass of nitrogen). Furthermore, the initial C/N ratios of 2, 3, 4, and 5 were controlled by changing the addition amount of the optimum carbon source in the DSM-1. Before the experiments, strain JM10B5a^T was incubated in NB at 30°C and 180 rpm for 24 h. The suspension was centrifuged and then washed 3 times with sterile physiological saline to remove the residual medium. The biomass was resuspended in sterile water with the initial OD_{600} adjusting to 1.0. The bacterial suspension was inoculated into a conical flask containing sterile medium with the inoculum amount of 4.0% and incubated at 30°C statically. Samples taken from flasks after 48 h of incubation were used for determining the OD_{600} and chemical analyses. The medium without bacterial inoculation was used as control treatment. All the experiments were performed in biological quadruplicate.

Analytical Methods and Statistical Analyses

The concentrations of NO_2^--N and NO_3^--N were measured using *N*-(1-naphthyl) ethylenediamine dihydrochloride and UV spectrophotometry, respectively, according to the standard analytical procedures (Association et al., 2005). All the data were presented as mean and standard error (SE). One-way ANOVA (multiple range test) was performed with Tukey's HSD test ($P < 0.05$) using SPSS Statistics 19.

RESULTS AND DISCUSSION

16S rRNA Gene Sequence Analyses and Chemotaxonomic Characterization

The almost complete 16S rRNA gene sequence of strain JM10B5a^T obtained by amplification (1,375 bp) was included in the complete 16S rRNA gene sequence assembled from genomic sequences (1,537 bp). The sequence comparison showed that strain JM10B5a^T fell into the genus *Pseudomonas* and shared the highest similarity with *P. stutzeri* CGMCC 1.1803^T (98.0%). All the other type strains showed similarities lower than 98.0% with strain JM10B5a^T. Based on phylogenetic analysis using the ML algorithm, strain JM10B5a^T was stably located in the genus *Pseudomonas* and formed a clade with *P. balearica* CCUG 44487^T (the similarity to JM10B5a^T was 97.0%) at the 79.0% bootstrap confidence level (**Figure 1**). The similarity and phylogenetic analysis based on the 16S rRNA gene sequences indicated that strain JM10B5a^T should represent a novel member of the genus *Pseudomonas*. Therefore, the type strains *P. stutzeri* CGMCC 1.1803^T and *P. balearica* CCUG 44487^T were purchased from the culture collection centers and used as references for further comparisons of phenotypic and chemotaxonomic characteristics.

The predominant cellular fatty acids (>10%) of strain JM10B5a^T were $C_{16:0}$ (22.0%), summed feature 3 ($C_{16:1}$ *ω6c*

[4]http://ggdc.dsmz.de/ggdc.php/

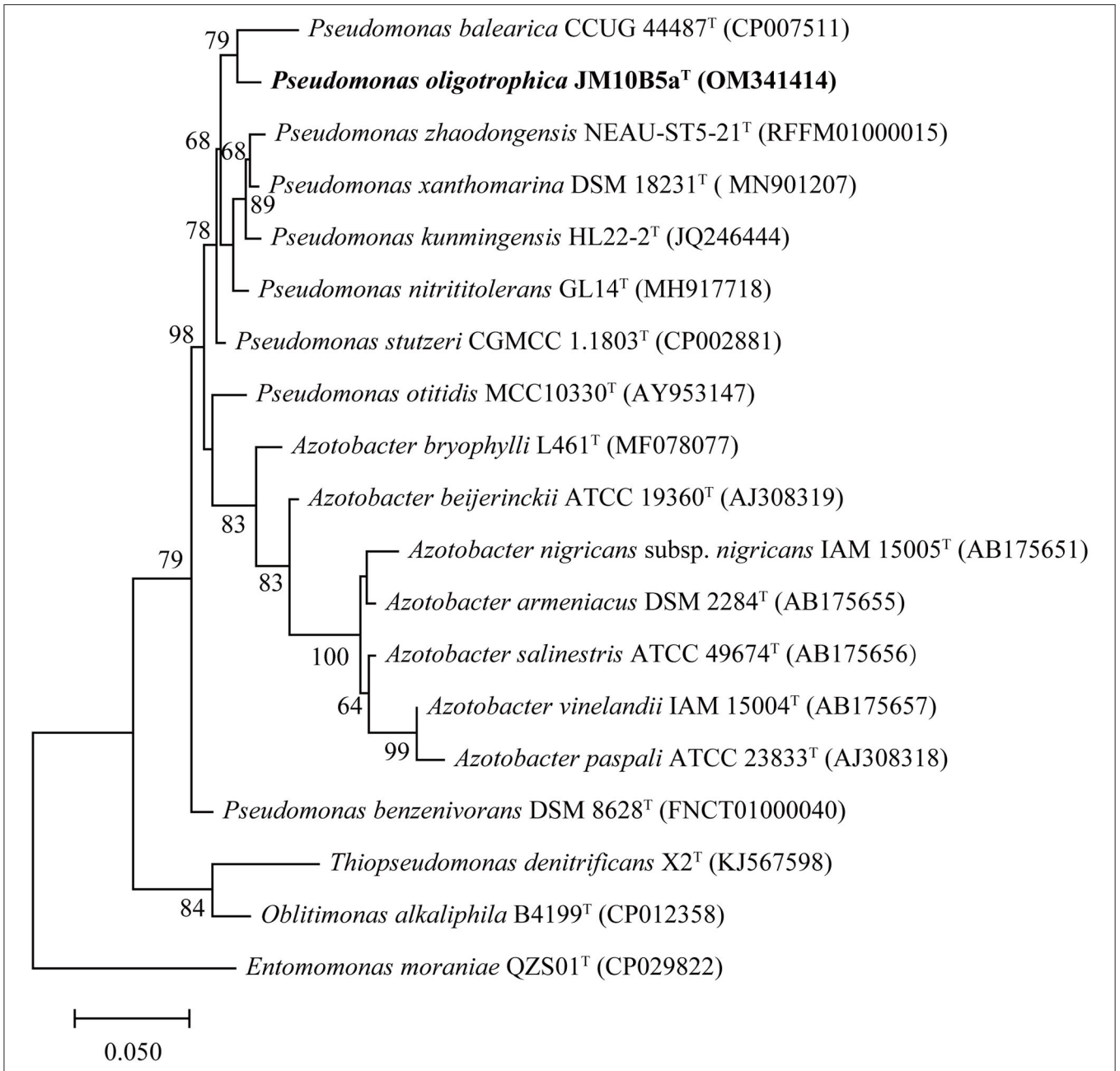

FIGURE 1 | ML tree based on 16S rRNA gene sequences of strain JM10B5a^T and the related type strains of genus *Pseudomonas*. Type strain *Entomomonas moraniae* QZS01^T was used as an outgroup. There were a total of 1,303 positions used to construct the phylogenetic tree. Bootstrap values higher than 60% were shown at branch points. Bar, 0.05 represents the number of substitutions per site.

and/or $C_{16:1}$ $\omega7c$, 21.3%), and summed feature 8 ($C_{18:1}$ $\omega6c$ and/or $C_{18:1}$ $\omega7c$, 29.1%), which were also detected in other *Pseudomonas* species (Mamtimin et al., 2021). Comparative fatty acid profiles between strain JM10B5a^T and the two related type strains are shown in **Table 1**. The fatty acid profile of JM10B5a^T was similar to that of other related strains, although there were minor quantitative differences observed. The predominant respiratory quinone of strain JM10B5a^T was ubiquinone-9 (Q-9) which was consistent with that of other members of the genus *Pseudomonas* (Zou et al., 2019; Mamtimin et al., 2021). The major polar lipids were phosphatidylethanolamine (PE), phosphatidylglycerol (PG), and diphosphatidylglycerol (DPG), which were consistent with the previously published data for *Pseudomonas* species (Zou et al., 2019; Li et al., 2020). In addition, minor amounts of two unidentified aminophospholipids (APLs)

TABLE 1 | Cellular fatty acid profiles of strain JM10B5a^T and the closely related type strains of genus *Pseudomonas*.

Fatty acid	JM10B5a^T	*P. stutzeri* CGMCC 1.1803^T	*P. balearica* CCUG 44487^T
Straight-chain saturated			
$C_{12:0}$	8.3	8.1	8.3
$C_{14:0}$	1.4	1.0	0.9
$C_{16:0}$	22.0	20.8	23.1
Hydroxy			
$C_{10:0}$ 3-OH	2.8	2.8	3.2
$C_{12:0}$ 3-OH	4.0	3.8	4.1
Branched saturated			
$C_{17:0}$ cyclo	5.2	2.0	6.0
iso $C_{17:0}$	TR	TR	0.8
Unsaturated			
$C_{19:0}$ cyclo ω8c	4.2	2.3	5.5
Summed Feature 3*	21.3	22.8	18.9
Summed Feature 8*	29.1	34.1	27.4

*All data were obtained from this study. Constituents <0.5% in three strains were not shown. TR, trace (<0.5%). *Summed features contain two or more fatty acids that cannot be separated by the MIDI system; summed feature 3 comprises $C_{16:1}$ ω6c and/or $C_{16:1}$ ω7c; summed feature 8 comprises $C_{18:1}$ ω6c and/or $C_{18:1}$ ω7c.*

and three unidentified phospholipids (PLs) were also present (**Supplementary Figure 1**).

Morphological Observations and Physiological Characterization

The morphological features of strain JM10B5a^T were studied on NA medium and formed irregular, filmy sheet, non-transparent, and ecru white colonies after 48 h of incubation at 30°C (**Supplementary Figure 2A**). Cells of strain JM10B5a^T were observed to be gram-stain-negative, aerobic, rod-shaped (0.6–0.7 × 1.4–1.5 μm), facultative anaerobic, and motile with a single polar flagellum (**Supplementary Figure 2B**). Growth was determined at 10–45°C (optimum, 25–30°C), at pH 5.5–11.0 (optimum, 6.0), and in 0–4.0% (w/v) NaCl (optimum, 0.5–2.0%). The activities of catalase and oxidase were positive, and the further details differentiating strain JM10B5a^T from the two related type strains are shown in **Table 2**. For instance, strain JM10B5a^T could not grow in the NB with a NaCl concentration of 5.0 while the two related type strains could grow; the optimum pH of strain JM10B5a^T was 6.0, which was inconsistent with that of *P. stutzeri* CGMCC 1.1803^T and *P. balearica* CCUG 44487^T of 6.5–7.5 and 8.5–9.5, respectively; the growth of strain JM10B5a^T was weaker than that of the two related type strains at 45°C. Besides, stain JM10B5a^T could be distinguished from the reference type strains by positive for adipic acid, trisodium citrate, esterase (C4), and lipase (C14) in the API 20NE and ZYM tests; and positive for D-galacturonic acid, D-glucuronic acid, gentiobiose, L-arginine, L-aspartic acid, L-galactonic acid lactone, mucic acid, quinic acid, α-hydroxybutyric acid, and γ-aminobutyric acid in the Biolog GNE III MicroPlate system. Importantly, strain JM10B5a^T exhibited the capability for complete denitrification that liberated copious amounts of nitrogen gas from nitrate. The denitrification characteristic of this strain was consistent with that of *P. stutzeri* and *P. balearica* strains (Bennasar et al., 1996; Li et al., 2021).

TABLE 2 | Differential characteristics of strain JM10B5a^T and the closely related type strains of genus *Pseudomonas*.

Characteristic	JM10B5a^T	*P. stutzeri* CGMCC 1.1803^T	*P. balearica* CCUG 44487^T
Growth			
NaCl concentration (optimum, w/v)	0–4.0 (0.5–2.0)	0–5.0 (0.5)	0–5.0 (1.0)
pH range (optimum)	5.5–11.0 (6.0)	6.0–11.0 (8.5–9.5)	5.5–11.0 (6.5–7.5)
Temperature (optimum, °C)	10–45 (25–30)	10–45 (30–37)	10–45 (30–37)
45°C	w	+	+
API ZYM and 20NE tests			
Adipic acid	+	+	−
Trisodium citrate	+	+	−
Esterase (C4)	+	−	−
Lipase (C14)	+	+	−
Biolog (GEN III) tests			
Dextrin	−	+	+
D-Galacturonic acid	+	−	−
D-Glucuronic acid	+	w	−
D-Maltose	−	+	+
D-Mannitol	−	+	−
D-Saccharic acid	+	−	−
Formic acid	−	+	−
Gentiobiose	+	−	−
L-Arginine	+	−	−
L-Aspartic acid	+	−	+
L-Galactonic acid lactone	+	−	−
L-Pyroglutamic acid	−	+	−
Mucic acid	+	−	−
Quinic acid	+	−	−
α-Hydroxy-butyric acid	+	−	+
γ-Amino butyric acid	+	−	−
G + C content (%)	67.2	63.6§	64.7§
Genome size (Mb)	4.0	4.5§	4.4§

All data were obtained from this study unless indicated otherwise.
§Data from draft genomes in the NCBI genome database.
+, positive; −, negative; w, weakly positive.

Genome Data and Comparative Genomic Analysis

The draft genome of strain JM10B5a^T was assembled into 20 contigs (>500 bp) with a genome size of 3,978,222 bp, and the estimated completeness and contamination were 100 and 0.1%, respectively, indicating that this genome was high quality according to the standards (Parks et al., 2015). Genomes of strains *P. stutzeri* CGMCC 1.1803^T and *P. balearica* CCUG 44487^T

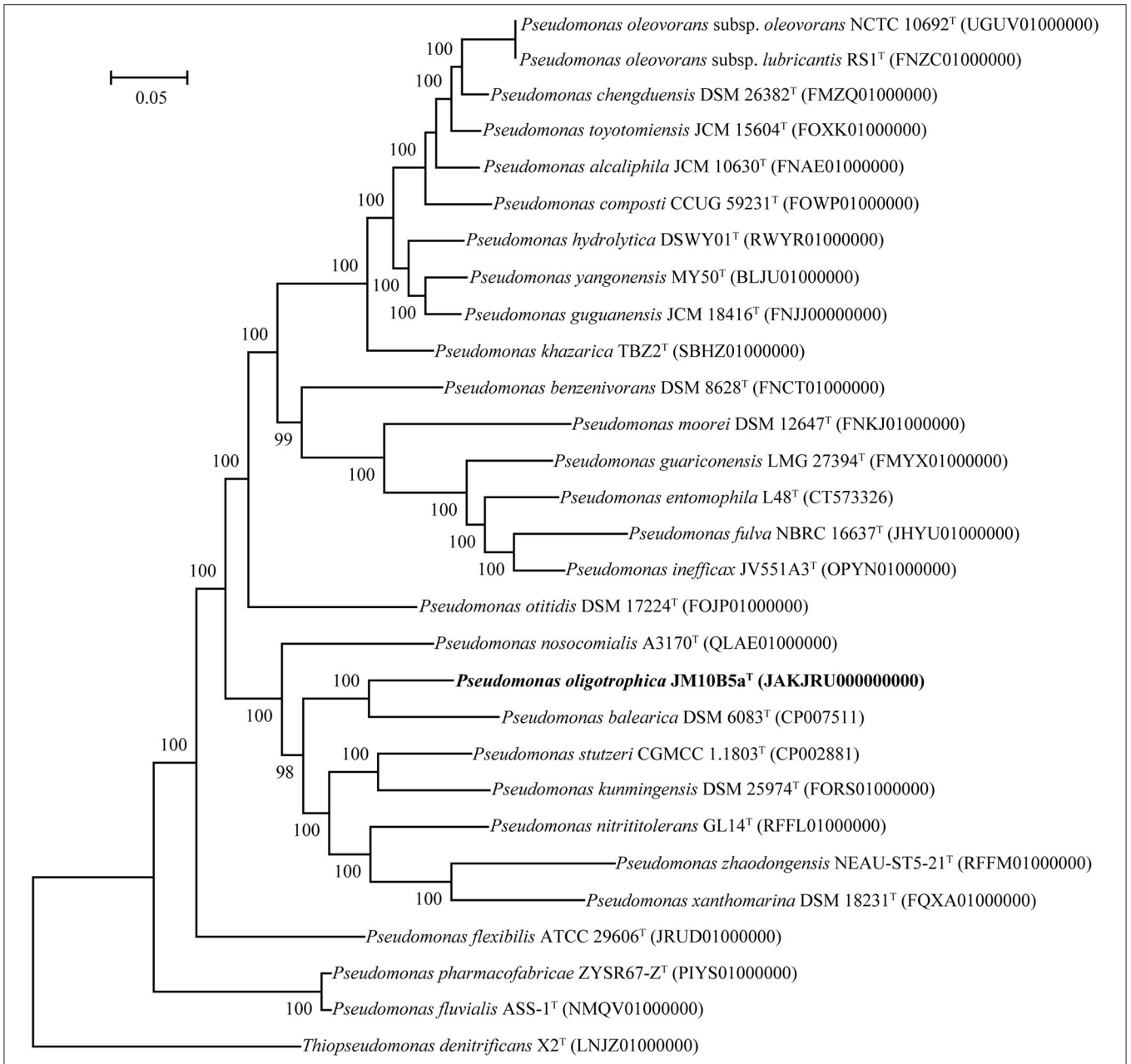

FIGURE 2 | Phylogenomic tree based on 92 bacterial core gene sets of strain JM10B5a^T and the related type strains of genus *Pseudomonas*. Type strain *Thiopseudomonas denitrificans* X2^T was used as an outgroup. Bootstrap values higher than 70% were shown at branch points. Bar, 0.05 represents the number of substations per site.

were obtained from the GenBank database with the numbers CP002881 and CP007511, respectively. Based on the Prokka annotation, a total of 3,744 genes, 3,679 protein-coding sequences (CDS), 60 tRNA genes, and 3 rRNA genes were found in the genome of strain JM10B5a^T. The genomic DNA G + C content of JM10B5a^T was 67.2%. Compared with the genomes of related type strains, JM10B5a^T had ANI values of 78.9–88.1% and dDDH values of 20.8–30.8% (**Supplementary Table 1**), which were all below 95.0 and 70% cutoff commonly used to define a bacterial species, respectively (Stackebrandt and Goebel, 1994; Richter and Rossello-Mora, 2009). To further determine the taxonomic position of strain JM10B5a^T, the phylogenomic tree based on the 92 bacterial core gene sets was reconstructed (Na et al., 2018). As shown in **Figure 2**, strain JM10B5a^T and *P. balearica* CCUG 44487^T formed a clade with 100% bootstrap value, which was consistent with the phylogenetic tree based on the 16S rRNA gene sequences. Therefore, the comprehensive analyses of OGRIs and phylogenomic tree further indicated that strain

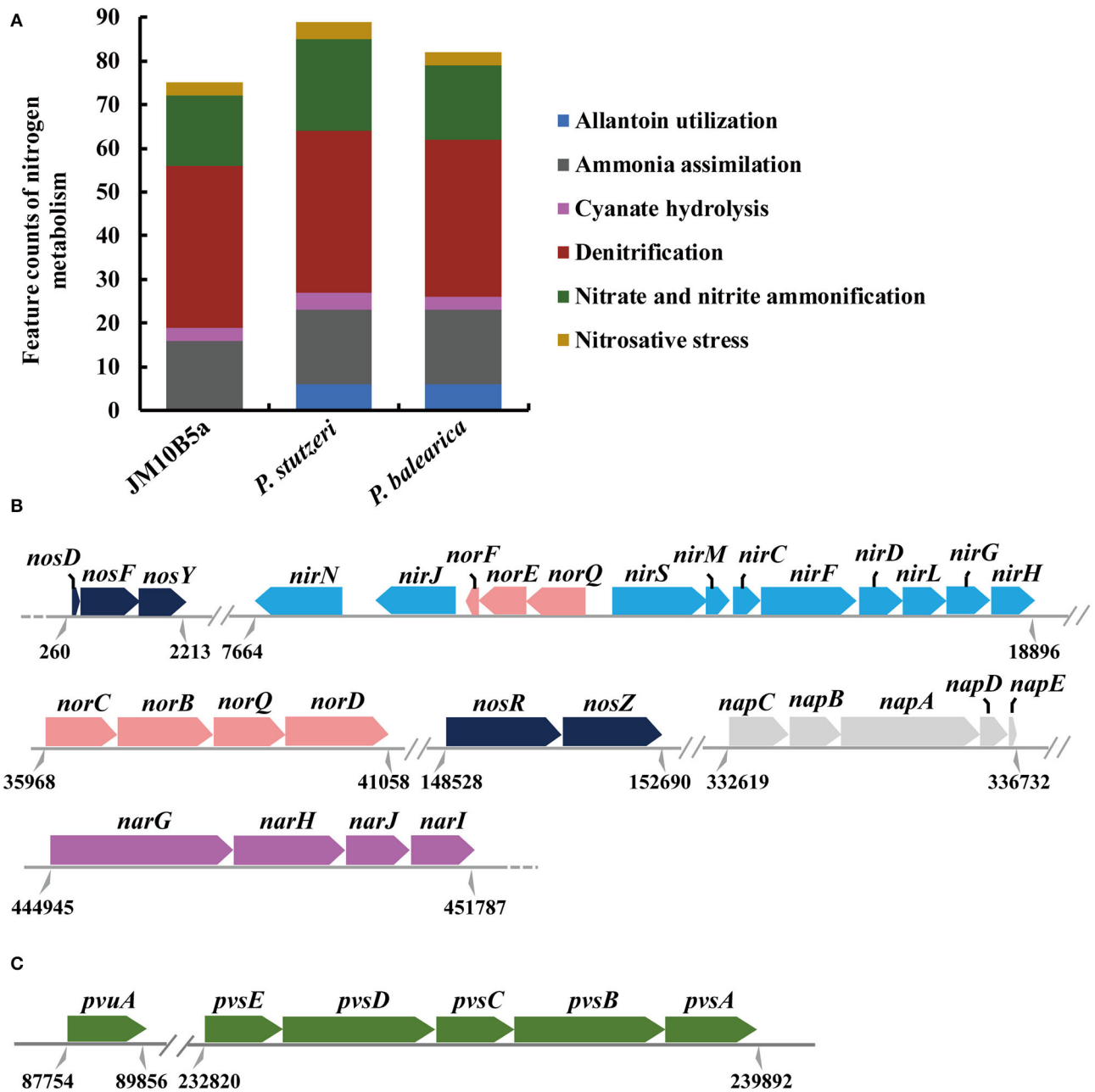

FIGURE 3 | Genomic analyses based on the RAST annotation. **(A)** Comparative analyses of the functional genes assigned to nitrogen metabolisms of strain JM10B5a^T and the related type strains of genus *Pseudomonas*. **(B)** Relative arrangements of the denitrification genes on the draft genome of strain JM10B5a^T. **(C)** The biosynthetic gene cluster for vibrioferrin on the draft genome of strain JM10B5a^T. Parallel double lines indicate a break in locus organization among scaffolds, and dotted black lines indicate where unrelated continuity loci are not shown. Numbers below the line symbolize the locations.

JM10B5a^T should represent a novel species within the genus of *Pseudomonas*.

According to the subsystem category distribution of RAST annotation, there were 190, 128, 402, and 336 genes associated with "RNA metabolism," "DNA metabolism," "amino acid and derivatives," and "carbohydrates," respectively, which might be important to the bacterial growth. In addition, 75 genes were identified in the nitrogen metabolism, including the functional genes related to denitrification and assimilation of nitrite and nitrate (**Figures 3A,B**). Nitrate reductase catalyzing the reduction in nitrate to nitrite plays an important role in the nitrogen cycle (Kuypers et al., 2018). Previous studies have shown that bacterial dissimilatory nitrate reduction could be catalyzed by two different enzymes: a membrane-bound nitrate

reductase (NAR, the catalytic subunit NarG encoded by *narG*) and periplasmic nitrate reductase (NAP, the catalytic subunit NapA encoded by *napA*) (Moreno-Vivian et al., 1999). Genes *narG* and *napA* were both contained in strain JM10B5a^T, which was consistent with *Pseudomonas* sp. JQ-H3 and *Paracoccus denitrificans* (Moreno-Vivian et al., 1999; Wang et al., 2019). The dissimilatory reduction in nitrite to nitric oxide can be catalyzed by two unrelated enzymes: a cytochrome cd1 nitrite reductase (cd1-NIR, encoded by *nirS*) or a Cu-containing nitrite reductase (Cu-NIR, encoded by *nirK*), which were widespread among bacteria and archaea (Kuypers et al., 2018). Gene *nirS* rather than *nirK* was identified in strain JM10B5a^T, which was consistent with *Pseudomonas* sp. JQ-H3, *P. bauzanensis* DN13-1, and *P. stutzeri* T13 (Wang et al., 2019; Zhang M. et al., 2020; Feng et al., 2021). In addition, genes *norB* encoding for nitric oxide reductase (NorB, the key enzyme for reducing nitric oxide to nitrous oxide) and *nosZ* encoding for nitrous oxide reductase (NosZ, the key enzyme for reducing nitrous oxide to nitrogen gas) were also identified. Therefore, it was speculated that strain JM10B5a^T could perform the complete denitrification pathway: NO_3^--N $\rightarrow$ NO_2^--N $\rightarrow$ NO $\rightarrow$ N_2O $\rightarrow$ N_2. Hence, strain JM10B5a^T was a novel denitrifying bacterium.

In addition, comparative genomic analyses showed that strain JM10B5a^T encoded 126 and 147 functional genes more than *P. balearica* CCUG 44487^T and *P. stutzeri* CGMCC 1.1803^T, respectively, and 67 genes of them were the shared differential genes (**Supplementary Table 2**). These genes were related to type I secretion system for aggregation, utilization of alkylphosphonate and tricarballylate, histidine ABC transporter, LysR family transcriptional regulator, and many other proteins. Most of these proteins were mainly affiliated with dehydratase, transferase, and biosynthesis of cofactors and vitamins. The genes encoding arginase and galactarate dehydratase made strain JM10B5a^T performing the positive for L-arginine and mucic acid (**Table 2**). Moreover, strain JM10B5a^T was found to harbor the complete operon *pvsABCDE* and vibrioferrin receptor gene *pvuA* (**Figure 3C**) that are required for the production of a siderophore vibrioferrin. This siderophore was shown to be responsible for vibrioferrin-mediated iron uptake in the terrestrial bacteria *Azotobacter vinelandii*, *Pseudomonas* sp., and the marine bacterium *Vibrio parahaemolyticus* (Yamamoto et al., 1994; Baars et al., 2016; Stanborough et al., 2018; Sood et al., 2019). It was reported that siderophore had a very high affinity to iron with the formation of Fe-siderophore which could facilitate the transport of iron through the membrane directly (Stintzi et al., 2000). Moreover, the denitrification efficiency might be enhanced with the improvement of iron transport from extracellular to intracellular (Jiang et al., 2020). Therefore, the biosynthesis of vibrioferrin might partly explain that the strain JM10B5a^T performed the high denitrification efficiency under the low C/N ratio condition.

Effect of Carbon Source on Denitrification by Strain JM10B5a^T

Heterotrophic denitrifying bacteria require organic carbon for cell growth and as the electron donor in the denitrification process (Rajta et al., 2020). Thus, carbon source was considered to be an important factor influencing denitrification. As expected, significant differences were observed using different carbon sources. As shown in **Figure 4A**, the strain JM10B5a^T could grow well with the OD_{600} of 0.42 when glucose was used as the sole carbon source. However, it exhibited a higher NO_3^--N removal efficiency of 99.5% when sodium acetate served as carbon source than that of 58.6% when glucose served as carbon source. As shown in **Figure 4B**, strain JM10B5a^T could grow quite well when glucose served as the carbon source (OD_{600} of 0.52), but it performed the relatively high NO_2^--N removal of 100% when sodium acetate served as the carbon source. These results indicated that sodium acetate was the optimum carbon source for the performance of denitrification for strain JM10B5a^T, which was consistent with *Bacillus pumilus*, *Arthrobacter* sp., and *Streptomyces lusitanus* (Elkarrach et al., 2021). Therefore, sodium acetate was employed in the following experiments.

Effect of Carbon/Nitrogen Ratio on Nitrate Removal by Strain JM10B5a^T

C/N ratio is a measure of the electron donor to acceptor ratio in the biological denitrification process. This factor can influence the denitrification efficiency and accumulation of NO_2^--N. To investigate the influence of C/N ratio on denitrification of strain JM10B5a^T, the initial concentration of NO_3^--N was fixed at ∼50.0 mg/L and the different initial C/N ratios (2, 3, 4, and 5) were controlled. As shown in **Figure 5**, strain JM10B5a^T grew poorly with the OD_{600} range of 0.10–0.15 at these low C/N ratios. The NO_3^--N was reduced completely at the C/N ratios of 3–5 which was distinctly higher than that of 84.4% at the C/N ratio of 2. Furthermore, there was no NO_2^--N accumulation observed at the C/N ratios of 3–5, but the NO_2^--N concentration of 19.3 mg/L was detected at the C/N ratio of 2. The low NO_3^--N removal efficiency and NO_2^--N accumulation at the C/N ratio of 2 were mainly due to the limited carbon source that could not provide sufficient energy for bacterial growth and electron donors for denitrification (Fan et al., 2021). These results were consistent with previous reports that denitrification efficiency could decrease under the extremely low carbon concentration (Zhao et al., 2018). Numerous studies have suggested that the optimum C/N ratios for most heterotrophic denitrifying bacteria were in the range of 8–15 (Guo et al., 2016; Liu et al., 2018; Zhao et al., 2018). For example, the C/N ratios of 10 and 15 were the most suitable for strains *P. stutzeri* XL-2 and *P. taiwanensis* J to achieve efficient nitrate removal, respectively (He et al., 2018; Zhao et al., 2018). In addition, some denitrifying bacteria could achieve complete denitrification at the relatively low C/N ratios. For example, Rout et al. (2017) used *Bacillus cereus* to remove nitrogen from domestic wastewater with 7.5 as the optimum C/N ratio; Zhang S. et al. (2020) reported that strain *Comamonas* sp. YSF15 could achieve complete denitrification at C/N of 3. Our results showed that strain JM10B5a^T could achieve the complete nitrate removal without accumulation of nitrite at the low carbon–nitrogen ratio of 3 (COD_{Cr}/TN ratio of 2.6), indicating that this strain could be a promising candidate for treating the oligotrophic wastewater.

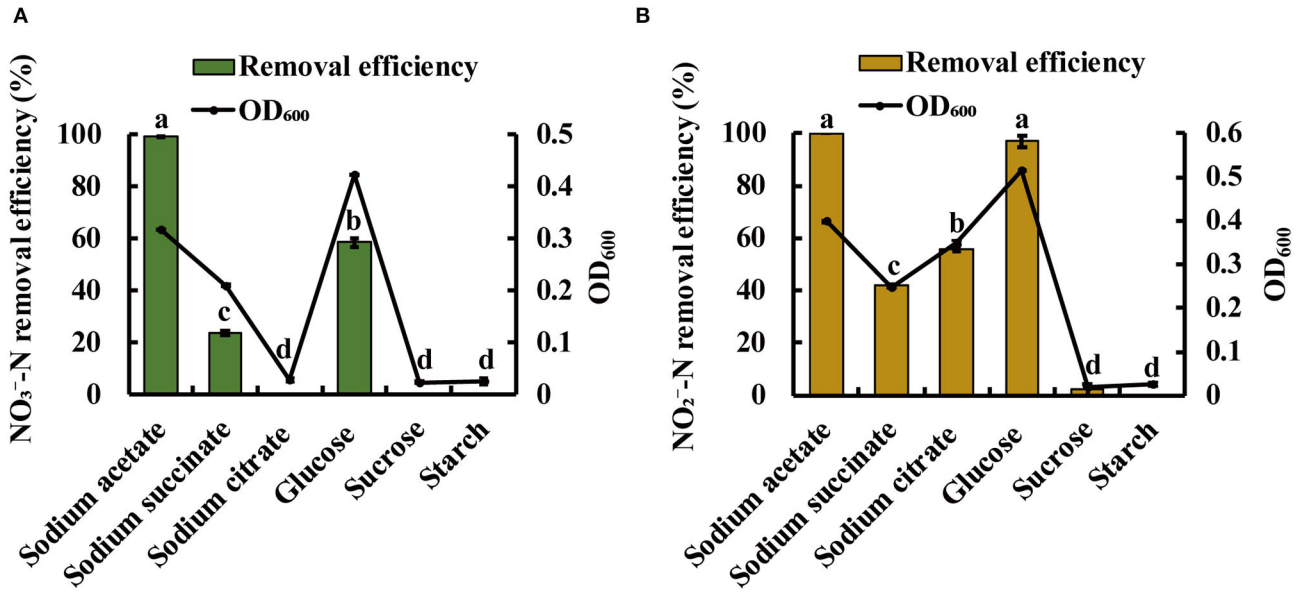

FIGURE 4 | Growth (OD_{600}) and NO_3^--N and NO_2^--N removal performance of strain JM10B5a^T under various common carbon sources. **(A)** NO_3^--N as the sole nitrogen source. **(B)** NO_2^--N as the sole nitrogen source. Values are mean ± SE (standard error) for four replicates.

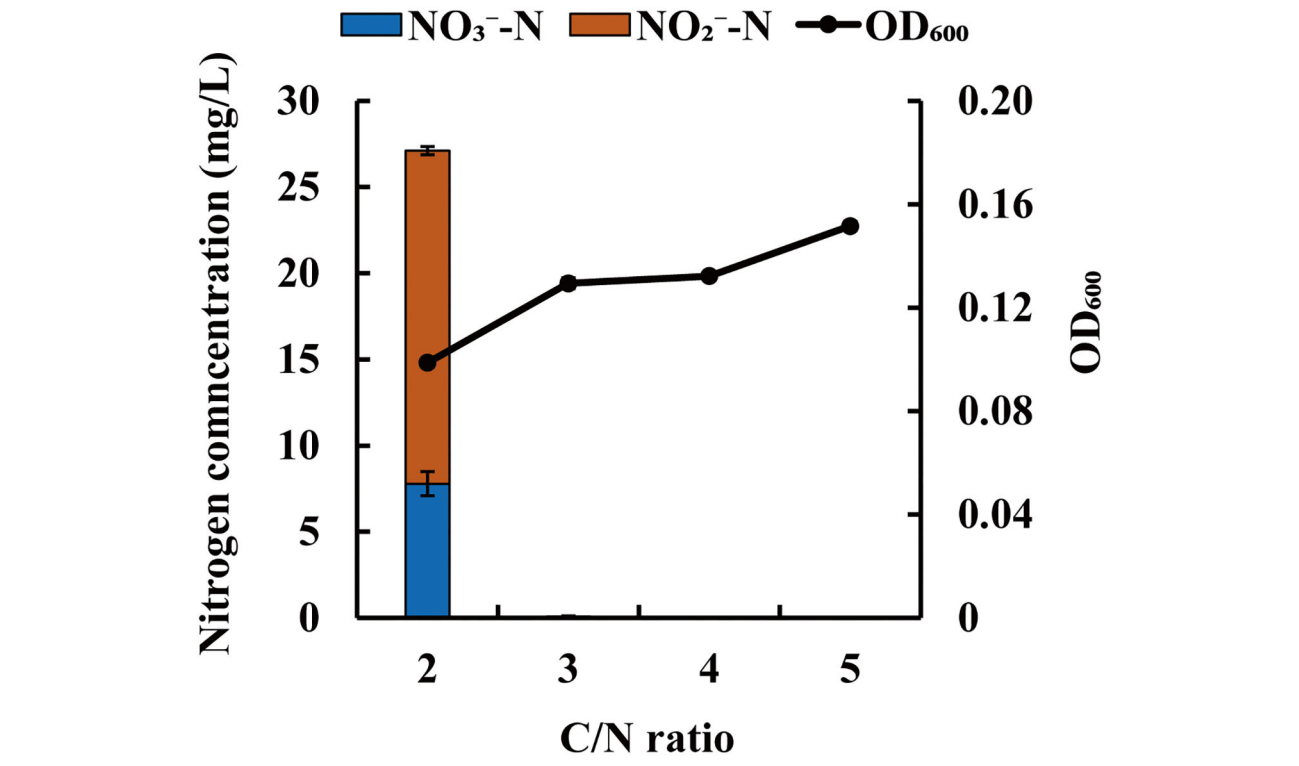

FIGURE 5 | Influence of C/N ratio on NO_3^--N removal characteristic of strain JM10B5a^T. Values are mean ± SE (standard error) for four replicates.

Description of *Pseudomonas oligotrophica* sp. nov.

Pseudomonas oligotrophica (o.li.go.tro'phi.ca. Gr. adj. *oligos*, few; Gr. adj. *trophikos*, nursing, tending, or feeding; N.L. fem. adj. *oligotrophica*, eating little, referring to a bacterium living on low-nutrient media).

Cells are rods (1.4–1.5 μm in length and 0.6–0.7 μm in width), gram-stain-negative, facultative anaerobic, and motile

by the polar flagellum. Colonies are irregular, filmy sheet, non-transparent, and ecru white after 48 h of incubation on NA agar at 30°C. Growth was determined at 10–45°C (optimum, 25–30°C), at pH 5.5–11.0 (optimum, 6.0), and in 0–4.0% (w/v) NaCl (optimum, 0.5–2.0%) and is positive for catalase and oxidase, and hydrolysis of Tween 20 and 60. In the API ZYM and 20NE system, it is positive for esterase (C4), esterase lipase (C8), lipase (C14), leucine arylamidase and naphtol-AS-B1-phosphoamidase, nitrate and nitrite reduction, β-glucosidase, D-glucose, D-maltose, potassium gluconate, capric acid, adipic acid, malic acid, and trisodium citrate. In the Biolog GNE III MicroPlate system, it is positive for gentiobiose, α-D-glucose, D-fructose, glycerol, L-alanine, L-arginine, L-aspartic acid, L-glutamic acid, D-galacturonic acid, L-galactonic acid lactone, D-gluconic acid, D-glucuronic acid, glucuronamide, mucic acid, quinic acid, D-saccharic acid, L-lactic acid, citric acid, α-ketoglutaric acid, D-malic acid, L-malic acid, bromosuccinic acid, γ-aminobutyric acid, α-hydroxybutyric acid, β-hydroxy-D, L-butyric acid, α-ketobutyric acid, propionic acid, and acetic acid. The major fatty acids are $C_{16:0}$, summed feature 3 ($C_{16:1}$ $\omega6c$ and/or $C_{16:1}$ $\omega7c$), and summed feature 8 ($C_{18:1}$ $\omega6c$ and/or $C_{18:1}$ $\omega7c$). The major polar lipids are PE, PG, and DPG, and the predominant respiratory quinone is Q-9. The DNA G + C content of strain JM10B05a^T is 67.2%. Accession numbers of the complete 16S rRNA gene sequence and draft genome in DDBJ/ENA/GenBank are OM341414 and JAKJRU000000000, respectively. The type strain, JM10B5a^T (= GDMCC 1.2828^T = JCM 35033^T), was isolated from pond water for juvenile *Litopenaeus vannamei* collected from Jiangmen city Guangdong Province, China.

DATA AVAILABILITY STATEMENT

The datasets presented in this study can be found in online repositories. The names of the repository/repositories and accession number(s) can be found in the article/**Supplementary Material**.

AUTHOR CONTRIBUTIONS

MZ, AL, and QY were involved in conceptualization and project administration. MZ involved in data curation, software, visualization, and writing—original draft. MZ and BX designed the formal analysis and methodology. AL, HZ, and BX were involved in funding acquisition. MZ, AL, QY, BX, and HZ investigated the study. HZ collected the resources and supervised the study. MZ and AL validated the study. MZ, QY, and BX were involved in writing—review and editing. All authors contributed to the article and approved the submitted version.

FUNDING

This work was financially supported by the Key-Area Research and Development Program of Guangdong Province (2020B0202080005), the National Natural Science Foundation of China (32070115, 11772133), and the GDAS' Special Project of Science and Technology Development (2020GDASYL-20200301003).

ACKNOWLEDGMENTS

We are very grateful to Mr. Fan Yang at Guangdong Microbial Culture Collection Center (Guangzhou, China) for purchasing the related type strains as references.

SUPPLEMENTARY MATERIAL

The Supplementary Material for this article can be found online at: https://www.frontiersin.org/articles/10.3389/fmicb.2022.882890/full#supplementary-material

REFERENCES

Association, A. P. H., Association, A. W. W., and Federation, W. E. (2005). *Standard Methods for the Examination of Water and Wastewater*. Washington, DC: American Public Health Association Press.

Baars, O., Zhang, X., Morel, F. M. M., and Seyedsayamdost, M. R. (2016). The siderophore metabolome of *Azotobacter vinelandii*. *Appl. Environ. Microbiol.* 82, 27–39. doi: 10.1128/AEM.03160-15

Bankevich, A., Nurk, S., Antipov, D., Gurevich, A. A., Dvorkin, M., Kulikov, A. S., et al. (2012). SPAdes: a new genome assembly algorithm and its applications to single-cell sequencing. *J. Comput. Biol.* 19, 455–477. doi: 10.1089/cmb.2012.0021

Bennasar, A., RosselloMora, R., Lalucat, J., and Moore, E. R. B. (1996). 16S rRNA gene sequence analysis relative to genomovars of *Pseudomonas stutzeri* and proposal of *Pseudomonas balearica* sp. nov. *Int. J. Syst. Bacteriol.* 46, 200–205. doi: 10.1099/00207713-46-1-200

Bernardet, J. F., Nakagawa, Y., and Holmes, B. (2002). Proposed minimal standards for describing new taxa of the family Flavobacteriaceae and emended description of the family. *Int. J. Syst. Evol. Microbiol.* 52, 1049–1070. doi: 10.1099/ijs.0.02136-0

Chen, C., Ali, A., Su, J., Wang, Y., Huang, T., and Gao, J. (2021). *Pseudomonas stutzeri* GF2 augmented the denitrification of low carbon to nitrogen ratio: possibility for sewage wastewater treatment. *Bioresour. Technol.* 333, 125169. doi: 10.1016/j.biortech.2021.125169

Chun, J., Oren, A., Ventosa, A., Christensen, H., Arahal, D. R., da Costa, M. S., et al. (2018). Proposed minimal standards for the use of genome data for the taxonomy of prokaryotes. *Int. J. Syst. Evol. Microbiol.* 68, 461–466. doi: 10.1099/ijsem.0.002516

Collins, M. D., and Jones, D. (1981). A note on the separation of natural mixtures of bacterial ubiquinones using reverse-phase partition thin-layer chromatography and high-performance liquid chromatography. *J. Appl. Bacteriol.* 51, 129–134. doi: 10.1111/j.1365-2672.1981.tb00916.x

Deng, L., Ngo, H. H., Guo, W., Wang, J., and Zhang, H. (2018). Evaluation of a new sponge addition-microbial fuel cell system for removing nutrient from low C/N ratio wastewater. *Chem. Eng. J.* 338, 166–175. doi: 10.1016/j.cej.2018.01.028

Deng, S., Li, D., Yang, X., Zhu, S., and Li, J. (2016). Process of nitrogen transformation and microbial community structure in the Fe(0)-carbon-based bio-carrier filled in biological aerated filter. *Environ. Sci. Pollut. Res. Int.* 23, 6621–6630. doi: 10.1007/s11356-015-5892-6

Di, Y., Xia, H., Jiao, Y., Zhang, X., Fang, Q., Li, F., et al. (2019). Biodegradation of polyhydroxybutyrate by *Pseudomonas* sp. DSDY0501 and purification and characterization of polyhydroxybutyrate depolymerase 3. *Biotechnology* 9, 359. doi: 10.1007/s13205-019-1871-9

Diep Thi, H., Chernomor, O., von Haeseler, A., Minh, B. Q., and Le Sy, V. (2018). UFBoot2: improving the ultrafast bootstrap approximation. *Mol. Biol. Evol.* 35, 518–522. doi: 10.1093/molbev/msx281

Dutra, F. M., Cidemar Alab, J. H., Costa Gomes, M. K., Furtado, P. S., Valenti, W. C., and Cupertino Ballester, E. L. (2020). Nitrate acute toxicity to post larvae and juveniles of *Macrobrachium amazonicum* (Heller, 1862). *Chemosphere* 242, 125229. doi: 10.1016/j.chemosphere.2019.125229

Elkarrach, K., Merzouki, M., Atia, F., Laidi, O., and Benlemlih, M. (2021). Aerobic denitrification using *Bacillus pumilus*, *Arthrobacter* sp., and *Streptomyces lusitanus*: novel aerobic denitrifying bacteria. *Bioresour. Technol. Rep.* 14, 100663. doi: 10.1016/j.biteb.2021.100663

Fan, Y., Su, J., Zheng, Z., Gao, J., and Ali, A. (2021). Denitrification performance and mechanism of a novel isolated *Acinetobacter* sp. FYF8 in oligotrophic ecosystem. *Bioresour. Technol.* 320 (Pt A), 124280. doi: 10.1016/j.biortech.2020.124280

Felsenstein, J. (1981). Evolutionary trees from DNA sequences: a maximum likelihood approach. *J. Mol. Evol.* 17, 368–376. doi: 10.1007/BF01734359

Feng, L., Yang, J., Ma, F., Xing, L., Pi, S., Cui, D., et al. (2021). Biological stimulation with Fe(III) promotes the growth and aerobic denitrification of *Pseudomonas stutzeri* T13. *Sci. Total. Environ.* 776, 145939. doi: 10.1016/j.scitotenv.2021.145939

Gao, L., Han, F., Zhang, X., Liu, B., Fan, D., Sun, X., et al. (2020). Simultaneous nitrate and dissolved organic matter removal from wastewater treatment plant effluent in a solid-phase denitrification biofilm reactor. *Bioresour. Technol.* 314, 123714. doi: 10.1016/j.biortech.2020.123714

Guo, L. J., Zhao, B., An, Q., and Tian, M. (2016). Characteristics of a novel aerobic denitrifying bacterium, *Enterobacter cloacae* strain HNR. *Appl. Biochem. Biotechnol.* 178, 947–959. doi: 10.1007/s12010-015-1920-8

He, T., Ye, Q., Sun, Q., Cai, X., Ni, J., Li, Z., et al. (2018). Removal of nitrate in simulated water at low temperature by a novel psychrotrophic and aerobic bacterium, *Pseudomonas taiwanensis* strain. *J. Biomed Res. Int.* 2018, 4984087. doi: 10.1155/2018/4984087

Hong, Y., Huang, G., An, C., Song, P., Xin, X., Chen, X., et al. (2019). Enhanced nitrogen removal in the treatment of rural domestic sewage using vertical-flow multi-soil-layering systems: experimental and modeling insights. *J. Environ. Manage.* 240, 273–284. doi: 10.1016/j.jenvman.2019.03.097

Huang, L., Ye, J., Xiang, H., Jiang, J., Wang, Y., and Li, Y. (2020). Enhanced nitrogen removal from low C/N wastewater using biodegradable and inert carriers: performance and microbial shift. *Bioresour. Technol.* 300, 122658. doi: 10.1016/j.biortech.2019.122658

Jain, C., Rodriguez,-R. L. M., Phillippy, A. M., Konstantinidis, K. T., and Aluru, S. (2018). High throughput ANI analysis of 90K prokaryotic genomes reveals clear species boundaries. *Nat. Commun.* 9, 5114. doi: 10.1038/s41467-018-07641-9

Jiang, M., Feng, L., Zheng, X., and Chen, Y. (2020). Bio-denitrification performance enhanced by graphene-facilitated iron acquisition. *Water Res.* 180, 115916. doi: 10.1016/j.watres.2020.115916

Kalyaanamoorthy, S., Minh, B. Q, Wong, T. K. F., von Haeseler, A., and Jermiin, L. S. (2017). ModelFinder: fast model selection for accurate phylogenetic estimates. *Nat. Methods* 14, 587–589. doi: 10.1038/nmeth.4285

Katoh, K., and Standley, D. M. (2014). MAFFT: iterative refinement and additional methods. *Methods Mol. Biol.* 1079, 131–146. doi: 10.1007/978-1-62703-646-7_8

Kumar, S., Stecher, G., Li, M., Knyaz, C., and Tamura, K. (2018). MEGA X: molecular evolutionary genetics analysis across computing platforms. *Mol. Biol. Evol.* 35, 1547–1549. doi: 10.1093/molbev/msy096

Kuypers, M. M. M., Marchant, H. K., and Kartal, B. (2018). The microbial nitrogen-cycling network. *Nat. Rev. Microbiol.* 16, 263–276. doi: 10.1038/nrmicro.2018.9

Lalucat, J., Gomila, M., Mulet, M., Zaruma, A., and Garcia-Valdes, E. (2021). Past, present and future of the boundaries of the *Pseudomonas* genus: proposal of *Stutzerimonas* gen. *Nov. Syst. Appl. Microbiol.* 45, 126289. doi: 10.1016/j.syapm.2021.126289

Lanyi, B. (1987). Classical and rapid identification methods for medically important bacteria. *Method. Microbiol.* 19, 1–67. doi: 10.1016/S0580-9517(08)70407-0

Li, B., Jing, F., Wu, D., Xiao, B., and Hu, Z. (2021). Simultaneous removal of nitrogen and phosphorus by a novel aerobic denitrifying phosphorus-accumulating bacterium, *Pseudomonas stutzeri* ADP-19. *Bioresour. Technol.* 321, 124445. doi: 10.1016/j.biortech.2020.124445

Li, J., Wang, L. H., Xiang, F. G., Ding, W. L., Xi, L. J., Wang, M. Q., et al. (2020). *Pseudomonas phragmitis* sp. nov., isolated from petroleum polluted river sediment. *Int. J. Syst. Evol. Microbiol.* 70, 364–372. doi: 10.1099/ijsem.0.003763

Ling, Y., Yan, G., Wang, H., Dong, W., Wang, H., Chang, Y., et al. (2021). Release mechanism, secondary pollutants and denitrification performance comparison of six kinds of agricultural wastes as solid carbon sources for nitrate removal. *Int. J. Environ. Res. Public Health* 18, 1232. doi: 10.3390/ijerph18031232

Liu, S., Chen, Q., Ma, T., Wang, M., and Ni, J. (2018). Genomic insights into metabolic potentials of two simultaneous aerobic denitrification and phosphorus removal bacteria, *Achromobacter* sp. GAD3 and *Agrobacterium* sp. LAD9. *FEMS Microbiol. Ecol.* 94, 4. doi: 10.1093/femsec/fiy020

Liu, X., Huang, M., Bao, S., Tang, W., and Fang, T. (2020). Nitrate removal from low carbon-to-nitrogen ratio wastewater by combining iron-based chemical reduction and autotrophic denitrification. *Bioresour. Technol.* 301, 122731. doi: 10.1016/j.biortech.2019.122731

Mamtimin, T., Anwar, N., Abdurahman, M., Kurban, M., Rozahon, M., Mamtimin, H., et al. (2021). *Pseudomonas lopnurensis* sp. nov., an endophytic bacterium isolated from Populus euphratica at the ancient Ugan river. *Antonie Van Leeuwenhoek* 114, 399–410. doi: 10.1007/s10482-021-01524-8

Meier-Kolthoff, J. P., Auch, A. F., Klenk, H. P., and Goeker, M. (2013). Genome sequence-based species delimitation with confidence intervals and improved distance functions. *BMC Bioinformat.* 14, 60. doi: 10.1186/1471-2105-14-60

Migula, W. (1894). Über ein neues system der bakterien. *Arb. Bakteriol. Inst. Karlsruhe*. 1, 235–238.

Minh, B. Q., Schmidt, H. A., Chernomor, O., Schrempf, D., Woodhams, M. D., von Haeseler, A., et al. (2020). IQ-TREE 2: new models and efficient methods for phylogenetic inference in the genomic era. *Mol. Biol. Evol.* 37, 2461. doi: 10.1093/molbev/msaa131

Minnikin, D. E., Odonnell, A. G., Goodfellow, M., Alderson, G., Athalye, M., Schaal, A., et al. (1984). An integrated procedure for the extraction of bacterial isoprenoid quinones and polar lipids. *J. Microbiol. Methods.* 2, 233–241. doi: 10.1016/0167-7012(84)90018-6

Moreno-Vivian, C., Cabello, P., Martinez-Luque, M., Blasco, R., and Castillo, F. (1999). Prokaryotic nitrate reduction: molecular properties and functional distinction among bacterial nitrate reductases. *J. Bacteriol.* 181, 6573–6584. doi: 10.1128/JB.181.21.6573-6584.1999

Na, S. I., Kim, Y. O., Yoon, S. H., Ha, S. M., Baek, I., and Chun, J. (2018). UBCG: Up-to-date bacterial core gene set and pipeline for phylogenomic tree reconstruction. *J. Microbiol.* 56, 280–285. doi: 10.1007/s12275-018-8014-6

Overbeek, R., Olson, R., Pusch, G. D., Olsen, G. J., Davis, J. J., Disz, T., et al. (2014). The SEED and the rapid annotation of microbial genomes using subsystems technology (RAST). *Nucleic Acids Res.* 42, D206–D214. doi: 10.1093/nar/gkt1226

Pang, Y., and Wang, J. (2021). Various electron donors for biological nitrate removal: a review. *Sci. Total. Environ.* 794, 148699. doi: 10.1016/j.scitotenv.2021.148699

Parks, D. H., Imelfort, M., Skennerton, C. T., Hugenholtz, P., and Tyson, G. W. (2015). CheckM: assessing the quality of microbial genomes recovered from isolates, single cells, and metagenomes. *Genome Res.* 25, 1043–1055. doi: 10.1101/gr.186072.114

Rajta, A., Bhatia, R., Setia, H., and Pathania, P. (2020). Role of heterotrophic aerobic denitrifying bacteria in nitrate removal from wastewater. *J. Appl. Microbiol.* 128, 1261–1278. doi: 10.1111/jam.14476

Rezvani, F., Sarrafzadeh, M. H., Ebrahimi, S., and Oh, H. M. (2019). Nitrate removal from drinking water with a focus on biological methods: a review. *Environ. Sci. Pollut. Res. Int.* 26, 1124–1141. doi: 10.1007/s11356-017-9185-0

Richter, M., and Rossello-Mora, R. (2009). Shifting the genomic gold standard for the prokaryotic species definition. *Proc. Natl. Acad. Sci. U. S. A.* 106, 19126–19131. doi: 10.1073/pnas.0906412106

Rout, P. R., Bhunia, P., and Dash, R. R. (2017). Simultaneous removal of nitrogen and phosphorous from domestic wastewater using *Bacillus cereus* GS-5 strain exhibiting heterotrophic nitrification, aerobic denitrification and denitrifying phosphorous removal. *Bioresour. Technol.* 244, 484–495. doi: 10.1016/j.biortech.2017.07.186

Rudra, B., and Gupta, R. S. (2021). Phylogenomic and comparative genomic analyses of species of the family Pseudomonadaceae: Proposals for the genera *Halopseudomonas* gen. nov. and Atopomonas gen. nov., merger of the genus Oblitimonas with the genus Thiopseudomonas, and transfer of some

misclassified species of the genus Pseudomonas into other genera. *Int. J. Syst. Evol. Microbiol.* 71, 005011. doi: 10.1099/ijsem.0.005011

Seemann, T. (2014). Prokka: rapid prokaryotic genome annotation. *Bioinformatics* 30, 2068–2069. doi: 10.1093/bioinformatics/btu153

Sood, U., Hira, P., Kumar, R., Bajaj, A., Rao, D. L. N., Lal, R., et al. (2019). Comparative genomic analyses reveal core-genome-wide genes under positive selection and major regulatory hubs in outlier strains of *Pseudomonas aeruginosa*. *Front. Microbiol.* 10, 53. doi: 10.3389/fmicb.2019.00053

Stackebrandt, E., and Goebel, B. M. (1994). Taxonomic Note: a place for DNA-DNA reassociation and 16s rRNA sequence analysis in the present species definition in bacteriology. *Int. J. Syst. Bacteriol.* 44, 846–849. doi: 10.1099/00207713-44-4-846

Stanborough, T., Fegan, N., Powell, S. M., Tamplin, M., and Chandry, P. S. (2018). Vibrioferrin production by the food spoilage bacterium *Pseudomonas fragi*. *FEMS Microbiol. Lett.* 365, 6. doi: 10.1093/femsle/fnx279

Stintzi, A., Barnes, C., Xu, L., and Raymond, K. N. (2000). Microbial iron transport via a siderophore shuttle: a membrane ion transport paradigm. *Proc. Natl. Acad. Sci. U. S. A.* 97, 10691–10696. doi: 10.1073/pnas.200318797

Sun, S., Wang, Y., Zang, T., wei, J., and Wu, H., Wei, C., et al. (2019). A biosurfactant-producing *Pseudomonas aeruginosa* S5 isolated from coking wastewater and its application for bioremediation of polycyclic aromatic hydrocarbons. *Bioresour. Technol.* 281, 421–428. doi: 10.1016/j.biortech.2019.02.087

Tindall, B., Sikorski, J., Smibert, R., and Krieg, N. (2007). "Phenotypic characterization and the principles of comparative systematics," in *Methods for General and Molecular Microbiology*, eds C. Reddy, T. Beveridge, J. Breznak, G. Marzluf, T. Schmidt, and L. Snyder, (Washington, DC: ASM Press), 330–393.

Wang, J. W., Cai, M., Nie, Y., Hu, B., Yang, Y., and Wu, X. L. (2020). *Pseudomonas jilinensis* sp. nov., isolated from oil production water of Jilin Oilfield in China. *Curr. Microbiol.* 77, 688–694. doi: 10.1007/s00284-019-01798-2

Wang, T., Wang, H., Chang, Y., Chu, Z., Zhao, Y., and Liu, R. (2018). Enhanced nutrients removal using reeds straw as carbon source in a laboratory scale constructed wetland. *Int. J. Environ. Res. Public Health* 15, 1081. doi: 10.3390/ijerph15061081

Wang, X., Wang, W., Zhang, Y., Sun, Z., Zhang, J., Chen, G., et al. (2019). Simultaneous nitrification and denitrification by a novel isolated *Pseudomonas* sp. JQ-H3 using polycaprolactone as carbon source. *Bioresour. Technol.* 288, 121506. doi: 10.1016/j.biortech.2019.121506

Wu, Z., Xu, F., Yang, C., Su, X., Guo, F., Xu, Q., et al. (2019). Highly efficient nitrate removal in a heterotrophic denitrification system amended with redox-active biochar: a molecular and electrochemical mechanism. *Bioresour. Technol.* 275, 297–306. doi: 10.1016/j.biortech.2018.12.058

Xie, E., Ding, A., Zheng, L., Dou, J., Anderson, B., Huang, X., et al. (2016). Screening and characterizing a denitrifying phosphorus-accumulating bacterium isolated from a circular plug-flow reactor. *Environ. Technol.* 37, 2823–2829. doi: 10.1080/09593330.2016.1167247

Xie, F., Thiri, M., and Wang, H. (2021). Simultaneous heterotrophic nitrification and aerobic denitrification by a novel isolated *Pseudomonas mendocina* X49. *Bioresour. Technol.* 319, 124198. doi: 10.1016/j.biortech.2020.124198

Yamamoto, S., Okujo, N., Yoshida, T., Matsuura, S., and Shinoda, S. (1994). Structure and iron transport activity of vibrioferrin, a new siderophore of Vibrio parahaemolyticus. *J. Biochem.* 115, 868–874. doi: 10.1093/oxfordjournals.jbchem.a124432

Yang, Z., Sun, H., Zhou, Q., Zhao, L., and Wu, W. (2020). Nitrogen removal performance in pilot-scale solid-phase denitrification systems using novel biodegradable blends for treatment of waste water treatment plants effluent. *Bioresour. Technol.* 305, 122994. doi: 10.1016/j.biortech.2020.122994

Yoon, S. H., Ha, S. M., Kwon, S., Lim, J., Kim, Y., Seo, H., et al. (2017). Introducing EzBioCloud: a taxonomically united database of 16S rRNA gene sequences and whole-genome assemblies. *Int. J. Syst. Evol. Microbiol.* 67, 1613–1617. doi: 10.1099/ijsem.0.001755

Zhang, H., Feng, J., Chen, S., Zhao, Z., Li, B., Wang, Y., et al. (2019). Geographical patterns of *nirS* gene abundance and *nirS*-type denitrifying bacterial community associated with activated sludge from different wastewater treatment plants. *Microb. Ecol.* 77, 304–316. doi: 10.1007/s00248-018-1236-7

Zhang, M., Li, A., Xu, S., Chen, M., Yao, Q., Xiao, B., et al. (2021). Sphingobacterium micropteri sp. nov. and Sphingobacterium litopenaei sp. nov., isolated from aquaculture water. *Int. J. Syst. Evol. Microbiol.* 71, 005091. doi: 10.1099/ijsem.0.005091

Zhang, M., Li, A., Yao, Q., Wu, Q., and Zhu, H. (2020). Nitrogen removal characteristics of a versatile heterotrophic nitrifying-aerobic denitrifying bacterium, *Pseudomonas bauzanensis* DN13-1, isolated from deep-sea sediment. *Bioresour. Technol.* 305, 122626. doi: 10.1016/j.biortech.2019.122626

Zhang, R. C., Chen, C., Wang, W., Shao, B., Xu, X. J., Zhou, X., et al. (2020). The stimulating metabolic mechanisms response to sulfide and oxygen in typical heterotrophic sulfide-oxidizing nitrate-reducing bacteria *Pseudomonas* C27. *Bioresour. Technol.* 309, 123451. doi: 10.1016/j.biortech.2020.123451

Zhang, S., Su, J., Zheng, Z., and Yang, S. (2020). Denitrification strategies of strain YSF15 in response to carbon scarcity: based on organic nitrogen, soluble microbial products and extracellular polymeric substances. *Bioresour. Technol.* 314, 123733. doi: 10.1016/j.biortech.2020.123733

Zhao, B., Cheng, D. Y., Tan, P., An, Q., and Guo, J. S. (2018). Characterization of an aerobic denitrifier *Pseudomonas stutzeri* strain XL-2 to achieve efficient nitrate removal. *Bioresour. Technol.* 250, 564–573. doi: 10.1016/j.biortech.2017.11.038

Zheng, Z., Ali, A., Su, J., Huang, T., Wang, Y., and Zhang, S. (2021). Fungal pellets immobilized bacterial bioreactor for efficient nitrate removal at low C/N wastewater. *Bioresour. Technol.* 332, 125113. doi: 10.1016/j.biortech.2021.125113

Zou, Y., He, S., Sun, Y., Zhang, X., Liu, Y., and Cheng, Q. (2019). *Pseudomonas urumqiensis* sp. nov., isolated from rhizosphere soil of *Alhagi sparsifolia*. *Int. J. Syst. Evol. Microbiol.* 69, 1760–1766. doi: 10.1099/ijsem.0.003390

Conflict of Interest: AL was employed by Guangdong BOWOTE BioSciTech, Co. Ltd.

The remaining authors declare that the research was conducted in the absence of any commercial or financial relationships that could be construed as a potential conflict of interest.

frontiers | Frontiers in Microbiology

ORIGINAL RESEARCH
published: 02 June 2022
doi: 10.3389/fmicb.2022.927650

Morphological and Spatial Heterogeneity of Microbial Communities in Pilot-Scale Autotrophic Integrated Fixed-Film Activated Sludge System Treating Coal to Ethylene Glycol Wastewater

*Fangxu Jia, Jiayi Chen, Xingcheng Zhao, Chenyu Liu, Yiran Li, Jinyuan Ma, Anming Yang and Hong Yao**

Beijing International Scientific and Technological Cooperation Base of Water Pollution Control Techniques for Antibiotics and Resistance Genes, Beijing Key Laboratory of Aqueous Typical Pollutants Control and Water Quality Safeguard, School of Environment, Beijing Jiaotong University, Beijing, China

OPEN ACCESS

Edited by:
Lei Miao,
Huazhong University of Science and Technology, China

Reviewed by:
Weihua Zhao,
Qingdao University of Technology, China
Yuanyuan Miao,
Qingdao University, China

***Correspondence:**
Hong Yao
yaohongts@163.com

Specialty section:
This article was submitted to Microbiotechnology, a section of the journal Frontiers in Microbiology

Received: *24 April 2022*
Accepted: *06 May 2022*
Published: *02 June 2022*

Citation:
Jia F, Chen J, Zhao X, Liu C, Li Y, Ma J, Yang A and Yao H (2022) Morphological and Spatial Heterogeneity of Microbial Communities in Pilot-Scale Autotrophic Integrated Fixed-Film Activated Sludge System Treating Coal to Ethylene Glycol Wastewater. Front. Microbiol. 13:927650. doi: 10.3389/fmicb.2022.927650

The understanding of microbial compositions in different dimensions is essential to achieve the successful design and operation of the partial nitritation/anammox (PN/A) process. This study investigated the microbial communities of different sludge morphologies and spatial distribution in the one-stage PN/A process of treating real coal to ethylene glycol (CtEG) wastewater at a pilot-scale integrated fixed-film activated sludge (IFAS) reactor. The results showed that ammonia-oxidizing bacteria (AOB) was mainly distributed in flocs (13.56 ± 3.16%), whereas anammox bacteria (AnAOB) was dominated in the biofilms (17.88 ± 8.05%). Furthermore, the dominant AnAOB genus in biofilms among the first three chambers was *Candidatus Brocadia* (6.46 ± 2.14% to 11.82 ± 6.33%), whereas it was unexpectedly transformed to *Candidatus Kuenenia* (9.47 ± 1.70%) and *Candidatus Anammoxoglobus* (8.56 ± 4.69%) in the last chamber. This demonstrated that the niche differentiation resulting from morphological (dissolved oxygen) and spatial heterogeneity (gradient distribution of nutrients and toxins) was the main reason for dominant bacterial distribution. Overall, this study presents more comprehensive information on the heterogeneous distribution and transformation of communities in PN/A processes, providing a theoretical basis for targeted culture and selection of microbial communities in practical engineering.

Keywords: anammox, the integrated fixed-film activated sludge (IFAS), partial nitritation/anammox (PN/A), heterogeneity, population shifts

INTRODUCTION

The anaerobic ammonia oxidation (anammox) was recognized as an efficient and sustainable alternative to the conventional biological denitrification process due to its advantages of no organic carbon required and aeration savings (Ma et al., 2016). Among the many anammox coupled nitrogen removal processes, one-stage partial nitritation/anammox (PN/A) was greatly favored due

to the more efficient and low cost (Lackner et al., 2014). Nevertheless, the long-term stable operation of the one-stage PN/A process still presents two major challenges: the balance of cooperation between anammox bacteria (AnAOB) and ammonia-oxidizing bacteria (AOB) and suppressing the growth of nitrite-oxidizing bacteria (NOB) (Zheng et al., 2016).

The integrated fixed-film activated sludge (IFAS) reactor served as an emerging technology that can be used to solve the above problems. It combined two types of sludge (biofilm and flocs) in a single system, which provided the optimal habitat for AnAOB and AOB cooperation, meanwhile inhibiting the growth of NOB by flocs sludge discharge (Zhang et al., 2022). Therefore, an increasing number of studies have begun to focus on the operation mode and wastewater treatment efficiency of IFAS, while the research on microbial community dynamics, especially for AnAOB population transformation in plug-flow mode, was limited. Due to differences in physiological characteristics of AnAOB at the genus level, the niche differentiation among genera likely occurred during the change in environmental conditions. For example, *Candidatus Brocadia* (K_{NO2-} = 34–350 μM) preferred to enrich in high nitrite concentrations than *Candidatus Kuenenia* (K_{NO2-} = 0.2–3 μM) (Zhang and Okabe, 2020); *C. Kuenenia* (K_{o2} = 0–200 μM) was able to survive in suspended sludge due to the higher oxygen tolerance compared with *C. Brocadia* (K_{o2} = 1–120 μM) and *Candidatus Scalindua* (K_{o2} = 10–20 μM) (Oshiki et al., 2016); *C. Brocadia* and *Candidatus Anammoxoglobus* can survive in the presence of organic matter due to their metabolic diversity (Kartal et al., 2007a,b). These studies suggested that different AnAOB genera may present interspecific competition based on differences in survival space and substrate concentration, resulting in the elimination or reduced abundance of inferior species in the habitat.

Currently, many studies have reported population shifts among various AnAOB genera under environmental and operating condition changes in upflow and completely mixed-mode reactors. For example, *C. Brocadia* in both suspended and biofilm sludge shifted to *C. Kuenenia* with the gradual reduction of hydraulic retention time in a UASB reactor (Park et al., 2015), and the original dominant *C. Brocadia* was shifted to *C. Anammoxoglobus* after increasing the propionic acid concentration in an SBR reactor (Kartal et al., 2007b) or gradually reducing temperature and ammonia in the CANON reactor (Gonzalez-Martinez et al., 2016). However, the above studies only tended to concentrate on revealing the relationship between AnAOB population shifts and surrounding environments or operations within the overall reactor, and less attention was paid to the morphological and spatial heterogeneity of the AnAOB genus at different zones in the plug-flow mode IFAS reactor. Furthermore, the IFAS reactor with a plug-flow mode is most likely to develop the population shift of AnAOB genera during long-term operation due to the degradation of pollutants along the flow direction, especially in the pilot- or full-scale IFAS for real industrial wastewater treatment.

Therefore, this study applied a pilot-scale IFAS reactor for the treatment of real coal to ethylene glycol (CtEG) wastewater and used 16S rRNA high-throughput sequencing and various biometrical methods to investigate the following two objectives: (1) the distribution of functional bacterial populations in sludge with different morphologies and spatial locations and (2) the potential factors influencing the transformation of dominant anammox genus. The results could provide a reference for the community composition and transformation of the PN/A process, which is essential to achieve IFAS systems efficiently treating similar types of wastewater in full-scale engineering applications.

MATERIALS AND METHODS

Reactor Construction and Wastewater

A simplified schematic of the pilot-scale IFAS reactor is illustrated in **Figure 1**. The effective volume of IFAS was 2 m^3 (volume ratio was 3:2:2:1 for each chamber) and operated under oxic phase (DO < 0.5 $mg \cdot L^{-1}$) for treatment of CtEG wastewater originating from the full-scale plant in Tongliao City, Inner Mongolia, China. The sponge carriers with mature anammox biofilms (dominated by *C. Brocadia*, **Supplementary Figure 1**) were used as seed sludge for the anammox reactor start-up. Additionally, the polyurethane sponge carriers (size of 10 × 10 × 10 mm, density of 0.9 $g \cdot cm^{-3}$, and specific surface area of 2,800 $m^2 \cdot m^{-3}$) were fixed in the reactor with a special design as follows: the sponge carriers were first filled into spherical cages and connected together with steel wires, and then the steel wires were fixed to the shelves (**Supplementary Figure 2**). In addition, the detail of the operational procedure and the wastewater characteristics were as previously reported (Yao et al., 2021).

Sampling and Microbial Community Analysis

Sludge samples were collected in triplicate from flocculent and biofilm sludge in each chamber at 132 days of the stabilization phase of the reactor. The sample names are as shown in **Figure 1** where F represents the floc, B represents the biofilm, t, m, and b represent the top, middle, and bottom, respectively, and the numbers 1–4 indicate the chamber numbers. Therefore, a total of 12 (4 × 3) flocculent sludge samples and 36 (12 × 3) biofilm samples were obtained.

Genomic DNA was extracted from each sample using the FastDNA SPIN Kit for Soil (QBIOgene Inc., Carlsbad, CA, United States). The 16S rDNA V3-V4 region was specifically amplified with bacterial universal primers 338F (5′-ACTCCTACGGGAGGCAGCAG-3′) and 806R (5′-GGACTACHVGGGTWTCTAAT-3′). Subsequently, the PCR products were purified using the AxyPrep DNA Gel Extraction Kit (Axygen Biosciences, Union City, CA, United States). Amplification products of all samples were sequenced on the Illumina MiSeq PE300 platform. Sequences shorter than 200 bps, homopolymers with 6 bps and primer mismatches, as well as quality scores below 25 and chimeras were removed. High-quality sequences were treated with the Mothur software program (version 1.44.3) using a 97% sequence similarity threshold to

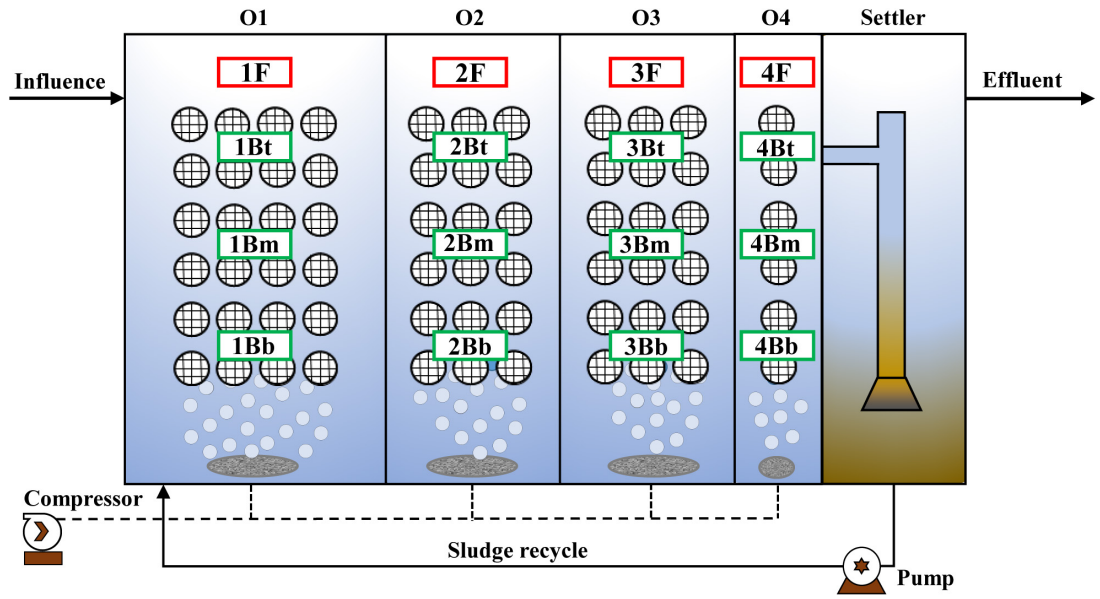

FIGURE 1 | Schematic diagram of the pilot-scale integrated fixed-film activated sludge (IFAS) reactor and sampling scheme.

generate operational taxonomic units (OTUs). Additionally, subsampling was performed to an equal sequencing depth of 24,338 reads per sample using the "single_rarefaction.py" module of the QIIME software (version 1.9.1). The raw sequencing data were uploaded to the NCBI Sequence Read Archive under accession no. PRJNA795428.

Spectral and Chemical Analytical Methods

Wastewater samples were collected in triplicate from each chamber at 132 days. The excitation-emission matrix (EEM) fluorescence spectroscopy protocol was modified according to previous research (Jia et al., 2016). In brief, the samples were diluted with deionized water to eliminate the inner-filter effect of fluorescence. The EEM fluorescence spectroscopy was measured using luminescence spectrometry (F-7000, Hitachi, Japan). The spectrometer displayed a maximum emission intensity of 5,000 arbitrary units (AUs). The EEM spectra were collected with subsequent scanning emission spectra from 290 to 550 nm by varying the excitation wavelength from 200 to 400 nm. To eliminate second-order Raleigh scattering, a 290-nm cutoff was used in scanning. The spectrum of deionized water was recorded as a blank.

The concentrations of COD, NH_4^+-N, NO_2^--N, and NO_3^--N were determined according to standard methods (APHA, 2005). Furthermore, pH, DO, and temperature were monitored with WTW-pH/Oxi 340i oxygen/pH probes (WTW Company, Germany). The chemical analyses were performed in duplicate using analytical grade chemicals.

Statistical Analysis

Principal component analysis (PCA) with Adonis pairwise test was performed using R (Version 4.1.0). The significantly different taxa in the microbial communities of each sample group were identified using the linear discriminant analysis (LDA) effect size (LEfSe) method.[1] In addition, the Welch's *t*-test was used to calculate statistical differences between core functional microorganisms in different groups using the SPSS software (version 26.0).

RESULTS

The Performance of the Partial Nitritation/Anammox System

The variation of pollutant concentration in the IFAS reactor during the stable operation stage (123–145 days) is shown in **Figure 2A**. During this stage, the nitrogen removal rate (NRR) was 0.5 ± 0.1 kg $N \cdot m^{-3} \cdot day^{-1}$, the COD removal rate was 62.0 ± 11.5%, and the total nitrogen removal efficiency (NRE) was 79.6 ± 4.4%. Furthermore, the values of the ratio between nitrate production and ammonium consumption (1.5 ± 2.3%) were obviously lower than the theoretical value of 11% (Miao et al., 2016), which were confirmed to be associated with the NO_3^--N reduction process by denitrification (Yao et al., 2021). In addition, the evolution of the pollutant concentration in each chamber of the reactor was also analyzed on day 132 (**Figure 2B**). To be specific, the largest contribution to NRE was achieved by the first chamber (69.3 ± 7.3%) and gradually improved to 76.1 ± 2.1% in the last chamber. Meanwhile, the COD removal rates showed a similar pattern along the plug-flow direction (35.8 ± 3.8% to 59.1 ± 2.9%).

To further understand the evolution of organic substance components in the wastewater of the PN/A system, EEM

[1]https://huttenhower.sph.harvard.edu/lefse/

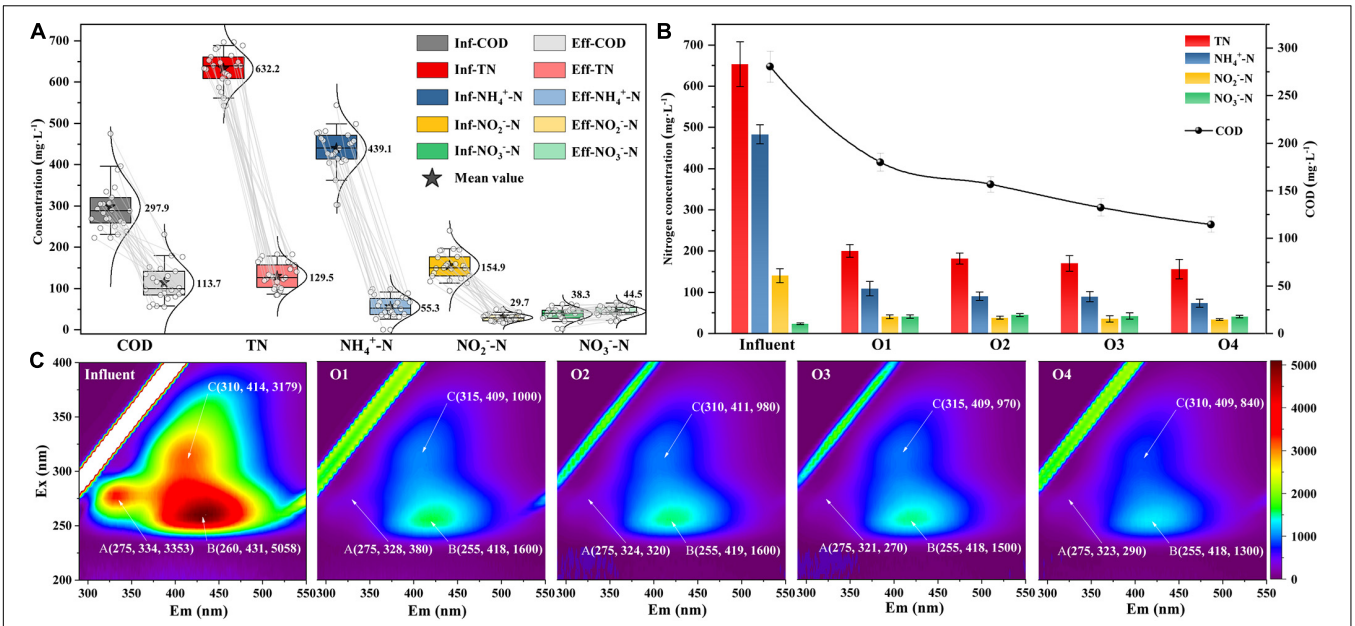

FIGURE 2 | (A) The pollutant removal performance of IFAS reactor during stable operation stage, **(B)** pollutant concentration, and **(C)** fluorescence components along the plug-flow direction in each chamber.

fluorescence spectral analysis was carried out (**Figure 2C**). According to the division principle of fluorescence spectral regions (Chen et al., 2003), three fluorescence peaks were identified from EEM fluorescence spectra of the wastewater samples in all chambers that can be attributed to soluble microbial by-product (SMP)-like (peak A, E_x/E_m = 275/321–334), the fulvic acid-like (peak B, E_x/E_m = 255–260/418–431), and humic acid-like (peak C, E_x/E_m = 310–315/409–414) component. Among the three peaks, peak B had the highest fluorescence intensity in influent and subsequently decreased from 68.4% (chamber 1) to 18.8% (chamber 4) with plug flow. The regularity of fluorescence intensity distributions of peak C (68.5–16.0%) coincided with that of peak B, whereas almost all the SMP-like substances (peak A) were degraded in the first chamber (88.7%) and virtually undetectable in the subsequent chambers. These results may be related to the extent of biodegradable organic matter, that is, humic acid and fulvic acid-like substances were refractory organics (Fang et al., 2019).

Microbial Community Composition

The 16S rRNA high-throughput sequencing was used to investigate the microbial communities in different chambers for floc and biofilm samples, which were collected at 132 days of the stable operation period in the IFAS reactor. The α-diversity parameters of the microbial communities in all samples are concluded in **Supplementary Table 1**. The Good's coverage of all OTUs was higher than 98.9%, and the rarefaction curves also showed clear and smooth horizontal asymptotes (**Supplementary Figure 3**), and both results suggest a near-complete sampling of the community. As for the Chao 1 index (**Supplementary Figure 4A**), group B (biofilm samples) was significantly higher than that of group F (floc samples) ($p < 0.001$), which indicated that the biomass abundance on the biofilm was higher than that of the flocculent sludge. In addition, the Chao 1 index of biofilm samples in each chamber displayed an obvious decreasing trend with flow direction, and the biofilm samples in chamber 1 (group 1B) was significantly higher than others ($p < 0.05$), which may be due to the higher nutrients in the front chamber that favors microbial colonization. In contrast to the Chao 1 index, the Shannon index of group F was significantly higher than that of group B ($p < 0.001$) and no significant difference between biofilm samples in each chamber (**Supplementary Figure 4B**). Apart from the above, there was no significant difference in the index of floc samples from each chamber and biofilm samples from different depths.

The microbial community structures of floc and biofilm samples from different chambers are depicted in **Figure 3**. At the phylum level, the predominant phyla for both floc and biofilm samples were *Chloroflexi*, *Proteobacteria, Planctomycetes,* and *Bacteroidetes*, which together accounted for more than 85% of the total microbial community detected. Obviously, the abundance of bacterial phyla detected in the two groups was dramatically different. Specifically, *Proteobacteria* and *Bacteroidetes* were dominant in the flocculent sludge, while *Chloroflexi* and *Planctomycetes* occupied higher proportions in the biofilm sludge. At the genus level, the dominant genera of flocculent sludge were *Denitratisoma* (14.8 ± 1.6%), *Nitrosomonas* (13.2 ± 0.7%), and *Thiobacillus* (6.4 ± 0.5%). While in the biofilm sludge, the dominant genera were three types of AnAOB, namely, *C. Brocadia* (7.6 ± 5.0%), *C. Kuenenia* (5.2 ± 3.3%), and *C. Anammoxoglobus* (5.1 ± 4.2%). In addition, *Ignavibacterium*,

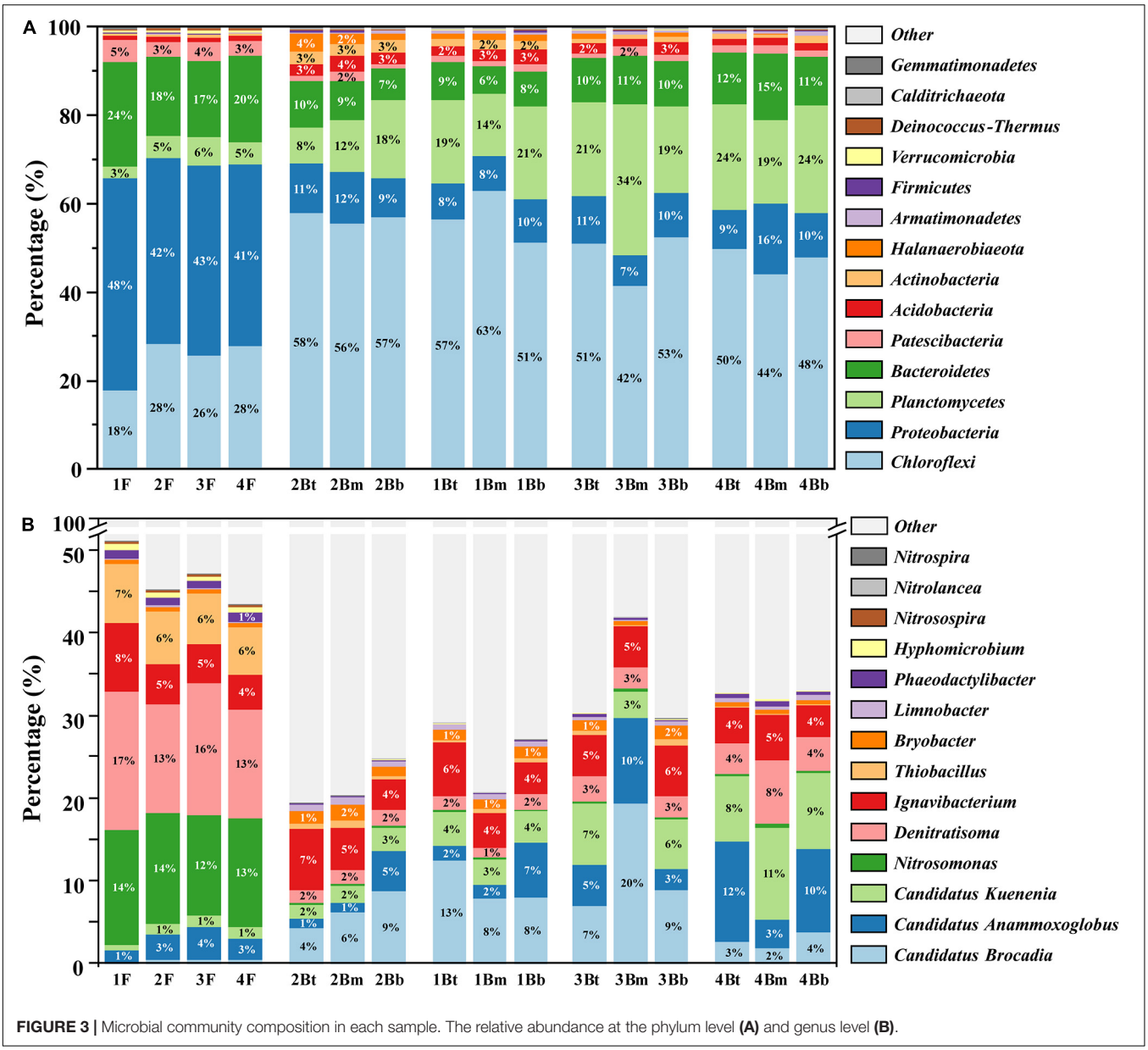

FIGURE 3 | Microbial community composition in each sample. The relative abundance at the phylum level **(A)** and genus level **(B)**.

as a type of fermentative bacterium, was dominantly observed in both flocculent (5.5 ± 1.7%) and biofilm (5.1 ± 1.1%) sludge.

Additionally, the PCA was used to distinguish sample cluster distribution in morphological and spatial dimensions. As shown in **Figure 4A**, floc and biofilm samples were clustered according to their respective sludge morphology and showed clear separation (p = 0.001). Meanwhile, an obvious grouping of the biofilm samples in each chamber was observed (p = 0.001) (**Figure 4B**). In addition, the grouping trends (chambers 1–4) were distinct shifts along PC1 axes from right to left, although there was a partial overlap between groups 1B and 2B. However, the samples at different depths of each chamber could not be separated effectively and showed large overlapping areas with each other (p = 0.931) (**Figure 4C**). The above results indicated that the difference in microbial community composition was significant in different morphologies and chambers, while not significant in different depths.

The significantly different taxa of sludge samples in different groups were further analyzed by the LEfSe algorithm (**Figure 5**). By comparing the F and B groups (**Figures 5A,C**), it was found that the most representative biomarkers (LDA score > 4) in flocculent were *Proteobacteria* (contain *Nitrosomonas*, *Denitratisoma*, and *Thiobacillus* members) and *Bacteroidetes*, while in biofilm sludge were *Chloroflexi* and *Planctomycetes* (contain *C. Brocadia* and *C. Kuenenia* members). These statistical results were basically consistent with the visual differences between the F and B groups (see above). As for biofilm samples in each chamber, the number of differential

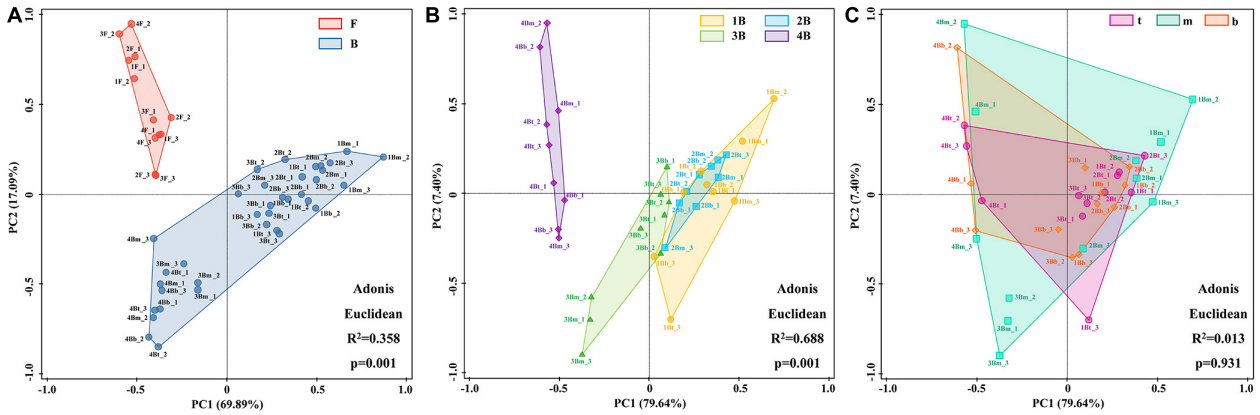

FIGURE 4 | Principal component analysis (PCA) of bacterial population distribution in different groups at the genus level. **(A)** Flocs vs. biofilms; **(B)** biofilms in each chamber; and **(C)** biofilms in different depths.

microorganisms decreased markedly compared with the F-B group (**Figures 5B,D**). The *Firmicutes* and *Spirochetes* were filtered as biomarkers in group 1B at the phylum level, even with lower LDA scores, whereas *C. Brocadia* and *Denitratisoma* were the most representative biomarkers in groups 3B and 4B at the genus level, respectively. As expected, there were no significantly different taxa in biofilm samples from different depths (data not shown), which showed the same results as the α -diversity.

Core Functional Microorganism

The distribution characteristics of core functional microorganisms of the PN/A process in flocculent and biofilm sludge from each chamber were compared (**Figure 6**). This system detected three types of AOB (*Nitrosomonas*, *Nitrosospira,* and *Unknown AOB*) and three types of AnAOB (*C. Brocadia*, *C. Kuenenia,* and *C. Anammoxoglobus*). As shown in **Figures 6A,C**, AOB was mainly concentrated in flocculent sludge (13.6 ± 3.2%), where *Nitrosomonas* was the dominant genus with 97% of the total AOB. Other genera of AOB exhibited an identical distribution pattern with *Nitrosomonas*, but the abundance was extremely low and can be ignored. In contrast, the AnAOB was mainly enriched in biofilm (17.9 ± 8.1%), and only a small amount of *C. Kuenenia* (1.2 ± 0.8%) and *C. Anammoxoglobus* (2.8 ± 1.8%) were detected in flocculent sludge with almost no detection of *C. Brocadia* (0.4 ± 0.3%) (**Figures 6B,D**). Among the biofilms of each chamber, the content of *C. Brocadia* increased from 6.5 ± 2.1% to 11.8 ± 6.3% in the first three chambers and decreased substantially to 2.8 ± 1.0% in the last chamber. Nevertheless, the abundance of *C. Kuenenia* and *C. Anammoxoglobus* gradually increased along with the plug-flow direction from 2.2 ± 0.6% to 9.5 ± 1.7% and 2.4 ± 2.1% to 8.6 ± 4.7%, respectively. Moreover, almost no significant differences in core functional microorganisms could be observed either between flocculent sludge in different chambers or between biofilm sludge in different depths. Besides, the abundance of NOB was extremely low in both flocculent (0.3 ± 0.02%) and biofilm sludge (0.03 ± 0.01%), thus it will not be discussed in this study.

DISCUSSION

Morphological Heterogeneity of Flocs and Biofilms

Balancing the cooperation between AOB and AnAOB for nitrite was key to the successful operation of the PN/A process. This study effectively solves this problem by integrating flocs and biofilms to separate functional bacteria in different spaces. As shown in **Figures 4**, **6**, AOB preferred to grow in flocculent sludge (13.6 ± 3.2%), while AnAOB was mainly distributed in biofilms (17.9 ± 8.1%). Previous studies indicated that the morphological heterogeneity of microbial community was determined by the differences in the characteristic of the floc and the biofilm (Laureni et al., 2019). In flocculent sludge, sufficient DO and ammonium supply allowed AOB with more survival advantage to enrich, which provided continuous nitrite to AnAOB (Wang et al., 2018). On the contrary, AnAOB was more prone to form aggregates in biofilms which was equivalent to prolonging the sludge retention time (SRT), providing an effective strategy for enriching slow-growing AnAOB (Zhang et al., 2022). Furthermore, the high mass transfer resistance of biofilm could be considered a reliable barrier to providing better protection for AnAOB against high DO and toxic compound interference (Zheng et al., 2016).

Although AnAOB preferred to be enriched in biofilms, a small fraction of AnAOB (mainly *C. Anammoxoglobus* and *C. Kuenenia*) was still detected in the flocculent sludge (**Figures 6B,D**), which was probably attributed to the differences in substrate affinity among the different genera of AnAOB. Specifically, *C. Kuenenia* possessed higher oxygen tolerance relative to other genera, which may allow it to survive in the flocs (Oshiki et al., 2016). Due to the capacity of *C. Anammoxoglobus* to degrade organic matter (Kartal et al., 2007b), it is reasonable to speculate that the small molecular organics originating

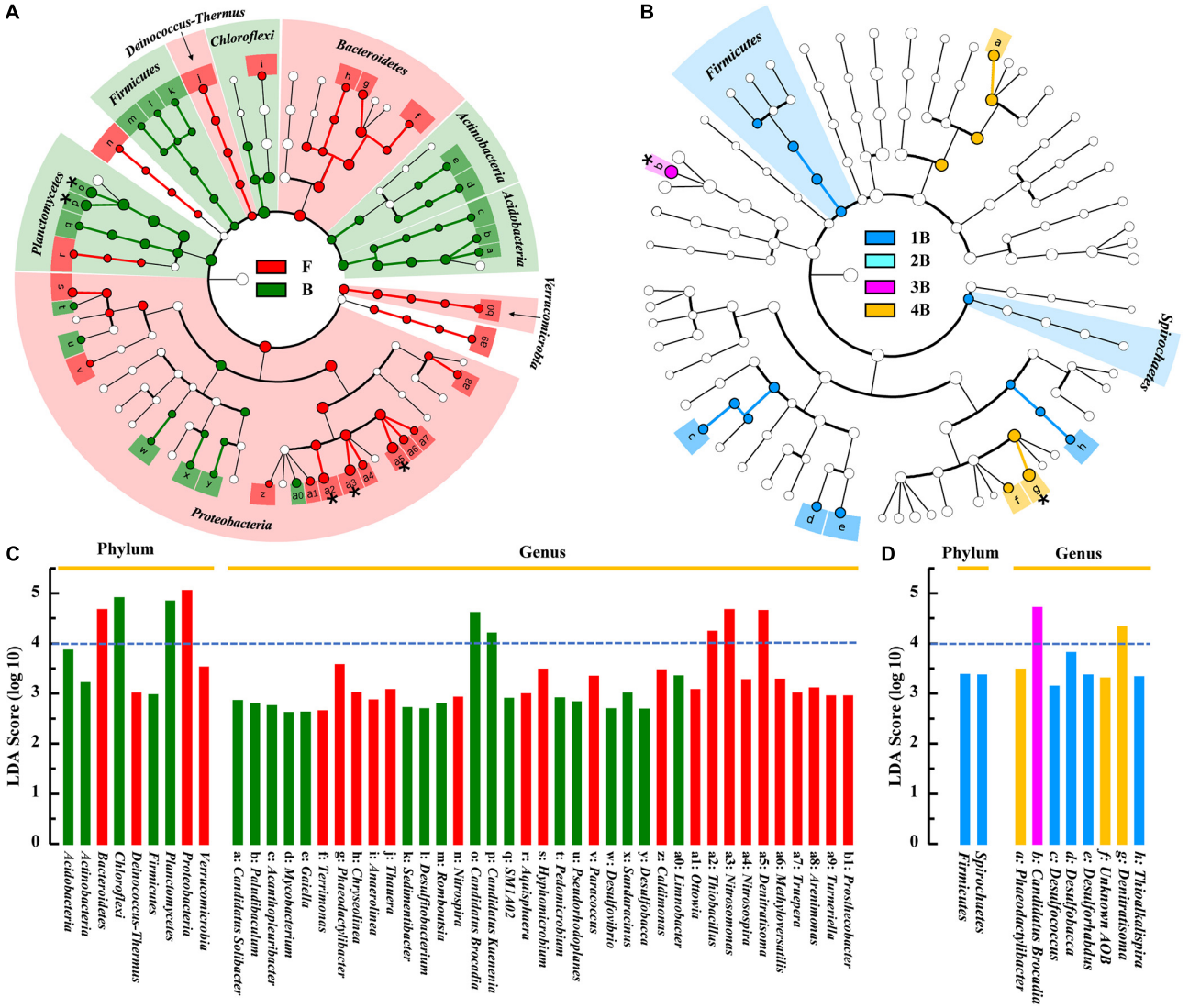

FIGURE 5 | Differential analysis of microbial communities in different groups of IFAS reactor by LEfSe. Phylogenetic dendrogram of biomarker bacteria in floc and biofilm samples **(A)** and in biofilm samples of each chamber **(B)**; the LDA score of the abundant biomarkers in floc and biofilm samples **(C)**, and in biofilm samples of each chamber **(D)**. The linear discriminant analysis (LDA) score larger than 4 was marked with an asterisk in the phylogenetic dendrogram.

from the CtEG wastewater biodegradation process (**Figure 2C**) could provide available substrates for its growth (Du et al., 2017). Coupled with the mass transfer limitation of organics in biofilms, allows *C. Anammoxoglobus* to survive in the floc sludge. For another, it is understandable that *C. Anammoxoglobus* and *C. Kuenenia* can easily grow on the surface of biofilm sludge based on the above-mentioned reasons. Therefore, a part of the microbial community flocculent sludge was probably contributed by biofilm detachment (Vlaeminck Siegfried et al., 2010; Yang et al., 2019b).

Based on the LEfSe analysis, the other differential microorganisms apart from AOB and AnAOB were also found in two types of morphological sludge. There into, the most representative biomarkers in flocs were *Denitratisoma* and *Thiobacillus* (**Figure 5C**), which possessed NO_x^- reduction capacity and were usually regarded as denitrifiers (Fahrbach et al., 2006; Deng et al., 2021). The lower DO of this system (< 0.5 mg·L^{-1}) allowed the above facultative anaerobic denitrifiers to reside in the flocculent sludge, thus acquiring more organics to provide a better habitat for AnAOB (Yang et al., 2019a). Moreover, such community distribution could further improve the total nitrogen removal efficiency of the PN/A system by reducing effluent nitrate (partial denitrification process), which has been confirmed by our previous study (Yao et al., 2021).

Spatial Heterogeneity in Each Chamber

At present, most studies focused on the overall differences in microbial communities in different periods of reactor operation, while less attention has been given to the variation of key

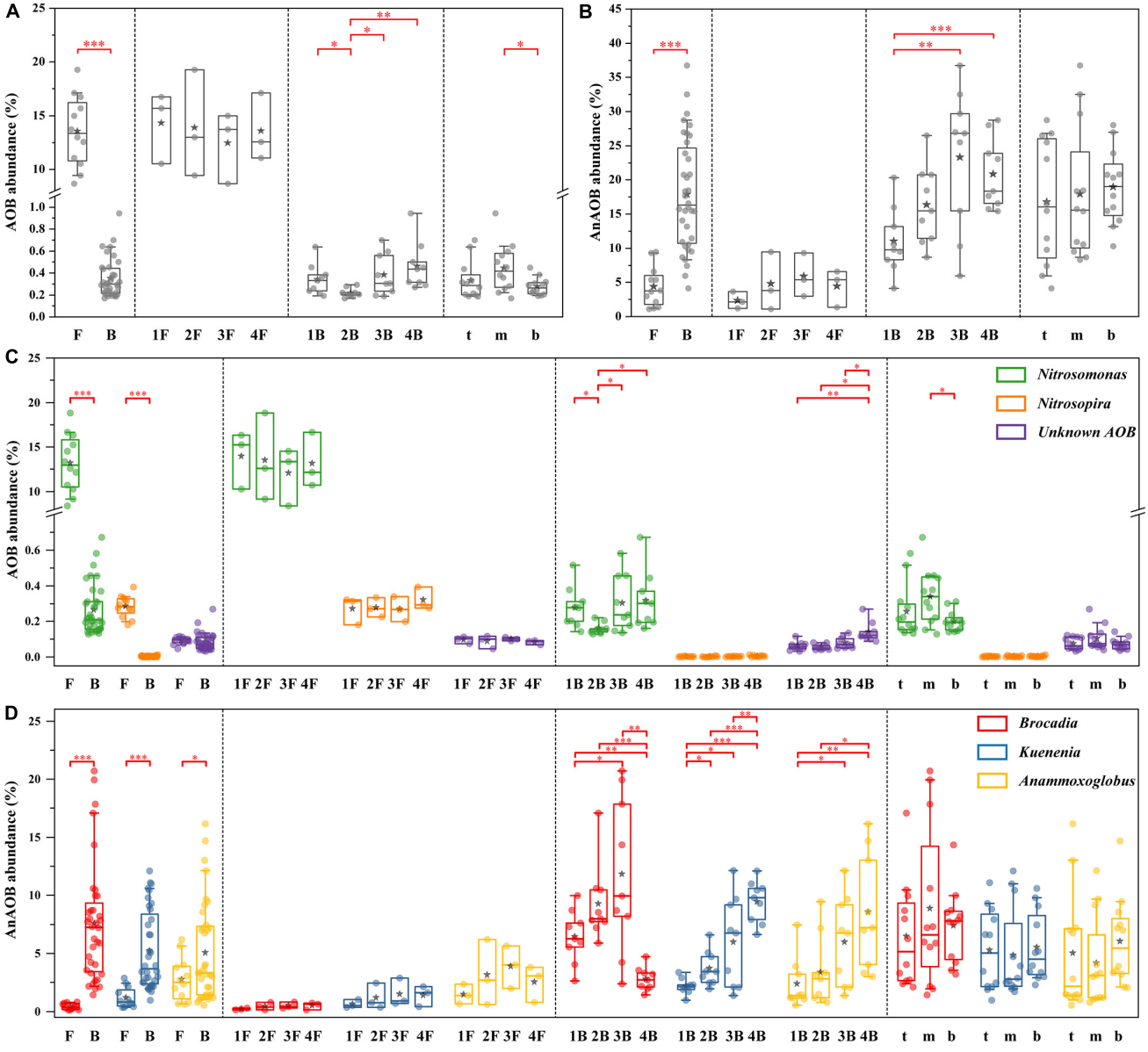

FIGURE 6 | Distribution of core functional microorganisms in different groups. The relative abundance of overall ammonia oxidizing bacteria (AOB) **(A)** and anammox bacteria (AnAOB) **(B)**; the relative abundance of AOB **(C)** and AnAOB **(D)** at genus level. Welch's *t*-test, asterisk (*) indicates $p < 0.05$, asterisk (**) indicates $p < 0.01$, asterisk (***) indicates $p < 0.001$.

functional bacteria at different locations in a reactor. To better reveal the spatial heterogeneity of microbial communities, this study explored the distribution of key functional microorganisms in different chambers and depths. The results indicated that the abundance of AOB and AnAOB in flocculent sludge were not significantly ($p > 0.05$) different between each chamber (**Figure 4**), which may be caused by the uniformly mixing of flocs with the help of sludge recycle and micro-aeration in a plug-flow mode IFAS reactor. Conversely, the abundance of AnAOB in biofilm sludge demonstrated significant differences ($p < 0.05$) between each chamber due to the long SRT of biofilm sludge.

The abundance of the AnAOB genus in the biofilm sludge showed a gradual increasing trend in each chamber (except for *C. Brocadia* in the last chamber, **Figures 6B,D**), which may be related to the continuous improvement of water quality along with the flow direction. In fact, some microorganisms with a strong degradation ability for toxic or refractory organics were detected in this system, such as *Ignavibacterium*, *Limnobacter*, and *Thiobacillus*, which gradually decreased the toxicity of the wastewater and provide a favorable living environment for AnAOB growth (Ma et al., 2015; Zheng et al., 2019; Li et al., 2020).

In addition, the population shift of AnAOB occurred in each chamber of the IFAS reactor (**Figure 6D**). Concretely,

C. Brocadia was the advantage AnAOB with a significantly higher abundance than *C. Kuenenia* and *C. Anammoxoglobus* in the first three chambers. The results of competition among AnAOB genera may be related to niche differences due to their respective growth characteristics. First, based on the theory of priority effect, that is, the establishment of species in a community can depend on the order of their arrival (Debray et al., 2022). In this study, the mature anammox biofilms dominated by *C. Brocadia* were used as the inoculation sludge in the IFAS system (**Supplementary Figure 1**), which made the *C. Brocadia* depletes resources preferentially, thereby inhibiting the establishment of a late arriver (*C. Kuenenia* and *C. Anammoxoglobus*). Second, the maximum specific growth rates of the *C. Brocadia* genus (0.0027–0.0088 h^{-1}) were higher than others, which suggested that it appeared to grow faster and more competitive in biofilms (Oshiki et al., 2016). Third, the *C. Brocadia* has the most hydrophobic surface in extracellular polymeric substances (EPS) than other AnAOB and thus exhibits a superior aggregation capability, which can promote the rapid development of microbial aggregates and enhance the retention effect in biofilms (Jia et al., 2017, 2021; Ali et al., 2018).

Furthermore, the abundance of *C. Brocadia* suddenly decreased in the last chamber and shifted to *C. Kuenenia* and *C. Anammoxoglobu*, which may be related to the following reasons. On the one hand, *C. Kuenenia* possessed a stronger ammonia affinity than *C. Brocadia* (Oshiki et al., 2016), which allowed *C. Kuenenia* to survive in a low ammonia environment, such as the last chamber in this study. On the other hand, *C. Anammoxoglobu* showed outstanding small molecule organic degradation ability compared with *C. Brocadia* (Oshiki et al., 2016). Therefore, some heterotrophic bacteria in this system can continuously decompose complex macromolecular organics into small molecules along the flow direction (He et al., 2021), allowing *C. Anammoxoglobu* to compete for more ecological niches using additional substrates, which also confirms the previous findings of the population shift from *C. Brocadia* to *C. Anammoxoglobu* under propionic condition (Kartal et al., 2007b).

Significance of This Study

In this study, the reasonable distribution of microbial communities in morphology and space was the key to the successful operation of the autotrophic IFAS system. This suggested that the coexistence of AOB and AnAOB with different physiological characteristics inside the single system was the premise to ensure the stable operation of the IFAS reactor. It is well known that the selection of suitable inoculated sludge is crucial for the successful start-up of the anammox process (Chi et al., 2018). Therefore, the results of niche differentiation in this study inspired the targeted selection of microbial communities in practical engineering applications.

Whether designing new reactors or modifying existing A/O or A/A/O to PN/A process, inoculating with mature anammox sludge of specific genera could be considered depending on the reactor type or water quality. This avoided the population shift of dominant anammox resulting from the long-term sludge adaptive domestication, thus greatly saving system start-up time and achieving stable operation. Based on the findings of this study, we recommended that the front area with high ammonia concentration should be artificially inoculated with *C. Brocadia* dominated sludge, whereas the later area with lower ammonia concentration should be employed with *C. Kuenenia* or *C. Anammoxoglobu* dominated sludge as inoculum in plug-flow PN/A reactor.

Regrettably, more detailed experimental evidence between wastewater chemical components and microbial community metabolism was lacking due to the limitations of the experimental conditions *in situ* of the pilot study. Moreover, the identification of anammox species niches remained a challenge. For further explanation of the morphological and spatial heterogeneity of the microorganisms in IFAS reactor, more attention should be paid to future studies to (1) monitor the changes in the composition and content of toxic or refractory organics from real wastewater; (2) conduct further laboratory studies to explore the effects of different substrate types and concentrations on the niche differentiation among AnAOB species; and (3) employ appropriate anammox inoculated sludge to verify the start-up effect of the PN/A system.

CONCLUSION

In this study, the PN/A process was successfully implemented in the pilot-scale IFAS system to treat CtEG wastewater, and the morphological and spatial heterogeneity of microbial community was investigated, with the key conclusions including:

- The IFAS reactor combined different morphologies of sludge (biofilm and floc) to provide an ideal habitat for AnAOB and AOB, respectively;
- Microenvironmental changes caused by the gradient distribution of substrates may be important factors influencing the dominant AnAOB population shift;
- The revelation of spatial heterogeneity provided supporting information for the targeted cultivation and selection of microbial communities in future engineering applications.

DATA AVAILABILITY STATEMENT

The datasets presented in this study can be found in online repositories. The names of the repository/repositories and accession number(s) can be found in the article/**Supplementary Material**.

AUTHOR CONTRIBUTIONS

FJ: writing—review and editing and funding acquisition. JC: investigation and visualization. XZ: writing—original draft. CL:

data curation. YL: methodology and investigation. JM and AY: investigation. HY: conceptualization, supervision, and funding acquisition. All authors contributed to the article and approved the submitted version.

FUNDING

This research was financially supported by the Beijing Outstanding Young Scientist Program (BJJWZYJH01201910004016), the National Natural Science Foundation of China (51908029), and the Fundamental Research Funds for the Central Universities (2019JBM088).

SUPPLEMENTARY MATERIAL

The Supplementary Material for this article can be found online at: https://www.frontiersin.org/articles/10.3389/fmicb.2022.927650/full#supplementary-material

REFERENCES

Ali, M., Shaw, D. R., Zhang, L., Haroon, M. F., Narita, Y., Emwas, A.-H., et al. (2018). Aggregation ability of three phylogenetically distant anammox bacterial species. *Water Res.* 143, 10–18. doi: 10.1016/j.watres.2018.06.007

APHA (2005). *Standard methods for the examination for water and wastewater american public health associationr, 21st Ed*. Washington, DC: American Public Health Association.

Chen, W., Westerhoff, P., Leenheer, J. A., and Booksh, K. (2003). Fluorescence excitation-emission matrix regional integration to quantify spectra for dissolved organic matter. *Environ. Sci. Technol.* 37, 5701–5710. doi: 10.1021/es034354c

Chi, Y.-Z., Zhang, Y., Yang, M., Tian, Z., Liu, R.-Y., Yan, F.-Y., et al. (2018). Start up of anammox process with activated sludge treating high ammonium industrial wastewaters as a favorable seeding sludge source. *Int. Biodeter. Biodegrad.* 127, 17–25. doi: 10.1016/j.ibiod.2017.11.007

Debray, R., Herbert, R. A., Jaffe, A. L., Crits-Christoph, A., Power, M. E., and Koskella, B. (2022). Priority effects in microbiome assembly. *Nat. Rev. Microbiol.* 20, 109–121. doi: 10.1038/s41579-021-00604-w

Deng, Y.-F., Wu, D., Huang, H., Cui, Y.-X., van Loosdrecht, M. C. M., and Chen, G.-H. (2021). Exploration and verification of the feasibility of sulfide-driven partial denitrification coupled with anammox for wastewater treatment. *Water Res.* 193:116905. doi: 10.1016/j.watres.2021.116905

Du, C., Cui, C.-W., Qiu, S., Shi, S.-N., Li, A., and Ma, F. (2017). Nitrogen removal and microbial community shift in an aerobic denitrification reactor bioaugmented with a *Pseudomonas* strain for coal-based ethylene glycol industry wastewater treatment. *Environ. Sci. Pollut. Res.* 24, 11435–11445. doi: 10.1007/s11356-017-8824-9

Fahrbach, M., Kuever, J., Meinke, R., Kämpfer, P., and Hollender, J. (2006). Denitratisoma oestradiolicum gen. nov., sp. nov., a 17 β-oestradiol-degrading, denitrifying betaproteobacterium. *Int. J. Syst. Evol. Microbiol.* 56, 1547–1552. doi: 10.1099/ijs.0.63672-0

Fang, Z., Li, L., Jiang, B., He, C., Li, Y., Xu, C., et al. (2019). Molecular composition and transformation of dissolved organic matter (DOM) in coal gasification wastewater. *Energy Fuels* 33, 3003–3011. doi: 10.1021/acs.energyfuels.8b04450

Gonzalez-Martinez, A., Rodriguez-Sanchez, A., Garcia-Ruiz, M. J., Muñoz-Palazon, B., Cortes-Lorenzo, C., Osorio, F., et al. (2016). Performance and bacterial community dynamics of a CANON bioreactor acclimated from high to low operational temperatures. *Chem. Eng. J.* 287, 557–567. doi: 10.1016/j.cej.2015.11.081

He, Z.-W., Zou, Z.-S., Sun, Q., Jin, H.-Y., Yao, X.-Y., Yang, W.-J., et al. (2021). Freezing-low temperature treatment facilitates short-chain fatty acids production from waste activated sludge with short-term fermentation. *Biores. Technol.* 2021:126337. doi: 10.1016/j.biortech.2021.126337

Jia, F., Yang, Q., Liu, X., Li, X., Li, B., Zhang, L., et al. (2017). Stratification of extracellular polymeric substances (EPS) for aggregated anammox microorganisms. *Environ. Sci. Technol.* 51, 3260–3268. doi: 10.1021/acs.est.6b05761

Jia, F. X., Peng, Y. Z., Li, J. W., Li, X. Y., and Yao, H. (2021). Metagenomic prediction analysis of microbial aggregation in anammox-dominated community. *Water Environ. Res.* 93, 2549–2558. doi: 10.1002/wer.1529

Jia, F. X., Yang, Q., Han, J. H., Liu, X. H., Li, X. Y., and Peng, Y. Z. (2016). Modeling optimization and evaluation of tightly bound extracellular polymeric substances extraction by sonication. *Appl. Microbiol. Biotechnol.* 100, 8485–8494. doi: 10.1007/s00253-016-7748-5

Kartal, B., Kuypers, M. M. M., Lavik, G., Schalk, J., Opden Camp, H. J. M., et al. (2007a). Anammox bacteria disguised as denitrifiers: nitrate reduction to dinitrogen gas via nitrite and ammonium. *Environ. Microbiol.* 9, 635–642. doi: 10.1111/j.1462-2920.2006.01183.x

Kartal, B., Rattray, J., van Niftrik, L. A., van de Vossenberg, J., Schmid, M. C., Webb, R. I., et al. (2007b). Candidatus "Anammoxoglobus propionicus" a new propionate oxidizing species of anaerobic ammonium oxidizing bacteria. *Syst. Appl. Microbiol.* 30, 39–49. doi: 10.1016/j.syapm.2006.03.004

Lackner, S., Gilbert, E. M., Vlaeminck, S. E., Joss, A., Horn, H., and van Loosdrecht, M. C. M. (2014). Full-scale partial nitritation/anammox experiences – An application survey. *Water Res.* 55, 292–303. doi: 10.1016/j.watres.2014.02.032

Laureni, M., Weissbrodt, D. G., Villez, K., Robin, O., de Jonge, N., Rosenthal, A., et al. (2019). Biomass segregation between biofilm and flocs improves the control of nitrite-oxidizing bacteria in mainstream partial nitritation and anammox processes. *Water Res.* 154, 104–116. doi: 10.1016/j.watres.2018.12.051

Li, Y., Li, J., Wang, D., Wang, G., Yue, X., Kong, X., et al. (2020). Denitrifying microbial community structure and bamA gene diversity of penol degraders in soil contaminated from the coking process. *Appl. Biochem. Biotechnol.* 190, 966–981. doi: 10.1007/s12010-019-03144-5

Ma, B., Wang, S., Cao, S., Miao, Y., Jia, F., Du, R., et al. (2016). Biological nitrogen removal from sewage via anammox: recent advances. *Biores. Technol.* 200, 981–990. doi: 10.1016/j.biortech.2015.10.074

Ma, Q., Qu, Y., Shen, W., Zhang, Z., Wang, J., Liu, Z., et al. (2015). Bacterial community compositions of coking wastewater treatment plants in steel industry revealed by Illumina high-throughput sequencing. *Biores. Technol.* 179, 436–443. doi: 10.1016/j.biortech.2014.12.041

Miao, Y., Zhang, L., Yang, Y., Peng, Y., Li, B., Wang, S., et al. (2016). Start-up of single-stage partial nitrification-anammox process treating low-strength swage and its restoration from nitrate accumulation. *Biores. Technol.* 218, 771–779. doi: 10.1016/j.biortech.2016.06.125

Oshiki, M., Satoh, H., and Okabe, S. (2016). Ecology and physiology of anaerobic ammonium oxidizing bacteria. *Environ. Microbiol.* 18, 2784–2796. doi: 10.1111/1462-2920.13134

Park, H., Sundar, S., Ma, Y., and Chandran, K. (2015). Differentiation in the microbial ecology and activity of suspended and attached bacteria in a nitritation-anammox process. *Biotechnol. Bioeng.* 112, 272–279. doi: 10.1002/bit.25354

Vlaeminck Siegfried, E., Terada, A., Smets Barth, F., De Clippeleir, H., Schaubroeck, T., Bolca, S., et al. (2010). Aggregate size and architecture determine microbial activity balance for one-stage partial nitritation and anammox. *Appl. Environ. Microbiol.* 76, 900–909. doi: 10.1128/AEM.02337-09

Wang, C., Liu, S., Xu, X., Zhang, C., Wang, D., and Yang, F. (2018). Achieving mainstream nitrogen removal through simultaneous partial nitrification, anammox and denitrification process in an integrated fixed film activated sludge reactor. *Chemosphere* 203, 457–466. doi: 10.1016/j.chemosphere.2018.04.016

Yang, S., Guo, B., Shao, Y., Mohammed, A., Vincent, S., Ashbolt, N. J., et al. (2019a). The value of floc and biofilm bacteria for anammox stability when treating ammonia-rich digester sludge thickening lagoon supernatant. *Chemosphere* 233, 472–481. doi: 10.1016/j.chemosphere.2019.05.287

Yang, S., Peng, Y., Zhang, L., Zhang, Q., Li, J., and Wang, X. (2019b). Autotrophic nitrogen removal in an integrated fixed-biofilm activated sludge (IFAS) reactor:

anammox bacteria enriched in the flocs have been overlooked. *Biores. Technol.* 288:121512. doi: 10.1016/j.biortech.2019.121512

Yao, H., Zhao, X., Fan, L., Jia, F., Chen, Y., Cai, W., et al. (2021). Pilot-scale demonstration of one-stage partial nitritation/anammox process to treat wastewater from a coal to ethylene glycol (CtEG) plant. *Environ. Res.* 2021:112540. doi: 10.1016/j.envres.2021.112540

Zhang, L., and Okabe, S. (2020). Ecological niche differentiation among anammox bacteria. *Water Res.* 171:115468. doi: 10.1016/j.watres.2020.115468

Zhang, W., Yu, D., Zhang, J., Miao, Y., Zhao, X., Ma, G., et al. (2022). Start-up of mainstream anammox process through inoculating nitrification sludge and anammox biofilm: Shift in nitrogen transformation and microorganisms. *Biores. Technol.* 347:126728. doi: 10.1016/j.biortech.2022.126728

Zheng, B., Zhang, L., Guo, J., Zhang, S., Yang, A., and Peng, Y. (2016). Suspended sludge and biofilm shaped different anammox communities in two pilot-scale one-stage anammox reactors. *Biores. Technol.* 211, 273–279. doi: 10.1016/j.biortech.2016.03.049

Zheng, M., Xu, C., Zhong, D., Han, Y., Zhang, Z., Zhu, H., et al. (2019). Synergistic degradation on aromatic cyclic organics of coal pyrolysis wastewater by lignite activated coke-active sludge process. *Chem. Eng. J.* 364, 410–419. doi: 10.1016/j.cej.2019.01.121

Conflict of Interest: The authors declare that the research was conducted in the absence of any commercial or financial relationships that could be construed as a potential conflict of interest.

Publisher's Note: All claims expressed in this article are solely those of the authors and do not necessarily represent those of their affiliated organizations, or those of the publisher, the editors and the reviewers. Any product that may be evaluated in this article, or claim that may be made by its manufacturer, is not guaranteed or endorsed by the publisher.

frontiers | Frontiers in Microbiology

ORIGINAL RESEARCH
published: 02 June 2022
doi: 10.3389/fmicb.2022.924084

Nitrogen Removal From Nitrate-Containing Wastewaters in Hydrogen-Based Membrane Biofilm Reactors *via* Hydrogen Autotrophic Denitrification: Biofilm Structure, Microbial Community and Optimization Strategies

Kun Dong[1,2†], Xinghui Feng[1,2†], Yi Yao[1,2], Zongqiang Zhu[1,2], Hua Lin[1,2], Xuehong Zhang[1,2], Dunqiu Wang[1,2] and Haixiang Li[1,2]*

[1]College of Environmental Science and Engineering, Guilin University of Technology, Guilin, China, [2]The Guangxi Key Laboratory of Theory and Technology for Environmental Pollution Control, Guilin, China

OPEN ACCESS

Edited by:
Chongjun Chen,
Suzhou University of Science and Technology, China

Reviewed by:
Bao-Cheng Huang,
Hangzhou Normal University, China
Lijie Zhou,
Shenzhen University, China

***Correspondence:**
Haixiang Li
2011042@glut.edu.cn

[†]These authors have contributed equally to this work and share first authorship

Specialty section:
This article was submitted to Microbiotechnology, a section of the journal Frontiers in Microbiology

Received: 20 April 2022
Accepted: 03 May 2022
Published: 02 June 2022

Citation:
Dong K, Feng X, Yao Y, Zhu Z, Lin H, Zhang X, Wang D and Li H (2022) Nitrogen Removal From Nitrate-Containing Wastewaters in Hydrogen-Based Membrane Biofilm Reactors via Hydrogen Autotrophic Denitrification: Biofilm Structure, Microbial Community and Optimization Strategies. Front. Microbiol. 13:924084. doi: 10.3389/fmicb.2022.924084

The hydrogen-based membrane biofilm reactor (MBfR) has been widely applied in nitrate removal from wastewater, while the erratic fluctuation of treatment efficiency is in consequence of unstable operation parameters. In this study, hydrogen pressure, pH, and biofilm thickness were optimized as the key controlling parameters to operate MBfR. The results of 653.31 μm in biofilm thickness, 0.05 MPa in hydrogen pressure and pH in 7.78 suggesting high-efficiency $NO_3^- - N$ removal and the $NO_3^- - N$ removal flux was 1.15 g·m^{-2} d^{-1}. 16S rRNA gene analysis revealed that *Pseudomonas*, *Methyloversatilis*, *Thauera*, *Nitrospira*, and *Hydrogenophaga* were the five most abundant bacterial genera in MBfRs after optimization. Moreover, significant increases of *Pseudomonas* relative abundances from 0.36 to 9.77% suggested that optimization could effectively remove nitrogen from MBfRs. Membrane pores and surfaces exhibited varying degrees of calcification during stable operation, as evinced by Ca^{2+} precipitation adhering to MBfR membrane surfaces based on scanning electron microscopy (SEM), atomic force microscopy (AFM) analyses. Scanning electron microscopy–energy dispersive spectrometer (SEM–EDS) analyses also confirmed that the primary elemental composition of polyvinyl chloride (PVC) membrane surfaces after response surface methodology (RSM) optimization comprised Ca, O, C, P, and Fe. Further, X-ray diffraction (XRD) analyses indicated the formation of $Ca_5F(PO_4)_3$ geometry during the stable operation phase.

Keywords: response surface methodology, microbial community, characterization, calcification, MBFR

INTRODUCTION

Abundant toxic and harmful pollutants have been discharged into natural environments in recent years, leading to significant deterioration in groundwater and surface water quality (Liu et al., 2022). Nitrate is mobile in water and soil, with excessive nitrate from sewage, agricultural fertilizers, or intensive agriculture easily entering groundwater and surface water systems, where it can cause greater harm to environments. Indeed, due to excessive eutrophication nitrate has become a serious environmental problem in most regions of the world, and in China, owing to the discharge of municipal wastewater. Nitrate cannot be easily removed by traditional denitrification technology in water purification plants. Rather, several physical and chemical techniques are used for nitrate in groundwater and surface water including ion exchange, chemical reduction, physical adsorption, and reverse osmosis (Della Rocca et al., 2007; Demirel and Bayhan, 2013). However, these physical and chemical methods are generally characterized by serious secondary pollution, high costs, and complex follow-up treatments, thereby considerably limiting their practical application. Consequently, the need to identify more efficient and green biological treatment technologies for nitrate removal has grown in recent years.

Membrane biofilm reactor treatment is a newly developed method for the efficient removal of nitrate from groundwaters and surface waters. MBfR operates under low carbon source and low oxygen availability conditions and combines microporous hollow fiber membrane diffusion aeration with autotrophic biofilm technology to remove oxidizing pollutants from water using hydrogen as a clean and inexpensive electron donor (Xia et al., 2016; Zhou et al., 2016). In MBfRs, microporous membranes act both as a channel for the transmission of hydrogen and as a carrier for microbial attachment, with electron donors (e.g., H_2) or electron acceptors (e.g., O_2) delivered to microorganisms living on membrane walls (Rittmann, 2011; Tang et al., 2012). H_2 diffuses from inside of the membrane to provide bubble-free hydrogen gas to the autotrophic microorganisms. Microbial respiration activity then oxidizes pollutants as electron acceptors and converts them into harmless byproducts. Importantly, hydrogen autotrophic microorganisms can use inorganic carbon as a carbon source and hydrogen as an electron donor to reduce oxidizing substances, thereby conserving energy. Hydrogen is a clean, non-toxic autotrophic denitrifying electron donor. MBfR using H_2 for denitrification leads to a very good hydrogen utilization efficiency (over 99%) and avoids risks from reactor explosion owing to hydrogen accumulation (Long et al., 2020). Moreover, the development of hydrogen production technology in recent years has led to reduced hydrogen production costs, rendering MBfR a promising, clean, and inexpensive electron donor strategy.

A number of MBfRs have been developed for contaminants such as nitrate, sulfate, bromate, perchlorate, and chromate (Chung et al., 2006; Van Ginkel et al., 2008; Li et al., 2017). In the case of hydrogen as an electron donor, the stoichiometries (Xia et al., 2010) in which $NO_3^- - N$ is reduced to nitrite and eventually to N_2 are shown by Eqs. (a), (b):

$$NO_3^- + H_2 \rightarrow NO_2^- + H_2O \quad \text{(a)}$$

$$2NO_2^- + 2H^+ + 3H_2 \rightarrow N_2 + 4H_2O \quad \text{(b)}$$

Nitrate reduction is clearly the source of alkaliniy in MBfRs *via* the consumption of 2 H^+ equivalents per N equivalent of NO_3^-, as shown in Eqs. (a), (b). Bicarbonate is added as an inorganic carbon source along with a combination of phosphate solutions (Na_2HPO_4 and KH_2PO_4) to the feed water to control pH in MBfRs.

Response surface methodology (RSM) is a statistical, mathematical modeling tool that can be used for reactor optimization. The Box–Behnken design (BBD), a kind of RSM design, has been used to investigate optimal levels of key factors for the removal rate of nitrate. During modeling, the system response ($NO_3^- - N$ removal rate) is firstly expressed as a function of several factors (pH concentration, hydrogen pressure, and biofilm thickness) and the system function relationship is expressed using reasonable experimental methods and graphical techniques to construct a suitable response surface model of the influencing factors of MBfR hydrogen autotrophic denitrification, followed by the use of RSM.

Calcification is also observed (e.g., *via* precipitates containing Ca^{2+}) on the surface of polyvinyl chloride (PVC) hollow fiber membranes during stable operation of MBfRs. Inorganic compounds such as $CaCO_3$ undergo precipitation reactions in dynamic equilibrium with MBfRs, wherein the hardness cations present in the MBfR combine with typical anions to form precipitates. Hardness ion precipitates in MBfRs include $CaCO_3$, $CaHPO_4$, $Ca(H_2PO_4)_2$, $Ca_5(PO_4)_3OH$, and $Ca_3(PO_4)_2$ (Tang et al., 2011). In addition, the precipitation of Ca^{2+} during denitrification and the long-term accumulation of $CaCO_3$ (comprising up to 25% of biofilm mass) outside the biofilm form a mineral solid buildup inside the biofilm, thereby increasing mass transfer resistance at the bottom of the biofilm. These dynamics then result in substrates not being able to freely diffuse inside the biofilm and even clogging the device, making the hollow fiber membrane filaments more brittle and leading to long-term negative impacts on the efficient operation of MBfRs (Lee and Rittmann, 2003; Hou et al., 2019). Increased Ca^{2+} on the hollow fiber membrane surface also leads to decreased hydrogen transfer efficiency and nitrogen removal performance in MBfRs. Three factors are related to calcification (i.e., the precipitation of Ca^{2+}) on the hollow fiber membrane surface and have been selected for optimization of the reactor to obtain stable and efficient denitrification performances: pH, hydrogen pressure, and biofilm thickness. Hydrogen autotrophic denitrification leads to increased pH, and Ca^{2+} precipitation is closely related to the solution pH. When Na_2HPO_4 and KH_2PO_4 are used as buffer solutions, the reactor solutions cannot effectively be controlled below pH 8.0, and the dynamic balance of free CO_2, HCO_3-, and CO_3^{2-} in solution directly affects the pH, thereby the precipitation and dissolution balance of Ca^{2+}. pH also plays a key role in the precipitation and dissolution

equilibrium of Ca^{2+}. Hydrogen as an electron donor is an important influencing factor for nitrate and nitrite removal. Insufficient hydrogen (i.e., low hydrogen pressures) during MBfR operation inhibit denitrification, while the supply mode at one end of the MBfR leads to low H_2 diffusion efficiency from the supply end due to insufficient hydrogen pressure, resulting in insufficient effective control of the pH in the biofilm at distant locations, leading to Ca^{2+} precipitation. The low solubility of hydrogen can also lead to excessive hydrogen, wherein it cannot be fully utilized by the biofilm, resulting in wasted resources. Biofilm thickness is the main factor affecting substrate transfer into the biofilm and pollutant removal efficiency, while biofilm thickness is closely related to Ca^{2+} precipitation. During MBfR operation when increasing calcium precipitation occurred on the biofilm surface, biofilm thickness increased, which led to limited substrate transfer and decreased pollutant removal efficiency.

In this study, PVC hollow fiber membranes were used as biofilm carriers in the reactor. RSM was then used to optimize the operating parameters of MBfR-hydrogen autotrophic denitrification. Calcification on the PVC hollow fiber membrane during the stable operation stage was characterized by scanning electron microscopy (SEM), X-ray diffraction (XRD), scanning electron microscopy–energy dispersive spectrometer (SEM–EDS), X-ray photoelectron spectroscopy (XPS), and atomic force microscopy (AFM). High-throughput sequencing was also used to assess the compositions of microbial communities. Optimal conditions were then investigated through RSM based on the BBD under different conditions. The above investigations were used to explore the operating parameters and surface morphological characteristics of hollow fiber membranes suitable for MBfR-hydrogen autotrophic denitrification, discuss the relationship between biofilm formation and calcification and provide a theoretical basis for reactor operation and control of membrane calcification.

MATERIALS AND METHODS

Experimental Set-Up and Control Strategy

Detailed MBfR parameters are listed in **Table 1** and **Figure 1**. A single peristaltic pump (BT101L-DG-1, Lead Fluid, Baoding, China) was used to control the nitrate-medium-feed influent rate at 0–3 ml/min. Synthetic domestication water followed a previously described recipe (Xia et al., 2010) and comprised (per liter): 0.128 g of KH_2PO_4, 0.434 g of $NaHPO_4$, 0.2 g of $MgSO_4{\cdot}7H_2O$, 0.001 g of $CaCl_2{\cdot}2H_2O$, 0.001 g of $FeSO_4{\cdot}7H_2O$, 0.252 g of $NaHCO_3$, and 1 ml of a stock solution containing trace elements. The trace element stock solution contained (per liter): 100 mg of $ZnSO_4{\cdot}7H_2O$, 30 mg of $MnCl_2{\cdot}4H_2O$, 300 mg of H_3BO_3, 0.1 mg of H_3BO_3, 200 mg of $CoCl_2{\cdot}6H_2O$, 10 mg of $CuCl_2{\cdot}2H_2O$, 10 mg of $NiCl_2{\cdot}6H_2O$, and 30 mg of Na_2SeO_3. The trace element solution was produced in a 25.0 l water distribution tank after purging with N_2 to remove dissolved oxygen (DO) in the influent and mixing the trace solution well by aeration. High recirculation speed (100 ml/min) and high recirculation rate (nearly 100:1 when the influent rate was 1 ml/min) were used in the experiment. Under these conditions, hydrogen autotrophic microorganisms can accumulate on the hollow fiber membrane faster and simultaneously enable the MBfR to reach a fully mixed state. In addition, pure H_2 was supplied to the interior of the hollow fiber through an inlet in the top center of the reactor, while the pressure range is controlled from 0.02 to 0.06 MPa. Further, a programmable logic controller (PLC) monitoring system connected to the pH and DO probes enables 24-h real-time monitoring of pH and DO inside the MBfR.

TABLE 1 | Physical characteristics of the MBfR system.

Parameter	Units	Value
Membrane material		PVC
Active volume	L	1.8
Number of HFM		40
HFM inner diameter	nm	1.0
HFM outer diameter	nm	1.66
Pure water flux	$L/m^2{\cdot}h$	400

PVC Hollow Fiber Membrane and Experimental Initiation

The main membrane module contained a bundle of 40 hydrophobic hollow fiber membranes (HFMs) constructed from PVC (Watercode, Guangzhou, China). Smaller pore size HFMs constructed with PVC and a pore size of 0.1 μm were used in the MBfR to deliver bubble-free H_2 through the HFM walls. The reactor volume was 1.8 l and the initial mixed liquor suspended solids (MLSS) concentration was 2,500 mg/l. Activated sludge was added with a 50 ml syringe, with a total volume of added activated sludge of 10% of the MBfR. The activated sludge consisted of sludge from the Qilidian wastewater plant in Guilin and mature hydrogen autotrophic denitrification sludge that was established in the laboratory, mixed at a ratio of 1:2.6 (50 ml of wastewater plant sludge and 130 ml of laboratory sludge). During the laboratory domestication stage when the influent concentration was 10 mg/l, the $NO_3^- - N$ removal flux was $0.83\,g{\cdot}m^{-2}\ d^{-1}$ after 76 days of domestication and the $NO_3^- - N$ standardized flux was $0.083\,g{\cdot}m^{-2}\ d^{-1}$, leading to a final removal rate of the MBfR reaching 90.32%. A layer of yellow–brown solids was also attached to the surface of the PVC hollow fiber membrane module and a uniformly distributed yellow–brown biofilm was observed. Thus, the MBfR start-up domestication stage was established. After the system was successfully initiated, the response surface was optimized on the basis of single-factor experiments to ensure experimental reliability.

Biofilm Structural Analysis

$NO_3^- - N$ removal rate is an important parameter for characterizing the performance of MBfR-hydrogen autotrophic denitrification and the $NO_3^- - N$ concentrations of all samples were measured by using a continuous flow analyzer (SAN^{++}, Skalar, Netherlands).

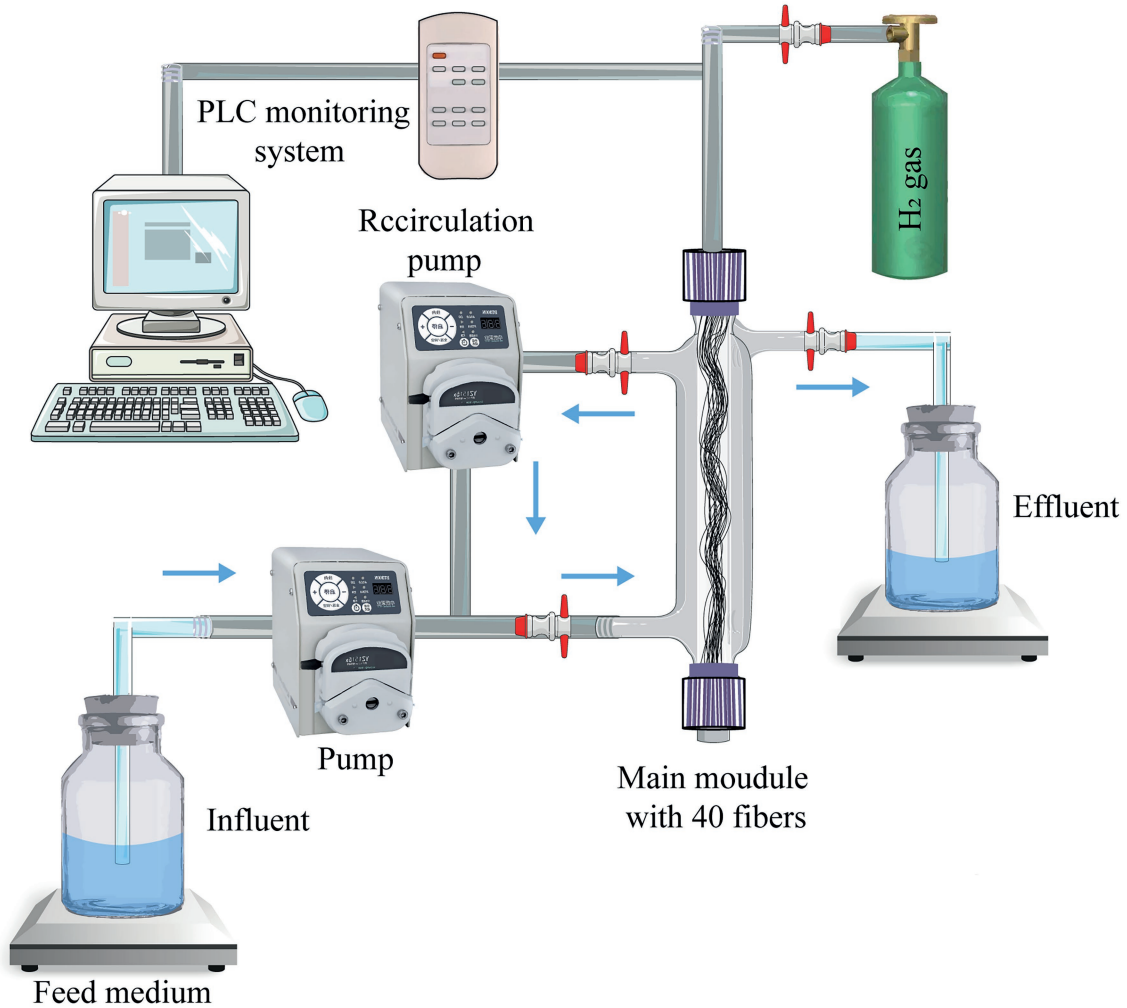

FIGURE 1 | Schematic of the hydrogen-based membrane biofilm reactor (MBfR) used to investigate nitrate reduction.

Several characterization analyses of the membrane modules based on PVC hollow fiber membranes were conducted in the stable operation stage by exploring calcification. Surface morphology, agglomeration, microstructure, and chemical composition characteristics of PVC hollow fiber membranes in the stable operation stage were assessed with SEM (MIRA3, Tescan, Czech Republic), and SEM–EDS (AZTEC X-MAXN 80, Oxford, United Kingdom). The SEM was operated with an acceleration voltage of 15 kV, a fixed angle of 35°, and an elemental analysis range of Be^{4} to Cf^{98}. XPS (ESCALAB250Xi, ThermoFisher Scientific, United States) with a monochromatic Al Kα source (1486.6 eV) was used to measure the elemental composition and chemical state of the membranes. In addition, crystal structures of the samples were assessed with XRD measurements and an X-ray diffractometer (X'PERT PRO, Panalytical, Holland) with a 2θ range of 5°–90° and a scan rate of $10°min^{-1}$. AFM (DIMENSION ICON, Bruker, United States) exhibited significant advantages by providing nanoscale resolution imaging capacities for studying the microscopic properties of materials and obtaining measurements such as the surface roughness of PVC hollow membrane samples.

MBfR biofilms can be used to identify bacterial species *via* high-throughput sequencing when $NO_3^- - N$ reductions are taking place. A 3 cm piece of the coupon fiber was cut from identical regions of each MBfR before and after optimization experiments. Biomass samples were then sent to Sangon Biotech Co., Ltd. (Shanghai, China) for microbial structural analysis. The 16S rRNA gene sequence libraries were then prepared using polymerase chain reaction (PCR) with universal primers and amplification of the V4–V5 hypervariable regions of genes. Operational taxonomic units (OTUs) at the 97% nucleotide identity threshold were generated, and taxonomic classification of each OTU representative was conducted at the genus level by using the Ribosomal Database Project Classifier.

RSM Optimization Design

In this study, $NO_3^- - N$ removal rate was the target index and a response surface model was constructed to evaluate

optimization of this rate. In particular, the response surface method was used to investigate the effects of biofilm thickness (A, 600–700 μm), hydrogen pressure (B, 0.02–0.06 mg/l), and pH (C, 6.5–8.5) on denitrification efficiency *via* the hydrogen autotrophic denitrification process, with the $NO_3^- - N$ removal rate as the response value. A total of 17 three-parameter experimental designs were conducted to evaluate the single and interactive effects of different conditions on the target responses to improve the denitrification performance of the reactor. A model was then established from the results to identify the best parameters to improve denitrification efficiency of hydrogen autotrophic denitrification. The mathematical relationships among variables (biofilm thickness, hydrogen pressure, and pH) and response values can be described by the following quadratic polynomial (Hellmuth et al., 1995):

$$Y = \beta_0 + \sum \beta_i X_i + \sum \beta_{ii} X_i^2 + \sum \beta_{ij} X_j \left(i,j = 1,2,\ldots,k\right) \quad \text{(c)}$$

where Y is the predicted response (i.e., the $NO_3^- - N$ removal rate), β_0 is the intercept term, and β_i, β_{ii}, and β_{ij} are the linear, quadratic, and interaction coefficients of the variables, respectively. X_i and X_j are the coefficients of biofilm thickness, hydrogen pressure, and pH. The validity of the model was then examined significantly *via* the second-order polynomial coefficients of determination (*R*-squared) and the analysis of variance (ANOVA) using the "Design Expert" software package (Version 8.0.6, Stat-Ease Inc., Minneapolis, MN, United States).

RESULTS AND DISCUSSION

RSM Models for Optimizing MBfR Hydrogen Autotrophic Denitrification

The interactions of the three reactor components and their optimal levels during the removal of nitrate were further analyzed by using response surface methodology. A normal plot of the residuals for nitrate removal by the MBfR was used to evaluate the reliability of the model (**Figure 2A**). The internally studentized residuals and normal % probability exhibited primarily linear function relationships and the data points were distributed around linear straight lines with a normal distribution (**Figure 2A**). The scatter of actual and predicted results for the nitrogen removal capacity of MBfRs based on the three-parameter experiment and RSM model was also evaluated (**Figure 2B**). Values obtained from the experimental results and those predicted by the model were randomly scattered around the linear straight line, while the experimental and predicted values barely deviated from the straight line, indicating that the error between the actual and predicted values was minimal. Three-dimensional response surface plots provided a visual representation of the relationships between the objective function and the design variable. Specifically, these represent surface derived from the function established by the relationship between two of the three variables mentioned above and the response value, requiring that all other parameters are constant to investigate the primary effects and interactions of the two factors (Polat and Sayan, 2019). The effects of (A) biofilm thickness and hydrogen pressure, (B) biofilm thickness and pH, and (C) hydrogen pressure and pH on the nitrate removal capacity of MBfRs were all evaluated (**Figure 3**). The $NO_3^- - N$ removal rate firstly increased and then decreased with increasing hydrogen pressure (from 0.02 to 0.06 MPa) and biofilm thickness (from 600 to 700 μm), respectively, at a specified influent concentration (**Figures 3A,B**). The mechanism underlying these dynamics was that increasing hydrogen pressure improved the use efficiency of hydrogen as electron donor and the stable concentration of $NO_3^- - N$ at 0.02 MPa was lower at 0.04 MPa, while the amount of electron donor (H_2) was insufficient for complete reduction of $NO_3^- - N$ to N_2. Thus, continuously increasing hydrogen pressure over a certain range can promote the removal of $NO_3^- - N$ to a certain extent. However, excessively high hydrogen pressures adversely affected the efficient operation of MBfRs and the removal of nitrate.

Biofilm thickness was also an important factor affecting the removal of $NO_3^- - N$. Increased biofilm thickness can lead to adverse effects on denitrification abilities of MBfRs *via* reduced substrate transfer efficiency that in turn affected $NO_3^- - N$ removal rates. The effects of different pH values on MBfR nitrate removal were also evaluated (**Figure 3C**). The nitrogen removal capacity of MBfRs clearly first increased and then decreased with increasing pH. Optimal conditions were obtained by using the Design Expert software package, suggesting optimal a biofilm thickness of 653.31 μm, hydrogen pressure of 0.05 MPa, and pH of 7.78. Specifically, the model predicted a $NO_3^- - N$ removal rate of 97.21%. The experimental conditions determined by the quadratic regression model were repeated three times to verify the reliability of the response surface model, while the average value of the total nitrogen removal rate obtained among the three experiments was 97.05% and the $NO_3^- - N$ removal flux reached 1.15 $g \cdot m^{-2}\ d^{-1}$. These values were essentially consistent with the theoretical prediction of the model and thus, the optimal $NO_3^- - N$ removal efficiency value obtained by RSM optimization is highly reliable and carries practical reference value.

Microbial Community Structure Analysis

To investigate the temporal dynamics of microbial communities in the MBfRs, the ten most abundant taxonomic groups at the genus and phylum levels were investigated among different phases (i.e., before RSM optimization phase A1 and at stable operation phase A2). A total of 181,527 16S rRNA gene sequences were generated in this study (94,766 for A1 and 84,761 for A2) by using Illumina-MiSeq sequencing. A total of 1,511 OTUs were generated from the sequences at the 97% nucleotide similarity level, and the samples collected from sample A2 were grouped, respectively, into 745 OTUs, among which 421 species were coincident. This suggested that the microbial species in the two samples were different. However, the number of unique OTU in the sample A1 was 766, and the number of unique OTU in the sample A2 was 324. At stable operation phase the species of microorganism on PVC hollow fiber membrane surface reduced, which indicated the

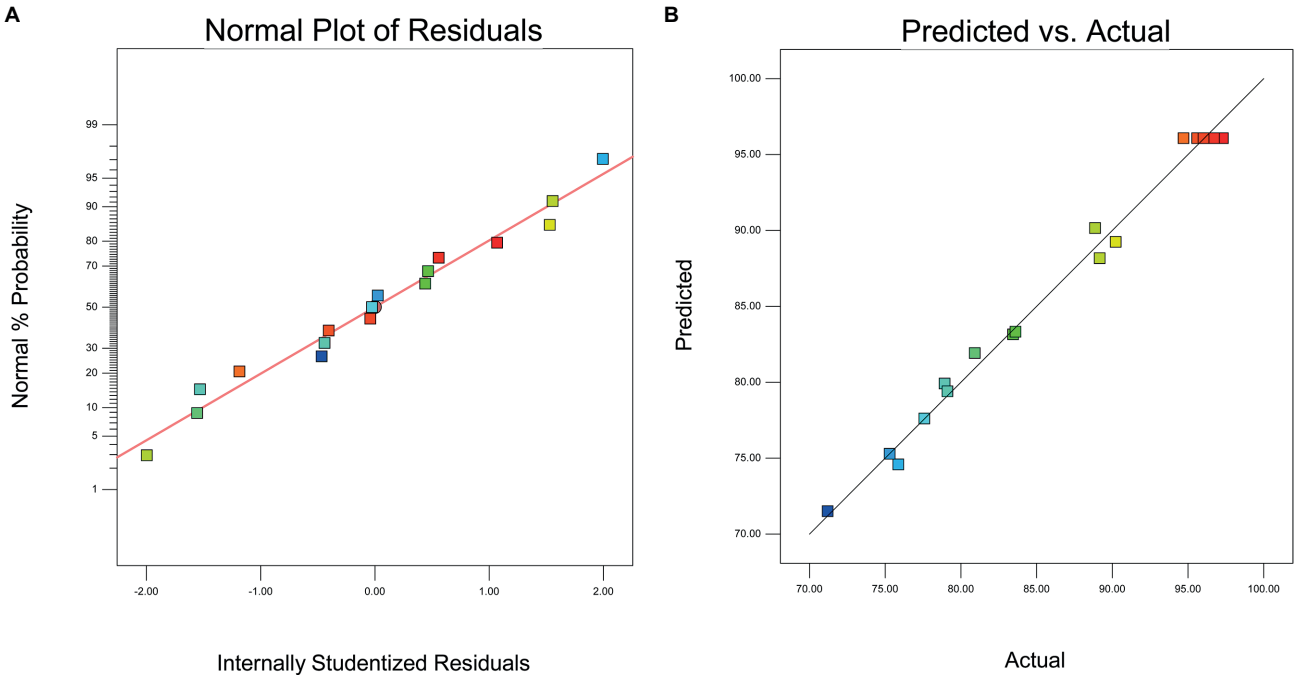

FIGURE 2 | **(A)** Normal plot of residuals and **(B)** plot of predicted vs. actual values.

bacteria associated with these OTUs may play an important role in the deepening of membrane surface calcification phenomenon.

Proteobacteria, *Bacteroidetes*, *Nitrospirae*, and *Chloroflexi* were the dominant phyla in the bacterial communities (**Figure 4B**), accounting for >75% of the A1 and A2 communities. The most abundant phyla associated with nitrogen removal in the MBfRs were the *Proteobacteria*, *Chloroflexi*, and *Bacteroidetes* (Chang et al., 2022), with relative abundances of 64.24, 14.80, 1.89, and 3.51% in A2 during the stable operation phase. *Proteobacteria* (abundances from 48.99 to 64.23%) have been previously shown as prominent during nitrate removal (Su et al., 2020). Moreover, the enrichment of *Proteobacteria* has been associated with removal of nitrogen pollutants and in key roles in removing total nitrogen (Lee et al., 2013). *Bacteroidetes* are another important phylum associated with wastewater biological treatment systems and have also been reported in typical association with denitrifying during denitrification (Zhou et al., 2022). In this study, *Bacteroidetes* were the second most abundant genus, with relative abundances >14% in both A1 and A2. Notably, the same predominant phyla were observed in A1 and A2, suggesting that optimization of the RSM denitrification performance of the MBfR did not affect the core microbiome of the reactor at the phylum level. Other, low relative abundance phyla were detected in the communities including *Nitrospirae*, *Acidobacteria*, *Firmicutes*, and *Planctomycetes*. Although these groups contributed little to the overall communities of A1 and A2, the entire communities nevertheless were likely involved in the improved hydrogen autotrophic denitrification performance of the MBfRs.

A total of 23 genera (relative abundance ≥1% in at least one sample) were identified in the two communities (**Figure 4A**). *Methyloversatilis* have been previously reported as denitrification bacteria (Li et al., 2019) and play a dominant role in NO_3^- removal in autotrophic reactors (Gao et al., 2015), accounting for 5.10 and 2.63% of the A1 and A2 communities, respectively. Comparison of the microbial communities of the A1 and A2 communities revealed that the microbial community structures of the membrane surface samples (A1 and A2) differed after RSM optimization. *Nitrosomonas*, which belong to ammonia-oxidizing bacteria, its proportions decreased from 5.75 to 1.87% of the communities, while anaerobic denitrification bacteria appeared, including *Pseudomonas* (12.75%), as previously described (Chang et al., 2022). These results suggested that the MBfR gradually became an anaerobic environment during the stable operation phase, thereby severely inhibiting the growth of nitrifying bacteria and providing optimal conditions for the growth of hydrogen autotrophic denitrifying bacteria. Notably, *Pseudomonas* relative abundances on the membrane surface of the two samples increased from 0.36 to 9.77%. *Pseudomonas* is a hydrogen autotrophic denitrifier and a nitrate-reducing taxa that has been shown to play a key role in hydrogen autotrophic denitrification during NO_3^- removal (Zhang et al., 2015). *Hydrogenophaga* is a well-known, but uncultured, hydrogen-oxidizing bacterial genus that characteristically reduces NO_3^- and can play a large role in H_2-based MBfR functioning (Jiang et al., 2020). In addition, *Thauera* have been previously considered the most active denitrifying bacteria in sewage treatment systems, and were the primary contributor to nitrogen wastewater denitrification in a previous study (Dong et al.,

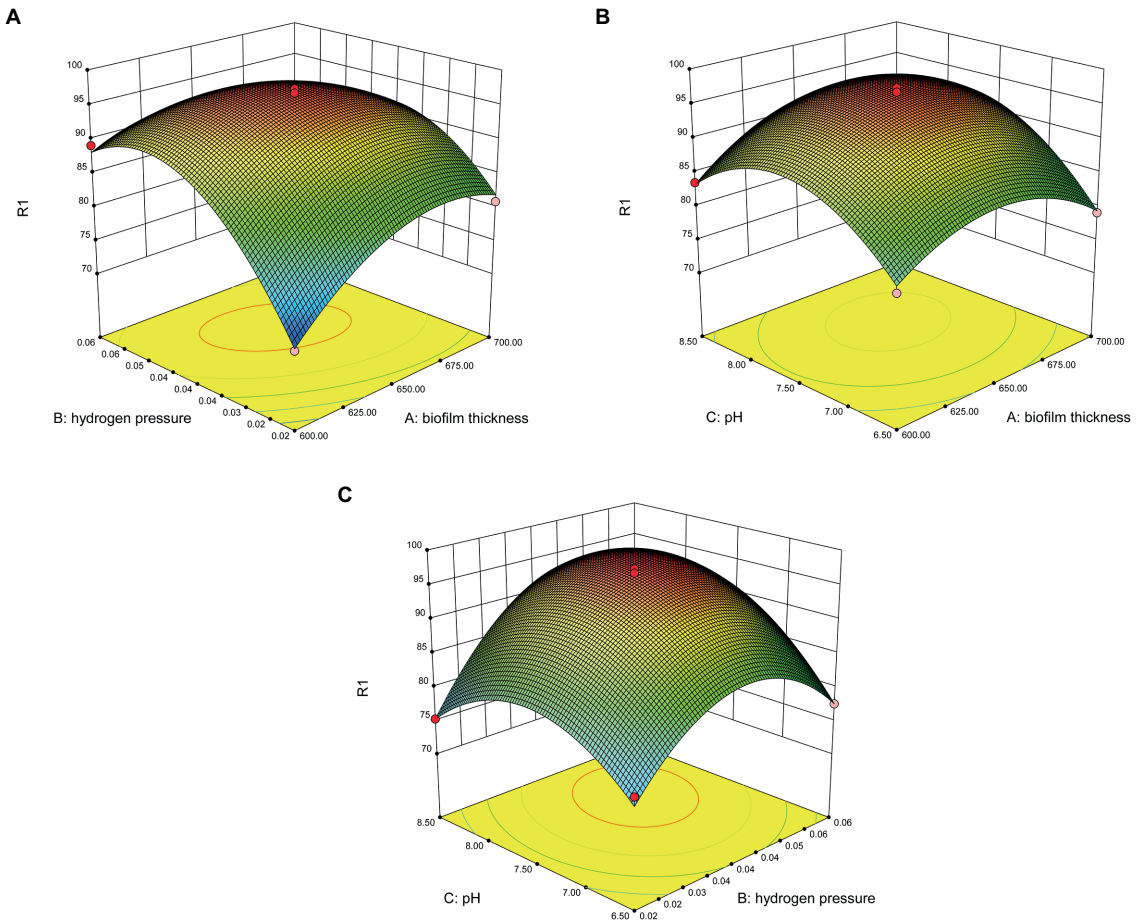

FIGURE 3 | Three-dimensional surface plots for the nitrate removal capacity of MBfR: **(A)** biofilm thickness vs. hydrogen pressure, **(B)** biofilm thickness vs. pH, and **(C)** hydrogen pressure vs. pH.

2021). Thus, *Thauera* can likely improve optimized MBfR denitrification performance. Overall, these results suggested that the microbial community structures of the biofilm considerably changed compared to the phase before RSM optimization, due to significant influences by MBfR operation and optimization.

Characterization of Calcification

Further analysis of our stably operating reactor revealed that biofilm formation was closely associated with Ca^{2+} concentration dynamics. Ca^{2+} has been previously observed as a common cation in water bodies that is associated with increased density of activated sludge and settling in activated sludge water treatment used in denitrification, while also simultaneously altering biofilm structures and affecting biofilm shedding (Liu et al., 2010). Calcification is more obvious in MBfRs operating for long periods of time, coinciding with increased Ca^{2+} deposits on biofilm surface and increased biofilm thickness on the hollow fiber membrane surfaces, causing more easy shedding. Slight calcification is helpful for biofilm formation, but severe calcification (which can be demonstrated by the thickness of the calcified layer) is detrimental to the growth of biofilm. Too thick biofilm will cause it to fall off more easily under the effect of hydraulic impact and vapor corrosion, resulting in lower denitrification efficiency. Consequently, the effects of calcification were characterized on the surfaces of the PVC hollow fiber membrane filaments in addition to the degree of Ca^{2+} enrichment by hollow fiber membrane filaments in MBfRs operating under stable anaerobic conditions.

SEM Characterization

Scanning electron microscopy was used to characterize the surface morphology of the PVC hollow fiber membranes (**Figure 5**). SEM analysis under various magnification levels indicated the presence of "particle"-like structures of the PVC hollow fiber membrane that were clearly visible on the surface during the stable operation phase (**Figures 5A,B**). Previous studies have shown that the surface structure of the PVC hollow fiber membrane in the early stage of the MBfR operation is mainly dominated by small pores and these membrane pores function as transport channels for hydrogen diffusion into biofilms in a bubble-free form (Nerenberg, 2016), while the membrane surface remains smooth without the presence of calcification.

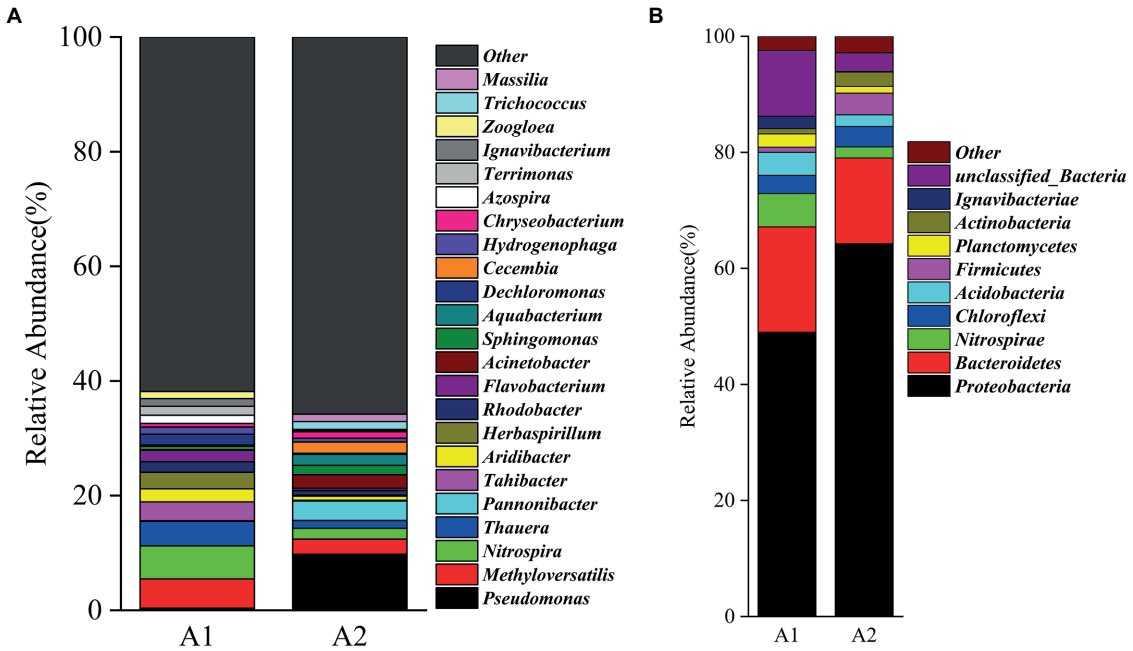

FIGURE 4 | Taxonomic classification of 16S rRNA gene sequences in the A1 and A2 samples from the PVC surfaces of MBfRs classified at the **(A)** genus and **(B)** phylum levels.

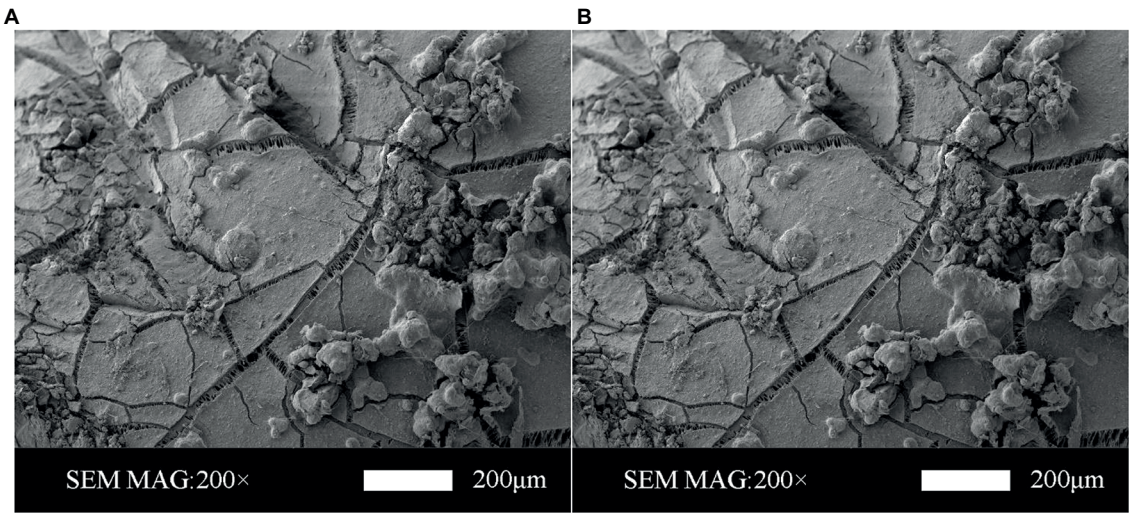

FIGURE 5 | Scanning electron microscopy (SEM) images of PVC hollow fiber membrane surfaces in the stable operation phase. Magnification is shown at **(A)** 200× and **(B)** 500×.

Although the $NO_3^- - N$ removal in MBfRs were improved in the stable operation stage, while the accumulated organic substances (Meng et al., 2010) were caused by the deposition of biopolymers on the membrane pores and the formation of gelatinous substances on the membrane surface that could enhance bacterial aggregation or binding to the surface. In addition, certain cations and anions were present in the MBfR, potentially leading to the phenomenon of concentration polarization on the surface of the PVC hollow fiber membrane that could lead to increases in salt concentrations on the membrane surface. Consequently, when the salt concentration exceeded the saturation concentration, chemical precipitation originating from inorganic crystals would occur on the membrane surface, leading to calcification. SEM visualizations revealed the presence of different shapes and sizes that can be clearly observed on the membrane surface, in addition to unique "particle"-like

structures that were covered by inorganic calcium precipitates and the presence of particulates of different shapes and sizes due to calcification of the membrane surface. This then resulted in a disordered porous structure that would allow a mixture of calcium precipitation and microbial binding to the membrane surface, leading to increased membrane thickness and an increase in the weight of the membrane, leading to easier peeling.

AFM and XPS Characterization

Biofilm material roughness of PVC hollow fiber membrane surfaces was measured during the stable operation phase with AFM analysis and is shown in three-dimensional imaging over an area of 10 μm × 10 μm (**Figure 6A**). Membrane surface roughness magnitude can indicate calcium ion adsorption on the membrane surface to some extent, wherein greater surface roughness suggests more ready inorganic precipitation of calcium ions adsorbed onto the membrane surface. Concomitantly, the thickness of the membrane is not easily controlled, resulting in poor denitrification efficiency and thereby triggering calcification. Surface morphology was characterized using the peak force mode of the Bruker AFM instrument and the AFM images and roughness parameters were identified by using the NanoScope Analysis 1.9 software package (Bruker).

The surfaces were rougher in the stable operation phase and exhibited a higher degree of biofilm layering (**Figure 6A**). Roughness parameters including average roughness (R_a), root mean squared roughness (R_q), and the maximum height between the top and the bottom (R_{max}) were used to quantitatively evaluate the surface properties of the PVC samples (Zhang et al., 2020). The R_q values differed among membranes (57.8 nm for stable operation phase samples), wherein roughest surfaces corresponded to the largest roughness values. The R_a also coincided with calcification, with a R_a reaching 42.8 nm during the stable operation phase and the R_{max} of the surface reaching 414 nm in the same phase. Sludge, microorganisms, and other substances adhere to PVC hollow fiber membrane surfaces, leading to clogging of membrane pores and adhesion of inorganic substances such as calcium ions, thereby accelerating the formation of the calcification layer on the membrane surface.

X-ray photoelectron spectroscopy technology was employed to characterize the effects of calcification during stable operation and assess the presence of Ca on the membrane surface showed in (**Figure 6B**). The XPS pattern of the reactor during stable operation was compared against the standard binding energy spectrum, revealing that the Ca 2p was split into three characteristic peaks. Among these, the peak areas of the Ca 2p1/2 and Ca 2p3/2 orbitals were 1:2, and the spin energy interval was 3.55 eV, which was consistent with the standard energy spectrum. In addition, an additional characteristic peak was observed at 353.4 eV that further confirmed the observed increased calcium material on the membrane surface.

SEM-EDS Characterization

The surface morphology and elemental composition of the PVC samples during the stable operation phase are shown in **Figure 7**. Larger sized particles were observed forming channels and adhering to the sample surface that were likely due to the scratching of the sample on the PVC hollow fiber membrane surfaces. The energy spectrum points sweep of the particles attached to the surface revealed that the main elemental compositions were Ca, O, C, P, and Fe (spectrum 1 in **Figures 7, 8**). Further exploration of the elemental composition observed in spectrum 1 revealed that the primary elemental composition of spectrum 1 comprised Ca, O, C, and P, while Ca content was low and the relative percentage of Ca in the area of spectrum 4 was 42.9 weight % (*wt.*%). These results were consistent with the continuous enrichment of calcium on the PVC hollow fiber membrane during operation, resulting in increased calcium precipitation owing to the adhesion of inorganic substances like calcium to the membrane surface. The high content of Ca^{2+} and other cations led to an increase in inorganic substances in the reactor, resulting in a bridging effect between the cations and the substances attached

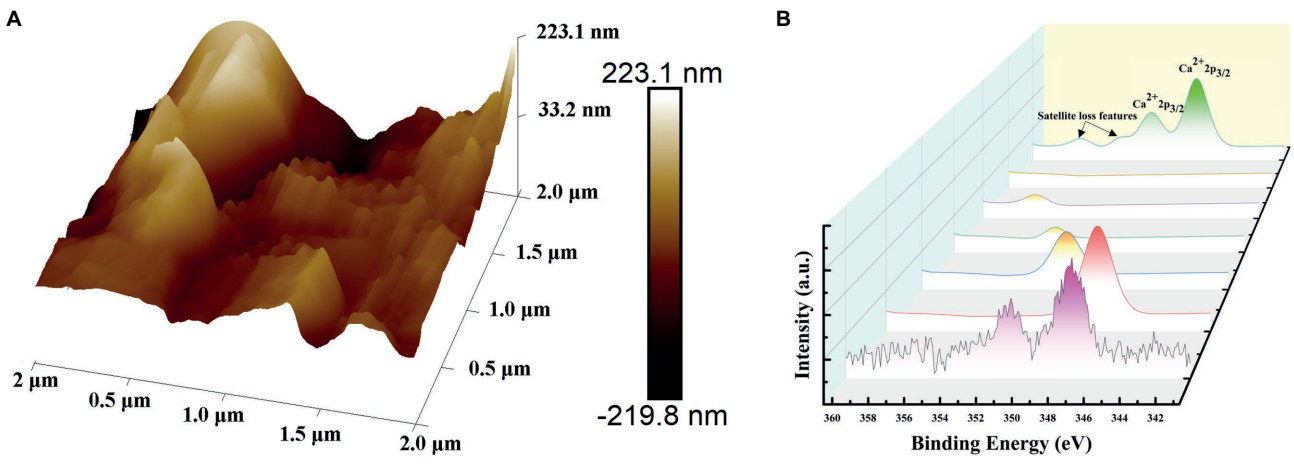

FIGURE 6 | Images of the PVC hollow fiber membrane surfaces showing Ca levels after operation during the stable phase. Showed in **(A)** Atomic force microscopy (AFM) and **(B)** X-ray photoelectron spectroscopy (XPS).

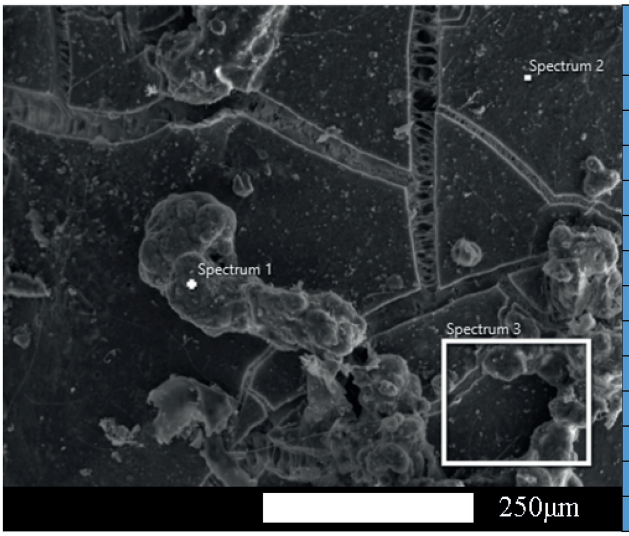

Elements	Spectrum 1	Spectrum 2	Spectrum 3
	Weight(%)	Weight(%)	Weight(%)
C	26.51	47.93	46.71
O	37.37	26.77	35.48
Mg	NA	0.37	NA
Al	NA	0.81	0.50
Si	NA	0.43	0.19
P	10.08	5.33	3.86
S	0.30	0.85	0.44
Cl	0.11	NA	NA
K	NA	0.20	0.13
Ca	24.53	5.36	6.72
Fe	0.73	11.87	5.96
Zn	0.38	NA	NA
Ba	NA	0.10	NA

FIGURE 7 | Scanning electron microscopy (SEM) morphology of the polyvinyl chloride (PVC) sample surface taken during stable operation, in addition to the point sweep energy spectra for spectrum 1, spectrum 2, and spectrum 3.

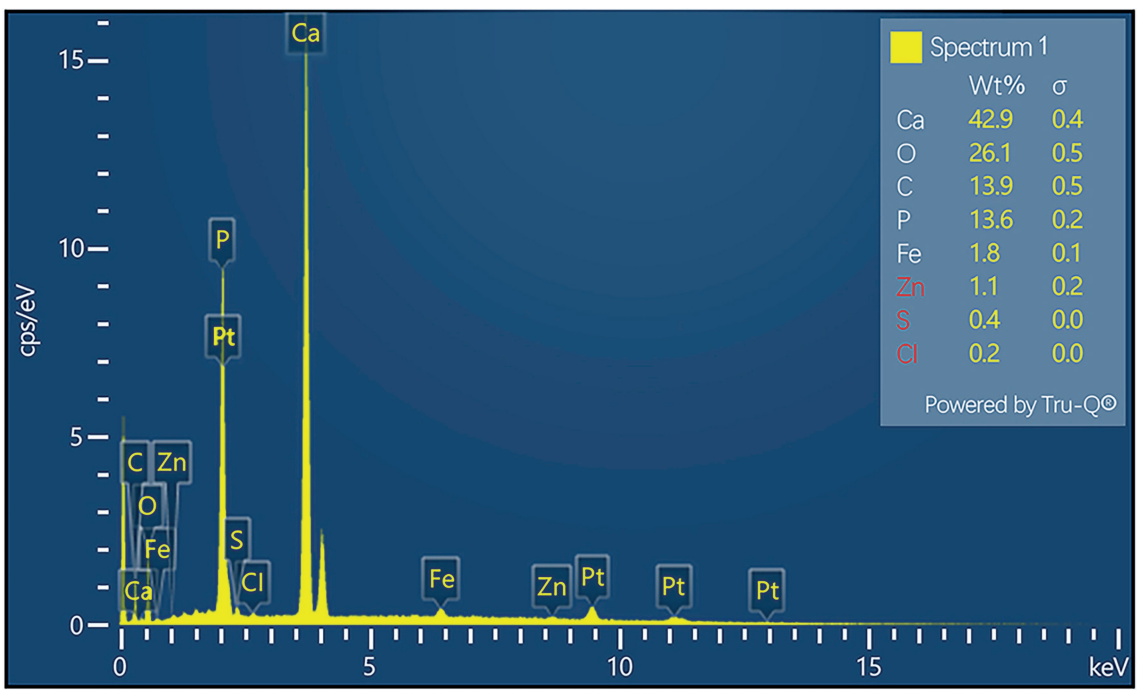

FIGURE 8 | Scanning electron microscopy–energy dispersive spectrometer (SEM–EDS) characterization of the elemental distribution of spectrum 1 of the polyvinyl chloride (PVC) sample surface during the stable operation phase.

to the membrane surface, thereby increasing the density of the membrane layer. Concomitantly, Ca^{2+} combined with specific acidic functional groups (e.g., R–COOH) can lead to the formation of complexes or gel layers, thereby further thickening the calcified layer and exacerbating the reduced membrane flux, leading to decreased membrane flux and reduced membrane life (Meng et al., 2010). PVC hollow fiber is a polymeric compound constructed from vinyl chloride that does not contain calcium, despite that calcium is the most abundant element on the surface of PVC hollow fibers during stable operation, which further confirming the presence of calcium-containing monomers or compounds on PVC hollow fiber surfaces. In addition to Ca, other elements were present based on the analyses including O, C, P, and Fe at *wt.*% of 26.10, 13.90, 13.60, and 1.80%, respectively. Thus,

other trace impurity elements can be introduced during sample preparation and neglected when evaluating reactor performance. Overall, the primary elemental composition of the PVC hollow fiber membrane surfaces during stable operation phase comprised Ca, O, C, P, and Fe, with particularly high Ca^{2+} concentrations reflecting calcium precipitation on membrane surfaces and clear calcification over time.

XRD Characterization

XRD patterns for PVC membrane sample surfaces were also analyzed during the stable operation phase (**Figure 9A**). Several obvious diffraction peaks were observed from surface samples in the range of 25–70°, although XRD curves also revealed bulges in the range of 20–40° into the back-bottom elevation. The overall diffraction peak position of the PVC sample was similar to that of $Ca_5F(PO_4)_3$ (PDF#01–071-3,848) based on comparison in MDI Jade 9. XRD refinement of the data and crystal structures of $Ca_5F(PO_4)_3$ (**Figures 9B,C**) indicated the presence of this compound in the optimized sample. Some of the diffraction peaks were compatible with $MgCl_2$ (PDF#70–2,746) that is involved in conducting the treatment, although multiple impurity peaks remained without suitable compounds corresponding to them. These results followed from the PVC membrane surface carrying significant amounts of impurity plugging due to uninterrupted inlet water present during the experimental process. This results in membrane pore blockage and calcium-containing inorganic substances adhesion, thereby leading to altered diffraction peaks of PVC and calcification development. These dynamics could be due to inorganic substances comprising impurities such as Ca, Mg, and their compounds being present in the feed water (Meng et al., 2010), in addition to the presence of harmful substances like P being present (as verified with SEM–EDS). These substances were attached to the calcified layer on the membrane surface, leading to impurities remaining in the PVC membrane pores that produce complex diffraction peaks.

CONCLUSION

In this study, a quadratic polynomial regression model of biofilm thickness, hydrogen pressure, and pH was established through

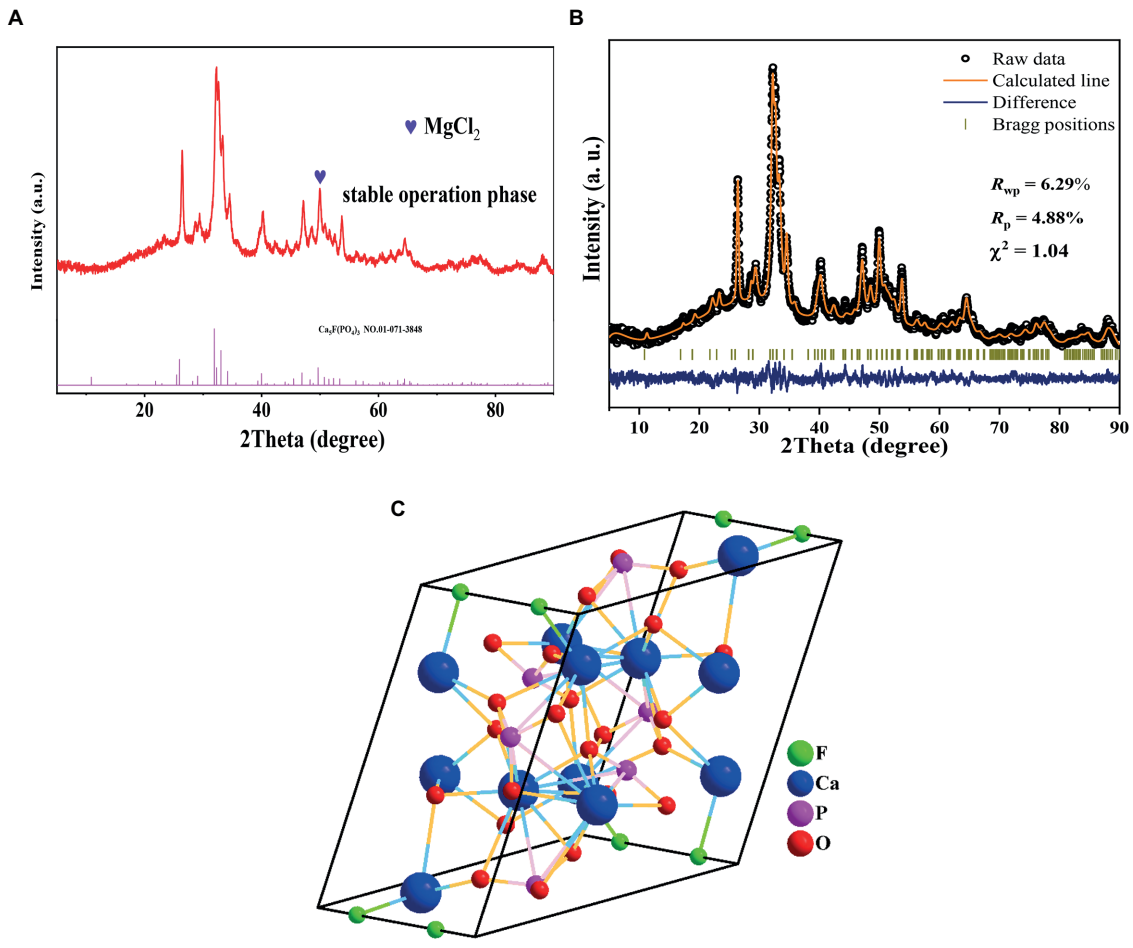

FIGURE 9 | (A) X-ray diffraction (XRD) analysis of polyvinyl chloride (PVC) membrane sample surface during stable operation. **(B)** XRD refinement of PVC membrane sample surfaces during stable operation. **(C)** Crystal structure of $Ca_5F(PO_4)_3$.

response surface analysis based on single-factor experiments. Modeling led to observed response surface conditions of the reactor exhibited the $NO_3^- - N$ removal flux was 1.15 g·m^{-2} d^{-1} when biofilm thickness was 653.31 μm, the hydrogen pressure was 0.05 MPa, and pH was 7.78. The model predicted the $NO_3^- - N$ removal rate with an accuracy of 97.21%. In addition,, obvious calcium precipitation increasing after long-term operation which provide suitable habitat for biofilm formation. However, the thicker calcium precipitation easily led to the tendency of the biofilm to fall off easily due to cavitation. During stable operation, SEM, XPS, and SEM–EDS analyses of the PVC hollow fiber membrane revealed a disordered porous structure with significant calcium precipitation and calcification leading to the blockage of membrane pores. Characterization of samples from the stable operation phase indicated the presence of elements such as Ca, O, C, P, and Fe. Further XRD characterization confirmed that $Ca_5F(PO_4)_3$ was added to the surface of the membrane filaments during the stable operation phase, in addition to the presence of other Ca and Mg elements and compounds. These results confirmed the presence of calcification on membrane surfaces during MBfR operation.

DATA AVAILABILITY STATEMENT

The original contributions presented in the study are included in the article/**Supplementary Material**, further inquiries can be directed to the corresponding author.

AUTHOR CONTRIBUTIONS

KD, XF, DW, and HaL: conceptualization and methodology. YY, KD, ZZ, and XF: project administration and data curation. HuL and KD: writing—original draft. KD and XF: writing—review and editing. KD, XF, YY, XZ, and HaL: supervision. All authors contributed to the article and approved the submitted version.

FUNDING

This study was funded by Guangxi Natural Science Foundation (grant number 2022GXNSFFA035033), The Guangxi Key Laboratory of Theory and Technology for Environmental Pollution Control (grant number Guikeneng 2001K008), the Natural Science Foundation of China (grant numbers 51878197, 51978188), the Basic Ability Enhancement Program for Young and Middle-aged Teachers of Guangxi (grant number 2021KY0265) and Innovation Project of Guangxi Graduate Education (grant number YCBZ2022117).

SUPPLEMENTARY MATERIAL

The Supplementary Material for this article can be found online at: https://www.frontiersin.org/articles/10.3389/fmicb.2022.924084/full#supplementary-material

REFERENCES

Chang, M., Liang, B., Zhang, K., Wang, Y., Jin, D., Zhang, Q., et al. (2022). Simultaneous shortcut nitrification and denitrification in a hybrid membrane aerated biofilms reactor (H-MBfR) for nitrogen removal from low COD/N wastewater. *Water Res.* 211:118027. doi: 10.1016/j.watres.2021.118027

Chung, J., Nerenberg, R., and Rittmann, B. E. (2006). Bio-reduction of soluble chromate using a hydrogen-based membrane biofilm reactor. *Water Res.* 40, 1634–1642. doi: 10.1016/j.watres.2006.01.049

Della Rocca, C., Belgiorno, V., and Meriç, S. (2007). Overview of *in-situ* applicable nitrate removal processes. *Desalination* 204, 46–62. doi: 10.1016/j.desal.2006.04.023

Demirel, S., and Bayhan, I. (2013). Nitrate and bromate removal by autotrophic and heterotrophic denitrification processes: batch experiments. *J. Environ. Health Sci. Eng.* 11:27. doi: 10.1186/2052-336X-11-27

Dong, K., Feng, X., Wang, W., Chen, Y., Hu, W., Li, H., et al. (2021). Simultaneous partial nitrification and denitrification maintained in membrane bioreactor for nitrogen removal and hydrogen autotrophic denitrification for further treatment. *Membranes (Basel)* 11:911. doi: 10.3390/membranes11120911

Gao, M., Wang, S., Jin, C., She, Z., Zhao, C., Zhao, Y., et al. (2015). Autotrophic perchlorate reduction kinetics of a microbial consortium using elemental sulfur as an electron donor. *Environ. Sci. Pollut. Res. Int.* 22, 9694–9703. doi: 10.1007/s11356-015-4147-x

Hellmuth, K., Pluschkell, S., Jung, J. K., Ruttkowski, E., and Rinas, U. (1995). Optimization of glucose oxidase production by Aspergillus Niger using genetic- and process-engineering techniques. *Appl. Microbiol. Biotechnol.* 43, 978–984. doi: 10.1007/BF00166912

Hou, D., Jassby, D., Nerenberg, R., and Ren, Z. J. (2019). Hydrophobic gas transfer membranes for wastewater treatment and resource recovery. *Environ. Sci. Technol.* 53, 11618–11635. doi: 10.1021/acs.est.9b00902

Jiang, M., Zhang, Y., Yuan, Y., Chen, Y., Lin, H., Zheng, J., et al. (2020). Nitrate removal and dynamics of microbial community of a hydrogen-based membrane biofilm reactor at diverse nitrate loadings and distances from hydrogen supply end. *Water* 12:3196. doi: 10.3390/w12113196

Lee, S.-H., Kondaveeti, S., Min, B., and Park, H.-D. (2013). Enrichment of clostridia during the operation of an external-powered bio-electrochemical denitrification system. *Process Biochem.* 48, 306–311. doi: 10.1016/j.procbio.2012.11.020

Lee, K.-C., and Rittmann, B. E. (2003). Effects of pH and precipitation on autohydrogenotrophic denitrification using the hollow-fiber membrane-biofilm reactor. *Water Res.* 37, 1551–1556. doi: 10.1016/s0043-1354(02)00519-5

Li, H., Lin, H., Xu, X., Jiang, M., Chang, C. C., and Xia, S. (2017). Simultaneous bioreduction of multiple oxidized contaminants using a membrane biofilm reactor. *Water Environ. Res.* 89, 178–185. doi: 10.2175/106143016X14609975746686

Li, H., Zhou, L., Lin, H., Zhang, W., and Xia, S. (2019). Nitrate effects on perchlorate reduction in a H2/CO2-based biofilm. *Sci. Total Environ.* 694:133564. doi: 10.1016/j.scitotenv.2019.07.370

Liu, L., Gao, D. W., Zhang, M., and Fu, Y. (2010). Comparison of Ca^{2+} and Mg^{2+} enhancing aerobic granulation in SBR. *J. Hazard. Mater.* 181, 382–387. doi: 10.1016/j.jhazmat.2010.05.02

Liu, C., Liang, Z., Yang, C., Cui, F., and Zhao, Z. (2022). Nitrite-enhanced N-nitrosamines formation during the simulated tetracycline polluted groundwater chlorination: experimental and theoretical investigation. *Chem. Eng. J.* 431:133363. doi: 10.1016/j.cej.2021.133363

Long, M., Zeng, C., Wang, Z., Xia, S., and Zhou, C. (2020). Complete dechlorination and mineralization of Para-chlorophenol (4-CP) in a hydrogen-based membrane biofilm reactor (MBfR). *J. Clean. Prod.* 276:123257. doi: 10.1016/j.jclepro.2020.123257

Meng, F., Liao, B., Liang, S., Yang, F., Zhang, H., and Song, L. (2010). Morphological visualization, componential characterization and microbiological identification of membrane fouling in membrane bioreactors (MBRs). *J. Membr. Sci.* 361, 1–14. doi: 10.1016/j.memsci.2010.06.006

Nerenberg, R. (2016). The membrane-biofilm reactor (MBfR) as a counter-diffusional biofilm process. *Curr. Opin. Biotechnol.* 38, 131–136. doi: 10.1016/j.copbio.2016.01.015

Polat, S., and Sayan, P. (2019). Application of response surface methodology with a Box–Behnken design for struvite precipitation. *Adv. Powder Technol.* 30, 2396–2407. doi: 10.1016/j.apt.2019.07.022

Rittmann, B. E. (2011). The membrane biofilm reactor is a versa tile platform for water and wastewater treatment. *Environ. Eng. Res.* 12, 157–175. doi: 10.4491/eer.2007.12.4.157

Su, J. F., Wang, Z., Huang, T. L., Zhang, H., and Zhang, H. (2020). Simultaneous removal of nitrate, phosphorous and cadmium using a novel multifunctional biomaterial immobilized aerobic strain Proteobacteria Cupriavidus H29. *Bioresour. Technol.* 307:123196. doi: 10.1016/j.biortech.2020.123196

Tang, Y., Zhou, C., Van Ginkel, S. W., Ontiveros-Valencia, A., Shin, J., and Rittmann, B. E. (2012). Hydrogen permeability of the hollow fibers used in H2-based membrane biofilm reactors. *J. Membr. Sci.* 407–408, 176–183. doi: 10.1016/j.memsci.2012.03.040

Tang, Y., Zhou, C., Ziv-El, M., and Rittmann, B. E. (2011). A pH-control model for heterotrophic and hydrogen-based autotrophic denitrification. *Water Res.* 45, 232–240. doi: 10.1016/j.watres.2010.07.049

Van Ginkel, S. W., Ahn, C. H., Badruzzaman, M., Roberts, D. J., Lehman, S. G., Adham, S. S., et al. (2008). Kinetics of nitrate and perchlorate reduction in ion-exchange brine using the membrane biofilm reactor (MBfR). *Water Res.* 42, 4197–4205. doi: 10.1016/j.watres.2008.07.012

Xia, S., Xu, X., Zhou, C., Wang, C., Zhou, L., and Rittmann, B. E. (2016). Direct delivery of CO_2 into a hydrogen-based membrane biofilm reactor and model development. *Chem. Eng. J.* 290, 154–160. doi: 10.1016/j.cej.2016.01.021

Xia, S., Zhong, F., Zhang, Y., Li, H., and Yang, X. (2010). Bio-reduction of nitrate from groundwater using a hydrogen-based membrane biofilm reactor. *J. Environ. Sci.* 22, 257–262. doi: 10.1016/s1001-0742(09)60102-9

Zhang, Y., Cui, K., Gao, Q., Hussain, S., and Lv, Y. (2020). Investigation of morphology and texture properties of WSi2 coatings on W substrate based on contact-mode AFM and EBSD. *Surf. Coat. Technol.* 396:125966. doi: 10.1016/j.surfcoat.2020.125966

Zhang, H., Zivel, M., Rittmann, B. E., and Krajmalnikbrown, R. (2015). Effect of dechlorination and sulfate reduction on the microbial community structure in denitrifying membrane-biofilm reactors. *Environ. Sci. Technol.* 44, 5159–5164. doi: 10.1021/es100695n

Zhou, C., Ontiveros-Valencia, A., Wang, Z., Maldonado, J., Zhao, H. P., Krajmalnik-Brown, R., et al. (2016). Palladium recovery in a H2-based membrane biofilm reactor: formation of Pd(0) nanoparticles through enzymatic and autocatalytic reductions. *Environ. Sci. Technol.* 50, 2546–2555. doi: 10.1021/acs.est.5b05318

Zhou, X., Xiong, W., Li, Y., Zhang, C., and Xiong, X. (2022). A novel simultaneous coupling of memory photocatalysts and microbial communities for alternate removal of dimethyl phthalate and nitrate in water under light/dark cycles. *J. Hazard. Mater.* 430:128395. doi: 10.1016/j.jhazmat.2022.128395

Conflict of Interest: The authors declare that the research was conducted in the absence of any commercial or financial relationships that could be construed as a potential conflict of interest.

Publisher's Note: All claims expressed in this article are solely those of the authors and do not necessarily represent those of their affiliated organizations, or those of the publisher, the editors and the reviewers. Any product that may be evaluated in this article, or claim that may be made by its manufacturer, is not guaranteed or endorsed by the publisher.

frontiers | Frontiers in Microbiology

ORIGINAL RESEARCH
published: 29 June 2022
doi: 10.3389/fmicb.2022.932940

Integration of Zeolite Membrane Bioreactor With Granular Sludge-Based Anammox in High-Efficiency Nitrogen Removal From Iron Oxide Red Wastewater

*Xing-Hui Feng[1,2], Xiao-Jun Wang[3], Hai-Xiang Li[1,2], Hai-Ya Zhang[4], Zong-Qiang Zhu[1,2], Yan-Peng Liang[1,2], Kun Dong[1] and Hong-Hu Zeng[1]**

[1] School of Environmental Science and Engineering, Guilin University of Technology, Guilin, China, [2] Collaborative Innovation Center for Water Pollution Control and Water Safety in Karst Area, Guilin University of Technology, Guilin, China, [3] School of Environment and Energy, South China University of Technology, Guangzhou, China, [4] Institute of Water Ecology and Environment, Chinese Research Academy of Environmental Science, Beijing, China

OPEN ACCESS

Edited by:
Chongjun Chen,
Suzhou University of Science and Technology, China

Reviewed by:
Da Kang,
Beijing University of Technology, China
Xiaojing Zhang,
Zhengzhou University of Light Industry, China

***Correspondence:**
Hong-Hu Zeng
zenghonghu@glut.edu.cn

Specialty section:
This article was submitted to Microbiotechnology, a section of the journal Frontiers in Microbiology

Received: 30 April 2022
Accepted: 23 May 2022
Published: 29 June 2022

Citation:
Feng X-H, Wang X-J, Li H-X, Zhang H-Y, Zhu Z-Q, Liang Y-P, Dong K and Zeng H-H (2022) Integration of Zeolite Membrane Bioreactor With Granular Sludge-Based Anammox in High-Efficiency Nitrogen Removal From Iron Oxide Red Wastewater. Front. Microbiol. 13:932940. doi: 10.3389/fmicb.2022.932940

Acquisition of stable nitritation and efficient anammox play a crucial role in partial nitritation (PN) combined with anammox for nitrogen removal from ammonium-rich wastewater. Due to the limitation of ammonia-oxidizing bacteria (AOB) enrichment and nitrite-oxidizing bacteria (NOB) control in traditional membrane biological reactor (MBR), it can result in a lower nitrite production rate (NPR) and unstable PN, eventually reducing the nitrogen removal rate (NRR) *via* PN-anammox. In this study, we developed a zeolite membrane biological reactor (ZMBR) to enhance the PN of iron oxide red wastewater (IORW), in which the biofilm derived from the zeolite surface can provide free ammonia (FA)-containing microenvironment for AOB enrichment and NOB inhibition. The results showed that ZMBR can tolerate a higher influent nitrogen loading rate (NLR) of 2.78 kg/(m^3·day) in comparison to the traditional MBR [2.02 kg/(m^3·day)] and the NPR in ZMBR and traditional MBR were 1.39 and 0.96 kg/(m^3·day), respectively. The mass concentration ratio of NO_2^--N/NH_4^+-N ranged from 1.05 to 1.33 in ZMBR, suggesting a suitable condition for nitrogen removal *via* anammox. Subsequently, the domesticated granular sludge obtained from a paper-making wastewater treatment was used as the carrier of anammox bacteria to remove nitrogen. After 93 days of operation, the NRR was observed to be 2.33 kg/(m^3·day) and high-throughput sequencing indicated that the relatively higher abundance (45.0%) of *Candidatus* Kuenenia stuttgartiensis was detected in the granular sludge of the bottom part of the reactor, which can produce more proteins and lipids, suggesting a good settleability. Overall, this study provides a high-efficient method to control PN and domesticate anammox for nitrogen removal from IORW.

Keywords: nitrogen removal, PN-anammox, granular sludge, IORW, alkalinity

INTRODUCTION

About 15 tons of iron oxide red wastewater (IORW) occurred per ton of finished product, which contains lots of ammonium (NH_4^+-N), Fe^{2+}, and SO_4^{2-}. The previous study has proved that aeration oxidation and alkaline neutralization are effective solutions for removing Fe^{2+} from which iron mud can be recycled and used as the inoculating crystal (Feng et al., 2019). However, the remaining NH_4^+-N is at high concentrations (700–1,000 mg/L) in the supernatant. The improper management or direct discharge of IORW could cause serious water eutrophication; accordingly, a low-carbon and low-cost technology for nitrogen removal is a significant requirement. Due to the presence of SO_4^{2-}, the traditional nitrification-denitrification technology might not be an acceptable process for nitrogen removal because sulfate-reducing bacteria (SRB) convert sulfate to H_2S, which would lead to serious secondary pollution and inhibition of nitrification.

Recently, the partial nitritation (PN) combined with anaerobic ammonium oxidation (PN-anammox) has been widely used in nitrogen removal system *via* anammox by using NH_4^+-N as the electron donor and NO_2^--N as the electron acceptor, and its engineering application, is drawing increasing attention from researchers. The PN-anammox reduces the need for organic carbon and aeration and decreases sludge production compared with traditional nitrification-denitrification (Lackner et al., 2014). Currently, a limiting step in PN-anammox is to obtain stable PN. Generally, ammonia-oxidizing bacteria (AOB) and nitrite-oxidizing bacteria (NOB) play a crucial role in the nitritation and nitratation process, respectively (Sinha and Annachhatre, 2007; Laureni et al., 2016). Nitrite accumulation depends on nitritation (Anthonisen et al., 1976) and AOB abundance increased, while NOB number decreased at high ammonium loading conditions (Shao et al., 2018). The literature reports numerous indirect methods to maintain effective AOB and inhibit NOB in the same reactor, for instance, controlling free nitrous acid (FNA) (Pedrouso et al., 2017), maintaining a low concentration of dissolved oxygen (DO) in a sequencing batch reactor (SBR) (Li et al., 2011) and regulating free ammonia (FA) in zeolite biological aeration filter (ZBAF). A previous study investigated the PN in two-stage ZBAF by controlling the alkalinity dosage resulting that stable PN being obtained in this combined system (Feng et al., 2019). In addition, high FA induced by Na_2CO_3 was avoided resulting that Na_2CO_3 as an alkalinity donor could save about 40% dosage than common $NaHCO_3$. Although ZBAF can be stable and low-cost in the PN from IORW, the low treatment efficiency and frequent backwashing requirement result that it might not be suitable for large-scale implementation. Moreover, the detached biofilm from zeolite would outflow along with the affluent, affecting the substance concentration (nitrite and ammonium). Besides, numerous theoretical and practical applications claim that membrane biological reactors (MBRs) have advantages in higher volumetric loading, better effluent quality, and less sludge loss (Barreto et al., 2017). These advantages from MBRs coupled with zeolite to maintain high-efficiency PN and used Na_2CO_3 as the alkalinity donor, which should have a wide market foreground and important engineering significance for IORW treatment. However, the premise is to achieve stable PN in a zeolite membrane biological reactor (ZMBR).

Anammox bacteria cultivated by feeding with real wastewater is another key step in nitrogen removal from IORW treatment because it has a high sensitivity to changing environmental conditions, which makes their cultivation extremely difficult (Ni and Meng, 2011). Besides, the growth rate of anammox bacteria is regarded as restrictive to engineering applications (Jin et al., 2012). Nitrogen removal efficiency is the common parameter to reflect anammox activity. The literature reports the different doubling times of anammox bacteria as 10–14 (Marc et al., 2006), 4.8 (Tang et al., 2011), and 1.8 days (Isaka et al., 2006). Different sludge morphologies (e.g., floc and granule) have different adhesive surfaces, which have differences in anammox bacteria enrichment. The characteristics of granular sludge mainly include well-defined shape, high settleability, enhanced microbial activities, and its application in domestic or industrial wastewater treatment (Sarma et al., 2017). Although flocculent sludge has a larger specific surface area that could offer more attachment sites for anammox bacteria than granular sludge, sludge loss would be a challenge in practical application. Moreover, extracellular polymeric substances (EPSs) are usually found in the metabolic activities of microorganisms and look like a gel-like network on the surface of granules and play a crucial role in maintaining their structural stability (Cai et al., 2017). Especially the proteins, lipids, and β-D-mannose are also beneficial to maintaining sludge structure and promoting sludge aggregation (Jia et al., 2017). In other words, EPS might be beneficial for the attachment of microorganisms to the sludge. Granular sludge is often considered a typical solid waste that needs reasonable disposal in papermaking plants. Because of this, using granular sludge as the carrier of anammox bacteria is also a potential resource utilization method, which still needs experimental verification.

In this study, the PN of IORW was conducted in ZMBR, followed by using granular sludge-based anammox for further nitrogen removal. The objective of this study was to: (1) obtain controllable PN of IORW in ZMBR and evaluate the biofilm formation on the surface of zeolite; (2) recycle granular sludge from the papermaking wastewater treatment process for the carrier of anammox bacteria; (3) investigate the living environment of anammox bacteria through EPS (proteins, β-D-mannose, and lipid) detection by using confocal laser scanning microscopy (CLSM); and (4) use ZMBR combined with granular sludge-based anammox for the nitrogen removal from IORW. The obtained result might provide a high-efficiency and cost-effective strategy for IORW treatment.

MATERIALS AND METHODS

Experimental Design

The ZMBR was designed as a rectangular vessel made of stalinite with a total volume of 10 L (working volume was 8 L) and the surface area of microfiltration polymeric membranes was 2 m^2 (the ratio of the addition of membrane to the working

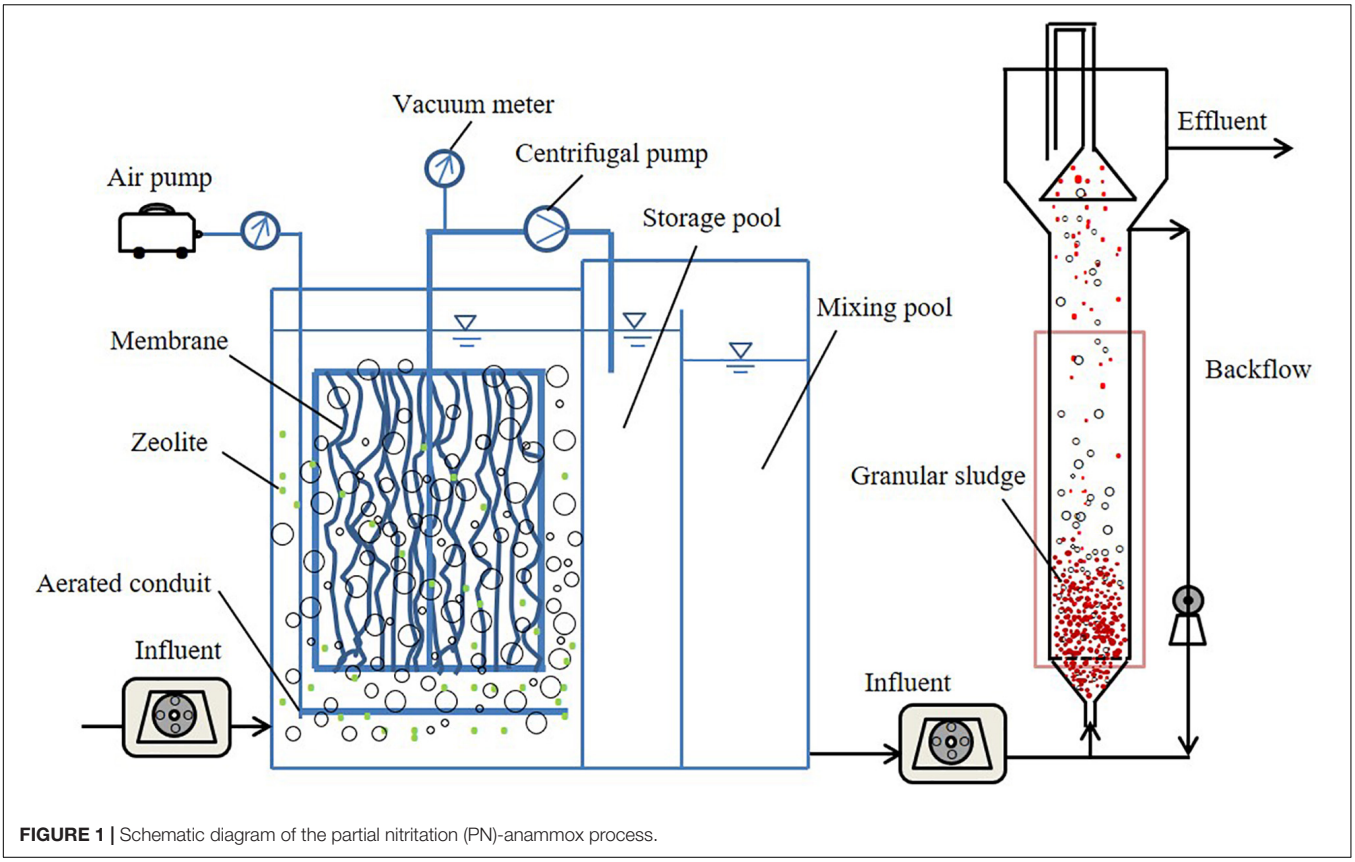

FIGURE 1 | Schematic diagram of the partial nitritation (PN)-anammox process.

volume of the reactor was 0.25 m^2/L). Natural zeolite was filled as the NH_4^+-N adsorbents that the average particle size was 0.5–1 mm (diameter) and the filling rate was ranged from 2 to 5% of the reactor volume. Based on upflow anaerobic sludge blanket (UASB) and anammox reactors, they were made of transparent acrylic plates of 1,000 mm in height and 80 mm in diameter. The total volume was 5 L and the sludge volume was about 1.5 L. The schematic diagram of the PN-anammox process is shown in **Figure 1**.

Experimental Wastewater and Sludge

Test wastewater was taken from the pretreatment process of an iron oxide red plant (Jiangmen, China) which has completed Fe^{2+} removal under the condition of aeration and added NaOH then static settlement. The concentration of NH_4^+-N was between 700 and 1,000 mg/L and SO_4^{2-} was in the range of 8,000–10,000 mg/L in the supernatant.

The seed sludge of nitritation was obtained from a refuse landfill (Guangzhou, China) and using clean water washed several times then cultivated under the laboratory condition (feed with alkalinity and NH_4^+-N). The granular sludge came from the sewage treatment process of a papermaking plant (Liuzhou, China). The seed sludge of anammox was taken from an anammox reactor that was fed with synthetic water in a laboratory and the dominant anammox bacteria were *Candidatus* Brocadia sinica and *Candidatus* Kuenenia stuttgartiensis.

Operational Strategies

The ZMBR startup was divided into three phases: Phase I, NH_4^+-N was enriched in the zeolite *via* adsorption; phase II, added 2 L seed sludge to activate PN [the mixed liquid suspended solids (MLSSs) was about 3,000 mg/L]; and phase III, gradually increase the influent NH_4^+-N concentration or shortening the hydraulic retention time (HRT) to increase influent nitrogen loading rate (NLR). Using an air pump to maintain the DO concentration in the range of 4–6 mg/L and the operating temperature was 28 ± 2°C in the ZMBR.

Using $MgSO_4$ (0.1 mg/L), KH_2PO_4 (0.05 mg/L) to provide essential microelement and Na_2CO_3 as alkalinity donor. According to the previous study, alkalinity/NH_4^+-N = 4.33 (mass concentration ratio) was an optimum ratio to obtain NO_2^--N/NH_4^+-N = 1.0–1.4 that is suitable for further treatment *via* anammox (Feng et al., 2019). The concentrations of NH_4^+-N, NO_2^--N, and NO_3^--N were detected in every 12 h to assess the nitritation efficiency and FA (Anthonisen et al., 1976), nitrite production rate (NPR), NLR, and nitrogen removal rate (NRR) were calculated by the following equations:

$$\mathrm{FA}\ (mg/L) = \frac{17}{14} \times \frac{NH_4^+ - N \times 10^{pH}}{\exp\left[6334/(273+T)\right] + 10^{pH}} \quad (1)$$

$$\mathrm{NPR}\ [\mathrm{kg\ N}\ /(m^3 \cdot \mathrm{d})] = 24 \times \frac{NO_2^- - N_{eff}}{HRT} \quad (2)$$

$$\text{NLR [kg N } /(m^3 \cdot \text{d})] = 24 \times \frac{TN_{in}}{HRT} \quad (3)$$

$$\text{NRR [kg N } /(m^3 \cdot \text{d})] = 24 \times \frac{TN_{in} - TN_{eff}}{HRT} \quad (4)$$

Anammox reactor was started up by inoculating with anammox sludge, increasing the influent substrate concentration (NH_4^+-N and NO_2^--N), and put on a heating jacket to maintain the temperature between 28 and 32°C.

Quantitative PCR Assays

Absolute quantification-PCR (AQ-PCR) technology was based on the known copy number variation (CNV) from the standard sample to obtain a standard curve. According to the cycle threshold (Ct) value, the absolute quantification of CNV from messenger RNA (mRNA) or DNA could be calculated according to the standard curve (Walker, 2001). Because of the relatively low abundance in NOB, it results that it was usually not detected by the common high-throughput sequencing technology. Therefore, PCR was employed to detect the relative ratio of AOB and NOB, which coexistence on the biofilm of zeolite.

$$\text{Ct} = -K\log X_0 + \text{b}$$

Ct refers to the cycle index when the fluorescence signal of the amplified product reaches the set threshold value and *K* was the slope and *b* as the y-intercept of standard curve.

This detection was supported by the Shanghai Sunny Biotechnology Corporation Ltd. The related primer information of AOB and NOB is given in **Table 1**. The real-time PCR samples were carried out by using 20 μl reaction volumes that contained 10 μl mixture A, which consist of 10 μl 2 × SYBR real-time PCR premixture and 0.4 μl from primer-F and -R (10 μM, the primer information from AOB and NOB was found in **Table 1**), 10 μl DNA diluent as template (using DNA extraction kit obtained 1.61 μg DNA in 50 μl solution, cat: DP305, TianGen Biotechnology Corporation Ltd., Beijing, China). The thermal cycling was performed under the following conditions: 95°C for 5 min, followed by 40 cycles of 95°C for 15 s, and a final extension at 60°C for 30 s. All the operations, primers, and analysis results were provided by Sunny Biotechnology Corporation Ltd. (Shanghai, China).

Confocal Laser Scanning Microscopy Observation

The samples from the anammox reactor were pretreated by staining and then observed by CLSM to detect the EPS (proteins, β-D-mannose, and lipid). The procedures of staining were adopted from a reference (Wu et al., 2018) and with a little modification that is described as follows: (1) Fluorescein isothiocyanate (FITC) (CAS No. 27072-45-3, Macklin, Shanghai, China) was applied to stain proteins; (2) Calcofluor white (CalW) (CAS No. 4404-43-47, Sigma-Aldrich Corporation, California, CA, United States) for β-D-mannose detection; and (3) Nile Red (CAS No. 7385-67-3, Macklin, Shanghai, China) was used to stain lipids.

The detailed staining steps were followed by adding a drop of FITC (10 mg/L, dimethyl sulfoxide as solvent) to the samples standing for 30 min and washing for three times by using phosphate-buffered saline (PBS) (0.01 M, pH = 7.4). Then, using CalW solution combined with 10% KOH (1:1) stained 1 min and washed with PBS several times. Next, put the samples in Nile red solution (5 mg/L, methanol as solvent) to stain for 5 min. Finally, a drop of the antifade mounting medium was added to the test samples. After staining, using PBS washing then put on the glass slide and observed by CLSM (Leica TCS SP8, Germany) and amplified about 4–10 times. The measuring parameter and observable color from different staining conditions are given in **Table 2**.

Chemical Analyses

Based on the standard examination of water and wastewater (Walter, 1961), the concentrations of ammonium, nitrite, and nitrate were periodically detected to evaluate the nitrogen removal performance and an automatic potentiometric titration was applied for the alkalinity measurement (based on $CaCO_3$ calculation, mg/L). A multifunctional portable instrument (HQ30d, HACH) was employed for the detection of temperature and DO. A pH meter (PHS-3C) was used to obtain the pH value. Using high-throughput sequencing technology, it investigates the bacterial community structure in sludge samples [this part was supported by The Beijing Genomics Institute (BGI) Corporation Ltd.].

RESULTS

Partial Nitritation Assessments in Zeolite Membrane Biological Reactor

Partial nitritation was maintained in ZMBR by gradually increasing the influent ammonium concentration and shortening HRT. As shown in **Figure 2**, ZMBR exhibited excellent nitritation efficiency and obtained 2.78 kg/(m^3·day) in NLR and

TABLE 1 | The related primer information of ammonia-oxidizing bacteria (AOB) and nitrite-oxidizing bacteria (NOB).

ID	Primer	Sequence(5′ to 3′)
amoA (AOB)	amoA-F	GGGGTTTCTACTGGTGGT
	amoA-R	CCCCTCKGSAAAGCCTTCTTC
Nitrobacter sp. 16S (NOB)	NxrB-F	ACGTGGAGACCAAGCCGGC
	NxrB-R	CCGTGCTGTTGAYCTCGTTGA
Nitrospira sp. 16S (NOB)	NSR-F	CCTGCTTTCAGTTGCTACCG
	NSR-R	GTTTGCAGCGCTTTGTACCG

TABLE 2 | Operation parameter and observable color of detection.

Dye	Emission wavelength (nm)	Excitation wavelength (nm)	Color
FITC	488	500–550	Green
CalW	400	410–480	Blue
Nile red	514	625–700	Red

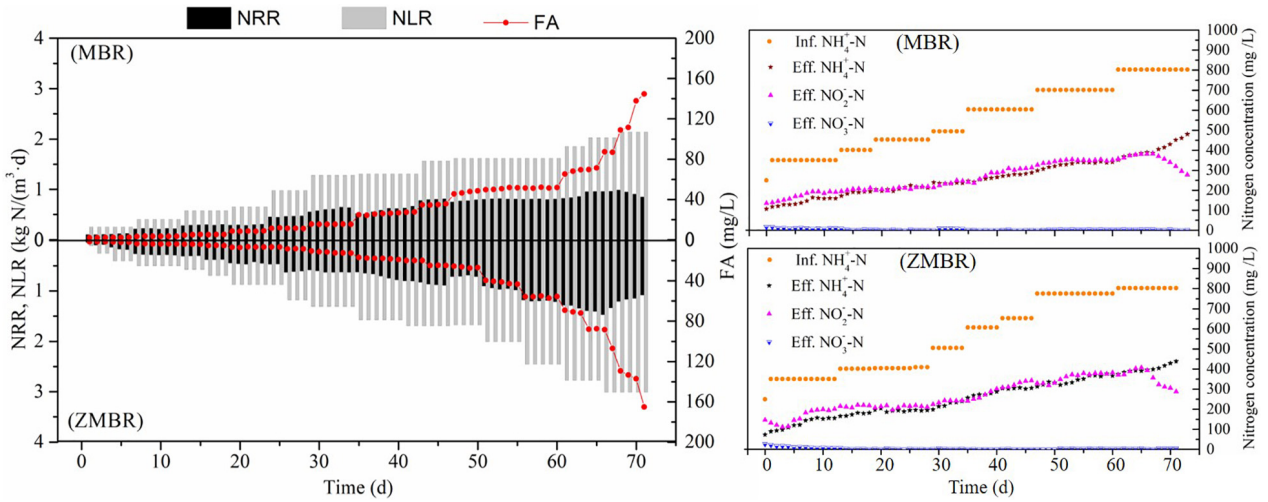

FIGURE 2 | Evaluation of the PN, free ammonia (FA), and the nitrogen concentrations in MBR and zeolite membrane biological reactor (ZMBR).

TABLE 3 | Copy numbers of AOB and NOB (calculated by standard curve).

Gene	Ct	Standard curve	*R*	X_0(copy/g)	SD
amoA	13.56	$Ct = -3.19\log X_0 + 34.83$	0.986	2.40×10^9	1.42×10^7
Nitrobacter sp. 16S	19.9	$Ct = -3.21\log X_0 + 35.74$	0.983	7.75×10^7	3.64×10^6
Nitrospira sp. 16S	29.20	$Ct = -3.18\log X_0 + 33.10$	0.996	1.30×10^4	0.85×10^3

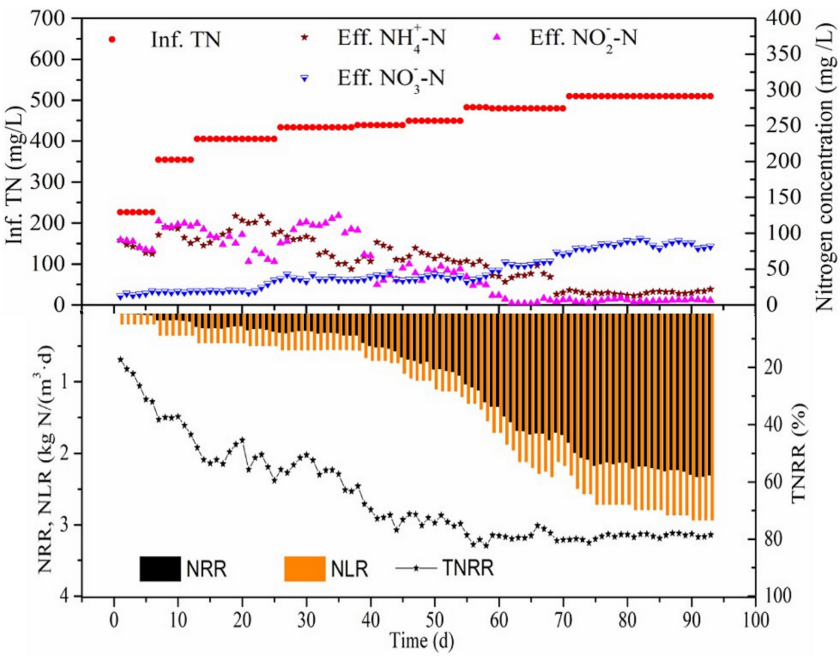

FIGURE 3 | Nitrogen removal from granular sludge-based anammox reactor.

1.40 kg/(m^3·day) in NPR by influent NH_4^+-N of 803 mg/L, while the MBR without zeolite achieved 2.02 kg/(m^3·day) (NLR) and NPR was 0.96 kg/(m^3·day). As compared to a previous study, it showed that the maximum influent NLR from one-stage ZBAF was 1.20 kg/(m^3·day) and obtained 0.76 kg/(m^3·day) in NPR by influent 550 mg/L NH_4^+-N from synthetic wastewater (Feng et al., 2019). The PN performed in two-stage ZBAF achieved the NPR up to 0.67 kg/(m^3·day) by influent 1.46 kg/(m^3·day) NLR at

752 mg/L NH_4^+-N from IORW (Feng et al., 2019). Dramatically, the PN in non-zeolite MBR would be seriously inhibited, if NLR was up to 2.14 kg/(m^3·day) then nitritation was gradually inhibited and FA increase to 109.0 mg/L. However, it would not be inhibited until the NLR is high to 3.01 kg/(m^3·day) in ZMBR and the corresponding FA was 88.5 mg/L. Due to the higher NLR maintained in ZMR, more DO was consumed to support high-efficient nitritation, which resulted that DO concentration in ZMBR (4–6 mg/L) being higher than ZBAF (3–6 mg/L). Moreover, PN in ZMBR can obtain the range of NO_2^--N/NH_4^+-N ratio was 1.07–1.33, which would provide the necessary influent substrate ratio for nitrogen removal *via* anammox. Stable PN is maintained in ZMBR, which can support nitrogen removal from high ammonium wastewater and profit by the low carbon and energy-saving of anammox.

In the PN phase, zeolite and biofilm played the role of NH_4^+-N adsorption-desorption and N biochemical conversion, respectively, which can be a key factor in maintaining high-efficiency PN. Due to zeolite, a special adsorptivity to ammonium and the FA concentration in liquid were lower than that on the surface of zeolite; therefore, AOB would easily grow on the biofilm than in suspended sludge. The biofilm on the surface of zeolite formed by different microorganisms and the dominant bacterial community (AOB) might be valid evidence to hold the efficient nitritation. According to the amplification and copy numbers in the biofilm from the surface of zeolite (**Table 3**), NOB can coexist with AOB on the biofilm and more copy numbers were obtained from AOB than from NOB. Since the FA inhibited NOB and AOB kept working, the ZMBR profited from the special existence of zeolite that supported a higher influent loading than the MBR.

Appraisal of the Granular Sludge-Based Anammox

Anammox bacteria are belonging to branching from Planctomycetes (Kuenen, 2008). At present, *Candidatus* Brocadia sinica, *Ca.* K. stuttgartiensis, *Candidatus* Jettenia asiatica, *Candidatus* Scalindua wagneri, and *Candidatus* Anammoxoglobus propionicus had been identified as the effective bacteria in anammox process (Hu et al., 2011; Mamoru et al., 2011). Microbial analysis at different taxonomy levels provides a further understanding of bacterial community function. *Ca.* K. stuttgartiensis can rapidly enrich in the IORW treatment process and dominate in granular sludge. The literature reports that *Ca.* K. stuttgartiensis has advantages in adapting to the environment of the nitrite-limiting environment (Park et al., 2015), while the other four prefer to grow in the substrate-rich anammox-based process (Gonzalezgil et al., 2015). Besides, sludge structure, inoculum, and organic matter might be other potential factors that affect bacterial community structure (Date et al., 2009). IORW is typical industrial wastewater and the possible affecting factors to anammox still need deep analysis. Generally, anammox was started by using seed sludge to shorten the startup time and rapidly increased treatment efficiency. In this study, granular sludge was obtained from a papermaking wastewater treatment process, which was applied as the microbial carrier and seeded with anammox sludge to further remove ammonium and nitrite. In the first 47 days, influent TN concentration was 226–450 mg/L (the NO_2^--N/NH_4^+-N ratio was in the range of 1.07–1.33) and effective nitrogen removal was achieved. As shown in **Figure 3**, the granular sludge-based anammox achieved stable nitrogen removal efficiency after 93 days' operation by influent IORW and the corresponding NRR was 2.33 kg/(m^3·day). The literature reports that overloads lead to system instability and the anammox process would be seriously inhibited when the nitrite concentration is higher than 280 mg/L (Trigo et al., 2006; Isaka et al., 2007).

Evolution of Microbial Community on Naturalized Granular Sludge

The granular sludge was used as a carrier of anammox bacteria in the further nitrogen removal process, which was obtained from a papermaking wastewater treatment process. According to the high-throughput sequencing detection, 632 operational taxonomic units (OTUs) and 1,093 OTUs were obtained from seed sludge samples and cultivating sludge in 90-day samples, respectively. Based on the classification at different taxonomy levels, the bacterial community structure from floc particle (settle at the bottom of the reactor), float sludge (floating on the surface of the liquid), and bottom sludge (accumulate at the bottom of the reactor) were similar, while the relative abundance exhibited significant difference when achieved stable anammox. As shown in **Figure 4**, the four most abundant bacteria at the phylum level were *Bacteroidetes* (28.5%), *Proteobacteria* (12.6%), *Chloroflexi* (8.9%), and *Chlorobi* (7.2%) in seed sludge sample, while it changed to *Planctomycetes*, *Proteobacteria*, and *Bacteroidetes* in the samples from floc particle, float sludge, and bottom sludge after 90 days of operation. Compared to the seed sludge, an obvious increase can be seen in *Planctomycetes* and *Proteobacteria*, which proved that anammox bacteria gradually increase on the granular sludge.

The granular sludge from the bottom has the most abundant *Ca.* K. stuttgartiensis (56.6%), followed by fine particle granular sludge (45.6%) and the last was float sludge (45.1%). The influent substances were from the bottom to the top (UASB) and the bottom sludge preferential using the substances than the floating sludge, which might be the reason for the different content of anammox bacteria. The reference reported that *Ca.* B. sinica and *Ca.* K. stuttgartiensis are usually dominant in large granules (greater than 400 μm in diameter) and *Ca.* J. asiatica was enriched in fine particles (less than 200 μm in diameter) that were cultivated with synthetic water (Liu et al., 2017). However, this study showed obvious differences compared to the reference because of different wastewater treatment and inoculation. In addition, the possible hydraulic and pneumatic shock cause channeling phenomenon with the result that substances maldistribution. This might easily lead to the different microenvironments with a high concentration of substances or severe shortage of substances concurrence. The other literature reports that the anammox activity would be completely lost when the anammox biomass aggregates exposure to a NO_2^--N solution of 100 mg/L (Van De Graaf et al., 1995) and the other results show that the NO_2^--N

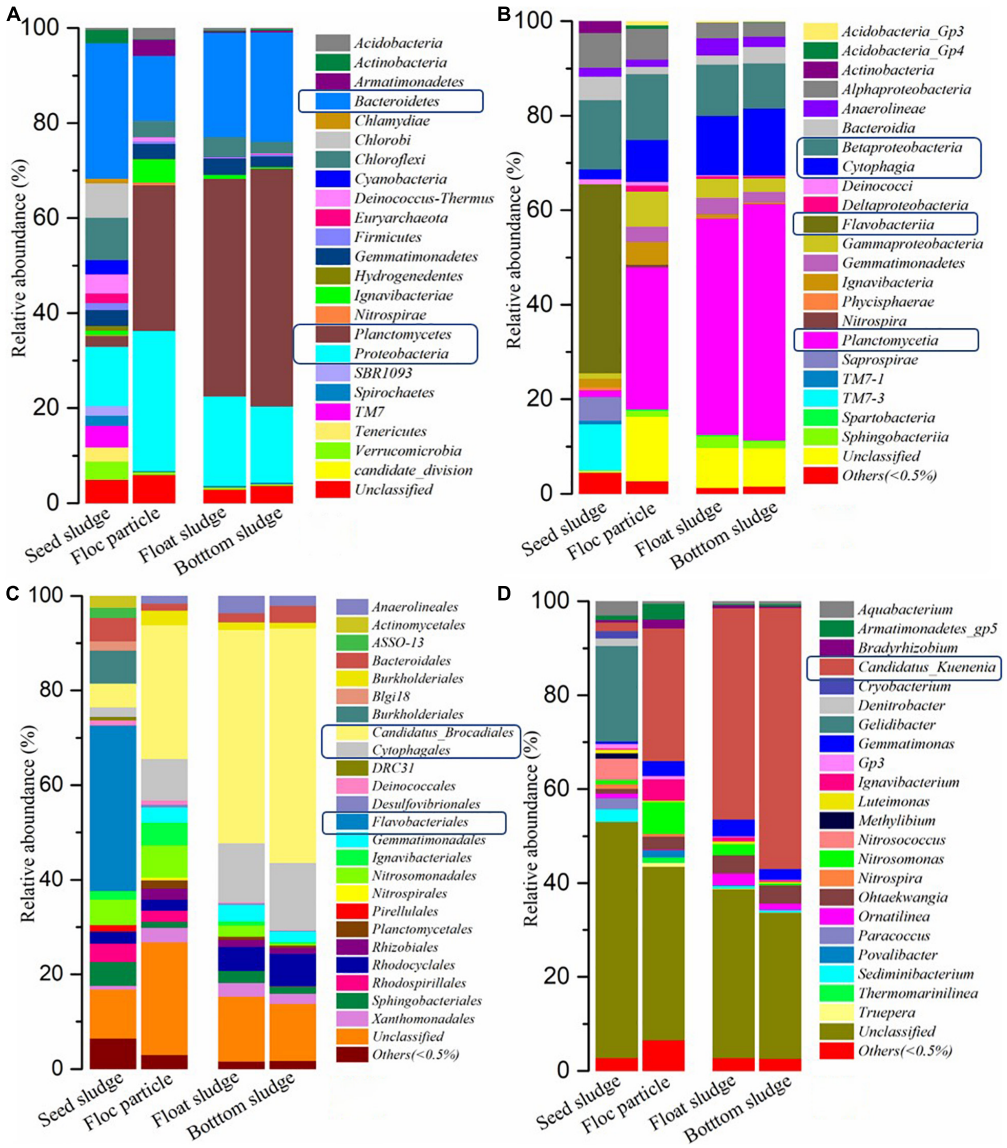

FIGURE 4 | Microbial community structure and relative abundance in different sludge samples. Taxonomy in phylum **(A)**, class **(B)**, order **(C)**, and genus **(D)**.

concentration of 40 mg/L over several days would lead to an irreversible inactivation (Hulle et al., 2010). This study believed that the tolerance to NO_2^--N concentration depends on the relative abundance of anammox bacteria. Moreover, substance distribution was another important factor in anammox bacteria enrichment.

DISCUSSION

Zeolite Plays a Key Role to Build a Microenvironment of High Free Ammonia

Zeolite has a special characteristic of absorption-desorption to NH_4^+-N, which should be the reason for the better performance than the process without zeolite. Besides, this kind of particularity can avoid NH_4^+-N substantial increase or decrease. Therefore, the ZMBR exhibited higher nitritation efficiency than the MBR by the same influent NLR, which might benefit from the stable concentration of NH_4^+-N and FA. As shown in **Figure 5**, zeolite was an efficient carrier that could maintain large areas of biofilm and lots of microorganisms attached to the biofilm and the biofilm formation on the zeolite might reduce a large amount of biofilm attached to the membranes. Moreover, the friction effect of the interfacial concrete from zeolite and membrane under aeration conditions might be another factor affecting a large amount of biofilm formation on the membrane. According to the above, the ZMBR obtained higher treatment efficiency than the MBR in the PN of IORW. Compared to the PN in a one-stage or two-stage ZBAF and SBR, the ZMBR has higher treatment efficiency and effluent quality. In addition, a previous

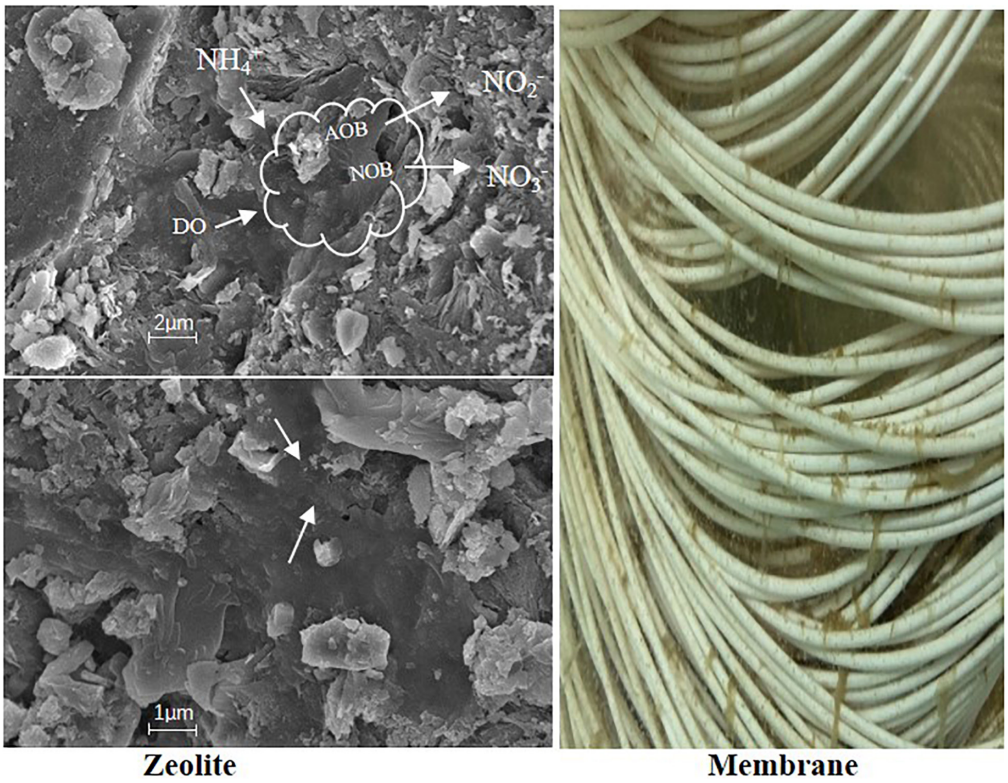

FIGURE 5 | Biofilm formation on the surface of zeolite and membrane.

study reported that using Na_2CO_3 as the alkalinity donor for PN could save about 40% dosage than common $NaHCO_3$, while it would bring higher FA and cause inhibition to PN (Feng et al., 2019). Thus, cost efficiency and high efficiency were achieved in the practical application. In this study, the ZMBR could maintain higher efficiency for PN than the MBR or ZBAF by using Na_2CO_3 as the alkalinity donor. Besides, the most practical merit of the ZMBR is its rapid startup, stable operation, and tolerance to high influent NLR, which provides a controllable and highly efficient method for the PN of IORW.

Granular Sludge-Based Cultivation and Its Morphology Structure Change

The granular sludge profited from better sludge settleability than flocculent sludge, which could achieve greater treatment efficiency. Moreover, the relative abundance of ammonium bacteria was directly affected by the nitrogen removal and the living environment of sludge might also be an important factor. Meanwhile, the different microbial structures would bring different excreta that might have positive or negative effects on the surface of sludge. This still needs further verification. Since granular sludge has different spatial distribution in the reactor resulting that a part of granular sludge float on the liquid and another part and floc sludge at the bottom of the reactor. This study disagrees with the opinion of dosing Fe^{2+} can suppress the flotation problem (Wang et al., 2018) because the residual concentration of Fe^{2+} in IORW is still at 15 ± 5 mg/L and believed that the continuous minute bubbles from anammox might be the main reason for the phenomenon of sludge floating. In addition, another study found that using vibration technology is an effective and quick method to form settleable granules (Zhang et al., 2019). The floc particle sludge should be formed from granular collision or decomposition. The efficient anammox consisted of these three different spatial distribution granular sludge and microorganism communities presenting different abundances.

Using CLSM observation technology can simultaneously exhibit the distribution and the relative abundance of different EPSs on the granular sludge. As shown in **Figure 6**, the fluorescence intensity indicated that proteins, lipids, and β-D-mannose were erratically distributed on the granular sludge and the proteins were patchily distributed on the granular sludge (the green color). Weaker fluorescence was found in lipid and β-D-mannose detection compared to the proteins. The EPS distribution revealed that the higher relative abundance of *Ca.* K. stuttgartiensis on granular sludge the better sludge settleability was maintained. Besides, EPSs might play a crucial role during fast anammox bacteria enrichment, which was different from the granular sludge with a low abundance of anammox bacteria (Ni et al., 2015). In addition, the aggregation property from EPS was usually applied to support the anammox bacteria preferably attached to the surface of sludge (Jia et al., 2017). Recent studies reveal that EPSs can enhance the NRR (Liu et al., 2018). EPS might contribute to the anammox bacteria

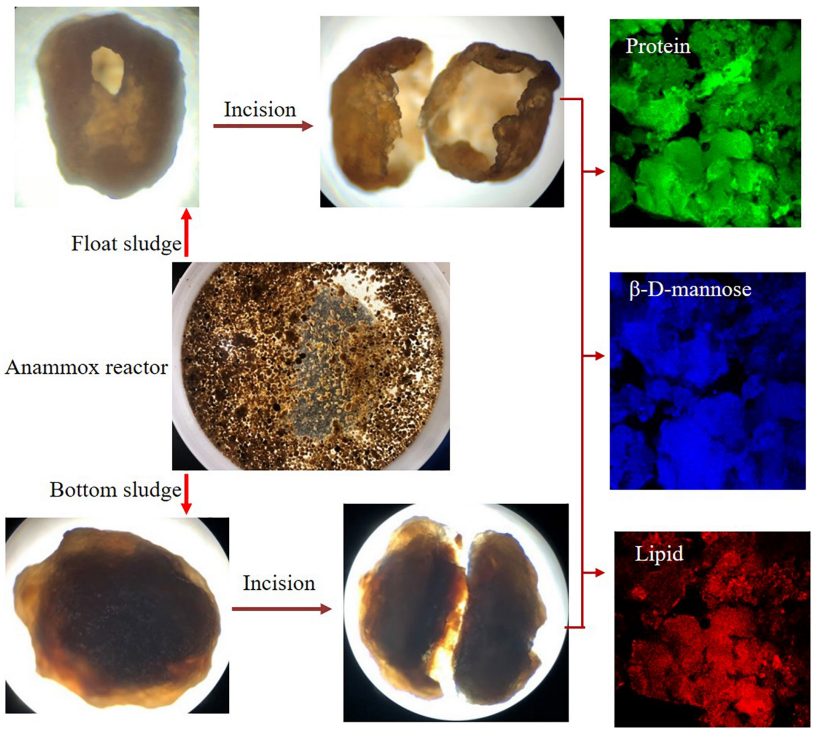

FIGURE 6 | Morphology structure and extracellular polymeric substance (EPS) detection of granular sludges.

attached to the surface of sludge. As a common carrier, granular sludge provides a suitable environment for anammox bacteria and is beneficial to the nitrogen removal of IORW. According to the microscopic image, a small cavity was common in float sludge in the cultivation phase, while the granular sludge at the bottom of the reactor was a solid sphere. The potential explanation was that ammonium and nitrite were simultaneously removed by anammox bacteria, which would produce a lot of gas on the surface of granular sludge, which can destroy the surface structure. Therefore, floc particles were released from the inside of the granular sludge, which might possible formatted new granular sludge because of the adhesion from abundant EPSs.

CONCLUSION

The stable PN was maintained in a ZMBR and obtained 2.78 kg/(m^3·day) in NLR and 1.40 kg/(m^3·day) in NPR by influent IORW with NH_4^+-N concentration at 803 mg/L treatment. Granular sludge was taken from a papermaking wastewater treatment process can be used as a bacterial carrier and *Ca.* K. stuttgartiensis gradually dominant on the sludge. Moreover, the morphology structure and EPSs distribution on granular sludge were investigated resulting that anammox bacteria activities and floc particles released from the inside of the granular sludge being an important reason for sludge floating. Based on the recycle utilization of granular sludge in anammox combined with ZMBR (PN-anammox) can obtain NRR was 2.33 kg/(m^3·day). Because of low-cost and high-efficient, this combined process would have great potential for IORW treatment and larger-scale engineering implementation.

DATA AVAILABILITY STATEMENT

The original contributions presented in the study are included in the article/supplementary material, further inquiries can be directed to the corresponding author.

AUTHOR CONTRIBUTIONS

X-HF, X-JW, and H-HZ: conceptualization and methodology. X-HF, KD, and Z-QZ: project administration and data curation. X-HF and KD: original draft. X-HF and H-YZ: review and editing. X-HF, Y-PL, and H-XL: supervision. All authors have contributed to the article and approved the submitted version of the manuscript.

FUNDING

This study was supported by the following research funds: the Guangxi Science and Technology Project (AD21220117), the Guangxi Natural Science Foundation (2022GXNSFFA035033), and the Guangxi Key Laboratory of Theory and Technology for Environmental Pollution Control (2001K008).

REFERENCES

Anthonisen, A. C., Loehr, R. C., Prakasam, T. B., and Srinath, E. G. (1976). Inhibition of nitrification by ammonia and nitrous acid. *J. Water Pollut. Control Federat.* 48, 835–852.

Barreto, C., Garcia, H. A., Hooijmans, C. M., Herrera, A., and Brdjanovic, D. (2017). Assessing the performance of an MBR operated at high biomass concentrations. *Int. Biodeterior. Biodegrad.* 119, 528–537.

Cai, X., Zhang, M., Yang, L., Lin, H., Wu, X., He, Y., et al. (2017). Quantification of interfacial interactions between a rough sludge floc and membrane surface in a membrane bioreactor. *J. Colloid. Interf. Sci.* 490, 710–718. doi: 10.1016/j.jcis.2016.12.005

Date, Y., Isaka, K., Ikuta, H., Sumino, T., Kaneko, N., Yoshie, S., et al. (2009). Microbial diversity of anammox bacteria enriched from different types of seed sludge in an anaerobic continuous-feeding cultivation reactor. *J. Biosci. Bioeng.* 107, 281–286. doi: 10.1016/j.jbiosc.2008.11.015

Feng, X., Wang, X., Chen, Z., and Chen, J. (2019). Nitrogen removal from iron oxide red wastewater *via* partial nitritation-Anammox based on two-stage zeolite biological aerated filter. *Bioresour. Technol.* 279, 17–24. doi: 10.1016/j.biortech.2019.01.113

Gonzalezgil, G., Sougrat, R., Behzad, A. R., Lens, P. N. L., and Saikaly, P. E. (2015). Microbial community composition and ultrastructure of granules from a full-scale anammox reactor. *Microb. Ecol.* 70, 118–131. doi: 10.1007/s00248-014-0546-7

Hu, B. L., Shen, L. D., Xu, X. Y., and Zheng, P. (2011). Anaerobic ammonium oxidation (anammox) in different natural ecosystems. *Biochem. Soc. T.* 39, 1811–1816. doi: 10.1042/BST20110711

Hulle, S. W. H. V., Vandeweyer, H. J. P., Meesschaert, B. D., Vanrolleghem, P. A., Dejans, P., and Dumoulin, A. (2010). Engineering aspects and practical application of autotrophic nitrogen removal from nitrogen rich streams. *Chem. Eng. J.* 162, 1–20.

Isaka, K., Date, Y., Sumino, T., Yoshie, S., and Tsuneda, S. (2006). Growth characteristic of anaerobic ammonium-oxidizing bacteria in an anaerobic biological filtrated reactor. *Appl. Microbiol. Biotechnol.* 70, 47–52. doi: 10.1007/s00253-005-0046-2

Isaka, K., Sumino, T., and Tsuneda, S. (2007). High nitrogen removal performance at moderately low temperature utilizing anaerobic ammonium oxidation reactions. *J. Biosci. Bioeng.* 103, 486–490. doi: 10.1263/jbb.103.486

Jia, F., Yang, Q., Liu, X., Li, X., Li, B., Zhang, L., et al. (2017). Stratification of Extracellular Polymeric Substances (EPS) for Aggregated Anammox Microorganisms. *Environ. Sci. Technol.* 51, 3260–3268. doi: 10.1021/acs.est.6b05761

Jin, R. C., Yang, G. F., Yu, J. J., and Zheng, P. (2012). The inhibition of the Anammox process: a review. *Chem. Eng. J.* 197, 67–79.

Kuenen, J. G. (2008). Anammox bacteria: from discovery to application. *Nat. Rev. Microbiol.* 6, 320–326. doi: 10.1038/nrmicro1857

Lackner, S., Gilbert, E. M., Vlaeminck, S. E., Joss, A., Horn, H., and Loosdrecht, M. C. M. V. (2014). Full-scale partial nitritation/anammox experiences – An application survey. *Water Res.* 55, 292–303. doi: 10.1016/j.watres.2014.02.032

Laureni, M., Falas, P., Robin, O., Wick, A., Weissbrodt, D. G., Nielsen, J. L., et al. (2016). Mainstream partial nitritation and anammox: long-term process stability and effluent quality at low temperatures. *Water Res.* 101, 628–639. doi: 10.1016/j.watres.2016.05.005

Li, J., Elliott, D., Nielsen, M., Healy, M. G., and Zhan, X. (2011). Long-term partial nitrification in an intermittently aerated sequencing batch reactor (SBR) treating ammonium-rich wastewater under controlled oxygen-limited conditions. *Biochem. Eng. J.* 55, 215–222.

Liu, W., Yang, D., Chen, W., and Xiao, G. (2017). High-throughput sequencing-based microbial characterization of size fractionated biomass in an anoxic anammox reactor for low-strength wastewater at low temperatures. *Bioresour. Technol.* 231, 45–52. doi: 10.1016/j.biortech.2017.01.050

Liu, Y., Guo, J., Lian, J., Chen, Z., Li, Y., Xing, Y., et al. (2018). Effects of extracellular polymeric substances (EPS) and N-acyl-L-homoserine lactones (AHLs) on the activity of anammox biomass. *Int. Biodeterior. Biodegrad.* 129, 141–147.

Mamoru, O., Masaki, S., Naoki, F., Hisashi, S., and Satoshi, O. (2011). Physiological characteristics of the anaerobic ammonium-oxidizing bacterium '*Candidatus Brocadia sinica*'. *Microbiology* 157, 1706–1713. doi: 10.1099/mic.0.048595-0

Marc, S., Eric, P., Sophie, M., Thomas, R., Angelika, L., Taylor, M. W., et al. (2006). Deciphering the evolution and metabolism of an anammox bacterium from a community genome. *Nature* 440, 790–794. doi: 10.1038/nature04647

Ni, S., and Meng, J. (2011). Performance and inhibition recovery of anammox reactors seeded with different types of sludge. *Water Sci. Technol.* 63, 710–718. doi: 10.2166/wst.2011.293

Ni, S., Sun, N., Yang, H., Zhang, J., and Ngo, H. H. (2015). Distribution of extracellular polymeric substances in anammox granules and their important roles during anammox granulation. *Biochem. Eng. J.* 101, 126–133.

Park, H., Sundar, S., Ma, Y., and Chandran, K. (2015). Differentiation in the microbial ecology and activity of suspended and attached bacteria in a nitritation-anammox process. *Biotechnol. Bioeng.* 112, 272–279. doi: 10.1002/bit.25354

Pedrouso, A., Río, Á. V. D., Morales, N., Vázquez-Padín, J. R., Campos, J. L., Méndez, R., et al. (2017). Nitrite oxidizing bacteria suppression based on in-situ free nitrous acid production at mainstream conditions. *Sep. Purif. Technol.* 186, 55–62.

Sarma, S. J., Tay, J., and Chu, A. (2017). Finding Knowledge Gaps in Aerobic Granulation Technology. *Trends Biotechnol.* 35, 66–78. doi: 10.1016/j.tibtech.2016.07.003

Shao, Y., Yang, S., Mohammed, A., and Liu, Y. (2018). Impacts of ammonium loading on nitritation stability and microbial community dynamics in the integrated fixed-film activated sludge sequencing batch reactor (IFAS-SBR). *Int. Biodeterior. Biodegrad.* 133, 63–69.

Sinha, B., and Annachhatre, A. P. (2007). Partial nitrification—operational parameters and microorganisms involved. *Rev. Environ. Sci. Biotechnol.* 6, 285–313.

Tang, C. J., Zheng, P., Wang, C. H., Mahmood, Q., Zhang, J. Q., Chen, X. G., et al. (2011). Performance of high-loaded ANAMMOX UASB reactors containing granular sludge. *Water Res.* 45, 135–144. doi: 10.1016/j.watres.2010.08.018

Trigo, C., Campos, J. L., Garrido, J. M., and Mendez, R. (2006). Start-up of the Anammox process in a membrane bioreactor. *J. Biotechnol.* 126, 475–487.

Van De Graaf, A. A., Mulder, A., Bruijn, P. D., Jetten, M. S., Robertson, L. A., and Kuenen, J. G. (1995). Anaerobic oxidation of ammonium is a biologically mediated process. *Appl. Environ. Microbiol.* 61, 1246–1251. doi: 10.1128/aem.61.4.1246-1251.1995

Walker, N. J. (2001). Real-time and quantitative PCR: applications to mechanism-based toxicology. *J. Biochem. Mol. Toxic.* 15, 121–127. doi: 10.1002/jbt.8

Walter, W. G. (1961). Apha standard methods for the examination of water and wastewater. *Am. J. Public Health* 51:940. doi: 10.2105/AJPH.51.6.940-a

Wang, B., Wu, D., Zhang, X., Mackey, H. R., and Chen, G. (2018). Sludge flotation, its causes and control in granular sludge upflow reactors. *Appl. Microbiol. Biotechnol.* 102, 6383–6392. doi: 10.1007/s00253-018-9131-1

Wu, L., Tang, B., Bin, L., Chen, G., Huang, S., Li, P., et al. (2018). Heterogeneity of the diverse aerobic sludge granules self-cultivated in a membrane bioreactor with enhanced internal circulation. *Bioresour. Technol.* 263, 297–305. doi: 10.1016/j.biortech.2018.05.004

Zhang, K., Lyu, L., Kang, T., Yao, S., Ma, Y., Pan, Y., et al. (2019). A rapid and effective way to cultivate anammox granular sludge through vibration. *Int. Biodeterior. Biodegrad.* 143:104704.

Conflict of Interest: The authors declare that the research was conducted in the absence of any commercial or financial relationships that could be construed as a potential conflict of interest.

frontiers | Frontiers in Microbiology

ORIGINAL RESEARCH
published: 07 July 2022
doi: 10.3389/fmicb.2022.934441

Denitrification Performance in Packed-Bed Reactors Using Novel Carbon-Sulfur-Based Composite Filters for Treatment of Synthetic Wastewater and Anaerobic Ammonia Oxidation Effluent

Yao Wang[1†], Baorui Liang[1†], Fei Kang[1], Youzhao Wang[1], Zhihong Yuan[2], Zhenning Lyu[1], Tong Zhu[1] and Zhijun Zhang[1*]*

[1] Institute of Process Equipment and Environmental Engineering, School of Mechanical Engineering and Automation, Northeastern University, Shenyang, China, [2] Shenyang Zhenxing Environmental Technology Co., Ltd., Shenyang, China

OPEN ACCESS

Edited by:
Chongjun Chen,
Suzhou University of Science and Technology, China

Reviewed by:
Lijuan Feng,
Zhejiang Ocean University, China
Niansi Fan,
Hangzhou Normal University, China

***Correspondence:**
Tong Zhu
tongzhu@mail.neu.edu.cn
orcid.org/0000-0002-3460-7316
Zhijun Zhang
286373480@qq.com
orcid.org/0000-0003-4281-5331

[†] These authors have contributed equally to this work and share first authorship

Specialty section:
This article was submitted to Microbiotechnology, a section of the journal Frontiers in Microbiology

Received: 02 May 2022
Accepted: 07 June 2022
Published: 07 July 2022

Citation:
Wang Y, Liang B, Kang F, Wang Y, Yuan Z, Lyu Z, Zhu T and Zhang Z (2022) Denitrification Performance in Packed-Bed Reactors Using Novel Carbon-Sulfur-Based Composite Filters for Treatment of Synthetic Wastewater and Anaerobic Ammonia Oxidation Effluent. Front. Microbiol. 13:934441. doi: 10.3389/fmicb.2022.934441

To avoid nitrate pollution in water bodies, two low-cost and abundant natural organic carbon sources were added to make up the solid-phase denitrification filters. This study compared four novel solid-phase carbon-sulfur-based composite filters, and their denitrification abilities were investigated in laboratory-scale bioreactors. The filter F_4 (mixture of elemental sulfur powder, shell powder, and peanut hull powder with a mass ratio of 6:2.5:1.5) achieved the highest denitrification ability, with an optimal nitrate removal rate (NRR) of 723 ± 14.2 mg NO_3^--N·L^{-1}·d^{-1} when the hydraulic retention time (HRT) was 1 h. The HRT considerably impacted effluent quality after coupling of anaerobic ammonium oxidation (ANAMMOX) and solid-phase-based mixotrophic denitrification process (SMDP). The concentration of suspended solids (SS) of the ANAMMOX effluent may affect the performance of the coupled system. Autotrophs and heterotrophs were abundant and co-existed in all reactors; over time, the abundance of heterotrophs decreased while that of autotrophs increased. Overall, the SMDP process showed good denitrification performance and reduced the sulfate productivity in effluent compared to the sulfur-based autotrophic denitrification (SAD) process.

Keywords: anaerobic ammonium oxidation, autotrophs, carbon-sulfur-based composite filter, heterotrophs, shell powder

INTRODUCTION

Nitrate, as a global contaminant, is frequently found in shallow groundwater, with adverse impacts on human health (e.g., methemoglobinemia and malformation) (Liang et al., 2021a). In addition, in saliva, the nitrites converted from nitrate might develop nitrosamines, which are known carcinogens, thus posing a huge risk to human health (Wang and Chu, 2016). Hence, removing nitrate in contaminated water is an urgent issue for the ecological environment.

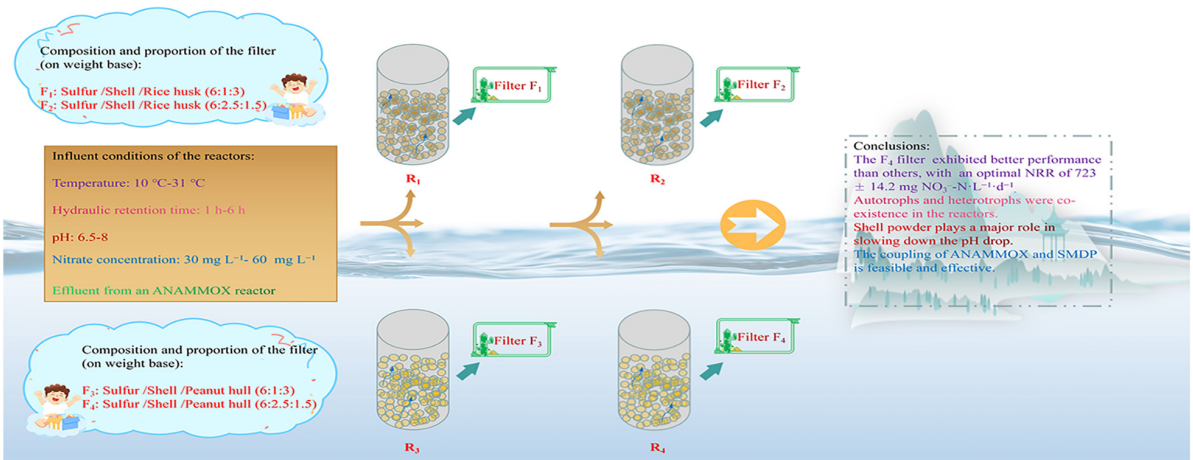

GRAPHICAL ABSTRACT | Novel filters for denitrification.

Various methods have been proposed to remove nitrate, including electrodialysis, ion exchange, distillation, and biological processes. Compared to physico/chemical processes, biological denitrification is a cost-effective method which is widely used in wastewater treatment plants (WWTPs) to treat nitrate-polluted wastewater, and heterotrophic denitrification (HD) is the preferred biological method due to its favorable denitrification rate (Liang et al., 2021a; Vo et al., 2021). Nevertheless, water-soluble organic carbon is generally required for denitrification due to the low carbon/nitrate (C/N) ratio of nitrate-polluted wastewater, which complicates this process and increases the operation costs.

$$55S_0 + 50NO_3^- + 38H_2O + 20CO_2 + 4NH_4^+ \rightarrow 4C_5H_7O_2N + 55SO_4^{2-} + 25N_2 + 64H^+ \quad (1)$$

As a biological-based denitrification method, autotrophic denitrification can be used as an alternative way. Sulfur-based autotrophic denitrification (SAD) has received considerable attention in recent years (Sahinkaya et al., 2011; Chung et al., 2014; Liang et al., 2020). The use of elemental sulfur in a packed-bed reactor is a preferred method and has been applied in pilot and full-scale reactors (Sahinkaya et al., 2014). However, the solubility of elemental sulfur limits the denitrification rate, and the increased sulfate production may also be a problem (Eq. 1). Accordingly, a variety of factors were investigated for packed-bed reactor, including hydraulic retention time (HRT), temperature, nitrate loading rate (NLR), and the types of solid-phase filters (Sahinkaya et al., 2014; Vo et al., 2021). Regarding the latter, previous research used a mixture of elemental sulfur and inorganic carbon particles, while this is not as effective as the denitrification filter formed by the thermal fusion of elemental sulfur and inorganic carbon sources (Liang et al., 2020). Moreover, solid organic carbon sources have also been explored [polycaprolactone (PCL), starch/PCL, etc.], and their denitrification levels for wastewater were moderate (Chu and Wang, 2011).

To overcome these problems, considering that mixotrophic denitrification (simultaneous autotrophic and heterotrophic) could compensate for the disadvantages of autotrophic and heterotrophic denitrification (Sahinkaya and Dursun, 2012), and because most of the liquid carbon sources are costly, the solid-phase-based mixotrophic denitrification process (SMDP) was investigated. So far, only a limited number of studies have focused on the SMDP: For example, the effects of different pH values on SMDP and the selection of suitable filters have not been systematically studied. Moreover, as an efficient and economical process for wastewater treatment, anaerobic ammonium oxidation (ANAMMOX) has been successfully applied and found to reduce the amount of aeration required for nitrogen removal (Gilbert et al., 2014). It is a chemolithotrophic process without organic carbon demand. The ANAMMOX process is the anoxic oxidation of ammonium with ammonium acting as the electron donor to produce nitrogen gas (Eq. 2; Strous et al., 1998). However, the by-product nitrate would accumulate and further treatment was required, while there is very little information available regarding the performance of the SMDP coupled with the ANAMMOX, and the adoption of ANAMMOX effluent in SMDP may achieve desirable nitrogen removal performance.

$$NH_4^+ + 1.32NO_2^- + 0.066HCO_3^- + 0.13H^+ \rightarrow 1.02N_2 + 0.26NO_3^- + 0.066CH_2O_{0.5}N_{0.15} + 2.03H_2O \quad (2)$$

In this study, two low-cost and abundant natural organic carbon sources were selected as HD materials and integrated into the SAD process, and parallel experiments were conducted in four SMDP reactors. The overall aims were as follows: (1) to compare the feasibility of four types of solid-phase filters for the SMDP; (2) to study the effects of influent pH on the denitrification ability of the SMDP; (3) to explore the feasibility of coupling SMDP with ANAMMOX; (4) to identify the variations in the microbial communities involved in the SMDP. These findings would provide a scientific

TABLE 1 | Influent conditions of the R_1–R_4 reactors in periods 1–6.

Periods	1	2	3	4	5	6
Days	0–5	6–20	21–40	41–60	61–80	81–180
HRT (h)	6	4	3	2	1	1
NLR (mg NO_3^--N·L^{-1}·d^{-1})	200	300	400	600	1200	720
NO_3^--N (mg L^{-1})	50					30
Average temperature (°C)	12	13	18	19	23	26

basis for the development of measures to further improve wastewater treatment.

MATERIALS AND METHODS

The Solid-Phase Filters

Four types of solid-phase filters were prepared for the SMDP. The elemental sulfur powder mixed with shell powder and rice husk powder according to the weight ratios of 6:1:3 and 6:2.5:1.5 was used to prepare F_1 and F_2, respectively. Filters F_3 and F_4 were prepared by mixing elemental sulfur powder with shell powder and peanut hull powder at weight ratios of 6:1:3 and 6:2:1.5, respectively. The mixed powders were, respectively, stirred under 150°C to form the molten material, which was poured into oval-shaped molds and naturally cooled to form the F_1–F_4 filters. The final products were in oval form, with a width of 5 mm, a height of 6 mm, and a length of 10 mm on average. The shell powder, elemental sulfur powder, rice husk powder, and peanut hull powder were obtained from a local technology company in Shenyang (Dongyuan, China), with a mean diameter of 600, 1500, 300, and 300 mesh, respectively.

Experimental Procedure

Four identical up-flow packed-bed column reactors (R_1–R_4) were conducted in this study. The reactors were made of plexiglass, with a height-to-diameter ratio of 6:1 and an effective volume of 1 L. The R_1–R_4 reactors were, respectively, filled with filters F_1, F_2, F_3, and F_4, with 1 kg per filter type. The R_1–R_4 reactors were conducted in parallel and operated continuously for 320 days, and the **Tables 1**, **2** list the detailed influent parameters.

During periods 1–6, the reactors were operated at ambient temperatures to evaluate the impact of temperature changes on the SMDP; meanwhile, the HRT and the influent nitrate concentration were adjusted to change the influent NLR to estimate SMDP performance under different conditions. Experiments were carried out indoors, starting at the coldest time, with an average temperature of 12°C (period 1). Hydrochloric acid solution and sodium bicarbonate solution were used to adjust the pH of the influent in period 7, fed-batch experiments were carried out to study the effects of different pH values on the performance of SMDP, batches 1 and 3 were performed in duplicate (corresponding to batches 2 and 4, respectively), and the HRT was also varied in period 7 (**Table 2**). Tap water supplemented with $NaNO_3$ agent was used as synthetic wastewater for the influent of the R_1–R_4 reactors.

During period 8, the influent of the R_1–R_4 reactors was changed to the effluent from a 6000 L ANAMMOX reactor in our laboratory (**Supplementary Figure 1**) and operated under various conditions, and the detailed influent parameters are summarized in **Table 2**. The effluent collected from the ANAMMOX reactor was reserved in a middle tank and then evenly pumped into the R_1–R_4 reactors. The influent temperature of the R_1–R_4 reactors was maintained at 29 ± 2°C during periods 7 and 8, and the dissolved oxygen (DO) was not controlled throughout the study. The seed sludge was taken from the bottom of the secondary sedimentation tank of a local WWTP (Shenyang, China), and the reactors were, respectively, inoculated with 100 mL seed sludge (with mixed liquor suspended solids (MLSS) of about 5.4 g L^{-1}) and operated under internal recycle mode with a flow rate of 15 L h^{-1} for 2 h to ensure an even distribution of the sludge throughout the reactor. After the internal recycle mode, the reactors were continuously fed with influent. The HRT was calculated considering the empty bed volume, and the HRT, NLR, and

TABLE 2 | Influent conditions of the R_1–R_4 reactors in periods 7 and 8.

		Period 7				Period 8		
Steps		1	2	3	4	1	2	3
Days	Batch 1	181–185	186–190	191–195	196–200	261–280	281–300	301–320
	Batch 2	201–205	206–210	211–215	216–220			
	Batch 3	221–225	226–230	231–235	236–240			
	Batch 4	241–245	246–250	251–255	256–260			
HRT (h)	Batch 1	3				4	3	2
	Batch 2							
	Batch 3	1						
	Batch 4							
NO_3^--N (mg L^{-1})		60				62 ± 2.3	61 ± 3.2	61 ± 2.6
NO_2^--N (mg L^{-1})						5.3 ± 1.3	5.8 ± 1.1	5.7 ± 1.4
NH_4^+-N (mg L^{-1})		2.2 ± 0.4				11.2 ± 3.3	11.9 ± 2.6	12.2 ± 2.4
Influent pH value		6.5	7	7.5	8	7.3–7.8		
Temperature (°C)					29 ± 2			

nitrate removal rate (NRR) were, respectively, calculated by the following equations:

$$HRT = \frac{R_v}{S_p} \quad (3)$$

$$NLR = \frac{C_a}{HRT} \times 24 \quad (4)$$

$$NRR = \frac{(C_a - C_b)}{HRT} \times 24 \quad (5)$$

where R_V is the empty bed volume of the reactor (L); S_p is the influent flow rate of the reactor (L h^{-1}); *Ca* is the influent nitrate concentration of the reactor (mg L^{-1}); and C_b is the effluent nitrate concentration of the reactor (mg L^{-1}).

Sampling and Analysis

The water samples were collected daily from the influent and effluent of the R_1–R_4 reactors, and the samples were filtered using 0.45-μm cellulose acetate membrane and analyzed for chemical oxygen demand (COD), MLSS, ammonium, nitrite, nitrate, suspended solids (SS), sulfate, and alkalinity according to standard methods (American Public Health Association [APHA], 2005). The pH and DO values were measured with digital instruments (VSTAR10, Thermo Fisher, China, and BDO-209F, Bell, China, respectively). For the sulfide measurements, the methylene blue method was adopted (Wang et al., 2016). The hemicellulose, lignin, and cellulose contents of rice husk powder and peanut hull powder were measured according to the methods of Hill et al. (1998).

DNA Extraction and Illumina MiSeq Sequencing

To identify the richness and diversity of microbial communities, the bio-samples on the surface of filters F_1, F_2, F_3, and F_4 in the R_1–R_4 reactors were collected. One bio-sample was collected from the top area of the R_1–R_4 reactors on days 80 and 320, respectively. The DNA was extracted using a PowerSoil DNA extraction kit (MP Biomedicals, United States), and after the sample collection, the extracted DNA was immediately placed at −20°C and then stored at −80°C until the next step. The V3–V4 hypervariable regions of 16S rRNA genes were amplified using the primers 338F (5′-ACTCCTACGGGAGGCAGCAG-3′) and 806R (5′-GGACTACHVGGGTWTCTAAT-3′). The AxyPrep DNA Purification Kit (AXYGEN, United States) was used to purify the PCR products. Afterward, all the purified 16S amplicons were pooled in equimolar and paired-end sequenced (2 × 300) on an Illumina MiSeq platform (Illumina, San Diego, CA, United States) in a biomedical laboratory (Majorbio, Shanghai, China). The raw 16S rRNA sequences have been deposited in the NCBI Sequence Read Archive (SRA) database under accession numbers PRJNA835999 and PRJNA836004.

RESULTS AND DISCUSSION

Performance of the Bioreactors

The performances of the R_1–R_4 reactors are depicted in **Figures 1**, **2**. The nitrate was almost entirely denitrified within 3 days in all reactors, indicating that the F_1–F_4 filters could start-up rapidly even at low temperatures (11–13°C) and display good denitrification performance. During period 1, a slight accumulation of ammonium was observed in R_1–R_4 reactors (**Figure 1**), which may be attributed to the dissimilatory nitrate reduction to ammonium (DNRA), caused by the high carbon-to-nitrogen ratio (C/N) (Rijn et al., 2006). To avoid such unfavorable factor, the HRT of the reactors was reduced in the period 2. However, all reactors showed a decrease in nitrate removal efficiency (NRE), which was 84.5 ± 4.1%, 86.9 ± 3.3%, 83.9 ± 2.6%, and 86.1 ± 1.8% for R_1, R_2, R_3, and R_4, respectively. Interestingly, the NRE of the reactors in the period 3 was similar as the period 2, even though the HRT in the period 3 was 3 h. The reason for this phenomenon may be due to the temperature fluctuations, as a lower temperature (≤15°C) could negatively affect the denitrification phenomenon (Sahinkaya et al., 2014), and compared with the period 2 (13°C), a higher temperature was observed in the period 3 (18°C). The HRT was further decreased in periods 4–5, the decreased NRE and the elevated nitrate concentrations in effluent were observed in all reactors, and the solubility of the solid-phase filter could be the main reason for the incomplete denitrification (Koenig and Liu, 2001). Above all, these results clearly indicated that the NRR was dependent of the HRT and temperature variation, and when the HRT was 2 h or 1 h in this study, it was hard to keep the effluent nitrate concentration always below 15 mg L^{-1}, indicating that it was difficult for F_1–F_4 filters to take into an account both a relatively faster flow rate (HRT ≤ 2 h) and a high influent nitrate concentration (50 mg L^{-1}). Given this scenario, the influent nitrate concentration was decreased to 30 mg L^{-1} to test the overall performance of the reactors in period 6.

In the first 15 days of period 6, the NRE of the R_1, R_2, R_3, and R_4 reactors was 53.5 ± 3.1%, 66.4 ± 3.6%, 58.9 ± 2.6%, and 70.1 ± 1.9%, respectively; and the NRE of the remaining days of period 6 (days 96–180) in the reactors was 39.5 ± 3.5%, 46.4 ± 2.7%, 41.9 ± 2.6%, and 50.1 ± 1.9%, respectively. This was in accordance with a previous study in packed-bed denitrification systems (Liang et al., 2021b). Although the average temperature in the reactors was 31°C during the last few days of period 6, which was closer to the optimum temperature of 35°C for nitrate reduction (Chen et al., 2018) than that in the other periods, the NRE values were still moderate. This may be due to the fact that after the filter had been working for a period of time, the release capacity of the organic carbon sources in the filter was weakened, which affects the denitrification capacity of the filter, because the HD rate was higher than the autotrophic denitrification rate (Oh et al., 2001). During periods 3–6, the F_4 filter showed a relatively higher denitrification performance than the others. Compared to the R_3 reactor, the nitrate concentration was higher in the R_1 effluent. Similarly, the nitrate concentration of the R_2 effluent was higher than that of R_4, suggesting that peanut hull may be more suitable as a denitrification source than rice husk. The cellulose, hemicellulose, and lignin contents of rice husk were 38.4, 20.3, and 21.6%, respectively, and 34.6, 18.2, and 28.2% for the peanut hull. Cellulose and hemicellulose are reported to be the carbon sources for HD process (Wen et al., 2010), but their contents in peanut hull are lower than those in rice husk, and the better denitrification performance obtained with peanut hull may

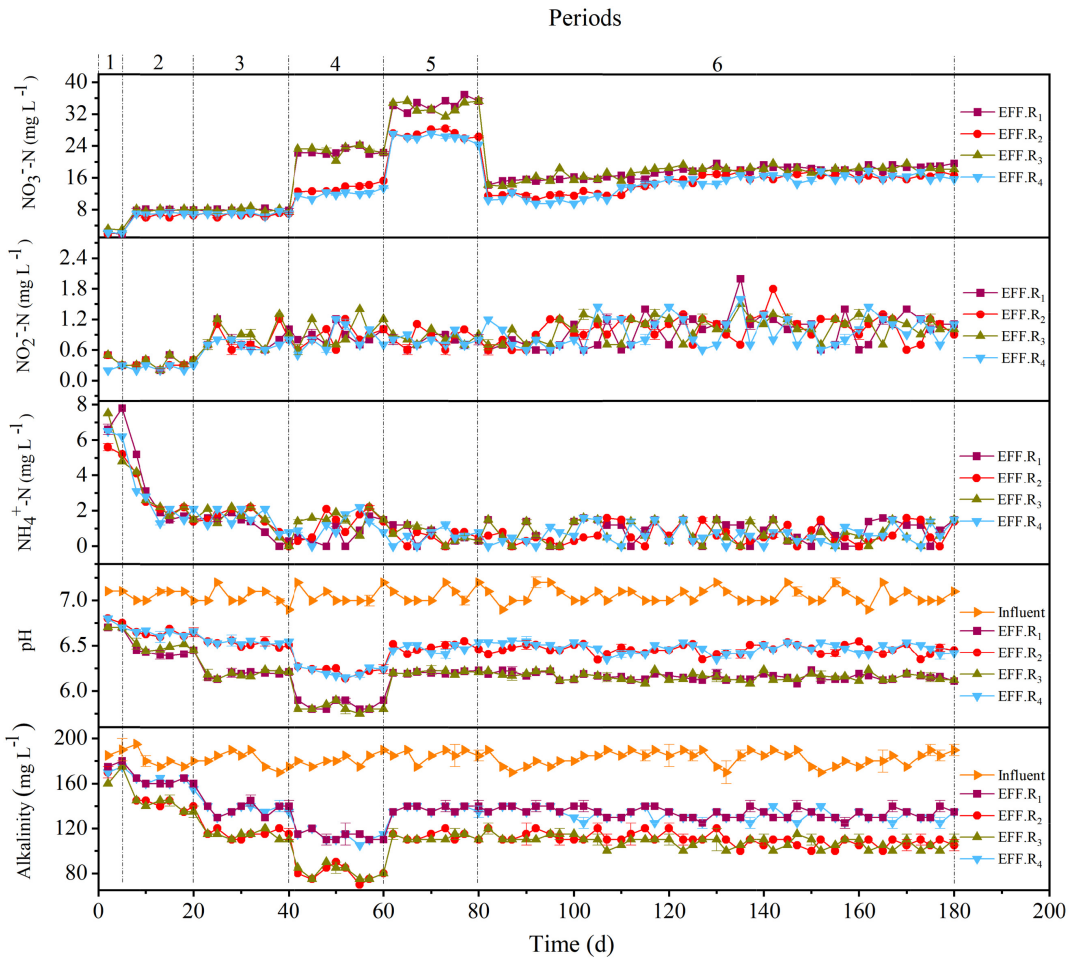

FIGURE 1 | Performances of the R_1–R_4 reactors during periods 1–6.

be due to the structural advantage given by the combination of peanut hull and elemental sulfur and the detailed release capacity of the carbon sources in the filters. Moreover, during periods 5–6, it was observed that the denitrification rates of the F_1 and F_3 filters were lower than those of F_2 and F_4, indicating that the content of natural organic carbon sources was not always proportional to the NRR, and a reasonable content of natural organic carbon sources may contribute to better denitrification. Notably, an optimal NRR of 723 ± 14.2 mg NO_3^--N·L^{-1}·d^{-1} was observed in the R_4 reactor (period 5), which demonstrated superior denitrification capacity compared to the other packed reactors (**Table 3**).

$$4S^0 + 4H_20 \rightarrow 3H_2S + SO_4^{2-} + 2H^+ \quad (6)$$

As shown in **Figure 2**, accumulations of COD were observed in all reactors during periods 1–2, with the average COD concentration of R_1, R_2, R_3, and R_4 reactors was 81.8 ± 31.2 mg L^{-1}, 58.6 ± 28.1 mg L^{-1}, 71.1 ± 35.8 mg L^{-1}, and 56.6 ± 28.6 mg L^{-1}, respectively. With the improvement of NLR in later periods, the average effluent COD concentration in all reactors decreased and reached an acceptable value (<50 mg L^{-1}). During periods 5–6, the average effluent COD concentration of all the reactors was similar, whereas the average NRR in R_1 and R_3 was lower than that in R_2 and R_4. The respective sulfate productivity values in the R_1, R_2, R_3, and R_4 reactors were 6.68 ± 0.33 mg SO_4^{2-}/mg NO_3^--N, 6.89 ± 0.29 mg SO_4^{2-}/mg NO_3^--N, 6.51 ± 0.32 mg SO_4^{2-}/mg NO_3^--N, and 6.78 ± 0.34 mg SO_4^{2-}/mg NO_3^--N in periods 1–6, which were lower than the theoretical value (7.54 mg SO_4^{2-}/mg NO_3^--N) calculated by Eq. 1. The accumulation of sulfate indicates that denitrification may still be dominated by SAD, and the lower sulfate productivity may be attributed to HD; specifically, the lower sulfate productivity of R_1 and R_3 may be attributed to the higher proportion of HD in the reactors. Moreover, the lower NRR in R_1 and R_3 may be related to the lower pH and alkalinity rates, and the effluent pH values in R_2 and R_4 were generally around 6.5 in periods 5–6, whereas in R_1 and R_3, these pH values were about 6.0–6.2. Generally, the pH range suitable for denitrification is 6.5–8.5 (Wang and Chu, 2016), the lower NRE of R_1 and R_3 may be due to the low content of the shell powder contained in the filters, because the content of shell powder in filters F_2 and F_4 was 2.5 times that of F_1 and F_3, and shell powder has a good effect on maintaining

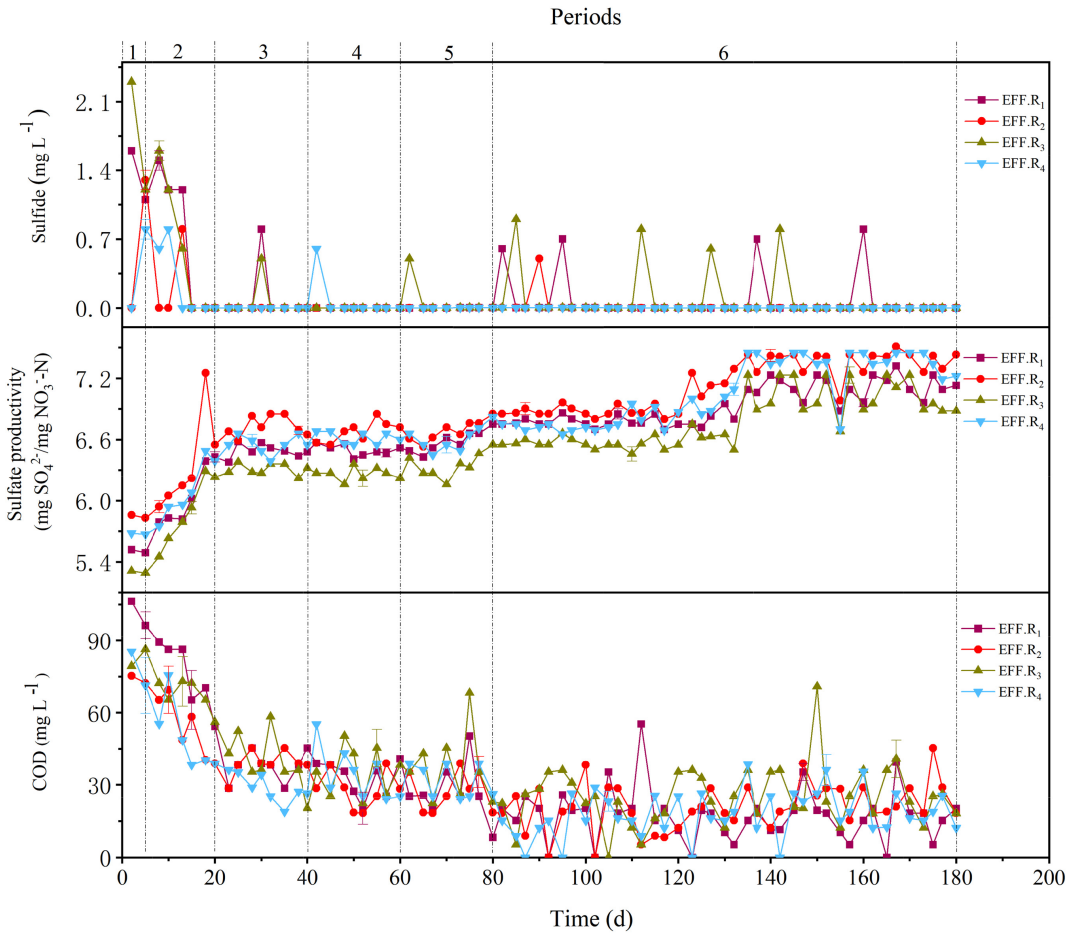

FIGURE 2 | Variations in sulfide, COD, and sulfate productivity in periods 1–6 of the R_1–R_4 reactors.

good denitrification performance due to its favorable alkalinity dissolution rate (Moon et al., 2004). Sulfide was occasionally found in the reactors and generally appeared in the R_1 and R_3 (**Figure 2**). The presence of sulfide might be attributed to the sulfur disproportionation process (Eq. 6), which is induced by the low nitrate load of the influent (Liang et al., 2021b). The higher sulfide content in R_1 and R_3 reactors in period 6 may be caused by the uneven distribution of denitrification capacity in the reactors. In general, the various proportions and compositions of the filter strongly affected the denitrification performance, and the F_4 could be the optimal filter due to its overall performance. Besides, the F_4 filter was composed of several low-cost substances and showed an excellent denitrification performance under different conditions, which further proves its economy and feasibility.

Effect of pH on the Solid-Phase-Based Mixotrophic Denitrification Process

The influent pH variations of the reactors under different conditions are depicted in **Figure 3**. When the HRT was 3 h, the NRR of the reactors was positively associated with an increase in pH value. During step 4, the average NRR of the R_1, R_2, R_3, and R_4 reactors was 376 ± 16.3 mg NO_3^--N·L^{-1}·d^{-1}, 411 ± 20.1 mg NO_3^--N·L^{-1}·d^{-1}, 382 ± 23.4 mg NO_3^--N·L^{-1}·d^{-1}, and 433 ± 17.7 mg NO_3^--N·L^{-1}·d^{-1}, respectively. These values were slightly higher than the NRR at pH of 7 or 7.5 in the four reactors (**Figure 3A**). On the contrary, when the pH was 6.5, the NRR of all the reactors showed a decreasing trend, and this may be due to the negative impact of the lower pH on denitrification (**Figure 3B**), because when the pH was lower than 6, denitrification will be inhibited (Yang et al., 2016).

When the HRT was 1 h, as the pH increased from 7.0 to 7.5, the NRR of the R_1 and R_3 reactors increased slightly, with the average NRR of the R_1, R_2, R_3, and R_4 reactors was 338 ± 12.8 mg NO_3^--N·L^{-1}·d^{-1}, 403 ± 16.8 mg NO_3^--N·L^{-1}·d^{-1}, 351 ± 19.6 mg NO_3^--N·L^{-1}·d^{-1}, and 422 ± 15.2 mg NO_3^--N·L^{-1}·d^{-1}, respectively. When the pH further increased to 8.0, the NRR of the four reactors hardly changed. Notably, when the pH decreased to 6.5, the NRR of all reactors began to decrease; in particular, the NRR in R_1 and R_3 decreased by about 40% compared to that at pH 7.5, whereas in R_2 and R_4, this value decreased by approximately 20%. These findings showed that the lower pH could significantly decrease the NRR, although the NRR also declined when the HRT was 3 h, and the decline

TABLE 3 | Comparison of studies on packed-bed denitrification.

Type of the reactor	Type of the packed filter	HRT (h)	Temperature (°C)	The maximum denitrification rate (mg-N·L^{-1}·d^{-1})	References
Column reactor	PHBV-Sawdust	1.5	/	146	Yang et al., 2020
Column reactor	Sulfur/Limestone	24–3	6–28	300	Sahinkaya et al., 2014
Column reactor	PCL/Starch	2–0.5	15–25	640	Shen et al., 2013
Column reactor	Polybutylene succinate/Bamboo powder	4	26	340	Qi et al., 2020
Column reactor	Sulfur/Shell/Peanut hull	6–1	10–31	723	This study

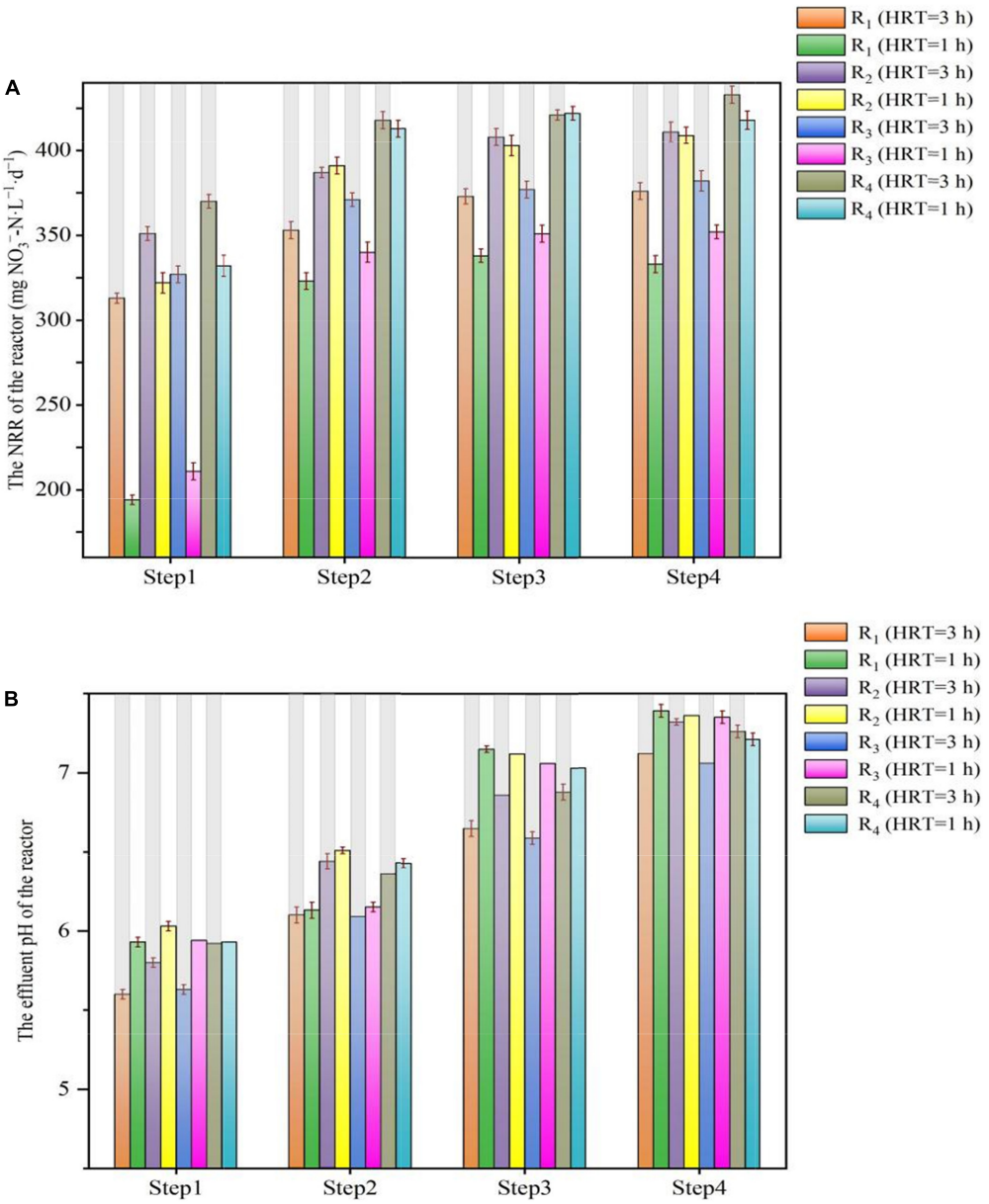

FIGURE 3 | Variations in NRR and effluent pH value in period 7 of the R_1–R_4 reactors. **(A)** NRR; **(B)** effluent pH value.

range was not as large as that with HRT of 1 h. Meanwhile, the increased pH value did not bring better NRR to all the reactors, while only a limited increase in NRR of the R_1 and R_3 reactors was observed. The reason for these phenomena may be attributed to the solubility of the solid-phase filter, and it could be speculated that as the pH decreases, even if the HD caused by the natural

solid organic carbon sources can counterbalance a certain drop in pH (Liang et al., 2021b), while shell powder would be the major role to slow down the pH drop. As the flow rate in the reactor increased, it was difficult for the solid-phase shell powder to provide sufficient alkalinity to alleviate the drop in pH, and the rapid drop in pH led to a decrease in NRR. This might explain why the NRR of the R_1 and R_3 was more susceptible to the decrease in influent pH value. Besides, when the HRT was 1 h, although a gradual increase in pH from 6.5 to 8.0 is theoretically beneficial for denitrification (Pang and Wang, 2021), there are limited electron donors released by elemental sulfur and natural organic carbon sources at this time. Hence, denitrification showed little benefit even if the pH increased.

Above all, the pH variations affected the NRR of the SMDP, and the rate of denitrification was affected by insufficient alkalinity supply when the influent pH was around 6.5. On the contrary, changes in pH will also affect the microbial activity and thus the denitrification capacity (Chen et al., 2018). When the electron donor in the reactor was insufficient, even if the pH was raised to the ideal range, it could hardly help the denitrification. Therefore, when SMDP or other denitrification reactors are adopted to remove the nitrate, the suitable pH should be considered in conjunction with the specific operation conditions (HRT, nitrate concentration, temperature, etc.).

Performance of the Solid-Phase-Based Mixotrophic Denitrification Process Coupled With Anaerobic Ammonium Oxidation

As shown in **Figure 4**, when the HRT was 4 h (step 1), the low nitrogen levels were observed in the effluent of the R_2 and R_4 reactors, with the average ammonium concentrations were also controlled within 5 mg L^{-1}, whereas the sum of the concentrations of nitrate, nitrite, and ammonium in the effluents of R_1 and R_3 reactors was greater than 15 mg L^{-1}. Lowering the HRT to 3 h in step 2 resulted in the nitrate accumulation in the reactors, with the NRE of the R_1, R_2, R_3, and R_4 reactors was 53.7 ± 3.1%, 71.5 ± 2.7%, 56.9 ± 2.6%, and 76.8 ± 3.2%, respectively. Further reduction in HRT from 3 h to 2 h in step 3 resulted in increased nitrate levels in all reactors, and the average nitrate concentration of the effluent in the R_1 and R_3 reactors was 38.6 ± 2.3 mg NO_3^--N·L^{-1} and 37.8 ± 1.9 mg NO_3^--N·L^{-1}, respectively. Compared with periods 3–4, a decrease in NRR was observed in steps 2 and 3 (within period 8), which could be explained by the following reasons: (1) The denitrification capacity may be weakened due to the consumption and loss of electron donors (elemental sulfur and natural organic carbon). (2) The mass transfer of the filter and nitrate was inhibited due to the increased sludge amount in the reactors (Zhou et al., 2011), because the sludge in the reactor was not artificially removed throughout the experiment. In addition, the ammonium concentrations in steps 2 and 3 were generally above 5 mg L^{-1}, and the optimal performance for the coupled system (SMDP and ANAMMOX) was obtained in step 1, as the HRT of the SMDP was decreased to 3 h or lower, an additional method (e.g., effluent reflux or backwashing) may be required to remove excess nitrogen to improve the quality of the effluent (Zhang et al., 2019; Liang et al., 2022).

In summary, coupling ANAMMOX with the SMDP can effectively reduce the excessive pollutant concentrations in ANAMMOX effluent. The HRT is an important factor for SMDP, which affects the overall performance of the coupled system. However, a potential problem of the coupled system was speculated because the average SS concentration in the ANAMMOX effluent was 42 mg L^{-1}, which was similar as a previous ANAMMOX reactor (Zhang et al., 2018). Compared with the tap water or the effluent of secondary sedimentation tank (SS < 10 mg L^{-1}), the high SS concentration of the ANAMMOX effluent may cause the blockage of SMDP, thereby affecting the overall denitrification performance, and the air–water backwashing method could be an effective way to remove excess sludge, which has been verified in a previous study (Zhou et al., 2021). Further verification of the optimization strategy for the coupled system is necessary in future research. Overall, as demonstrated in this study, the F_4 filter represents an effective and more favorable performance throughout the study, which provided a novel and feasible method for the SMDP process and solid-phase-based denitrification technology.

Comparative Analysis of Microbial Community

The results of the bacterial communities assigned to the phylum and genus levels, with the relative abundance of the most abundant (>1%), are summarized in **Figure 5**. Overall, 13 bacterial phyla were found in the eight bio-samples (**Figure 5A**). *Proteobacteria* were the largest phyla in all the bio-samples, which have been detected as the autotrophic denitrifying bacteria in previous study (Han et al., 2020). In all reactors, the relative abundance of *Proteobacteria* increased over time, from 53–72.2% at S_1–S_4 (S_1, S_2, S_3, and S_4: microbial communities on day 80 of the R_1, R_2, R_3, and R_4, respectively) to 67–83.6% at S_5–S_8 (S_5, S_6, S_7, and S_8: microbial communities on day 320 of the R_1, R_2, R_3, and R_4, respectively). The remaining dominant phyla were *Bacteroidetes* and *Chloroflexi*, and their abundances in S_5–S_8 were both decreased. *Bacteroidetes*, *Chloroflexi*, *Firmicutes*, and *Actinobacteria* are related to the biodegradation of organic matters (Miura et al., 2007; Xin and Qiu, 2021), and similar to the *Bacteroidetes* and *Chloroflexi*, the abundances of phyla *Firmicutes* and *Actinobacteria* also decreased over time. This shift might have been caused by changes in the amounts of organic carbon sources in the filters. Furthermore, increase in abundance of *Desulfobacterota* was observed in the R_2 and R_4, which is known as the sulfate-reducing bacteria (Frolov et al., 2021); meanwhile, the abundance of *Campilobacterota* in the R_2 and R_4 was also increased, *Campilobacterota* has been reported as the sulfide-oxidizing bacteria (Carrier et al., 2020), and the increase in its abundance was likely benefiting from the *Desulfobacterota* in the R_2 and R_4.

The genera *Ferritrophicum*, *Simplicispira*, and *Thermomonas* were found to be dominant in the bio-samples S_1–S_4 (**Figure 5B**). *Ferritrophicum* was reported as the denitrifying bacteria in the sulfur-based autotrophic system (Wan et al., 2019), and in this

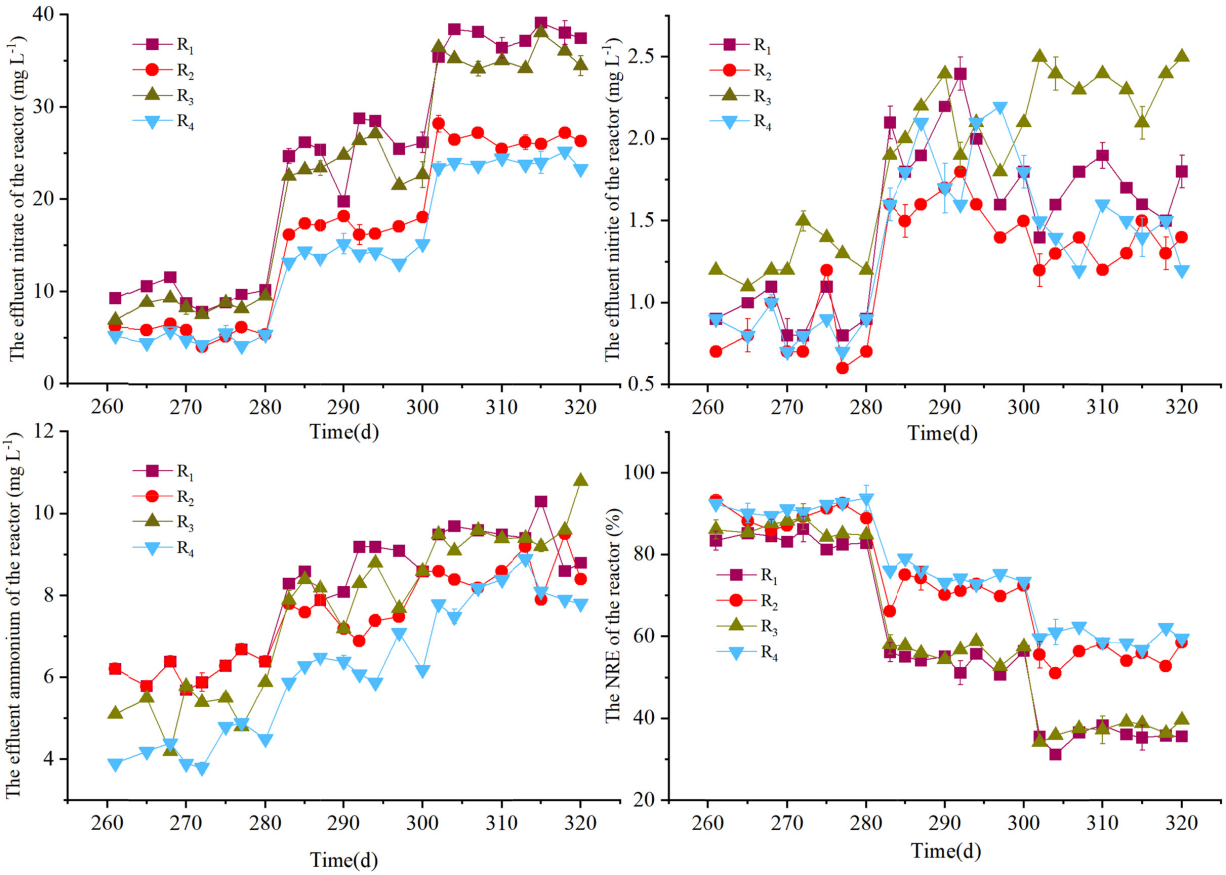

FIGURE 4 | Variations in nitrate, nitrite, ammonium, and NRE in period 8 of the R_1–R_4 reactors.

study, the abundance of *Ferritrophicum* increased in all the reactors. *Thiobacillus*, the typical denitrifying bacteria in SAD processes (Zhang et al., 2020; Dominika et al., 2021), was present at low abundances in S_1–S_4, and its abundance significantly increased in S_5–S_8. Conversely, the abundance of *Simplicispira* decreased to almost negligible levels in S_5–S_8, which probably due to its function was to degrade the organic carbon (Feng et al., 2017). The reason for these phenomena may be that the compositions of the filters changed with operation. The autotrophs and heterotrophs were both abundant in S_1–S_4. The heterotrophs in S_1–S_4, including *Ferruginibacter*, *Bacteroides*, *Trichococcus*, *Dokdonella*, *Herminiimonas*, *Sphingobium*, and *Cellulomonas*, are associated with the degradation of organics or HD processes (Chen et al., 2016; Han et al., 2020; Tian et al., 2021; Xin and Qiu, 2021; Zhang et al., 2021), and their abundances were both decreased or disappeared in S_5–S_8. The abundance of *Rhodanobacter* increased in R_1 and R_3 reactors, even though these bacteria are related to the degradation of carbohydrates (Xin and Qiu, 2021). *Ignavibacterium* has been reported as the nitrite-reducing bacteria (Chai et al., 2020) and was only found in S_7, most likely because of the high nitrite concentration of the ANAMMOX effluent. *Chlorobaculum* is sulfur-oxidizing bacteria that could oxidize sulfide and elemental sulfur to sulfate (Zhang et al., 2021), its appearance in S_8 may be attributed to the sulfur disproportionation process or the SAD process, whereas the sulfide was hardly found in the R_4 effluent (**Figure 2**), and it is thus considered that the *Chlorobaculum* may give extra advantage to ensure the quality of the effluent.

In all reactors, the autotrophs and heterotrophs were both abundant on day 80; however, on day 320, the heterotrophs decreased significantly accompanied by the increase of autotrophs. Although the abundance of heterotrophs in S_5 and S_7 was higher than that in S_6 and S_8, the structure, proportion, and composition of the filter itself likely played a decisive role in the process of denitrification. Comparatively, the F_4 filter showed a better performance under different conditions, providing a powerful option for optimizing the SMDP and the coupling of SMDP and ANAMMOX.

Engineering Implications and Future Research

The SMDP-based denitrification system provided considerable nitrogen removal performance in laboratory-scale bioreactors, besides, the composition of the filters and the long-term experimental results also demonstrate its economy and reliability. Although the conventional HD processes are still

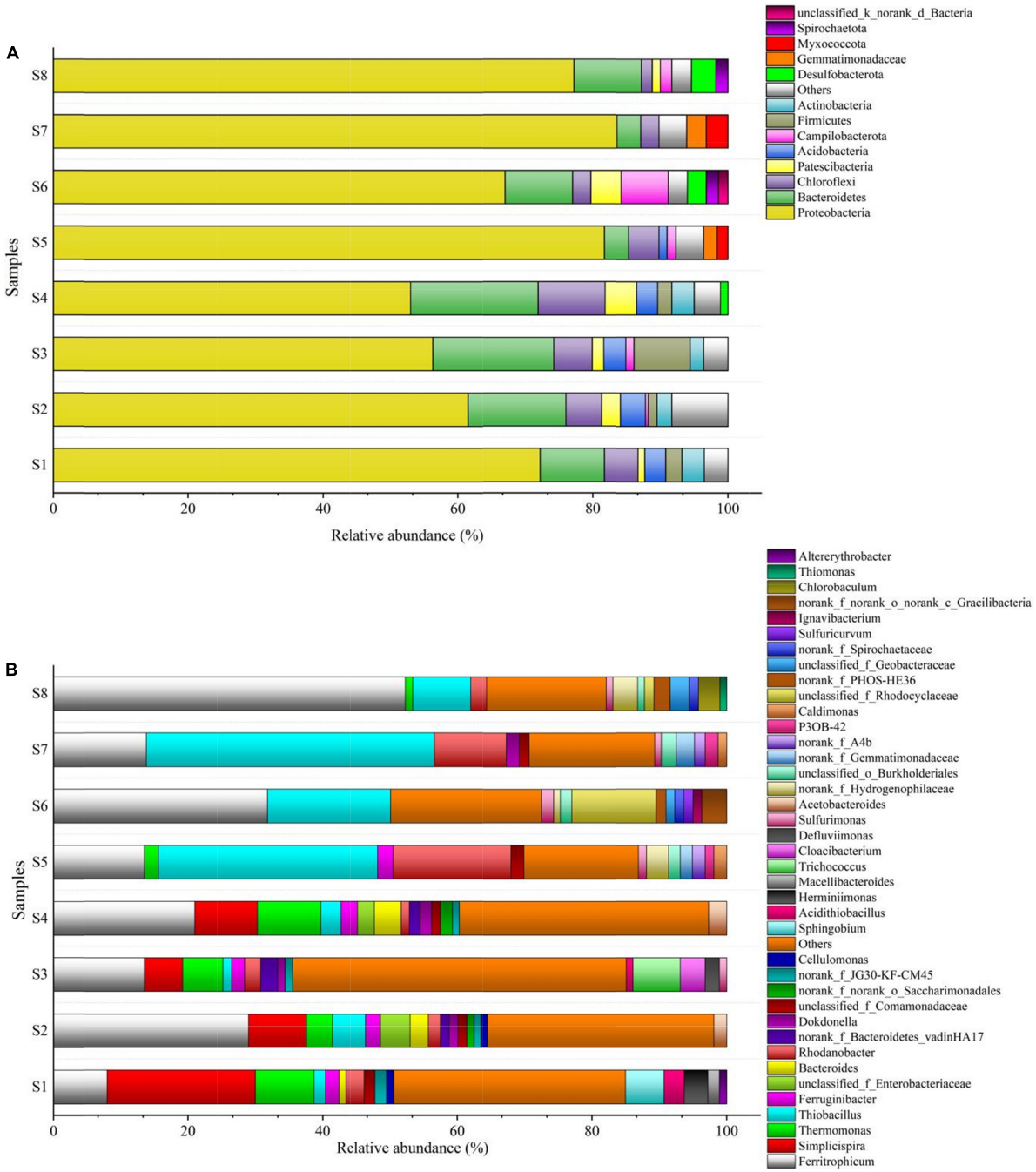

FIGURE 5 | Taxonomic classification of the eight bio-samples at **(A)** phylum level; **(B)** genus level.

widely applied in WWTPs, it is expected that the SMDP process can reduce the cost of denitrification, such as installing an SMDP device in the effluent of the secondary sedimentation tank, thereby reducing or avoiding the addition of organic carbon sources in the previous process (e.g., pre-denitrification tank). Similarly, compared to the HD processes, some scholars have found that the SAD processes were more cost-effective (Vandekerckhove et al., 2018; Wang et al., 2021). In addition, compared to the conventional nitrification/denitrification processes, the ANAMMOX process has the potential to save more than 90% of operational costs (Zhang et al., 2018), and it can be speculated that the sludge production would also be reduced through the ANAMMOX–SMDP coupled system. Furthermore, the implementation of SMDP process coupled with other efficient nitrogen removal processes [e.g., partial-denitrification–ANAMMOX (PD/A), partial-nitritation–ANAMMOX (PN/A),

etc.] may be meaningful to improve nitrogen removal rates. In general, the SMDP process represents a good denitrification effect and has strong practical engineering significance.

CONCLUSION

The solid-phase carbon-sulfur-based composite filters were successfully investigated in reactors. Changes in influent pH significantly impacted denitrification, and the content of shell powder played an important part in the filter to alleviate water acidification. The enhanced denitrification performance was observed in the R_4 reactor, and the R_4 was also the superior reactor in ANAMMOX–SMDP coupled systems. This study confirmed the overall performance of the SMDP, with F_4 as a promising filter for the purification of nitrogen-contaminated wastewater (e.g., the effluent of the secondary sedimentation tank of WWTPs).

DATA AVAILABILITY STATEMENT

The data presented in this study are deposited in the NCBI SRA database under accession numbers PRJNA835999 and PRJNA836004.

AUTHOR CONTRIBUTIONS

YaW: conceptualization, data curation, investigation, formal analysis, writing – original draft, and visualization. BL: conceptualization, supervision, and editing. FK: conceptualization and editing. YoW: supervision and editing. ZY and ZL: supervision. TZ: funding acquisition, writing – original draft, and editing. ZZ: funding acquisition, supervision, writing – original draft, and editing. All authors contributed to the article and approved the submitted version.

FUNDING

This work was supported by the Ningxia Provincial Natural Science Foundation of China (Grant No. 2020AAC03272). This study received funding from Shenyang Zhenxing Environmental Technology Co., Ltd. The funder had the following involvement with the study: data collection and analysis.

SUPPLEMENTARY MATERIAL

The Supplementary Material for this article can be found online at: https://www.frontiersin.org/articles/10.3389/fmicb.2022.934441/full#supplementary-material

REFERENCES

American Public Health Association [APHA] (2005). *Standard Methods for the Examination of Water and Wastewater*. Washington, DC: American Public Health Association/American Water Works Association/Water Environment Federation.

Carrier, V., Svenning, M. M., Gründger, F., Niemann, H., Dessandier, P. A., and Panieri, G. (2020). The impact of methane on microbial communities at marine arctic gas hydrate bearing sediment. *Front. Microbiol.* 11:1932. doi: 10.3389/fmicb.2020.01932

Chai, F. G., Li, L., Xue, S., and Liu, J. X. (2020). Auxiliary voltage enhanced microbial methane oxidation co-driven by nitrite and sulfate reduction. *Chemosphere* 250:126259. doi: 10.1016/j.chemosphere.2020.126259

Chen, F. M., Li, X., Gu, C. W., Huang, Y., and Yuan, Y. (2018). Selectivity control of nitrite and nitrate with the reaction of S_0 and achieved nitrite accumulation in the sulfur autotrophic denitrification process. *Bioresour. Technol.* 266, 211–219. doi: 10.1016/j.biortech.2018.06.062

Chen, Y. S., Zhao, Z., Peng, Y. K., Li, J., Xiao, L., and Yang, L. Y. (2016). Performance of a full-scale modified anaerobic/anoxic/oxic process: high-throughput sequence analysis of its microbial structures and their community functions. *Bioresour. Technol.* 220, 225–232. doi: 10.1016/j.biortech.2016.07.095

Chu, L. B., and Wang, J. L. (2011). Nitrogen removal using biodegradable polymers as carbon source and biofilm carriers in a moving bed biofilm reactor. *Chem. Eng. J.* 170, 220–225. doi: 10.1016/j.cej.2011.03.058

Chung, J., Amin, K., Kim, S., Yoon, S., Kwon, K., and Bae, W. (2014). Autotrophic denitrification of nitrate and nitrite using thiosulfate as an electron donor. *Water Res.* 58, 169–178. doi: 10.1016/j.watres.2014.03.071

Dominika, G., Joanna, M., and Jacek, M. (2021). Sulfate reducing ammonium oxidation (SULFAMMOX) process under anaerobic conditions. *Environ. Technol. Innov.* 22:101416. doi: 10.1016/j.eti.2021.101416

Feng, L. J., Chen, K., Han, D. D., Zhao, J., Lu, Y., Yang, G. F., et al. (2017). Comparison of nitrogen removal and microbial properties in solid-phase denitrification systems for water purification with various pretreated lignocellulosic carriers. *Bioresour. Technol.* 224, 700–707. doi: 10.1016/j.biortech.2016.11.002

Frolov, E. N., Gololobova, A. V., Klyukina, A. A., Bonch-Osmolovskaya, E. A., Pimenov, N. V., Chernyh, N. A., et al. (2021). Diversity and activity of sulfate-reducing prokaryotes in kamchatka hot springs. *Microorganisms* 9:2072. doi: 10.3390/microorganisms9102072

Gilbert, E. M., Agrawal, S., Karst, S. M., Harald, H., Nielsen, P. H., and Lackner, S. (2014). Low temperature partial nitritation/anammox in a moving bed biofilm reactor treating low strength wastewater. *Environ. Sci. Technol.* 48, 8784–8792. doi: 10.1021/es501649m

Han, F., Zhang, M. R., Shang, H. G., Liu, Z., and Zhou, W. L. (2020). Microbial community succession, species interactions and metabolic pathways of sulfur-based autotrophic denitrification system in organic-limited nitrate wastewater. *Bioresour. Technol.* 315:123826. doi: 10.1016/j.biortech.2020.123826

Hill, C. A. S., Khalil, H. P. S. A., and Hale, M. D. (1998). A study of the potential of acetylation to improve the properties of plant fibres. *Ind. Crops Prod.* 8, 53–63. doi: 10.1016/S0926-6690(97)10012-7

Koenig, A., and Liu, L. H. (2001). Kinetic model of autotrophic denitrification in sulphur packed-bed reactors. *Water Res.* 35, 1969–1978. doi: 10.1016/S0043-1354(00)00483-8

Liang, B. R., Chang, M. D., Zhang, K., Liu, D. D., Qiu, X. L., Yao, S., et al. (2020). Investigation of different solid carbonate additives in elemental-sulfur-based autotrophic denitrification process coupled with anammox process. *Environ. Technol. Innov.* 20:101149. doi: 10.1016/j.eti.2020.101149

Liang, B. R., Kang, F., Wang, Y., Zhang, K., Wang, Y. Z., Yao, S., et al. (2022). Denitrification performance of sulfur-based autotrophic denitrification and biomass-sulfur-based mixotrophic denitrification in solid-phase denitrifying reactors using novel composite filters. *Sci. Total Environ.* 823:153826. doi: 10.1016/j.scitotenv.2022.153826

Liang, B. R., Zhang, K., Liu, D. D., Yao, S., Chen, S. T., Ma, F., et al. (2021a). Exploration and verification of the feasibility of sulfur-based autotrophic denitrification process coupled with vibration method in a modified anaerobic baffled reactor for wastewater treatment. *Sci. Total Environ.* 786:147348. doi: 10.1016/j.scitotenv.2021.147348

Liang, B. R., Kang, F., Yao, S., Zhang, K., Wang, Y. Z., Chang, M. D., et al. (2021b). Exploration and verification of the feasibility of the sulfur-based autotrophic denitrification integrated biomass-based heterotrophic denitrification systems for wastewater treatment: from feasibility to application. *Chemosphere* 287:131998. doi: 10.1016/j.chemosphere.2021.131998

Miura, Y., Watanabe, Y., and Okane, S. (2007). Significance of chloroflexi in performance of submerged membrane bioreactors (MBR) treating municipal wastewater. *Environ. Sci. Technol*. 41, 7787–7794. doi: 10.1021/es071263x

Moon, H. S., Ahn, K. H., Lee, S., Nam, K., and Kim, J. Y. (2004). Use of autotrophic sulfur-oxidizers to remove nitrate from bank filtrate in a permeable reactive barrier system. *Environ. Pollut.* 129, 499–507. doi: 10.1016/j.envpol.2003.11.004

Oh, S. E., Yoo, Y. B., Young, J. C., and Kim, I. S. (2001). Effect of organics on sulfur-utilizing autotrophic denitrification under mixotrophic conditions. *J. Biotechnol.* 92, 1–8. doi: 10.1016/S0168-1656(01)00344-3

Pang, Y. M., and Wang, J. L. (2021). Various electron donors for biological nitrate removal: a review. *Sci. Total Environ*. 794:148699. doi: 10.1016/j.scitotenv.2021.148699

Qi, W. H., Taherzadeh, M. J., Ruan, Y. J., Deng, Y. L., Chen, J. S., Lu, H. F., et al. (2020). Denitrification performance and microbial communities of solid-phase denitrifying reactors using poly (butylene succinate)/bamboo powder composite. *Bioresour. Technol*. 305:123033. doi: 10.1016/j.biortech.2020.123033

Rijn, J. V., Tal, Y., and Schreier, H. J. (2006). Denitrification in recirculating systems: theory and applications. *Aquac. Eng.* 34, 364–376. doi: 10.1016/j.aquaeng.2005.04.004

Sahinkaya, E., and Dursun, N. (2012). Sulfur-oxidizing autotrophic and mixotrophic denitrification processes for drinking water treatment: elimination of excess sulfate production and alkalinity requirement. *Chemosphere* 89, 144–149. doi: 10.1016/j.chemosphere.2012.05.029

Sahinkaya, E., Dursun, N., Kilic, A., Demirel, S., Uyanik, S., and Cinar, S. (2011). Simultaneous heterotrophic and sulfur oxidizing autotrophic denitrification process for drinking water treatment: control of sulfate production. *Water Res.* 45, 6661–6667. doi: 10.1016/j.watres.2011.09.056

Sahinkaya, E., Kilic, A., and Duygulu, B. (2014). Pilot and full-scale applications of sulfur based autotrophic denitrification process for nitrate removal from activated sludge process effluent. *Water Res.* 60, 210–217. doi: 10.1016/j.watres.2014.04.052

Shen, Z. Q., Zhou, Y. X., Hu, J., and Wang, J. L. (2013). Denitrification performance and microbial diversity in a packed-bed bioreactor using biodegradable polymer as carbon source and biofilm support. *J. Hazard. Mater.* 250-251, 431–438. doi: 10.1016/j.jhazmat.2013.02.026

Strous, M., Heijnen, J. J., Kuenen, J. G., and Jetten, M. S. M. (1998). The sequencing batch reactor as a powerful tool for the study of slowly growing anaerobic ammonium-oxidizing microorganisms. *Appl. Microbiol. Biotechnol.* 50, 589–596. doi: 10.1007/s002530051340

Tian, W., Xiang, X., and Wang, H. M. (2021). Differential impacts of water table and temperature on bacterial communities in pore water from a subalpine Peatland, Central China. *Front. Microbiol.* 12:649981. doi: 10.3389/fmicb.2021.649981

Vandekerckhove, T. G. L., Kobayashi, K., Janda, J., Nevel, S. V., and Vlaeminck, S. E. (2018). Sulfur-based denitrification treating regeneration water from ion exchange at high performance and low cost. *Bioresour. Technol.* 257, 266–273. doi: 10.1016/j.biortech.2018.02.047

Vo, T. K. Q., Kang, S., An, S. A., and Kim, H. S. (2021). Exploring critical factors influencing on autotrophic denitrification by elemental sulfur-based carriers in up-flow packed-bed bioreactors. *J. Water Process. Eng.* 40:101866. doi: 10.1016/j.jwpe.2020.101866

Wan, D. J., Li, Q., Liu, Y. D., Xiao, S. H., and Wang, H. J. (2019). Simultaneous reduction of perchlorate and nitrate in a combined heterotrophic-sulfur-autotrophic system: secondary pollution control, pH balance and microbial community analysis. *Water Res.* 165:115004. doi: 10.1016/j.watres.2019.115004

Wang, J. L., and Chu, L. B. (2016). Biological nitrate removal from water and wastewater by solid-phase denitrification process. *Biotechnol. Adv.* 34, 1103–1112. doi: 10.1016/j.biotechadv.2016.07.001

Wang, S. S., Cheng, H. Y., Zhang, H., Su, S. G., Sun, Y. L., Wang, H. C., et al. (2021). Sulfur autotrophic denitrification filter and heterotrophic denitrification filter: comparison on denitrification performance, hydrodynamic characteristics and operating cost. *Environ. Res.* 197:111029. doi: 10.1016/j.envres.2021.111029

Wang, X. W., Zhang, Y., Zhang, T. T., Zhou, J. T., and Chen, M. X. (2016). Waste activated sludge fermentation liquid as carbon source for biological treatment of sulfide and nitrate in microaerobic conditions. *Chem. Eng. J.* 283, 167–174. doi: 10.1016/j.cej.2015.07.062

Wen, Y., Chen, Y., Zheng, N., Yang, D. H., and Zhou, Q. (2010). Effects of plant biomass on nitrate removal and transformation of carbon sources in subsurface-flow constructed wetlands. *Bioresour. Technol.* 101, 7286–7292. doi: 10.1016/j.biortech.2010.04.068

Xin, X. D., and Qiu, W. (2021). Linking microbial mechanism with bioelectricity production in sludge matrix-fed microbial fuel cells: freezing/thawing liquid versus fermentation liquor. *Sci. Total Environ.* 752:141907. doi: 10.1016/j.scitotenv.2020.141907

Yang, W., Lu, H., Khanal, S. K., Zhao, Q., Meng, L., and Chen, G.-H. (2016). Granulation of sulfur-oxidizing bacteria for autotrophic denitrification. *Water Res.* 104, 507–519. doi: 10.1016/j.watres.2016.08.049

Yang, Z. C., Sun, H. M., Zhou, Q., Zhao, L., and Wu, W. Z. (2020). Nitrogen removal performance in pilot-scale solid-phase denitrification systems using novel biodegradable blends for treatment of waste water treatment plants effluent. *Bioresour. Technol.* 305:122994. doi: 10.1016/j.biortech.2020.122994

Zhang, K., Kang, T., Yao, S., Liang, B., Chang, M., Wang, Y., et al. (2020). A novel coupling process with partial nitritation-anammox and short-cut sulfur autotrophic denitrification in a single reactor for the treatment of high ammonium-containing wastewater. *Water Res.* 180:115813. doi: 10.1016/j.watres.2020.115813

Zhang, K., Lyu, L., Yao, S., Kang, T., Ma, Y., Pan, Y., et al. (2019). Effects of vibration on anammox-enriched biofilm in a high-loaded upflow reactor. *Sci. Total Environ.* 685, 1284–1293. doi: 10.1016/j.scitotenv.2019.06.082

Zhang, K., Yang, B., Ma, Y. G., Lyu, L. T., Pan, Y., Wang, Y. Z., et al. (2018). A novel anammox process combined with vibration technology. *Bioresour. Technol.* 256, 277–284. doi: 10.1016/j.biortech.2018.01.128

Zhang, M., Gao, J., Liu, Q. L., Fan, Y. J., Zhu, C. J., Liu, Y. Z., et al. (2021). Nitrite accumulation and microbial behavior by seeding denitrifying phosphorus removal sludge for partial denitrification (PD): the effect of COD/NO_3^- ratio. *Bioresour. Technol.* 323:124524. doi: 10.1016/j.biortech.2020.124524

Zhou, W. L., Sun, Y. J., Wu, B. T., Zhang, Y., Huang, M., Miyanaga, T., et al. (2011). Autotrophic denitrification for nitrate and nitrite removal using sulfur-limestone. *J. Environ. Sci.* 23, 1761–1769. doi: 10.1016/S1001-0742(10)60635-3

Zhou, Y., Chen, F. X., Chen, N., Peng, T., Dong, S. S., and Feng, C. P. (2021). Denitrification performance and mechanism of biofilter constructed with sulfur autotrophic denitrification composite filler in engineering application. *Bioresour. Technol.* 340:125699. doi: 10.1016/j.biortech.2021.125699

Conflict of Interest: ZY was employed by Shenyang Zhenxing Environmental Technology Co., Ltd.

The remaining authors declare that the research was conducted in the absence of any commercial or financial relationships that could be construed as a potential conflict of interest.

Publisher's Note: All claims expressed in this article are solely those of the authors and do not necessarily represent those of their affiliated organizations, or those of the publisher, the editors and the reviewers. Any product that may be evaluated in this article, or claim that may be made by its manufacturer, is not guaranteed or endorsed by the publisher.

frontiers | Frontiers in Microbiology

TYPE Original Research
PUBLISHED 02 August 2022
DOI 10.3389/fmicb.2022.970548

OPEN ACCESS

EDITED BY
Chongjun Chen,
Suzhou University of Science and Technology, China

REVIEWED BY
Bo Hu,
Chang'an University, China
Mabruk Adams,
National University of Ireland Galway, Ireland

*CORRESPONDENCE
Zhijun Zhang
286373480@qq.com
Tong Zhu
tongzhu@mail.neu.edu.cn
Baorui Liang
1810136@stu.neu.edu.cn

†These authors have contributed equally to this work and share first authorship

SPECIALTY SECTION
This article was submitted to Microbiotechnology, a section of the journal Frontiers in Microbiology

RECEIVED 16 June 2022
ACCEPTED 14 July 2022
PUBLISHED 02 August 2022

CITATION
Wang Y, Liang B, Kang F, Wang Y, Zhao C, Lyu Z, Zhu T and Zhang Z (2022) An efficient anoxic/aerobic/aerobic/anoxic process for domestic sewage treatment: From feasibility to application. *Front. Microbiol.* 13:970548. doi: 10.3389/fmicb.2022.970548

An efficient anoxic/aerobic/aerobic/anoxic process for domestic sewage treatment: From feasibility to application

Yao Wang†, Baorui Liang*†, Fei Kang, Youzhao Wang, Chaoyue Zhao, Zhenning Lyu, Tong Zhu* and Zhijun Zhang*

School of Mechanical Engineering and Automation, Institute of Process Equipment and Environmental Engineering, Northeastern University, Shenyang, China

In this paper, the anoxic/aerobic/aerobic/anoxic (AOOA) process was proposed using fixed biofilms in a continuous plug-flow multi-chamber reactor, and no sludge reflux operation was performed during the 190days of operation. The reactor volume ratio of 1.5:2:1.5:1 (A/O/O/A) with the dissolved oxygen (DO) concentration of 2mgL^{-1} in the aerobic zone was the optimal condition for reactor operation. According to the results obtained from the treatment of real domestic sewage, when the hydraulic retention time (HRT) was 6h, the effluent of the reactor could meet the discharge standard even in cold conditions (13°C). Specifically, the elemental-sulfur-based autotrophic denitrification (ESAD) process contributed the most to the removal of total inorganic nitrogen (TIN) in the reactor. In addition, the use of vibration method was helpful in removing excess sludge from the biofilms of the reactor. Overall, the AOOA process is an efficient and convenient method for treating domestic sewage.

KEYWORDS

biofilm, domestic sewage, elemental-sulfur-based autotrophic denitrification, multi-chamber, no sludge reflux, vibration

Introduction

Nitrogen pollution in water bodies is already a worldwide issue, and excessive accumulation of nutrients is the main cause of this problem (Wang et al., 2019). In China, there are still many water bodies suffering from eutrophication, which is most likely caused by nitrogen pollution (Jiang et al., 2019). Although the Chinese Government agency stipulates that the total nitrogen concentration in the effluent of wastewater treatment plants (WWTPs) cannot be higher than 15 mg L^{-1}, due to the low content of organic matter in the influent, many WWTPs find it difficult to meet this discharge standard (Feng et al., 2021). Thus, the development of efficient technology to further improve the effluent quality of WWTPs is urgently needed.

For the WWTPs, nitrification and denitrification (ND) processes are often used due to their high efficiencies. However, when the amount of organic matter in the influent of ND

process is not enough to complete denitrification, additional organic matter is needed, which will increase the difficulty and cost of operation. From this point of view, to reduce the dependence on organic matter in sewage treatment processes and the cost, many processes have been proposed, including the partial nitrification–denitrification (PND), anaerobic ammonia oxidation (anammox), partial nitritation-anammox (PN-A), and partial-denitrification-anammox (PD-A; Zhang et al., 2018; Du et al., 2020; Peng et al., 2020; Feng et al., 2021). Nonetheless, the implementation of these processes requires stringent conditions, which limits their widespread application. For instance, the slow growth of anammox bacteria and the need for strict restriction of nitrite-oxidizing bacteria (NOB) limit the application of anammox-based processes for nitrogen removal from sewage (Zhang et al., 2019; Du et al., 2020). Moreover, the ever-changing influent concentration of dissolved oxygen (DO) and ammonium will affect the performance of partial nitrification process, thus resulting in the instability of PND system (Li et al., 2020).

Compared with other reactors, the multi-chamber reactor has shown to be helpful in improving the removal efficiency of pollutants in water bodies (Liang et al., 2021a). Furthermore, the biofilm reactor can help to improve the quality of effluent and reduce the loss of bacteria (Zhang et al., 2015), whereas the multi-chamber reactor coupled with biofilm may improve the capacity of domestic sewage treatment. Nevertheless, the effects of structural changes of the biofilm-coupled multi-chamber reactor on domestic sewage treatment have not been studied in detail. Moreover, as an effective method for removing pollutants from water bodies, the effect of vibration method on the treatment of domestic sewage after coupling biofilms with multi-chamber reactor is unclear.

In this study, a lab-scale multi-chamber reactor coupled with biofilm was tested under different conditions for the treatment of domestic sewage. The objectives of this study were: (1) to compare the influence of changes in the structure of the reactor on the treatment of domestic wastewater; (2) to study the performance of the reactor under different DO concentrations and influent chemical oxygen demand/total inorganic nitrogen (COD/TIN) ratios; (3) to study the impact of vibration method on the reactor; (4) to analyze the changes in the microbial community in the reactor at different times. The results of this study would help to simplify the operation of domestic sewage treatment and improve the treatment capacity.

Materials and methods

Reactor configuration

A continuous plug-flow reactor with an effective working volume of 15.4 l was used in this study. The reactor was divided into four different chambers by three baffles, and the chambers were orderly adopted as the anoxic part 1 (A1), aerobic part 2 (O2), aerobic part 3 (O3), and anoxic part 4 (A4; Figure 1). The reactor was made of plexiglass with a rectangular shape, had a width of 15 cm, an effective water height of 17 cm, and a length of 60.4 cm. The baffle position between chambers A1 and O2 was made movable so as to allow easy adjustability, yielding the desired working volumes in A1 and O2 at any moment. This was used to study the effect of changes in the volumes of A1 and O2 on the removal of pollutants, and the working volumes of O3 and A4 were fixed at 3.8 and 2.6 l, respectively. The pH probe connected to a pH controller (MIK-pH 8.0, Meacon, China) was used to control the metering pump (DS2-PU2, Xin Xishan, China), which was used to maintain the influent pH of A4 at about 7.0 ± 0.1.

The biofilm frame had a rectangular shape and was welded using several stainless-steel rods, with a width of 13 cm, a height of 22 cm, and a length of 5 cm. Two identical biofilm frames were filled into the A1, O2, and O3 chambers, respectively, and the nylon biofilms were immobilized on biofilm frames to serve as the carriers for microorganisms (Figure 1). The biofilm frames were combined with a rectangular plate, and six eccentric DC motors (BGB37-528, Baishizhili, China, 12 V DC motor) were installed on the top of the plate. The vibration of biofilm frames was driven by operating motors, and a DC speed regulator (DC-12 V, Gewa, China) was adopted to regulate the motor speed.

Seed sludge and sewage

The synthetic domestic sewage used for the influent was made from tap water supplemented with glucose and NH_4Cl as the COD and ammonium sources, respectively. The $NaHCO_3$ (0.7 g l^{-1}) solution was used as the pH regulator for the A4 chamber. The seed sludge of the O2 and O3 chambers was purchased from an environmental technology company in Shenyang (Dongyuan, China), which is applied for the ND process of the domestic sewage. For the A1 and A4 chambers, the seed sludge was obtained from Donggang WWTP (Rizhao, China). The real domestic sewage adopted in the reactor was obtained from the Donggang WWTP, its main compounds are presented in Table 1.

Reactor start-up and experimental procedure

In the A4 chamber, 800 g of oyster shell was evenly filled into the lower part to further improve the pH value, and 1,800 g of the elemental-sulfur-based autotrophic denitrification (ESAD) filter was evenly filled into the upper part for the denitrification process (Figure 1). The composition and structure of the ESAD filter were consistent with those of the USS filter used in our previous study (Liang et al., 2020). The ESAD process was adopted because of its low sludge yield and good denitrification capacity as compared to other denitrification processes (Sahinkaya et al., 2014). The size of the oyster shell and the ESAD filter were screened at around 6 cm^3. The volume of the seed sludge [the concentration of mixed liquor suspended solids (MLSS) was around 4.1 g L^{-1}] which was

10.3389/fmicb.2022.970548

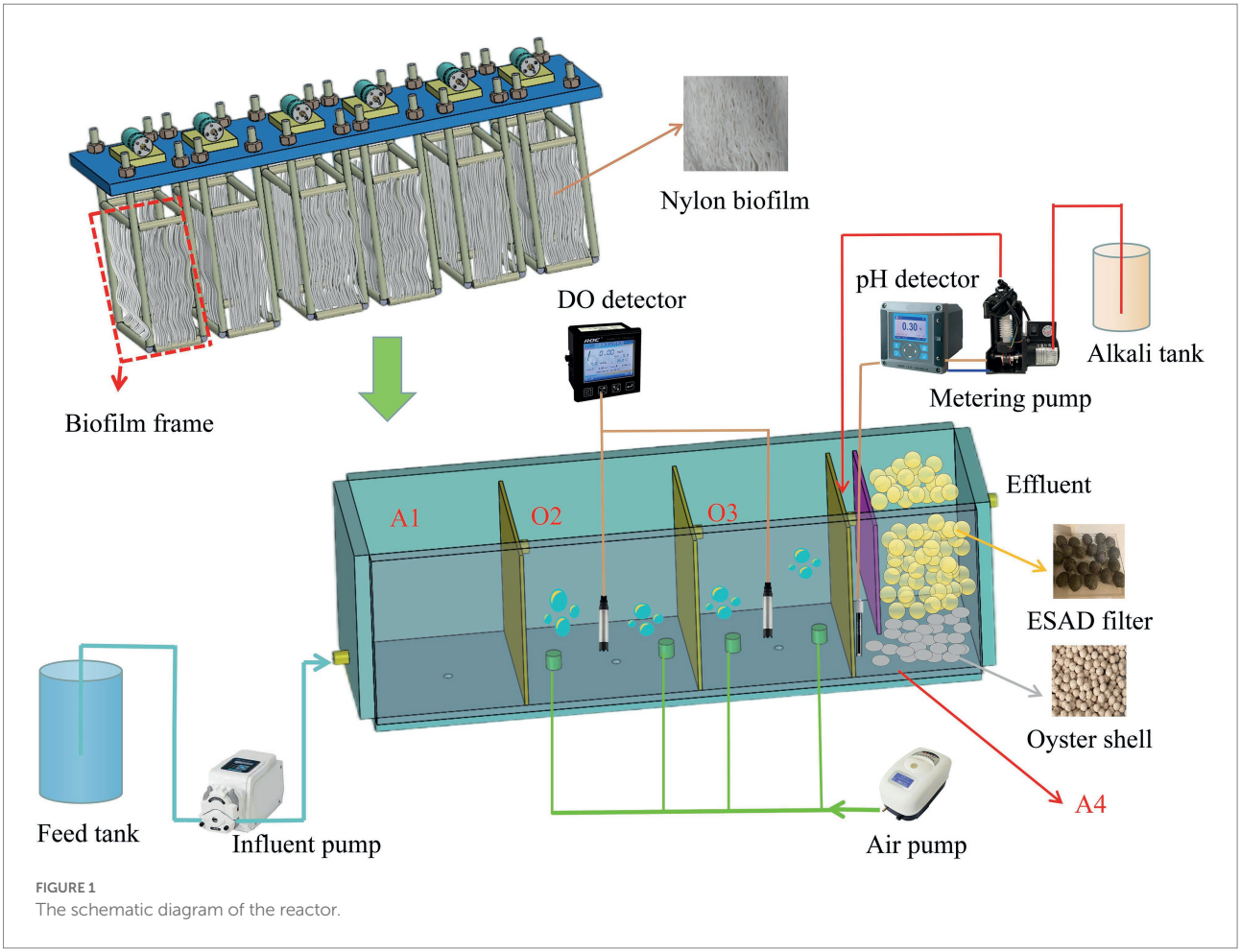

FIGURE 1
The schematic diagram of the reactor.

TABLE 1 Influent parameters of the reactor.

Periods	I	II	III	IV
Days	1–70	71–110	111–160	161–190
HRT (h)	12–4	5	5	5 and 6
COD/TIN	4	4	2–6	3.5
Average temperature (°C)	29 ± 2			13 ± 2
Ammonium (mg L^{-1})	50			48.2 ± 15.3
Sulfate (mg L^{-1})	52.3 ± 4.6			69.3 ± 5.9
COD (mg L^{-1})	200		100–300	168.7 ± 30.6
DO concentration of O2 and O3 (mg L^{-1})	3	1–4	2	

inoculated into the A1 and A4 chambers in volumes of 600 and 400 ml, respectively, while for O2 and O3 inoculated sludge (with the MLSS concentration of around 3.8 g L^{-1}), these volumes were 800 and 600 ml, respectively. After the reactor was filled with seed sludge, the motors were turned on to promote the vibration of biofilm frames to help the seed sludge attach onto the nylon biofilm carriers. This situation lasted for 24 h before continuous feeding experiments, the DO concentration of O2 and O3 was maintained at around 3 mg L^{-1} until period II.

After inoculation, the reactor was operated for 190 days with continuous feeding and was divided into four periods. Period I was planned to test the reactor performance under different hydraulic retention times (HRT), and to compare the performance of reactor under different volume ratios, the volume ratios of A1/O2 were changed (Table 2). During period II, to investigate the effect of changes in the concentration of DO on the reactor, the DO concentrations of O2 and O3 chambers were changed and two batches of repeated experiments were carried out. Similarly, batch experiments were carried out in period III to study the effects of different COD/TIN ratios on the reactor (Table 3), and throughout periods I to III, the water temperature of the reactor was controlled at 29°C ± 2°C using heaters.

During period IV, to study the effects of real domestic sewage and changes in ambient temperature, the heaters in the reactor were turned off to keep the reactor operating at ambient temperatures, and the influent of the reactor was changed from synthetic sewage to real sewage (Table 1). No reflux operation was performed throughout the study, and during days 120–190, to mitigate the impact of sludge accumulation on the biofilm frames, vibrations were performed every 20 days, which lasted for 1 h each time. According to the actual conditions of the vibrations of the biofilm frames, the speed of the motor was stabilized at 600 r/min during the vibrations. After the

TABLE 2 Operating parameters of the reactor during period I.

Days	1–5	6–9	10–13	14–20	21–25	26–30	31–35 and 51–55	36–40 and 56–60	41–45 and 61–65	46–50 and 66–70
Operation conditions										
HRT (h)	12	8	6	5	4	5	5	5	5	5
Volume ratio (A1/O2/O3/A4)	2:1.5:1.5:1						2:1.5:1.5:1	2.5:1:1.5:1	1.5:2:1.5:1	1:2.5:1.5:1
Influent COD (mg L^{-1})	200									
Influent ammonium (mg L^{-1})	50									
Effluent characteristics										
COD (mg L^{-1})	10.3 ± 2.3	10.7 ± 2.6	13.1 ± 3.2	12.4 ± 2.3	24.4 ± 8.7	12.8 ± 3.6	18.2 ± 6.8	11.1 ± 4.3	15.7 ± 3.9	23.1 ± 11.6
Ammonium (mg L^{-1})	2.1 ± 1.1	3.5 ± 0.4	4.2 ± 0.6	2.9 ± 0.9	10.6 ± 2.6	3.6 ± 1.5	3.9 ± 0.9	12.3 ± 2.6	1.95 ± 0.4	4.6 ± 0.7
TNE (mg L^{-1})	3.1 ± 1.3	8.2 ± 1.5	10.1 ± 1.6	6.2 ± 1.1	16.8 ± 3.1	7.6 ± 0.8	11.3 ± 1.4	18.3 ± 3.2	3.5 ± 0.8	10.5 ± 1.3
COD removal efficiency (%)	94.9	94.7	93.5	93.7	87.8	93.6	90.9	94.4	92.1	88.4
ARE (%)	95.8	93	91.6	94.2	78.8	92.8	92.2	75.4	96.1	90.8

TABLE 3 Operation parameters of the reactor during periods II and III.

Periods		II				III				
Days	Batch 1	71–75	76–80	81–85	86–90	111–115	116–120	121–125	126–130	131–135
	Batch 2	91–95	96–100	101–105	106–110	136–140	141–145	146–150	151–155	156–160
DO concentration of O2 and O3 (mg L^{-1})		1	2	3	4			2		
Influent COD/TIN		4				2	3	4	5	6
Influent COD (mg L^{-1})		200				100	150	200	250	300

vibrations, the reactor was briefly stopped (for 15 min), thus temporal cessation of sewage feed supply, allowing the suspended sludge to settle, and then the sludge was discharged through the outlet at the bottom of the reactor. The HRT was calculated considering the empty bed volume, and the following equations were used to calculate the HRT, TIN, and total nitrogen in effluent (TNE):

$$HRT = \frac{B_a}{R_b} \quad (1)$$

$$TIN = N_a + N_i + N_N \quad (2)$$

$$TNE = E_a + E_i + E_N \quad (3)$$

where R_b is the influent flow rate of the reactor (L h^{-1}); B_a is the empty bed volume of the reactor (L); *Na*, *Ni*, and *NN* are the ammonium, nitrate, and nitrite concentrations (mg L^{-1}) in the influent of the reactor, respectively; *Ea*, *Ei*, and *EN* are the ammonium, nitrate, and nitrite concentrations (mg L^{-1}) in the effluent of the reactor, respectively.

Analytical methods

The samples collected from the inlet, A1, O2, O3, and A4 (outlet) were tested on daily basis. Before the measurements, the 0.45 μm membrane filters were adopted to filter the samples, then the following parameters were analyzed according to APHA (2005): COD, sulfate, MLSS, nitrate, nitrite, and ammonium. For the sulfate, the samples were only collected from the inlet and A4 effluent. The concentration of MLSS in the effluent from A4 chamber was monitored once a week. The digital probes (Pro20i, YSI, United States and PHS-3C, LeiCi, China) were, respectively, adopted to measure the DO and pH values.

DNA extraction and Illumina MiSeq sequencing

Microbial samples were collected from different chambers of the reactor to study microbial communities. For the A1, O2, and O3 chambers, the sludge was taken from four different points on the two biofilm frames in each chamber and then mixed to form the finished sample, while for the finished sample of A4 chamber, the sludge on the surface of ESAD filters was collected from four different points and mixed. The samples were collected on day 30 and 190, respectively, and one sample was taken at a time from each chamber. The PowerSoil DNA extraction kit (FastDNA Spin Kit for Soil, MP Biomedicals, United States) was used to extract the DNA, and according to the standard protocols (Majorbio, Shanghai, China), the V3–V4 hypervariable region of the bacterial 16S rRNA gene was targeted by primers 338F (5′-ACTCCTACGGGAGGCAGCAG-3′) and 806R

(5′-GGACTACHVGGGTWTCTAAT-3′). Both the amplicons were pooled in equimolar, and paired-end sequenced (2 × 300) on a MiSeq sequencing platform (Illumina, San Diego, USA).

Results and discussion

Performance of the reactor under different HRTs and volume ratios

During period I, the variations in COD and nitrogen concentrations of the reactor are shown in Table 2. On days 1–30, to study the effect of changes in influent flow rate on the reactor, the overall performance of the reactor was observed under different HRTs. After 5 days of operation, the average effluent COD, ammonium, and TNE concentrations of the reactor were 10.3 ± 2.3, 2.1 ± 1.1, and 3.1 ± 1.3 mg L^{-1}, respectively, indicating that the reactor can start up quickly and achieve the desired pollutant removal performance. When the COD and ammonium effluent concentrations were, respectively, lower than 50 and 5 mg L^{-1} for three consecutive days, the HRT of the reactor gradually decreased. Throughout period I, the COD concentration in the effluent of the reactor was always lower than 50 mg L^{-1}, while the average ammonium concentration increased to 10.6 ± 2.6 mg L^{-1} when the HRT was 4 h. This may have been caused by the faster flow rate of sewage that weakened the treatment efficiency of ammonium in the reactor. Therefore, the HRT of the reactor was stabilized at 5 h, and then the two repeat batches of volume change experiments were performed at 30–70 days.

The A1/O2/O3/A4 volume ratio was first set at 2:1.5:1.5:1, which was then successively changed to 2.5:1:1.5:1, 1.5:2:1.5:1, and 1:2.5:1.5:1, respectively. The reactor was run continuously for 5 days at each volume ratio, and this was repeated on days 51–70. Under the four different volume ratios, the COD concentrations of the effluent from the reactor were always lower than 50 mg L^{-1}, and the removal of COD was mainly carried out in the A1 chamber. Compared to other volume ratios, the reactor obtained the lowest COD removal efficiency when the ratio was 1:2.5:1.5:1, with the effluent concentration of COD was 23.1 ± 11.6 mg L^{-1} (Table 2).

The change of the volume has a great influence on the concentration of nitrogen in the effluent of the reactor, the effluent average ammonium concentration of 12.3 ± 2.6 mg L^{-1} was obtained under the volume ratio of 2.5:1:1.5:1 in period I. This could be attributed to the decrease in the volume of aerobic zone, whereas for the other three volume ratios, due to the larger volumes of the aerobic zone, the ammonium removal efficiencies (ARE) of the reactor were both greater than 90%. The optimal ARE was 96.1% by volume ratio of 1.5:2:1.5:1, with the effluent average TNE concentration of 3.5 ± 0.8 mg L^{-1}. In a word, the application of anoxic/aerobic/aerobic/anoxic (AOOA) process in the reactor shows that the reactor can start-up quickly and efficiently treat COD and TIN in domestic sewage, the optimal volume ratio is considered to be 1.5:2:1.5:1 in the experiment, and the volume ratio of the reactor was fixed at 1.5:2:1.5:1 in the next periods.

Performance of the reactor under different DO concentrations

To verify the adaptability of the reactor under different conditions, the DO concentrations of the chambers O2 and O3 were varied on days 71–110. Continuous aeration was carried out, and the DO concentration was set at 1, 2, 3, and 4 mg L^{-1} successively with repeat batch experiments were adopted, the experimental results are shown in Figure 2. The ARE decreased to 69.9%, resulting in effluent ammonium concentration of reactor to be 15.05 ± 0.62 mg NH_4^+-N·L^{-1} for the DO concentration of 1 mg L^{-1}. Especially in chamber O3, only a decrease in ammonium concentration of about 10 mg NH_4^+-N·L^{-1} was observed, this was worse than the removal performance of ammonium at other DO concentrations (22.2 ± 1.42, 26.4 ± 1.86, and 16.1 ± 1.05 mg NH_4^+-N·L^{-1}, corresponding to DO concentrations of 2, 3, and 4 mg L^{-1}, respectively). The reason for this phenomenon could be attributed to the nitrification activity was weakened when the DO concentrations were lower than 1.3 mg L^{-1} (Kim et al., 2021).

When the DO concentration was set at 2 mg L^{-1}, the effluent average ammonium, TNE, and nitrate decreased to 0.83 ± 0.22, 3.55 ± 0.36, and 2.61 ± 0.45 mg L^{-1}, respectively, with the TIN removal efficiency in chamber O3 increased from 7.2% (DO = 1 mg L^{-1}) to 18.4% (DO = 2 mg L^{-1}). As the DO concentration was further increased to 3 mg L^{-1}, the average ammonium and nitrate concentrations in the effluent of the reactor were increased to 2.79 ± 0.31 and 5.83 ± 0.27 mg L^{-1}, respectively, with the TIN removal efficiency of the reactor decreasing from 92.9% (DO = 2 mg L^{-1}) to 82.8% (DO = 3 mg L^{-1}). Although the reactor could meet the standard of level A at the DO concentrations of 2 and 3 mg L^{-1} (GB18918-2002, discharge standard of pollutants for municipal WWTPs), while considering that when the DO concentration was 2 mg L^{-1}, the reactor achieved better pollutant removal performance and required lower aeration intensity, this may be the optimal DO concentration for the reactor. Unexpectedly, the performance of the reactor was also weakened when the DO concentration was set at 4 mg L^{-1}, with the effluent ammonium of the reactor being 9 mg L^{-1}, and the nitrate concentration in the O2 effluent was 17.3 ± 1.36 mg L^{-1}, which was higher than the nitrate concentration of O2 effluent under other DO concentrations during period II. This may be attributed to the occurrence of heterotrophic denitrification (HD) processes in O2 chamber, since the activity of HD could be inhibited when the DO concentration was higher than 4 mg L^{-1} and the DO is likely to be consumed by heterotrophic bacteria (Gutierrez-Wing et al., 2012; Du et al., 2020), thus leading to the accumulation of nitrate. Moreover, compared with the DO concentrations of 2 and 3 mg L^{-1}, a higher ammonium accumulation was observed when the operational DO

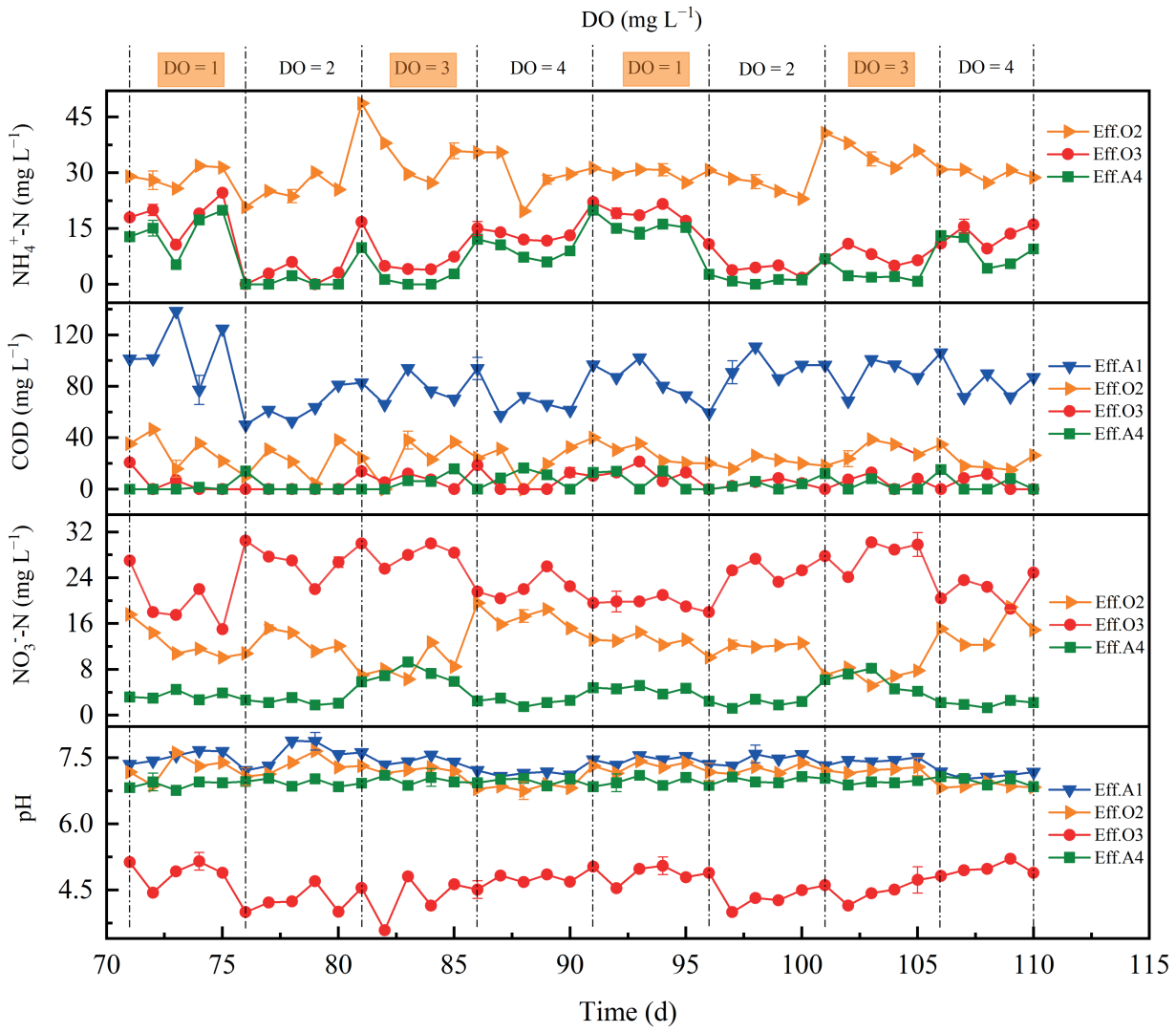

FIGURE 2
Performance of the reactor during period II.

concentration increased to 4.0 mg L^{-1}, the reason may be that the nitrifiers were inhibited and the shape of the biofilm was affected by excessive aeration intensity, which leads to negative effects.

During period II, the COD removal mainly occurred in chambers A1 and O2. A certain amount of COD in O2 could contribute to the occurrence of HD process, while the COD/TIN ratio in O3 was generally lower than 2. Therefore, it was difficult to realize complete HD process in the O3 chamber due to poor COD resources, which could not provide enough electrons (Liang et al., 2021b). Aside from COD measurements, it was found that the change of pH value was closely related to the performance of reactor, when the DO concentration was lower than 4 mg L^{-1}, there were no significant differences in the pH values between the inlet and outlet of chamber O2, and decreased only in the effluents of O3 and A4 (Figure 2). It could be speculated that the removal of nitrogen in chamber O2 was probably induced by the simultaneous nitrification and denitrification (SND) process, because one of the features of SND is the acid–base equilibrium before and after the operation (Lai et al., 2020). The occurrence of SND process may benefit from the use of biofilms, which supports the coexistence of anoxic and aerobic conditions (Layer et al., 2020). The decrease in pH and the nitrate accumulation of the O3 effluent were presumably caused by the nitrification process, with the nitrification process being the fundamental mechanism in chamber O3, because the main function of nitrification process is to convert ammonium into nitrate (Pan et al., 2022).When the DO concentration wa s set at 4 mg L^{-1}, a decrease in pH of O2 effluent was observed, which was likely attributable to the inhibition of HD caused by the higher DO concentration, thus affecting the acid–base balance of O2 effluent. Notably, when the DO concentrations were 1 and 4 mg L^{-1}, a recovery period was likely needed to restore the performance of the reactor, suggesting that the DO concentration is an important factor when the reactor is challenged with the environmental variations.

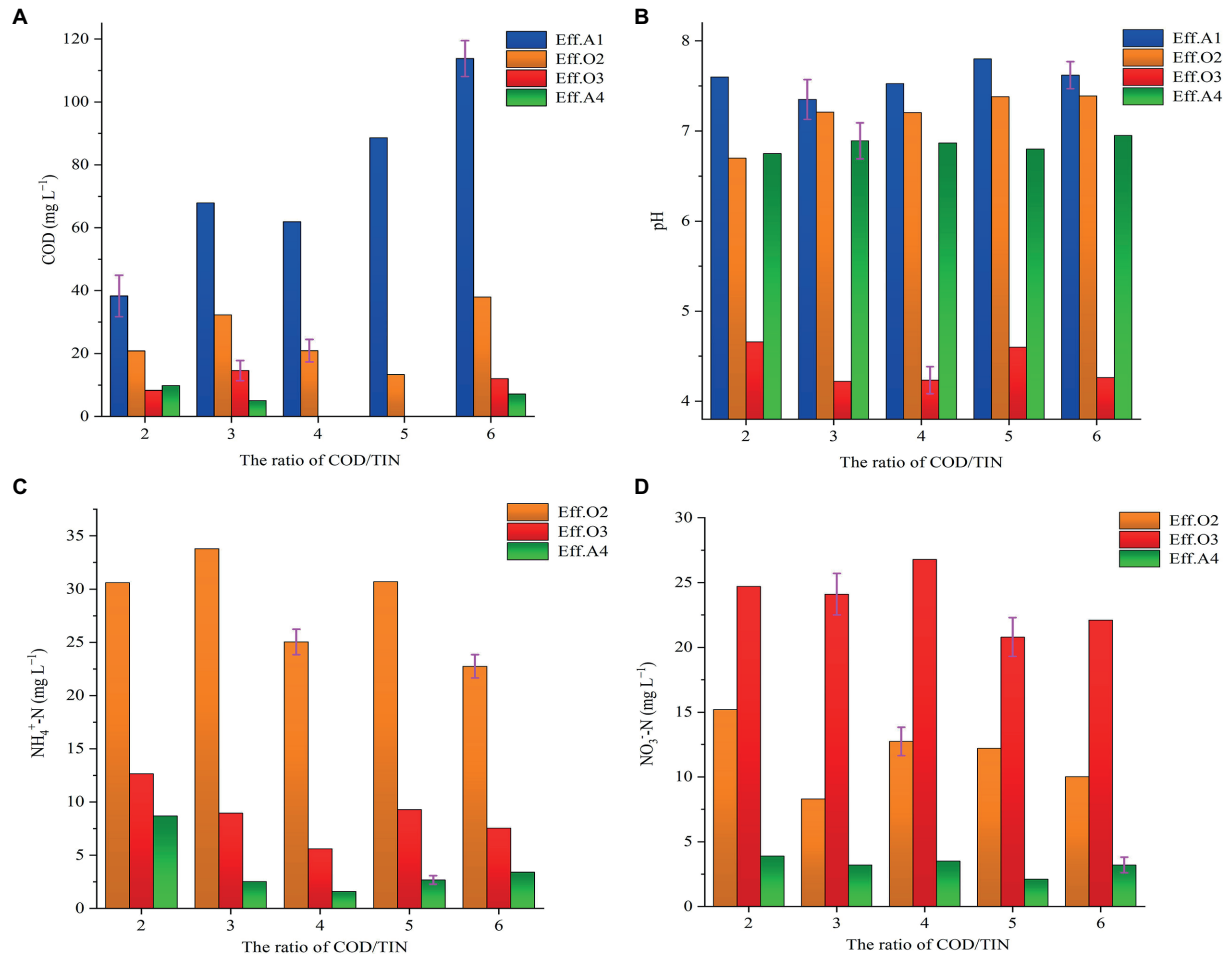

FIGURE 3
Variations of COD, pH, ammonium, and nitrate in period III of the reactor **(A)** COD; **(B)** pH; **(C)** ammonium; and **(D)** nitrate.

$$55S_0 + 50NO_3^- + 38H_2O + 20CO_2 + 4NH_4^+ \rightarrow 4C_5H_7O_2N + 55SO_4^{2-} + 25N_2 + 64H^+ \quad (4)$$

The pH of the A4 influent was first automatically increased to about 7.0 ± 0.1, and then naturally increased after passing through the oyster shells, with the average pH of the period II further increased to about 7.4 ± 0.1 before the ESAD process. In the reactor, the chamber A4 contributed the most (39.2%–54.6%) to TIN removal efficiency (Supplementary Table S1), and could simultaneously remove ammonium and nitrate in the sewage. However, the accumulation of sulfate is a major problem in the ESAD process. When the DO concentration was 2 and 3 mg L^{-1}, the average sulfate productivity was 6.60 ± 0.58 and 6.82 ± 0.48 mg SO_4^{2-}/mg NO_3^--N, respectively, while the sulfate concentration in the effluent of the reactor was always lower than 250 mg L^{-1} (maximum value set by US EPA). According to Eq. 4, the theoretical sulfate productivity was 7.54 mg SO_4^{2-}/mg NO_3^--N, the lower sulfate productivity could be attributed to the use of shell powder in the USS filter, because shell powder contains a small fraction of organic matter, which may facilitate the occurrence of HD process (Liang et al., 2022).

Performance of the reactor under different COD/TIN ratios

During period III, different COD/TIN ratios were adopted to elucidate the effects on the reactor. Similar to period II, COD was mainly consumed in chambers A1 and O2 during period III (Figure 3). When the COD/TIN ratio was set at 2, the ARE of the reactor was reduced to 82.6% with the ammonium removal effect deteriorated, while this ratio was generally greater than 93% for the COD/TIN ratio of higher than 2. In addition, when the COD/TIN ratio was 2, it was observed that the pH decrease in the O2 effluent was more severe and a higher nitrate concentration was obtained compared to other COD/TIN ratios. This was likely due to the limited COD concentration in the chamber O2, since carbon could act as an energy source for microbes (Xi et al., 2022). Thereafter, with the COD/TIN ratio gradually increased from 2 to

6, the reactor exhibited stable performance and the effluent average concentrations of ammonium and TNE were lower than 5 and 15 mg L^{-1}, respectively. Although the COD concentration in the O3 influent was relatively high when the COD/TIN ratio was 6, the nitrate concentration in O3 effluent was not effectively reduced, which proved that lower concentrations of COD had limited effects on denitrification. Overall, the proposed AOOA process demonstrated outstanding performance in removing pollutants from sewage and is also simple to operate.

By comparing phases II and III that ran under the same operating conditions, a higher nitrate concentration was observed in the reactor's effluent on days 121–125 (8.35 ± 0.58 mg L^{-1}), with the MLSS concentration of 17.6 mg L^{-1}. This could be explained by the hampering of the mass transfer between the nitrate and the ESAD filter was influenced due to the gradually accumulated sludge in the chamber A4, so it leads to the increase of nitrate in the effluent. To alleviate this potential problem, the oyster shell and ESAD filter were manually taken out and excess sludge was washed away, they were then filled back into chamber A4 successively. For the ESAD filter, only a small amount of sludge was left on its surface for subsequent denitrification process. This resulted in nitrate concentration of 5.23 ± 0.35 mg L^{-1} on days 146–150, suggesting that the removal of excess sludge from ESAD filter could help in improving the denitrification capacity.

Performance of the reactor to treat real sewage and under vibration conditions

Switching from synthetic domestic sewage to real domestic sewage resulted in effluent COD and ammonium concentrations of 32.4 ± 10.3 and 16.8 ± 0.42 mg L^{-1} (days 161–173), respectively, with the ARE decreased to 65.1%. This could have been caused by the activity of the nitrification process, which was suppressed due to the low temperature (Gao et al., 2022), leading to low ARE and a build-up of ammonium in the effluent. Consistent with this study, with the decrease of temperature, other researchers have also found a decrease in the activity of the nitrification reaction (Kim et al., 2006; Hoang et al., 2014). Considering that the reactor could not adapt to the influent load at this time under such cold conditions, the HRT of the reactor was increased from 5 to 6 h to explore whether the risk of effluent ammonium could be reduced. With continuous operation, a recovery trend was observed with the average ARE increased to 90.1% (days 174–190), indicating that at lower temperature, prolonging the HRT is the key method to cope with the decrease of ARE in the reactor. The effluent nitrate was always lower than 5 mg L^{-1} throughout period IV, indicating favourable denitrification performance of the ESAD process, even the average water temperature was only 13°C. Compared with other periods, a higher concentration of effluent COD was observed in period IV (33.6 ± 12.9 mg L^{-1}), which may be due to the reason that real domestic sewage contained a certain amount of non-biodegradable organic matter, which led to the increase of remaining COD. Moreover, the average pH value of O2 effluent during period IV decreased to acidic to a certain extent (Figure 4), while the average pH value of O3 effluent was slightly higher than the other periods. This may be due to a decrease in the contribution of HD processes in O2 and an increase in O3.

To control the possible reduction in treatment efficiency of the reactor caused by the gradually thickening biofilms, the vibration method was adopted to remove excess sludge on the biofilms. The overall performance of the reactor on the day of vibrations, the day before the vibrations and the day after the vibrations are recorded in Supplementary Table S2. The results verified that the vibrations had no negative impact on the performance of the reactor. Although the effluent COD of the reactor rose to a certain extent after the vibrations, it was still within the acceptable range (<50 mg L^{-1}). Overall, the proposed AOOA process would be an applicable pathway even without the reflux operation, and the implementation of the vibration method also ensures long-term and efficient operation of the reactor.

Evolution of the microbial community

The samples were collected from the reactor to discover the changes in the microbial communities, distributions of bacterial sequences at phylum and genus levels as shown in Supplementary Table S1 and Figure 5, respectively (relative abundance ≥ 1%). At the phylum level (Supplementary Figure S1), the *Bacteroidetes* was the most dominant phylum in the A1 chamber. Its abundance increased from 35.6% (day 30) to 49.5% (day 190). The enrichment of *Bacteroidetes* could be related to its function, as it has been reported to be mainly used for the degradation of organic matter (Hou et al., 2021). For the chambers O2 and O3, the dominant phyla were *Proteobacteria* and *Bacteroidetes*, their coexistence may be helpful in removing ammonium (Chen et al., 2016). Similar to previous ESAD studies, the phylum *Proteobacteria* was found to be the most abundant bacteria in A4 chamber. This could be due to the fact that *Proteobacteria* can play an important role in degrading the organic matter and nitrate (Zhao et al., 2022).

From the genus assignment results, the *Bacteroides* exhibited a higher proportion than other genera in A1 chamber on day 30 (Figure 5A), this was probably due to its enrichment could promote the degradation of glucose (Wang et al., 2021a). Notably, the *Bacteroides* was not observed on day 190, with greater abundances of *Macellibacteroides*, *Trichococcus*, and *paraclostridium* were observed in A1 chamber, their existences have been confirmed could help to degrade the organic matters (Yan et al., 2020; She et al., 2021; He et al., 2022). The changes in the microbial community within the A1 chamber may be attributed to changes in the influent conditions and environmental factors.

For the chambers O2 and O3, the enrichment of genus *Rhodanobacter* was observed throughout the study (Figure 5B), it is worth noting that the *Rhodanobacter* could be a prominent role in the reactor, because it can degrade the ammonium and convert

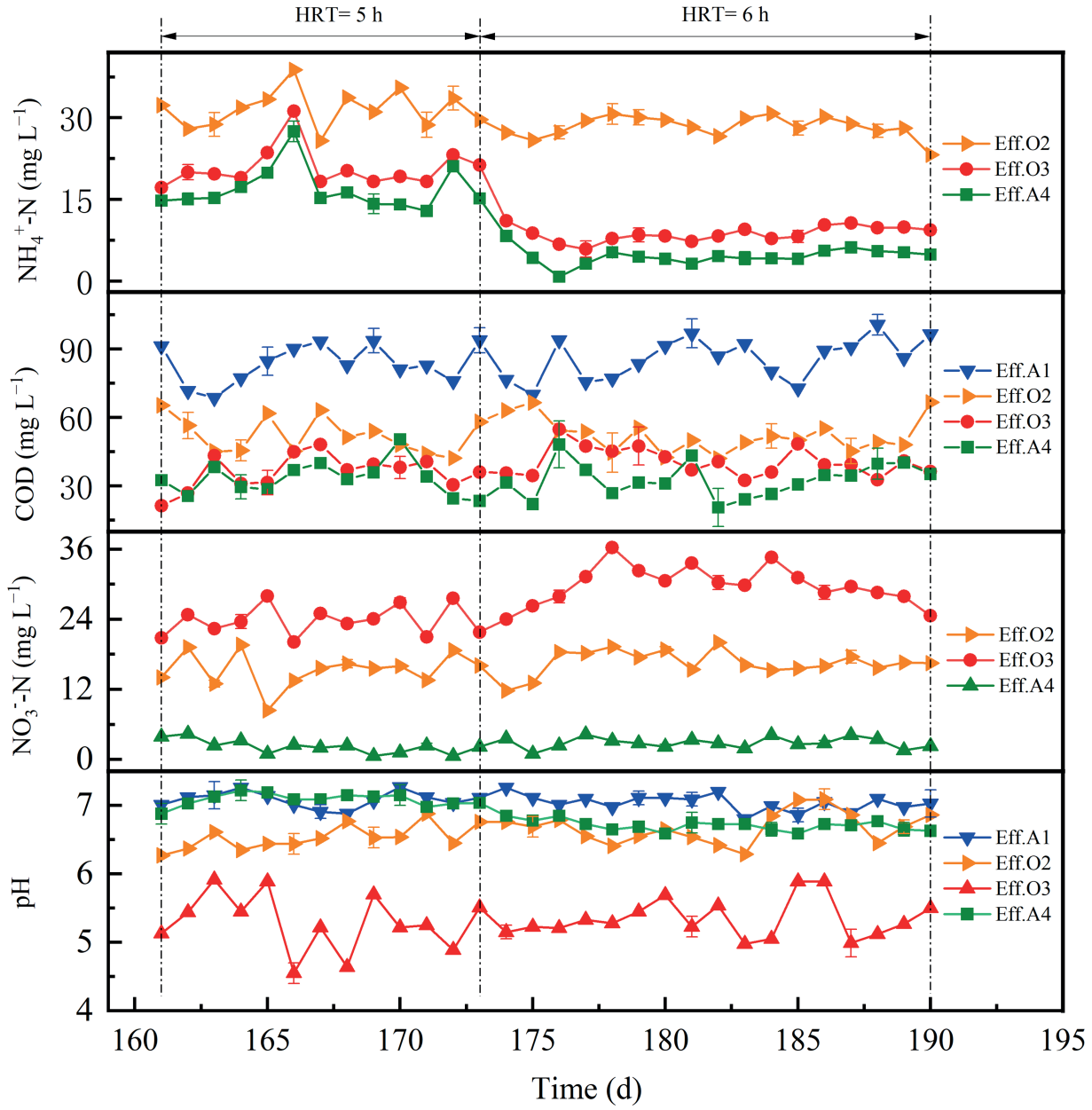

FIGURE 4
Performance of the reactor during period IV.

nitrate into nitrogen gas (Wang et al., 2020). Meanwhile, the genera *Chujaibacter* and *Nitrospira* were also dominant in chambers O2 and O3, the *Nitrospira* is known as a nitrification-related bacterium during nitrification process (Li et al., 2022a), and *Chujaibacter* is reported to be positively correlated with *Nitrospira* (Sato et al., 2021). The presence of genera *Bradyrhizobium*, *Mesorhizobium*, *Dokdonella*, *Ferruginibacter*, *Holophaga*, and *Hyphomicrobium* could be related to the denitrification processes or organic degradation (Chen et al., 2021; Liang et al., 2021b; Wang et al., 2021b; Qian et al., 2022; Li et al., 2022b), this is helpful in removing COD and nitrate in the chambers O2 and O3, and the *unclassified_f__Comamonadaceae* was able to reduce nitrate by using organic carbons (Zhang et al., 2022). In general, the main functions of bacteria in the O2 and O3 chambers may be to get involved in the nitrification process, denitrification process and removal of organic matter, which further verified the removal trend of pollutants in the reactor.

In A4 chamber, the dominant genera were *Thiobacillus*, *Sulfurimonas*, and *Ferritrophicum* on day 30. However, on day 190, the *Thiobacillus* and *Sulfurimonas* were not observed, while the abundance of *Ferritrophicum* increased to 69.6% (Figure 5A). *Thiobacillus* and *Sulfurimonas* were identified as the major denitrifying genera in the ESAD process (Vandekerckhove et al., 2018). Significant changes in their abundances may have been caused

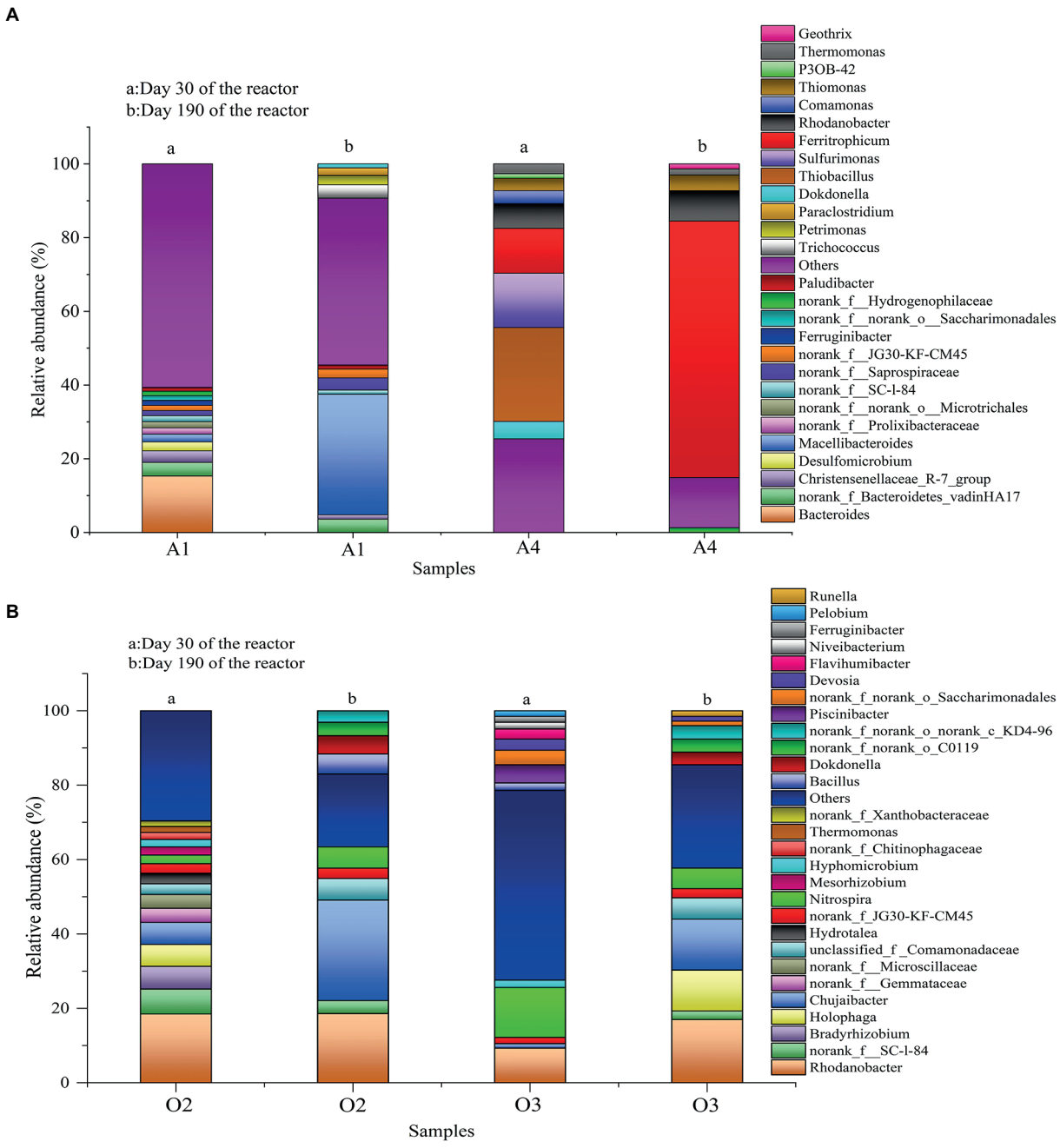

FIGURE 5
Changes in microbial community in the reactor **(A)** genus level of chambers A1 and A4; **(B)** genus level of chambers O2 and O3.

by the washing of ESAD filters. Furthermore, *Ferritrophicum* was verified as a denitrification bacterium (Wan et al., 2019), its enrichment is helpful for the denitrification process, which also indicates that although washing ESAD filter will cause changes in the structure of bacterial community, the main bacteria are still the denitrifying bacteria. The existence of *Rhodanobacter* may be that the ESAD filter could block the bacteria in O3 effluent, which helps in realising the ND processes simultaneously, and further contributes to the decrease of sulfate productivity in the effluent.

Conclusion

The AOOA process was successfully explored to treat domestic sewage. In chambers O2 and O3, the control of DO has a great influence on the removal of pollutants in the reactor. An increase in ammonium concentration was observed in the reactor effluent when the temperature decreased to 13°C ± 2°C, and extending the HRT from 5 to 6 h could alleviate this problem. The AOOA process is a promising method for treating domestic

sewage, especially for the domestic sewage which is difficult to be centrally treated, the proposed AOOA process has a simple operation and requires lower investment costs.

Data availability statement

The raw 16S rRNA sequences have been deposited in the National Center for Biotechnology Information Sequence Read Archive database under accession number PRJNA849697.

Author contributions

YaW: conceptualization, data curation, investigation, funding acquisition, writing–original draft, and visualization. BL: conceptualization, data curation, formal analysis, and funding acquisition. FK: conceptualization and editing. YoW: funding acquisition. CZ and ZL: supervision. TZ: funding acquisition, writing–original draft, and editing. ZZ: funding acquisition, data curation, writing–original draft, and editing. All authors contributed to the article and approved the submitted version.

Funding

This work was supported by the National Key Research and Development Program of China (grant no. 2020YFC1806402), Major Key and Core Technology Research Project (direction of water pollution control industry chain), Science and Technology Plan of Shenyang in 2020 (grant no. 20-202-4-37), and the Ningxia Provincial Natural Science Foundation of China (grant no. 2020AAC03272).

Conflict of interest

The authors declare that the research was conducted in the absence of any commercial or financial relationships that could be construed as a potential conflict of interest.

Publisher's note

All claims expressed in this article are solely those of the authors and do not necessarily represent those of their affiliated organizations, or those of the publisher, the editors and the reviewers. Any product that may be evaluated in this article, or claim that may be made by its manufacturer, is not guaranteed or endorsed by the publisher.

Supplementary material

The Supplementary material for this article can be found online at: https://www.frontiersin.org/articles/10.3389/fmicb.2022.970548/full#supplementary-material

References

APHA (2005). American Water Works Association (AWWA), and Water Environment Federation (AEF) (2005). *Standard Methods for the Examination of Water and Wastewater*. Washington, DC, USA.

Chen, Z. Q., Li, D., Liu, H. G., and Wen, Q. X. (2021). Effects of polyurethane foam carrier addition on anoxic/aerobic membrane bioreactor (A/O-MBR) for coal gasification wastewater (CGW) treatment: performance and microbial community structure. *Sci. Total Environ.* 789:148037. doi: 10.1016/j.scitotenv.2021.148037

Chen, Z. G., Wang, X. J., Yang, Y. Y., and Yuan, Y. L. (2016). Partial nitrification and denitrification of mature landfill leachate using a pilot-scale continuous activated sludge process at low dissolved oxygen. *Bioresour. Technol.* 218, 580–588. doi: 10.1016/j.biortech.2016.07.008

Du, R., Cao, S. B., Zhang, H. Y., Li, X. C., and Peng, Y. Z. (2020). Flexible nitrite supply alternative for mainstream anammox: advances in enhancing process stability. *Environ. Sci. Technol.* 54, 6353–6364. doi: 10.1021/acs.est.9b06265

Feng, Y., Peng, Y. Z., Wang, B., Liu, B., and Li, X. Y. (2021). A continuous plug-flow anaerobic/aerobic/anoxic/aerobic (AOAO) process treating low COD/TIN domestic sewage: realization of partial nitrification and extremely advanced nitrogen removal. *Sci. Total Environ.* 771:145387. doi: 10.1016/j.scitotenv.2021.145387

Gao, X. J., Xu, Z. Z., Peng, Y. Z., Zhang, L., and Ding, J. (2022). The nitrification recovery capacity is the key to enhancing nitrogen removal in the AOA system at low temperatures. *Sci. Total Environ.* 818:151674. doi: 10.1016/j.scitotenv.2021.151674

Gutierrez-Wing, M. T., Malone, R. F., and Rusch, K. A. (2012). Evaluation of polyhydroxybutyrate as a carbon source for recirculating aquaculture water denitrification. *Aquacult. Eng.* 51, 36–43. doi: 10.1016/j.aquaeng.2012.07.002

He, Z. W., Zou, Z. S., Sun, Q., Jin, H. Y., Yao, X. Y., Yang, W. J., et al. (2022). Freezing-low temperature treatment facilitates short-chain fatty acids production from waste activated sludge with short-term fermentation. *Bioresour.Technol.* 347:126337. doi: 10.1016/j.biortech.2021.126337

Hoang, V., Delatolla, R., Abujamel, T., Mottawea, W., Gadbois, A., Laflamme, E., et al. (2014). Nitrifying moving bed biofilm reactor (MBBR) biofilm and biomass response to long term exposure to 1 degrees C. *Water Res.* 49, 215–224. doi: 10.1016/j.watres.2013.11.018

Hou, Y. R., Li, B., Feng, G. C., Zhang, C. F., He, J., Li, H. D., et al. (2021). Responses of bacterial communities and organic matter degradation in surface sediment to *Macrobrachium nipponense* bioturbation. *Sci. Total Environ.* 759:143534. doi: 10.1016/j.scitotenv.2020.143534

Jiang, C. C., Xu, S. J., Wang, R., Feng, S. G., Zhou, S. N., Wu, S. M., et al. (2019). Achieving efficient nitrogen removal from real sewage via nitrite pathway in a continuous nitrogen removal process by combining free nitrous acid sludge treatment and DO control. *Water Res.* 161, 590–600. doi: 10.1016/j.watres.2019.06.040

Kim, T., Hite, M., Rogacki, L., Sealock, A. W., Sprouse, G., Novak, P. J., et al. (2021). Dissolved oxygen concentrations affect the function but not the relative abundance of nitrifying bacterial populations in full-scale municipal wastewater treatment bioreactors during cold weather. *Sci. Total Environ.* 781:146719. doi: 10.1016/j.scitotenv.2021.146719

Kim, D. J., Lee, D. I., and Keller, J. (2006). Effect of temperature and free ammonia on nitrification and nitrite accumulation in landfill leachate and analysis of its nitrifying bacterial community by FISH. *Bioresour. Technol.* 97, 459–468. doi: 10.1016/j.biortech.2005.03.032

Lai, C. M., Guo, Y., Cai, Q., and Yang, P. (2020). Enhanced nitrogen removal by simultaneous nitrification denitrification and further denitrification (SND-DN) in a moving bed and constructed wetland (MBCW) integrated bioreactor. *Chemosphere* 261:127744. doi: 10.1016/j.chemosphere.2020.127744

Layer, M., Villodres, M. G., Hernandez, A., Reynaert, E., Morgenroth, E., and Derlon, N. (2020). Limited simultaneous nitrification-denitrification (SND) in aerobic granular sludge systems treating municipal wastewater: mechanisms and practical implications. *Water Res. X.* 7:100048. doi: 10.1016/j.wroa.2020.100048

Li, C. T., Cui, Q., Li, Y., Zhang, K., Lu, X. Q., and Zhang, Y. (2022b). Effect of LDPE and biodegradable PBAT primary microplastics on bacterial community after four months of soil incubation. *J. Hazard. Mater.* 429:128353. doi: 10.1016/j.jhazmat.2022.128353

Li, J. Y., Du, Q. P., Peng, H. Q., Zhang, Y. L., Bi, Y. Q., Shi, Y., et al. (2020). Optimization of biochemical oxygen demand to total nitrogen ratio for treating landfill leachate in a single-stage partial nitrification denitrification system. *J. Clean. Prod.* 266:121809. doi: 10.1016/j.jclepro.2020.121809

Li, M. L., Zhang, L. L., Qin, C. L., Lu, P. L., Bai, H. C., Han, X. K., et al. (2022a). Temporal changes of microbial community structure and nitrogen cycling processes during the aerobic degradation of phenanthrene. *Chemosphere* 286:131709. doi: 10.1016/j.chemosphere.2021.131709

Liang, B. R., Chang, M. D., Zhang, K., Liu, D. D., Qiu, X. L., Yao, S., et al. (2020). Investigation of different solid carbonate additives in elemental-sulfur-based autotrophic denitrification process coupled with anammox process. *Environ. Technol. Innov.* 20:101149. doi: 10.1016/j.eti.2020.101149

Liang, B. R., Kang, F., Wang, Y., Zhang, K., Wang, Y. Z., Yao, S., et al. (2022). Denitrification performance of sulfur-based autotrophic denitrification and biomass-sulfur-based mixotrophic denitrification in solid-phase denitrifying reactors using novel composite filters. *Sci. Total Environ.* 823:153826. doi: 10.1016/j.scitotenv.2022.153826

Liang, B. R., Kang, F., Yao, S., Zhang, K., Wang, Y. Z., Chang, M. D., et al. (2021b). Exploration and verification of the feasibility of the sulfur-based autotrophic denitrification integrated biomass-based heterotrophic denitrification systems for wastewater treatment: from feasibility to application. *Chemosphere* 287:131998. doi: 10.1016/j.chemosphere.2021.131998

Liang, B. R., Zhang, K., Liu, D. D., Yao, S., Chen, S. T., Ma, F., et al. (2021a). Exploration and verification of the feasibility of sulfur-based autotrophic denitrification process coupled with vibration method in a modified anaerobic baffled reactor for wastewater treatment. *Sci. Total Environ.* 786:147348. doi: 10.1016/j.scitotenv.2021.147348

Pan, D. D., Shao, S. C., Zhong, J. F., Wang, M. H., and Wu, X. W. (2022). Performance and mechanism of simultaneous nitrification-denitrification and denitrifying phosphorus removal in long-term moving bed biofilm reactor (MBBR). *Bioresour. Technol.* 348:126726. doi: 10.1016/j.biortech.2022.126726

Peng, L., Xie, Y. K., Beeck, W. V., Zhu, W. Q., Tendeloo, M. V., Tytgat, T., et al. (2020). Return-sludge treatment with endogenous free nitrous acid limits nitrate production and N_2O emission for mainstream partial Nitritation/Anammox. *Environ. Sci. Technol.* 54, 5822–5831. doi: 10.1021/acs.est.9b06404

Qian, Z. Z., Zhuang, S. Y., Gao, J. S., Tang, L. Z., Harindintwali, J. D., and Wang, F. (2022). Aeration increases soil bacterial diversity and nutrient transformation under mulching-induced hypoxic conditions. *Sci. Total Environ.* 817:153017. doi: 10.1016/j.scitotenv.2022.153017

Sahinkaya, E., Kilic, A., and Duygulu, B. (2014). Pilot and full-scale applications of sulfur based autotrophic denitrification process for nitrate removal from activated sludge process effluent. *Water Res.* 60, 210–217. doi: 10.1016/j.watres.2014.04.052

Sato, Y., Tanaka, E., Hori, T., Futamata, H., Murofushi, K., Takagi, H., et al. (2021). Efficient conversion of organic nitrogenous wastewater to nitrate solution driven by comammox *Nitrospira*. *Water Res.* 197:117088. doi: 10.1016/j.watres.2021.117088

She, Y. C., Wei, W. X., Ai, X. H., Hong, J. M., and Xin, X. D. (2021). Synergistic pretreatment of CaO and freezing/thawing to enhance volatile fatty acids recycling and dewaterability of waste activated sludge via anaerobic fermentation. *Chemosphere* 280:130939. doi: 10.1016/j.chemosphere.2021.130939

Vandekerckhove, T. G. L., Kobayashi, K., Janda, J., Nevel, S. V., and Vlaeminck, S. E. (2018). Sulfur-based denitrification treating regeneration water from ion exchange at high performance and low cost. *Bioresour. Technol.* 257, 266–273. doi: 10.1016/j.biortech.2018.02.047

Wan, D. J., Li, Q., Liu, Y. D., Xiao, S. H., and Wang, H. J. (2019). Simultaneous reduction of perchlorate and nitrate in a combined heterotrophic-sulfur-autotrophic system: secondary pollution control, pH balance and microbial community analysis. *Water Res.* 165:115004. doi: 10.1016/j.watres.2019.115004

Wang, L. X., Liu, T., Chen, S., and Quan, X. (2021a). Enhancing the treatment of petrochemical wastewater using redox mediator suspended biofilm carriers. *Biochem. Eng. J.* 173:108087. doi: 10.1016/j.bej.2021.108087

Wang, D. B., Tao, L. J., Yang, J. N., Xu, Z. Y., Yang, Q., Zhang, Y., et al. (2021b). Understanding the interaction between triclocarban and denitrifiers. *J. Hazard. Mater.* 401:123343. doi: 10.1016/j.jhazmat.2020.123343

Wang, W., Wei, D. Y., Li, F. C., Zhang, Y. W., and Li, R. H. (2019). Sulfur-siderite autotrophic denitrification system for simultaneous nitrate and phosphate removal: From feasibility to pilot experiments. *Water Res.* 160, 52–59. doi: 10.1016/j.watres.2019.05.054

Wang, L. M., Zhou, Y., Peng, F. Q., Zhang, A. G., Pang, Q. Q., Bian, J. J., et al. (2020). Intensified nitrogen removal in the tidal flow constructed wetlandmicrobial fuel cell: insight into evaluation of denitrifying genes. *J. Clean. Prod.* 264:121580. doi: 10.1016/j.jclepro.2020.121580

Xi, H. P., Zhou, X. T., Arslan, M., Luo, Z. J., Wei, J., Wu, Z. R., et al. (2022). Heterotrophic nitrification and aerobic denitrification process: promising but a long way to go in the wastewater treatment. *Sci. Total Environ.* 805:150212. doi: 10.1016/j.scitotenv.2021.150212

Yan, P. X., Zhao, Y. B., Zhang, H., Chen, S. S., Zhu, W. B., Yuan, X. F., et al. (2020). A comparison and evaluation of the effects of biochar on the anaerobic digestion of excess and anaerobic sludge. *Sci. Total Environ.* 736:139159. doi: 10.1016/j.scitotenv.2020.139159

Zhang, K., Lyu, L., Yao, S., Kang, T., Ma, Y., Pan, Y., et al. (2019). Effects of vibration on anammox-enriched biofilm in a high-loaded upflow reactor. *Sci. Total Environ.* 685, 1284–1293. doi: 10.1016/j.scitotenv.2019.06.082

Zhang, K., Yang, B., Ma, Y. G., Lyu, L. T., Pan, Y., Wang, Y. Z., et al. (2018). A novel anammox process combined with vibration technology. *Bioresour. Technol.* 256, 277–284. doi: 10.1016/j.biortech.2018.01.128

Zhang, L. L., Zhang, C., Hu, C. Z., Liu, H. J., Bai, Y. H., and Qu, J. H. (2015). Sulfur-based mixotrophic denitrification corresponding to different electron donors and microbial profiling in anoxic fluidized-bed membrane bioreactors. *Water Res.* 85, 422–431. doi: 10.1016/j.watres.2015.08.055

Zhang, X. X., Zhang, X. N., Wu, P., Ma, L. P., Chen, J. J., Wang, C. C., et al. (2022). Hydroxylamine metabolism in mainstream denitrifying ammonium oxidation (DEAMOX) process: achieving fast start-up and robust operation with bio-augmentation assistance under ambient temperature. *J. Hazard. Mater.* 421:126736. doi: 10.1016/j.jhazmat.2021.126736

Zhao, Y. R., Zhang, Q., Peng, Y., Peng, Y. Z., Li, X. Y., and Jiang, H. (2022). Advanced nitrogen elimination from domestic sewage through two stage partial nitrification and denitrification (PND) coupled with simultaneous anaerobic ammonia oxidation and denitrification (SAD). *Bioresour.Technol.* 343:125986. doi: 10.1016/j.biortech.2021.125986

frontiers | Frontiers in Microbiology

TYPE Original Research
PUBLISHED 22 August 2022
DOI 10.3389/fmicb.2022.969722

OPEN ACCESS

EDITED BY
Ren-Cun Jin,
Hangzhou Normal University, China

REVIEWED BY
Jiexu Ye,
Zhejiang University of Technology, China
Reshmi Upreti,
University of Washington, United States

*CORRESPONDENCE
Zhigang Zhao
zhaozhigang@hrfri.ac.cn

SPECIALTY SECTION
This article was submitted to Microbiotechnology, a section of the journal Frontiers in Microbiology

RECEIVED 15 June 2022
ACCEPTED 01 August 2022
PUBLISHED 22 August 2022

CITATION
Zhang R, Luo L, Wang S, Guo K, Xu W and Zhao Z (2022) Screening and characteristics of ammonia nitrogen removal bacteria under alkaline environments. *Front. Microbiol.* 13:969722. doi: 10.3389/fmicb.2022.969722

Screening and characteristics of ammonia nitrogen removal bacteria under alkaline environments

Rui Zhang[1,2], Liang Luo[1,2], Shihui Wang[1,2], Kun Guo[1,2], Wei Xu[1,2] and Zhigang Zhao[1,2]*

[1]Key Open Laboratory of Cold Water Fish Germplasm Resources and Breeding of Heilongjiang Province, Heilongjiang River Fisheries Research Institute, Chinese Academy of Fishery Sciences, Harbin, China, [2]Engineering Technology Research Center of Saline-Alkaline Water Fisheries (Harbin), Chinese Academy of Fishery Sciences (CAFS), Harbin, China

The toxicity of ammonia nitrogen (AN) has always caused severe harm to aquatic animals in intensive aquaculture conditions, especially in saline-alkali aquaculture waters. The application of AN removal bacteria is a safe and effective method for controlling the AN concentration in aquaculture water through direct conversion to bacterial protein. However, there is still a lack of AN removal bacteria that are appropriate for saline-alkali aquaculture conditions. In this study, three AN removal strains, namely, *Bacillus idriensis* CT-WN-B3, *Bacillus australimaris* CT-WL5-10, and *Pseudomonas oleovorans* CT-WL5-6, were screened out under alkaline conditions from the alkali-tolerant strains distributed in carbonate saline-alkali soil and water environments in Northeast China. Under different pH (8.0–9.0), salinities (10–30 g/L NaCl), alkalinities (10–30 mmol/L $NaHCO_3$), and AN concentrations (1–3 mg/L), corresponding to the actual conditions of saline-alkali aquaculture waters, the AN removal rates and relative characteristics of these strains were analyzed. The results showed that all of the three strains were efficient on AN removal under various conditions, and the highest removal rate reached up to 3×10^{-13} mg/cfu/h. Both CT-WL5-10 and CT-WL5-6 were most efficient under pH 9.0 with 3 mg/L initial AN, while pH 8.5 with 2 mg/L AN was the best fit for CT-WN-B3. In 96-h pure incubation of these strains in alkali media, approximately 90% AN was removed, and pH values were decreased by 2.0 units within 12 h accompanied by the growth of the strains. In addition, salinity and alkalinity slightly disturbed the removal rates of CT-WL5-10 and CT-WL5-6, but there were at least 65% AN removed by them within 24 h. These results indicated that all three strains have good application prospect in saline-alkali aquaculture waters.

KEYWORDS

ammonia nitrogen removal bacteria, alkali-tolerance, ammonia nitrogen removal rate, alkaline environment, water quality purification

Introduction

High stocking densities and high-protein feeds have always been used to maximize the output in intensive aquaculture systems, while the water pollution caused by such systems is becoming increasingly significant. The feces from aquatic animals and the residual high-protein feed in the aquaculture process eventually form large amounts of ammonia nitrogen (AN) through microbial metabolism in the water (Avnimelech, 1999; Cai et al., 2010; Wu et al., 2017), and the resulting toxicity directly impacts the survival and growth of aquatic animals (Alcaraz et al., 1999; Mummert et al., 2003; Armstrong et al., 2012). AN consists of ammonium (NH_4^+-N) and the toxic component—ammonia (NH_3) (Alcaraz et al., 1999; Körner et al., 2001; Zhang et al., 2018). Ammonia can enter aquatic animals through the gills or skin membranes due to its fat solubility, damage gill epidermal cells, increase the ammonia concentration in blood and tissues, reduce the oxygen-carrying capacity of blood, and destroy the excretory system and osmotic balance of the organism (Alcaraz et al., 1999; Timmons et al., 2002; Jiang et al., 2004). Then, symptoms such as dyspnea, food intake reduction, and resistibility decrease occur gradually, which ultimately cause great reductions in the survival rate of aquatic animals (Alcaraz et al., 1999; Timmons et al., 2002).

In saline-alkali waters, the AN toxicity is much stronger as high pH could shift the equilibrium state toward ammonia (NH_3) direction in $NH_3{\cdot}H_2O \rightleftharpoons NH_4^+ + OH^-$ and could enhance the proportion of ammonia in the same concentration of AN (Mayes et al., 1986; USEPA, 1999; Körner et al., 2001; Wu et al., 2017). This leads to a more severe impairment of aquatic animals and restricts the development of aquaculture in saline-alkali waters seriously. Therefore, the effective control of AN concentrations in saline-alkali aquatic waters has become a key problem that urgently needs to be solved. In recent years, a zero-exchange water quality management system based on heterotrophic AN removal bacteria has been employed to address AN pollution (Crab et al., 2007; Martínez-Córdova et al., 2014). In this system, high carbon-nitrogen ratios are guaranteed to stimulate the growth of heterotrophic bacteria and directly convert AN into bacterial proteins (Avnimelech et al., 1994; Avnimelech, 1999, 2005; Ebeling et al., 2006). This system has been successfully promoted for use in freshwater ponds with intensive aquaculture. The applied bacteria are appropriate for ordinary fresh water environment because of their neutral isolation conditions (Hou et al., 2006; Muthukrishnan et al., 2012; Xin et al., 2014; Diao et al., 2015; Yun et al., 2018; Chen et al., 2019; Lei et al., 2019). However, there is still a lack of AN removal bacteria that are suitable for saline-alkali aquaculture waters.

In this study, the AN removal strains were screened out from the alkali-tolerant microflora distributed in the carbonate saline-alkali soil and water environments in Northeast China. According to the real conditions of saline-alkali aquaculture waters, their AN removal rates and action characteristics were analyzed under different pH levels, salinities, alkalinities, and initial AN concentrations. This study provides a theoretical basis for AN regulation and water quality purification in saline-alkali aquaculture waters.

Materials and methods

Strains

The alkali-tolerant strains used in this study are shown in **Supplementary Table 1**. In our previous study, water and sediment samples were randomly collected from 9 saline-alkali aquaculture ponds in Daqing, Heilongjiang Province, in June 2020. Then, alkali-tolerant strains, which can tolerate pH 9.5–10.0 stress, were isolated from the samples and identified by 16S rRNA gene similarity comparisons and phylogenetic analysis (Zhang et al., 2022). Totally, 24 alkali-tolerant strains were isolated (**Supplementary Table 1**) and used for the screening of AN removal bacteria.

Medium

An activation medium (LB) containing 10.0 g of tryptone, 5.0 g of yeast, and 10.0 g of NaCl in 1,000 ml of filtered water was prepared, and the pH was adjusted to 7.0 with NaOH.

A primary screening medium containing 5.0 g of glucose, 0.183 g of $(NH_4)_2SO_4$ (corresponding to 50 mg/L of AN), 1.0 g of NaCl, 0.5 g of K_2HPO_4, 0.25 g of $MgSO_4{\cdot}7H_2O$, and 15.0 g of agar powder in 1,000 ml of filtered water was prepared, and the pH was adjusted to 7.0 with NaOH.

A rescreening medium containing 5.0 g of glucose, 0.037 g of $(NH_4)_2SO_4$ (corresponding to 10 mg/L of AN), 1.0 g of NaCl, 0.5 g of K_2HPO_4, and 0.25 g of $MgSO_4{\cdot}7H_2O$ in 1,000 ml of filtered water was prepared, and the pH was adjusted to 7.0 with NaOH.

An AN removal detection medium containing 1.0 g of NaCl; 0.5 g of K_2HPO_4; 0.25 g of $MgSO_4{\cdot}7H_2O$; 0.0037, 0.0074, or 0.0111 g of ammonium sulfate (corresponding to 1, 2, or 3 mg/L of AN), and a certain amount of glucose (guaranteed to achieve C/N 20:1) in 1,000 ml of filtered water was prepared, and the pH levels were adjusted to the required values (e.g., 6.0, 8.0, 8.5, and 9.0) with HCl or NaOH. To explore the effect of salinity and alkalinity on the removal rate, a certain amount of NaCl (10, 20, or 30 g/L) or $NaHCO_3$ (10, 20, or 30 mmol/L) was added to the media as required, and NaOH was used to guarantee pH 9.0.

Strain isolation

Primary screening: In total, 24 alkali-tolerant strains were purely cultured in activation media overnight at 30°C and 150 rpm, and centrifuged at 12,000 rpm and 4°C for 10 min. The supernatants were discarded, washed two times with aseptic water, and resuspended in the same volumes of aseptic water. Then, the suspensions were gradient diluted to 10^{-4}, 10^{-5}, and 10^{-6} with aseptic water. A volume of 100 μl of each of the diluted solutions of the 24 strains was spread on the primary screening media, respectively, and incubated at 30°C for 5 days. The strains that grew well were picked out.

Rescreening: The screened strains were reactivated, and the cell suspensions were prepared according to the same method as used in the "primary screening" step. Then, the bacterial suspension was inoculated into the rescreening medium at a 1% inoculation amount and incubated at 30°C and 150 rpm for 24 h. The cultures were centrifuged at 12,000 rpm and 4°C for 10 min, and the supernatants were taken to determine the AN concentrations. The AN removal strains were picked out on the basis of AN removal rates (R).

Determination of ammonia nitrogen concentration, growth curve, and pH curve

The cultures incubated in different media were centrifuged at 12,000 rpm and 4°C for 10 min. The AN concentrations of the supernatants were determined using Nessler reagent colorimetry according to the description by APHA (1992). During the cultivation process, the pH and OD_{600nm} values of cultures were directly measured at 0, 4, 8, 12, 24, 48, 72, and 96 h by pH meter (Shanghai Apera Instrument Co., Ltd., PH400) and spectrophotometer from Shanghai Yoke Instrument Co., Ltd. (752N), respectively. The experiment included three replicates.

Biomass detection

The biomass of the culture was detected using the plate colony counting method; 10 ml culture was centrifuged at 12,000 rpm and 4°C for 10 min; the sediments were resuspended in the same volume of aseptic water; and the gradient was diluted to 10^{-2}, 10^{-3}, 10^{-4}, and 10^{-5}. A volume of 100 μL of each of the diluted solutions was spread on the activation media and incubated at 30°C for 24 h. Then, the colony counter was used to calculate the viable count of the cultures.

Calculation of ammonia nitrogen removal rate

AN removal rates (R) were calculated using the following formulas:

$$\begin{aligned} R\ (mg/cfu/h) &= [A-B]\ (mg/L)\ /biomass\ (cfu/L)/24\ (h) \\ &\quad (or) \\ R\ (mg/cfu) &= [A-B]\ (mg/L)\ /biomass\ (cfu/L), \end{aligned}$$

where A is the initial AN concentration and B is the residual AN concentration.

Statistical analysis

The experimental data are expressed as the mean ± standard error (mean ± S.E.). All statistical analyses were performed using SPSS 19.0 for Windows. Data obtained from the experiment were analyzed by one-way ANOVA after the homogeneity of variance test. When significant differences were found, Duncan's multiple range tests were used to identify differences among the experimental groups. Differences were considered significant at $P < 0.05$.

Phylogenetic tree

To analyze the phylogenetic relationships of the AN removal strains reported previously (Hou et al., 2006; Zhang et al., 2011; Chen et al., 2012, 2019; Xin et al., 2014; Diao et al., 2015; Huang et al., 2015a, 2018; Su et al., 2016; Xu et al., 2016; Yun et al., 2018; Hu et al., 2020) and screened out in this study, their 16S rRNA gene sequences were downloaded from NCBI and compared using MEGA 6.0. Then, the neighbor-joining method was used to select Bootstrap and construct a phylogenetic tree for 1,000 repeats. The 16S rRNA has been uploaded to Genbank,[1] and the accession numbers are listed in **Supplementary Table 1**.

Results

Strain isolation

A total of 6 strains that grew well in the primary screening medium were picked out, namely, CT-SL8-3, CT-WN-B3, CT-WN-B4, CT-WN-B8, CT-WL5-10, and CT-WL5-6. These strains were inoculated into the rescreening media, and the AN concentrations were determined after a 24-h incubation

1 https://www.ncbi.nlm.nih.gov/nuccore/

period. All 6 strains removed 35–85% AN (Table 1) after 24 h, and the removal percentages of *Bacillus idriensis* CT-WN-B3, *Bacillus australimaris* CT-WL5-10, and *Pseudomonas oleovorans* CT-WL5-6 were significantly higher than those of the other strains ($P < 0.05$). Among them, *P. oleovorans* CT-WL5-6 removed more than 80% of AN within 24 h (Table 1). The nitrite concentrations were also determined, which is worth mentioning, but no signal was detected.

TABLE 1 AN removal percentage of the strains with 10 mg/L initial AN.

Strains	AN removal percentage (%)
Bacillus firmus CT-SL8-3	36.48 ± 1.50^{a}
Bacillus idriensis CT-WN-B3	64.56 ± 0.56^{c}
Bacillus zhangzhouensis CT-WN-B4	43.52 ± 1.46^{b}
Bacillus horikoshii CT-WN-B8	41.95 ± 1.83^{ab}
Bacillus australimaris CT-WL5-10	74.10 ± 1.12^{d}
Pseudomonas oleovorans CT-WL5-6	83.68 ± 2.59^{e}

Each value represents the average value ± S.E. (n = 3), and values with different superscripts are significantly different ($P < 0.05$).

Analysis of ammonia nitrogen removal rate under different pH

To assess the AN removal ability, the average removal rates within 24 h were detected in different conditions. *B. idriensis* CT-WN-B3 exhibited a relatively stable removal rate in alkali pH media, which showed the highest rate at pH 8.5 with 2 mg/L initial AN and exhibited the lowest rate in groups with 1 mg/L initial AN ($P < 0.05$) (Figure 1A). However, CT-WN-B3 neither can grow nor remove AN in acidic conditions (Supplementary Figure 1), indicating that is AN removal function is alkali-pH dependent. After a 24-h incubation, the increasing initial AN concentration of the alkali medium caused a gradual increase in the AN removal rate of *B. australimaris* CT-WL5-10, which can remove AN most efficiently in pH 9.0 media with 3 mg/L initial AN concentration ($P < 0.05$) (Figure 1B). Increased initial AN concentration led to a gradual increase in the removal rate by CT-WL5-6, which was always up to 2.5×10^{-13} mg/cfu/h in 3 mg/L initial AN groups (Figure 1C). These results indicated that both initial AN concentration and pH affected their AN removal capability. In addition, CT-WL5-10 and CT-WL5-6 showed distinct removal rates in acidic media (Supplementary Figure 1), and this suggested that these two strains can function effectively in a wide pH range rather than alkali-pH only.

Ammonia nitrogen removal characteristics of *Bacillus idriensis* CT-WN-B3

To analyze the dynamic situation of AN removal process, this study monitored the growth of the strains within 96 h, as well as the accompanying changes of AN concentrations and pH values in pH 9.0 media. As shown in Figure 2A, AN concentration increased within 0–4 h and then decreased in all of the 3 groups. In 3 mg/L group, AN dramatically decreased within 4–24 h and then decreased slowly until the lowest level ($P < 0.05$) (Figure 2A). The best growth was exhibited in 3 mg/L group ($P < 0.05$), which reached the stable stage in approximately OD_{600nm} 0.1 within 24 h. While in 1 or 2 mg/L group, the biomass did not reach the maximum until 72 h (Figure 2B). Accompanied by the growth, the culture pH decreased rapidly within 4 h and tended to be stable after 12 h. Although the 3 mg/L group exhibited the most rapid pH decrease (Figure 2C), no significant differences were observed after 24 h ($P > 0.05$). As shown in Figure 2D, the removal rate (mg/cfu) was gradually increased in the 3 mg/L group, and the highest rate was observed in the 2 mg/L group within 24 h. These results suggested that CT-WN-B3 has a sustained and stable effect in the 3 mg/L group and provides the most efficient AN removal during the first 24 h in the 2 mg/L group (pH 9.0).

Ammonia nitrogen removal characteristics of *Bacillus australimaris* CT-WL5-10

In the media with 3 mg/L initial AN, the AN concentration decreased rapidly within 4–24 h and then tended to be stable. Comparatively, a gradual removal was caused by CT-WL5-10 within 4–48 h in the other two groups. While no significant difference was observed after 48 h between these groups ($P > 0.05$), an approximate 0.3 mg/L of final AN was guaranteed (Figure 3A). CT-WL5-10 gradually grew during the whole period and showed the most vigorous growth in the 3 mg/L group ($P < 0.05$) (Figure 3B). Additionally, the 3 mg/L group exhibited the fastest pH decrease and reached a significantly lower level than that of the 1 mg/L group by the end of the experiment ($P < 0.05$) (Figure 3C). The highest removal rate (mg/cfu) was detected at 24 h in the 3 mg/L group and in the 2 mg/L group, and the removal rate was relatively stable after 24 h (Figure 3D). These results indicated that the strain can remove AN most efficiently during 12–24 h in the 3 mg/L group and during the first 12 h in the 2 mg/L group and reminded an initial AN concentration-dependent removal rate of CT-WL5-10.

Ammonia nitrogen removal characteristics of *Pseudomonas oleovorans* CT-WL5-6

The AN was decreased rapidly by CT-WL5-6 within 24 h and then tended to be stable in pH 9.0 media with 2 mg/L

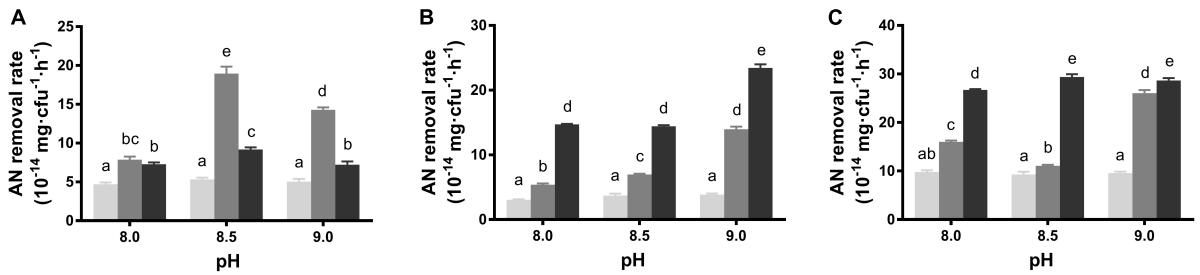

FIGURE 1
AN removal rate under alkali pH and low initial AN concentrations. The removal rates in different conditions of *B. idriensis* CT-WN-B3 **(A)**, *B. australimaris* CT-WL5-10 **(B)**, and *P. oleovorans* CT-WL5-6 **(C)** were shown, and values with different superscripts were significantly different ($P < 0.05$). In **(A–C)**, columns in light gray, dark gray, and black color, respectively, represent 1, 2, and 3 mg/L initial AN concentration group.

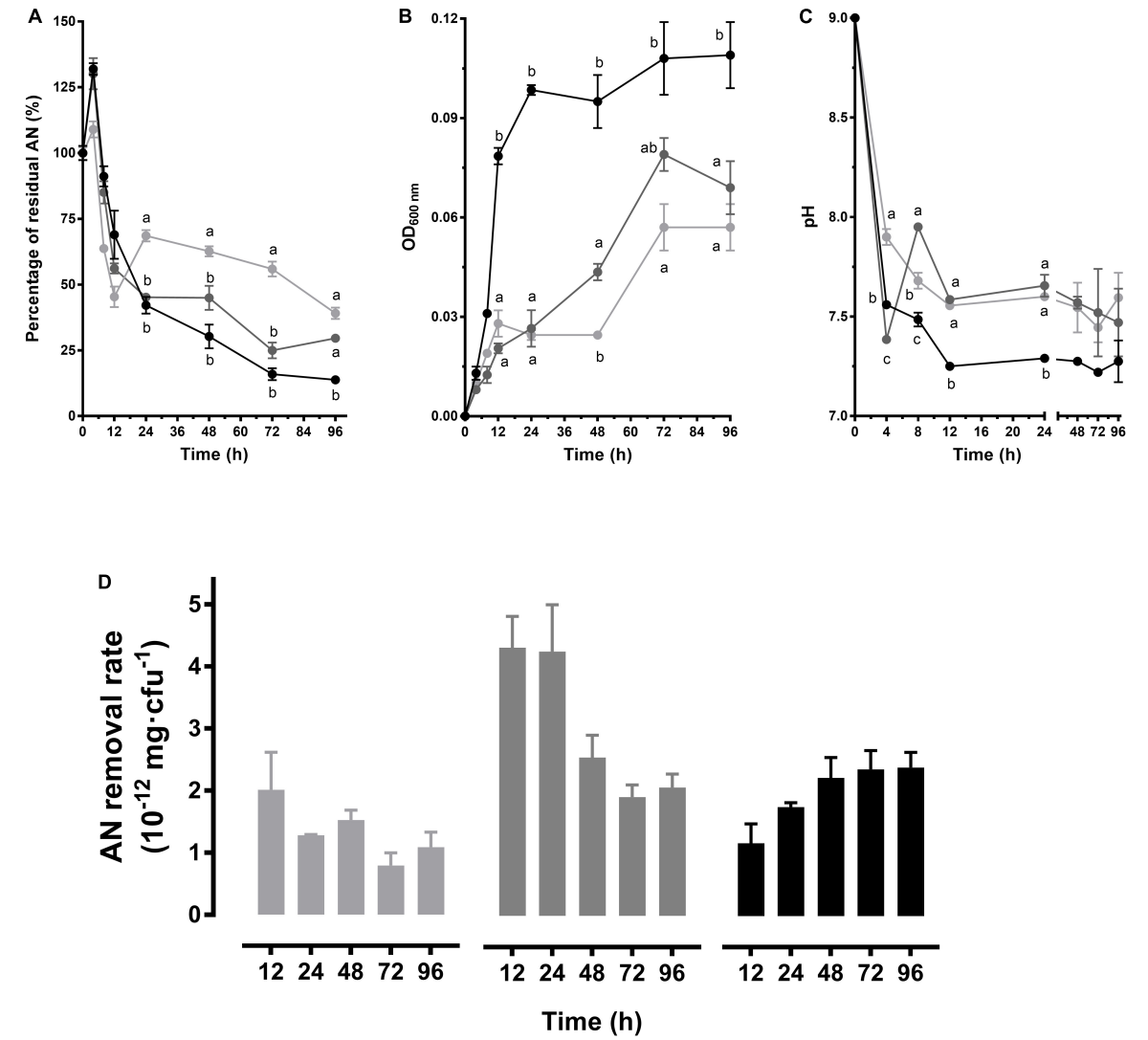

FIGURE 2
AN removal characteristics of *B. idriensis* CT-WN-B3. The residual AN percentage **(A)**, $OD_{600\,nm}$ **(B)**, and pH **(C)** determined within 96 h were shown. Values of each time point with different superscripts in **(A–C)** were significantly different ($P < 0.05$). **(D)** The removal rate (AN quantity per cell) in 0–12 h, 0–24 h,. . ., 0–96 h of incubation. In **(A–D)**, lines or column in light gray, dark gray, and black color, respectively, represents 1, 2, and 3 mg/L initial AN concentration group.

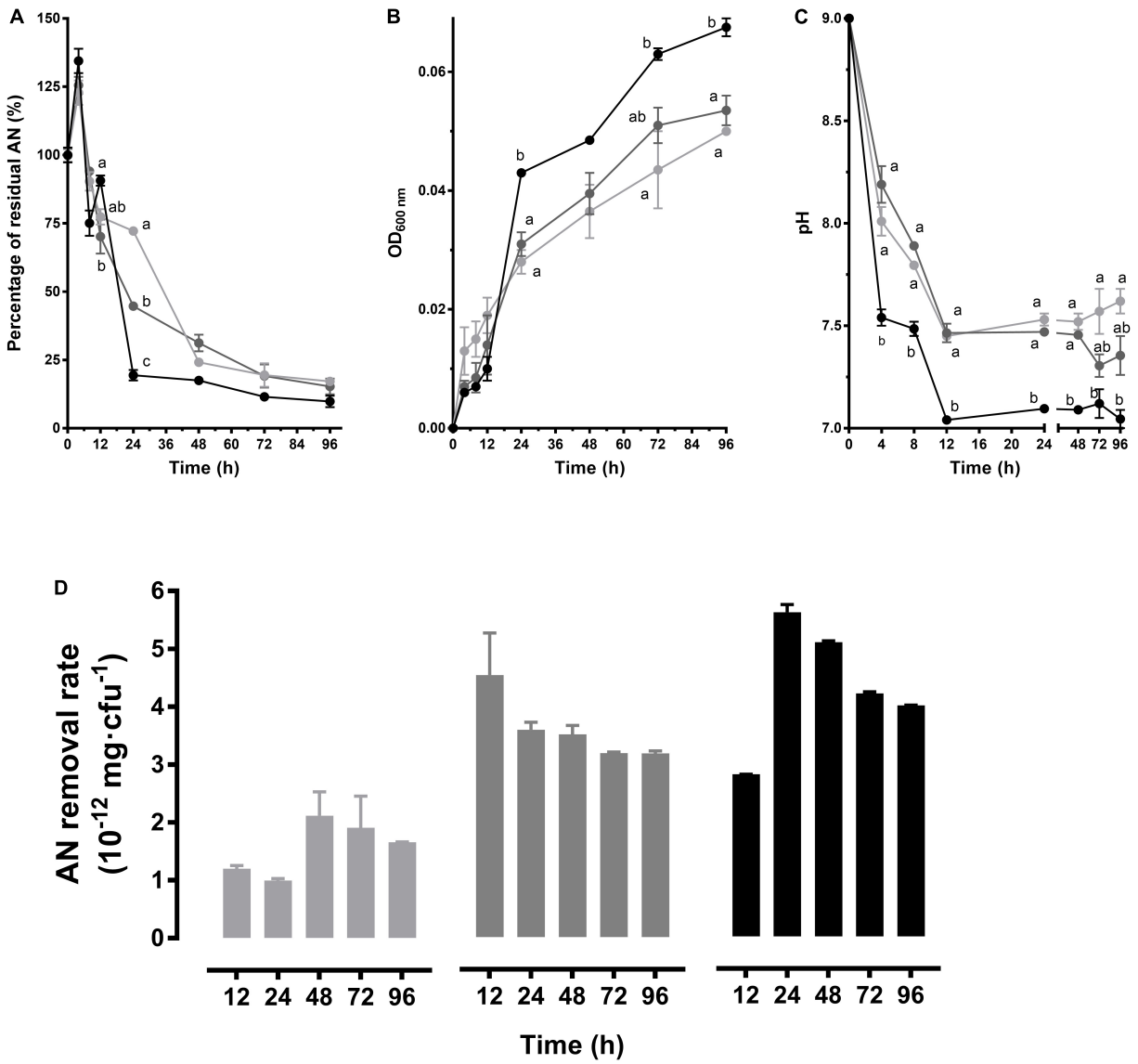

FIGURE 3
AN removal characteristics of *B. australimaris* CT-WL5-10. The residual AN percentage **(A)**, $OD_{600\,nm}$ **(B)**, and pH **(C)** determined within 96 h were shown. Values of each time point with different superscripts in **(A–C)** were significantly different ($P < 0.05$). **(D)** The removal rate (AN quantity per cell) in 0–12 h, 0–24 h,. . ., 0–96 h of incubation. In **(A–D)**, lines or column in light gray, dark gray, and black color, respectively, represents 1, 2, and 3 mg/L initial AN concentration group.

or 3 mg/L AN, and in the 1 mg/L group, the AN was tardily decreased until 72 h (Figure 4A). As to the growth in the 3 mg/L group, the biomass increased most rapidly within 48 h until the same level as the other 2 groups (Figure 4B). The most rapid pH decrease was also exhibited in the 3 mg/L group, but no significant difference was observed after 48 h ($P > 0.05$) (Figure 4C). Among different conditions, CT-WL5-6 removed AN most efficiently in the 3 mg/L group during 0–24 h. In the 2 mg/L group, the highest removal rate (mg/cfu) was detected at 24 h (Figure 4D). This indicated that CT-WL5-6 removed AN more efficiently under high initial AN concentrations, and an approximate 0.3 mg/L final concentration of AN could be reached regardless of the initial concentrations (Figure 4D).

Salinity and alkalinity effect on ammonia nitrogen removal rate

Salinity and alkalinity in saline-alkali aquaculture water are two main factors that could not be ignored. To explore their effect on AN removal, the removal rates of the three

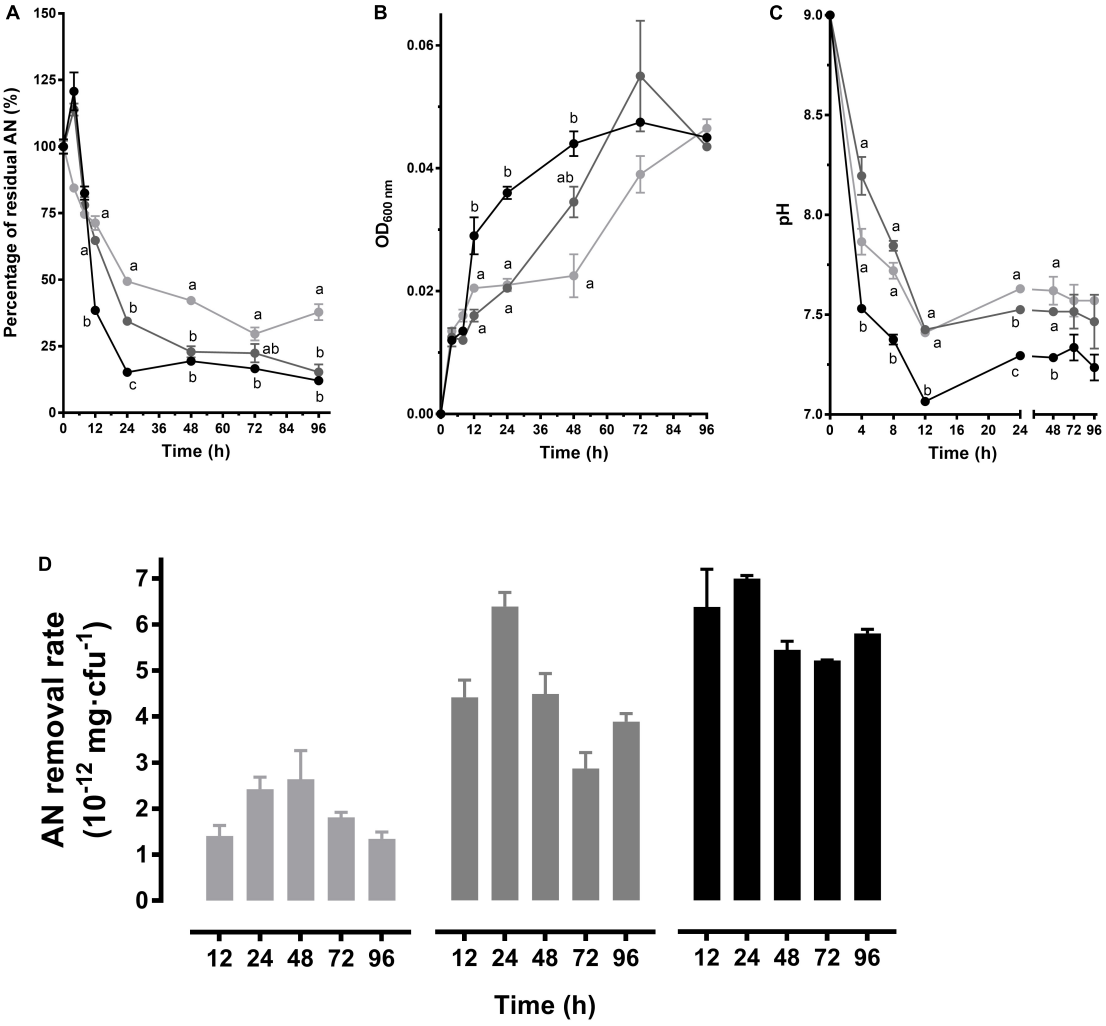

FIGURE 4
AN removal characteristics of *P. oleovorans* CT-WL5-6. The residual AN percentage **(A)**, $OD_{600\,nm}$ **(B)**, and pH **(C)** determined within 96 h were shown. Values of each time point with different superscripts in **(A–C)** were significantly different ($P < 0.05$). **(D)** The removal rate (AN quantity per cell) in 0–12 h, 0–24 h,. . ., 0–96 h of incubation. In **(A–D)**, lines or column in light gray, dark gray, and black color, respectively, represents 1, 2, and 3 mg/L initial AN concentration group.

screened strains were analyzed under different salinities (10–30 g/L NaCl) or alkalinities (10–30 mmol/L $NaHCO_3$) in alkali media (pH 9.0). When NaCl was supplemented into media, invariant percentages of AN were removed after a 24-h incubation of CT-WN-B3 or CT-WL5-6 ($P > 0.05$) (Figure 5A). That should be caused by their undiminished removal rates ($P > 0.05$) (Figure 5B) compared with the control group (0 g/L NaCl). However, less amount of AN was removed by CT-WL5-10 under different salinities (Figure 5A), and the removal rate was also lower than that of the control group. As similar as the results of salinity treatment, there was no significant change in the AN removal level of CT-WN-B3 after $NaHCO_3$ was supplemented (Figure 6A), even in its removal efficiency (Figure 6B). However, CT-WL5-10 and CT-WL5-6 removed less amount of AN (Figure 6A), and their AN removal percentage showed the same changing trend as their AN removal rate (Figure 6B). These results suggested that salinity and alkalinity cannot affect the AN removal application of CT-WN-B3, but both of them can disturb the AN removal reaction of CT-WL5-10. As to CT-WL5-6, the AN removal efficiency can be significantly reduced by alkalinity rather than salinity.

Discussion

In this study, an oligotrophic medium with $(NH_4)_2SO_4$ as the only nitrogen source was used to isolate AN removal strains from the alkali-tolerant bacteria that are distributed in carbonate saline-alkali soils and water environments in Northeast China (Zhang et al., 2022). First, the strains that

were able to grow by using AN were screened out in a neutral medium (pH 7.0). Then, their AN removal rates in alkaline (pH 8.0) media were determined, and three strains with high AN removal rates were picked out, namely, *B. idriensis* CT-WN-B3, *B. australimaris* CT-WN5-10, and *P. oleovorans* CT-WL5-6. According to the actual conditions of saline-alkali aquaculture waters, the AN removal characteristics were analyzed under various conditions, including different pH levels (8.0–9.0), salinities (10–30 g/L NaCl), alkalinities (10–30 mmol/L NaHCO3), and AN concentrations (1–3 mg/L).

The reported strains with AN removal function mainly consisted of *Bacillus* (Hou et al., 2006; Zhang et al., 2011; Xu et al., 2016; Huang et al., 2018; Yun et al., 2018). Other strains with the same function have also been reported, such as *Acinetobacter* (Xin et al., 2014; Huang et al., 2015a), *Pseudomonas* (Diao et al., 2015), *Sphingomonas* (Yun et al., 2018), *Vibrio* (Su et al., 2016), *Rhodococcus* (Chen et al., 2012), and *Nitratireductor* (Hu et al., 2020). The phylogenetic tree based on the 16S rRNA sequences of reported AN removal bacteria and the three strains screened out in this study (**Figure 5**) clearly revealed that all of the *Bacillus* strains, including CT-WN-B3 and CT-WL5-10, which were most closely related to *Bacillus licheniformis* and *Bacillus megaterium*, were clustered into one large clade (the threshold was 100%). CT-WL5-6 was clustered in a stable manner with the reported *Pseudomonas* AN removal bacteria (the threshold was 99%)

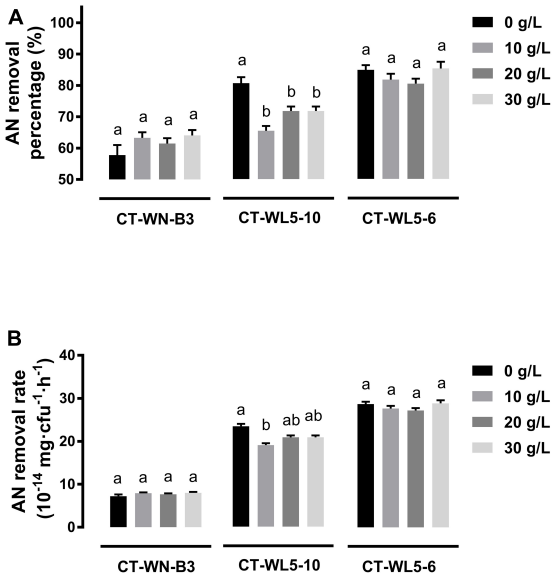

FIGURE 5
Salinity effect on AN removal. The AN removal percentage **(A)** and AN removal rate (AN quantity per cell per hour) **(B)** of strains after 24 h incubation in media with different salinities were shown. Values in each strain group with different superscripts in **(A,B)** were significantly different ($P < 0.05$). Columns in different colors represent different NaCl concentrations.

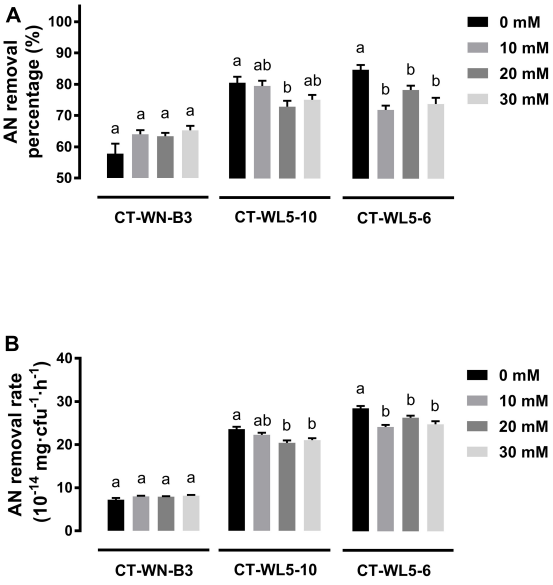

FIGURE 6
Alkalinity effect on AN removal. The AN removal percentage **(A)** and AN removal rate (AN quantity per cell per hour) **(B)** of strains after 24 h incubation in media with different alkalinities were shown. Values in each strain group with different superscripts in **(A,B)** were significantly different ($P < 0.05$). Columns in different colors represent different $NaHCO_3$ concentrations.

(**Figure 7**). These results suggested similar AN removal function and action characteristics, from an evolutionary perspective, within the strains belonging to *Bacillus* or *Pseudomonas*. In this study, the AN removal capability of *B. idriensis* and *B. australimaris* were reported for the first time and that of *P. oleovorans* under alkaline conditions was also supplemented.

These three strains were able to grow under alkaline conditions, which was followed by rapid AN removal and pH decrease. Compared with conventional microbial media, the growth of microorganisms might be inhibited in oligotrophic media, especially under alkaline stress. The biomass levels of the three strains range between $OD_{600\,nm}$ 0.04 and 0.10. These results are consistent with the levels reported for other strains, for example, *Delftia lacustria* SF9 and *Acinetobacter* sp. Sxf14 (Huang et al., 2015a,b) grew slowly under oligotrophic conditions, and the maximum $OD_{600\,nm}$ was less than 0.060.

During the AN removal processes of the strains isolated in this study, the AN level of the cultures increased at first and then rapidly decreased (**Figures 2B**, **3B**, **4B**). This was probably because the bacteria cells ingested abundant organic nitrogen from activation medium, and after being transferred into AN removal medium, the unfinished metabolism of organic nitrogen was continued. Then amounts of AN were produced during the metabolism (Ebeling et al., 2006; Avnimelech, 2015). This is probably corresponding to the results that AN removal bacteria can covert peptones into large amounts of AN

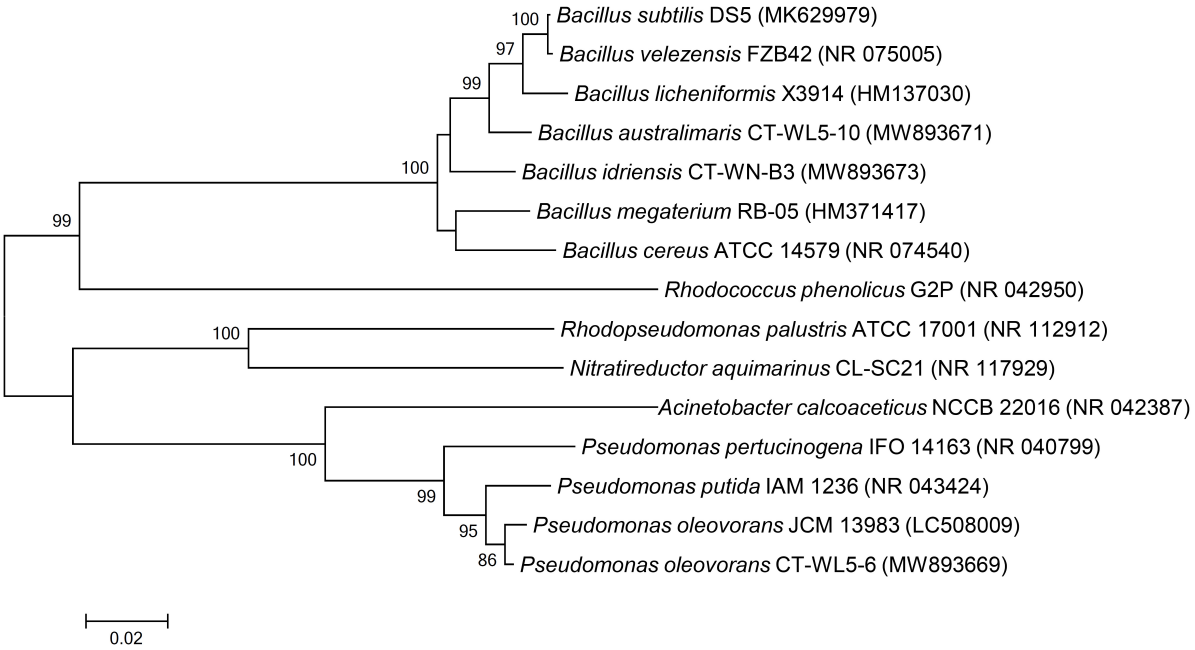

FIGURE 7
Phylogenetic analysis of AN removal strains. The 16S rRNA gene sequences of the isolated strains were compared with the reported AN removal bacteria by MEGA 6.0 software, and the phylogenetic tree was constructed by the neighbor-joining method. Black circle marked the bacteria isolated in this study.

(Huang et al., 2018). In addition, the above process is considered to be related to the physiological status of the bacterial cells, and hence, the increase is more obvious in richer N source groups (3 mg/L > 2 mg/L > 1 mg/L) (**Figures 2B**, **3B**, **4B**). As the growth began to enter an exponential phase, the accumulated organic nitrogen was used up, and AN began to be consumed, which manifested as a high level of AN removal. A close relationship between strain growth and AN removal has always been exhibited; for example, the AN removal rate was synchronized with the growth of *Bacillus licheniformis* X3914 (Zhang et al., 2011). Chen et al. (2012) considered that AN removal mainly occurred in the exponential growth period. Similarly, Wang et al. (2016) found that within the first 12 h of their experiment, the growth status of *Acinetobacter baumannii* WJ6 was nearly the same as the degree of AN removal. In this study, it was also found that the strains entered a platform growth period after rapid growth, which was accompanied by a significant AN removal within 24 h (**Figures 2–4**). It was also noticed that the propagation of strains is not absolutely related to AN removal, for example, the growth level of CT-WN-B3 in the 2 mg/L initial AN media was much lower than that in the 3 mg/L group, but the same AN quantity was removed in these two groups within 48 h (**Figures 2A,B**). The highest rate was detected within 0–24 h in the 2 mg/L group (**Figure 2D**). CT-WL5-10 showed an indistinctive growth difference between the 2 mg/L and 1 mg/L group in 96 h, but a larger quantity of AN removal (0–24 h) and a higher removal rate were detected in the former (**Figures 3A,B,D**), and so is CT-WL5-6 (**Figures 4A,B,D**). These results suggested that the AN removal is not only because of the utilization of nitrogen source during growth but also because of a functional specialty of these strains, which is considered affected by both initial AN concentration and pH (**Figure 1** and **Supplementary Figure 1**).

As far as CT-WN-B3 is concerned, the highest AN removal rate was observed in pH 8.5 media with 2 mg/L initial AN (**Figure 1A**). Compared with the other strains, CT-WN-B3 exhibited an undisputedly stronger growth ability (**Figures 2B**, **3B**, **4B**), which could rapidly propagate to $OD_{600\,nm}$ > 0.10 and decrease the pH at the same time (**Figures 1C,D**). These results suggested that CT-WN-B3 has the advantage of forming a dominant ecological niche and reducing AN toxicity in saline-alkali aquaculture waters. Furthermore, CT-WN-B3 is more targeted to AN removal at high pH levels (**Figure 1** and **Supplementary Figure 1**), and neither salinity nor alkalinity affects its AN removal effect (**Figures 6**, **7**). All these results mean an excellent application prospect of CT-WN-B3 in saline-alkali aquaculture waters. The high removal efficiency of *P. oleovorans* has been reported (Diao et al., 2015), and this study further confirmed the AN removal properties of *P. oleovorans* under alkaline conditions. The AN removal rates of CT-WN5-10 and CT-WL5-6 changed more significantly with initial AN concentration (**Figures 1A,B**, **3D**, **4D**), which might be caused by their stronger alkali tolerance. As the strain propagated continuously within 96 h, pH decreased rapidly and only about

0.3 mg/L AN remained (Figures 3A,B, 4A,B). The AN removal efficiency of CT-WN5-10 and CT-WL5-6 was considerable, although they were indeed disturbed by salinity and alkalinity (Figures 6, 7). In addition, the AN removal rates of CT-WN5-10 and CT-WL5-6 in acid media were obviously higher than that in the alkali media (Figure 1 and Supplementary Figure 1). These results remind us that CT-WN5-10 and CT-WN5-6 have a wider range of application prospect for water quality control in aquaculture waters.

Totally, three AN removal strains were screened out under alkaline conditions, namely, *B. idriensis* CT-WN-B3, *B. australimaris* CT-WN5-10, and *P. oleovorans* CT-WL5-6. Because of its propagation capability as well as distinguished and stable AN removal rate under different conditions, CT-WN-B3 is considered to have application prospects in saline-alkali aquaculture waters to reduce AN toxicity. The AN removal efficiencies of CT-WN5-10 and CT-WL5-6 were indeed disturbed by salinity and alkalinity, but their high removal rates can still support for controlling the AN concentration. These strains are meaningful for AN regulation and water quality purification in saline-alkali aquaculture waters.

Data availability statement

The datasets presented in this study can be found in online repositories. The names of the repository/repositories and accession number(s) can be found in the article/Supplementary material.

Author contributions

RZ: writing-original draft, investigation, data analysis, writing-review, and project. LL: resources, investigation, and software. SW: visualization and project. KG: methodology and data analysis. WX: writing-review. ZZ: writing-review, editing, and project. All authors contributed to the article and approved the submitted version.

Funding

This study was supported by the Central Public-Interest Scientific Institution Basal Research Fund, HRFRI (No. HSY202107M) and the Central Public-Interest Scientific Institution Basal Research Fund, CAFS (Nos. 2021XT05 and 2020TD56).

Conflict of interest

The authors declare that the research was conducted in the absence of any commercial or financial relationships that could be construed as a potential conflict of interest.

Publisher's note

All claims expressed in this article are solely those of the authors and do not necessarily represent those of their affiliated organizations, or those of the publisher, the editors and the reviewers. Any product that may be evaluated in this article, or claim that may be made by its manufacturer, is not guaranteed or endorsed by the publisher.

Supplementary material

The Supplementary Material for this article can be found online at: https://www.frontiersin.org/articles/10.3389/fmicb.2022.969722/full#supplementary-material

SUPPLEMENTARY FIGURE 1
AN removal rates under acid pH and low initial AN concentrations. The removal rates in different conditions of *B. idriensis* CT-WN-B3, *B. australimaris* CT-WL5-10, and *P. oleovorans* CT-WL5-6 were shown, and values with different superscripts were significantly different ($P < 0.05$). Columns in different colors represent different initial AN concentration in media.

References

Alcaraz, G., Chiappa-Carrara, X., Espinoza, V., and Vanegas, C. (1999). Acute toxicity of ammonia and nitrite to white shrimp *Penaeus setiferus* postlarvae. *J. World Aquac. Soc.* 30, 90–97. doi: 10.1111/j.1749-7345.1999.tb00321.x

APHA (1992). *Standard methods for the examination of water and wastewater*, 18th Edn. Washington, DC: American Public Health Association.

Armstrong, B. M., Lazorchak, J. M., Murphy, C. A., Haring, H. J., Jensen, K. M., and Smith, M. E. (2012). Determining the effects of ammonia on fathead minnow (*Pimephales promelas*) reproduction. *Sci. Total Environ.* 420, 127–133. doi: 10.1016/j.scitotenv.2012.01.005

Avnimelech, Y., Kochva, M., and Diab, S. (1994). Development of controlled intensive aquaculture systems with limited water exchange and adjusted carbon to nitrogen ratio. *Israel. J. Aquac. Bamidgeh* 46, 119–131.

Avnimelech, Y. (1999). Carbon/nitrogen ratio as a control element in aquaculture systems. *Aquaculture* 176, 227–235. doi: 10.1016/S0044-8486(99)00085-X

Avnimelech, Y. (2005). Tilapia harvest microbial flocs in active suspension research pond. *Glob. Aquac. Alliance* 8, 57–58.

Avnimelech, Y. (2015). *Biofloctechnology: A practical hand book*. Baton Rouge, LA: The world aquaculture society, 1–224.

Cai, J. H., Shen, Q. Y., and Zheng, X. Y. (2010). Advancement in researches of ammonia pollution hazards on aquaculture and its treatment technology. *J. Zhejiang Ocean Univ.* 2, 167–172, 195.

Chen, J., Zheng, J., Shi, T., Li, T., Wang, P., Mao, Y., et al. (2019). Isolation and identification of a strain of probiotic *Bacillus* from a breeding outdoor pond of shrimp (*Litopenaeus vannamei*) and optimization of its fermentation formula. *J. Fish. Res.* 41, 175–186.

Chen, P., Li, J., Li, Q. X., Wang, Y., Li, S., Ren, T., et al. (2012). Simultaneous heterotrophic nitrification and aerobic denitrification by bacterium *Rhodococcus* sp. CPZ24. *Bioresour. Technol.* 116, 266–270. doi: 10.1016/j.biortech.2012.02.050

Crab, R., Avnimelech, Y., Defoirdt, T., Bossier, P., and Verstraete, W. (2007). Nitrogen removal techniques in aquaculture for a sustainable production. *Aquaculture* 270, 1–14. doi: 10.1016/j.aquaculture.2007.05.006

Diao, W., An, X., Wang, C., and Li, L. (2015). Isolation and identification of ammonia degrading bacteria from marine shrimp and crab polyculture ponds. *Fish. Sci.* 34, 83–88.

Ebeling, J. M., Timmons, M. B., and Bisogni, J. J. (2006). Engineering analysis of the stoichiometry of photoautotrophic, autotrophic, and heterotrophic removal of ammonia-nitrogen in aquaculture systems. *Aquaculture* 257, 346–358. doi: 10.1016/j.aquaculture.2006.03.019

Hou, Y., Sun, J. D., Xu, J. Q., and Xu, C. L. (2006). Degrading Characters of ammonia-nitrogen in aquatic water of *Bacillus megaterium*. *J. Shenyang Agric. Univ.* 37, 607–610.

Hu, X., Wen, G., Tian, Y., Su, H., Xu, W., Xu, Y., et al. (2020). Removal effect of strain NB5 on ammonia nitrogen under different aquaculture conditions. *South China Fish. Sci.* 16, 89–96.

Huang, H., He, L., Lei, Y., Zhang, Y., Gong, M., Zou, W., et al. (2018). Characterization of growth and ammonia removal of *Bacillus* strain under low nitrogen source condition. *Acta Sci. Cirumstantiae* 38, 183–192. doi: 10.13671/j.hjkxxb.2017.0260

Huang, T., He, X., Zhang, H., Zhou, S., and Bai, S. (2015a). Nitrogen removal characteristics of the heterotrophic nitrification-aerobic denitrification bacterium *Acinetobacter* sp. Sxf14. *Chin. J. Appl. Environ. Biol.* 21, 201–207.

Huang, T., Bai, S., Zhang, H., Zhou, S., and He, X. (2015b). Identification and denitrification characteristics of an oligotrophic heterotrophic nitrification and aerobic denitrification bacteria. *Chin. J. Environ. Eng.* 9, 5665–5671.

Jiang, L. X., Pan, L. Q., and Xiao, G. Q. (2004). Effects of ammonia-N on immune parameters of white shrimp *Litopenaeus vannamei*. *J. Fish. Sci. China* 11, 537–541. doi: 10.1007/BF02911033

Körner, S., Das, S. K., Veenstra, S., and Vermaat, J. E. (2001). The effect of pH variation at the ammonium/ammonia equilibrium in wastewater and its toxicity to *Lemna gibba*. *Aquat. Bot.* 71, 71–78. doi: 10.1016/S0304-3770(01)00158-9

Lei, Y., Zhang, Q., Chen, Y., Fan, L. Y., and Zheng, Y. (2019). Screening and identification of microecological bacteria for the efficient degradation of ammonia nitrogen in shrimp aquaculture. *Fujian Agric. Sci. Technol.* 10, 16–20.

Martínez-Córdova, L. R., Emerenciano, M., Miranda-Baeza, A., and Martínez-Porchas, M. (2014). Microbial-based systems for aquaculture of fish and shrimp: An updated review. *Rev. Aquac.* 6, 1–18.

Mayes, M. A., Alexander, H. C., Hopkins, D. L., and Latvaitis, P. B. (1986). Acute and chronic toxicity of ammonia to freshwater fish: A site-specific study. *Environ. Toxicol. Chem.* 5, 437–442. doi: 10.1002/etc.5620050503

Mummert, A. K., Neves, R. J., Newcomb, T. J., and Cherry, D. S. (2003). Sensitivity of juvenile freshwater mussels (*Lampsilis fasciola*, *Villosa iris*) to total and un-ionized ammonia. *Environ. Toxicol. Chem.* 22, 2545–2553. doi: 10.1897/02-341

Muthukrishnan, A., Sabaratnam, S., and Chong, V. C. (2012). Ammonical-nitrogen removal by an aerobic heterotrophic bacterium, *Microbacterium* sp. VCM11. *Malaysian J. Sci.* 31, 76–82.

Su, Z., Li, Y., Pan, L., and Xue, F. (2016). An investigation on the immunoassays of an AN-degrading bacterial strain in aquatic water. *Aquaculture* 450, 17–22. doi: 10.1016/j.aquaculture.2015.07.001

Timmons, M. B., Ebeling, J. M., Wheaton, F. W., Summerfelt, S. T., and Vinci, B. J. (2002). *Recirculating aquaculture systems*, 2nd Edn. New York, NY: Cayuga Aqua Ventures, 769.

USEPA (1999). *1999 Update of ambient water quality criteria for ammonia*. Washington, DC: Environmental Protection Agency.

Wang, J., Ding, G., Lin, W., and Peng, L. (2016). Characteristics of growth and heterotrophic nitrification-aerobic denitrification for *Acinetobacter baumannii* wj6 strain. *Water Purif. Technol.* 35:76.

Wu, K., Zhong, Z., Chen, Y., Weng, S., and He, J. (2017). The relationship between climate change, feeding management and ammonia, rdtrite and nitrate nitrogen in the *Litopenaeus vannamei* aquaculture ponds. *Acta Sci. Natural. Univ. Sunyatseni* 56, 102–114. doi: 10.13471/j.cnki.acta.snus.2017.01.017

Xin, X., Yao, L., Lu, L., Leng, L., Zhou, Y. Q., and Guo, J. Y. (2014). Identification of a high ammonia nitrogen tolerant and heterotrophic nitrification-aerobic denitrification bacterial strain TN-14 and its nitrogen removal capabilities. *Environ. Sci.* 35, 3926–3932. doi: 10.13227/j.hjkx.2014.10.040

Xu, S., Yang, N., Feng, L., Ren, Y., and Wang, W. (2016). Study on *Bacillus* screening and their purification of water quality analysis from sea shrimp farming areas. *J. Qingdao Agric. Univ. (Nat. Sci.).* 33, 317–320.

Yun, L., Yu, Z., Li, Y., Luo, P., Jiang, X., Tian, Y., et al. (2018). Ammonia nitrogen and nitrite removal by a heterotrophic *Sphingomonas* sp. strain LPN080 and its potential application in aquaculture. *Aquaculture* 500, 477–484. doi: 10.1016/j.aquaculture.2018.10.054

Zhang, L., Xu, E. G., Li, Y., Liu, H., Vidal-Dorsch, D. E., and Giesy, J. P. (2018). Ecological risks posed by ammonia nitrogen (AN) and un-ionized ammonia (NH3) in seven major river systems of China. *Chemosphere* 202, 136–144. doi: 10.1016/j.chemosphere.2018.03.098

Zhang, Q. H., Feng, Y. H., Wang, J., Guo, J., Zhang, Y. H., Gao, J. Z., et al. (2011). Study on the characteristics of the ammonia-nitrogen and residual feeds degradation in aquatic water by *Bacillus licheniformis*. *Acta Hydrobiol. Sin.* 35, 498–503. doi: 10.1016/S1671-2927(11)60313-1

Zhang, R., Luo, L., Wang, S., Guo, K., Xu, W., and Zhao, Z. (2022). Screening and functional analysis of alkalitolerant microorganisms in carbonate-type saline-alkali ponds in Northeast China. *Chin. J. Fish.* Available online at: http://kns.cnki.net/kcms/detail/23.1363.S.20220518.1031.002.html (accessed May 18, 2022).

frontiers | Frontiers in Microbiology

TYPE Review
PUBLISHED 16 November 2022
DOI 10.3389/fmicb.2022.968812

OPEN ACCESS

EDITED BY
Ren-Cun Jin,
Hangzhou Normal University, China

REVIEWED BY
Nídia Dana Lourenço,
New University of Lisbon,
Portugal
Da Kang,
Beijing University of Technology, China

*CORRESPONDENCE
Kiprotich Kosgey
kiprotichcharapkosgey@gmail.com
Sheena Kumari
SheenaK1@dut.ac.za

SPECIALTY SECTION
This article was submitted to Microbiotechnology, a section of the journal Frontiers in Microbiology

RECEIVED 14 June 2022
ACCEPTED 28 October 2022
PUBLISHED 16 November 2022

CITATION
Kosgey K, Zungu PV, Bux F and Kumari S (2022) Biological nitrogen removal from low carbon wastewater. *Front. Microbiol.* 13:968812. doi: 10.3389/fmicb.2022.968812

Biological nitrogen removal from low carbon wastewater

Kiprotich Kosgey*, Phumza Vuyokazi Zungu, Faizal Bux and Sheena Kumari*

Institute for Water and Wastewater Technology, Durban University of Technology, Durban, South Africa

Nitrogen has traditionally been removed from wastewater by nitrification and denitrification processes, in which organic carbon has been used as an electron donor during denitrification. However, some wastewaters contain low concentrations of organic carbon, which may require external organic carbon supply, increasing treatment costs. As a result, processes such as partial nitrification/anammox (anaerobic ammonium oxidation) (PN/A), autotrophic denitrification, nitritation-denitritation and bioelectrochemical processes have been studied as possible alternatives, and are thus evaluated in this study based on process kinetics, applicability at large-scale and process configuration. Oxygen demand for nitritation-denitritation and PN/A is 25% and 60% lower than for nitrification/denitrification, respectively. In addition, PN/A process does not require organic carbon supply, while its supply for nitritation-denitritation is 40% less than for nitrification/denitrification. Both PN/A and nitritation-denitritation produce less sludge compared to nitrification/denitrification, which saves on sludge handling costs. Similarly, autotrophic denitrification generates less sludge compared to heterotrophic denitrification and could save on sludge handling costs. However, autotrophic denitrification driven by metallic ions, elemental sulfur (S) and its compounds could generate harmful chemicals. On the other hand, hydrogenotrophic denitrification can remove nitrogen completely without generation of harmful chemicals, but requires specialized equipment for generation and handling of hydrogen gas (H_2), which complicates process configuration. Bioelectrochemical processes are limited by low kinetics and complicated process configuration. In sum, anammox-mediated processes represent the best alternative to nitrification/denitrification for nitrogen removal in low- and high-strength wastewaters.

KEYWORDS

nitrogen removal, anammox process, DEAMOX process, bioelctrochemical process, autotrophic denitrification, low carbon wastewater

Introduction

Nitrogen in wastewater presents serious ecological challenges to the receiving water bodies, including eutrophication and toxicity to aquatic life. It is dissolved as ammonium (NH_4^+), nitrite (NO_2^-), nitrate (NO_3^-) and organic compounds (e.g., amino acids and CN^-) in wastewaters (Wiesmann, 1994; Wang et al., 2012). When organics are degraded by

microorganisms, organic nitrogen is transformed to NH_4^+ (Wiesmann, 1994). In mainstream wastewater, the concentration of NH_4^+ and organic nitrogen is about 40 and 20 mg-N/L, respectively (Wiesmann, 1994). Nitrogen and COD concentrations vary depending on the source of wastewater (Tables 1, 2). Chemical oxygen demand (COD) to nitrogen ratio (C/N) ratios in mainstream wastewaters are typically ≥2, while those in sidestream wastewaters generally contain lower concentrations (Li et al., 2018a). COD concentrations are high in industrial wastewaters (Table 2). For instance, effluents from a biodiesel plant, was reported to contain COD concentration of up to 403,540 mg/L (Mousazadeh et al., 2021).

Nitrification/denitrification represents the traditional nitrogen removal process that has been applied in the past several decades in municipalities across the globe (Grady et al., 2011). In this conventional process, NH_4^+ is sequentially oxidized to NO_3^- by ammonia oxidizing bacteria (AOB) in the first stage, and by nitrite oxidizing bacteria (NOB) in the second stage, then the NO_3^- is removed through denitrification in the last stage (Figure 1). However, the economic aspects of this process indicate that it is more costly compared to nitritation-denitritation and partial nitrification/anammox (anaerobic ammonium oxidation) processes because it consumes more COD, produces more sludge and requires more aeration (Hellinga et al., 1998; Kartal et al., 2013). These challenges relating to COD consumption are magnified in the treatment of low-COD wastewaters such as reject wastewater and landfill leachate, as supplementation with external COD sources is inevitable (Table 1).

Autotrophic denitrification could play a vital role in the treatment of wastewaters with high NO_3^- concentrations such as some industrial wastewaters and groundwater (Pu et al., 2014). Compared to heterotrophic denitrification, this process is associated with lower sludge production and utilization of simple elements/ions, and could be applicable in treatment of wastewaters containing nitrogen and electron donors such as sulfide (S^{2-}), SCN^- (thiocyanate), hydrogen gas (H_2), etc. (Cardoso et al., 2006; Di Capua et al., 2019). However, autotrophic denitrification driven by metallic elements and ions as well as those driven by S and its compounds have been reported to generate harmful chemicals that require downstream treatment to avert environmental disasters (Di Capua et al., 2019).

The PN/A process has generated a lot of interest from water practitioners leading to the development of over 100 full-scale systems (Lackner et al., 2014a; Bowden et al., 2015). However, the process still requires further improvements to emerge as an efficient alternative for nitrogen removal. Moreover, there is need to develop the process for mainstream applications because of the associated benefits (Li et al., 2018a). Furthermore, PN/A converts a fraction of NH_4^+ to NO_3^-, which reduces process efficiency (Daverey et al., 2013), and would thus be necessary to incorporate systems for NO_3^--removal downstream.

Cyanide (CN^-) and its derivatives which are present in some industrial wastewaters such as coal gasification and gold/silver mining industries (Table 2), is highly toxic and its removal is necessary to avert environmental disasters (Kjeldsen, 1999; Chen et al., 2008). Some physical and chemical processes have been developed for its removal from wastewater, but these processes are generally characterized by high costs (Akcil et al., 2003). Therefore, biological processes have generated a lot of interest because they are cheap and safe, as they do not generate harmful secondary chemical wastes. Microalgae, plants, bacteria and fungi have all been determined to be able to remediate against CN^- contamination (Chapatwala et al., 1998; Ezzi and Lynch, 2002; Gurbuz et al., 2004). This study thus incorporates biodegradation of CN^- and its derivatives as they can be transformed to NH_4^+ and other nitrogen compounds ("Biological degradation of cyanide" and "Autotrophic denitrification"). Furthermore, since SCN^- can be utilized as electron donor (Pan et al., 2018), it is necessary to analyze their influence on nitrogen removal.

In the recent past, there have been reviews on different low carbon nitrogen removal processes, including those covering ANAMMOX-mediated processes (Adams et al., 2022), autotrophic denitrification (Di Capua et al., 2019; Li et al., 2022), and bioelectrochemical processes (Albina et al., 2019; Cecconet et al., 2020; Jung et al., 2020) among other biological processes (Winkler and Straka, 2019; Abeysiriwardana-Arachchige et al., 2020; Mohsenpour et al., 2021). Despite the useful insights presented in those previous reports, many aspects of low carbon nitrogen removal processes were not adequately addressed including the process kinetics, applicability at full-scale level, actual COD consumption/g-N removed, by-product and sludge generation. Furthermore, the previous reviews either focused on aspects of a

TABLE 1 Nitrogen and COD concentrations in low- and high-strength wastewaters.

	NH_4^+ conc. (mg-N/L)	NO_3^- conc. (mg-N/L)	COD conc. (mg/L)	C/N[a]	Remarks	References
1	1,000	-	810	0.8	Reject water	Hellinga et al. (1998)
2	223–229	-	1,090–1,270	5–6	Abattoir wastewater	Lemaire et al. (2008)
3	1,128 ± 141	0.77 ± 0.3	1956 ± 597	1–2.6	Reject water from digested sludge	Noutsopoulos et al. (2018)
4	66 ± 17	2.09 ± 0.2	4,244 ± 2,100	25.8–129.5	Reject water from primary sludge thickening unit	
5	142.7 ± 40.9	-	1,223 ± 336	4.8–15.3	Slaughterhouse wastewater	Dobbeleers et al. (2020)
6	1,500	-	2,700	1.8	Landfill leachate	Magrí et al. (2021)

[a]Calculated.

TABLE 2 Summary of nitrogen and COD concentrations in industrial and mining wastewaters.

	NH_4^+ conc. (mg-N/L)	NO_3^- conc. (mg-N/L)	COD conc. (mg/L)	CN^-/ SCN^- (mg/L)	C/N[a]	Remarks	References
1	-	-	-	840	-	Wastewater from gold leaching process	Song et al. (2021)
2	110–165	55-80	2,750	0.5–3.5/22–45	16–25	Coal gasification wastewater	Wang et al. (2012)
3	325	201	-	-	-	Wastewater from fertilizer factory	Leaković et al. (2000)
4	56–132	0.5-1.2	900–2000	-	7–36	Wastewater from petrochemical industry	Qin et al. (2007)

[a]Calculated.

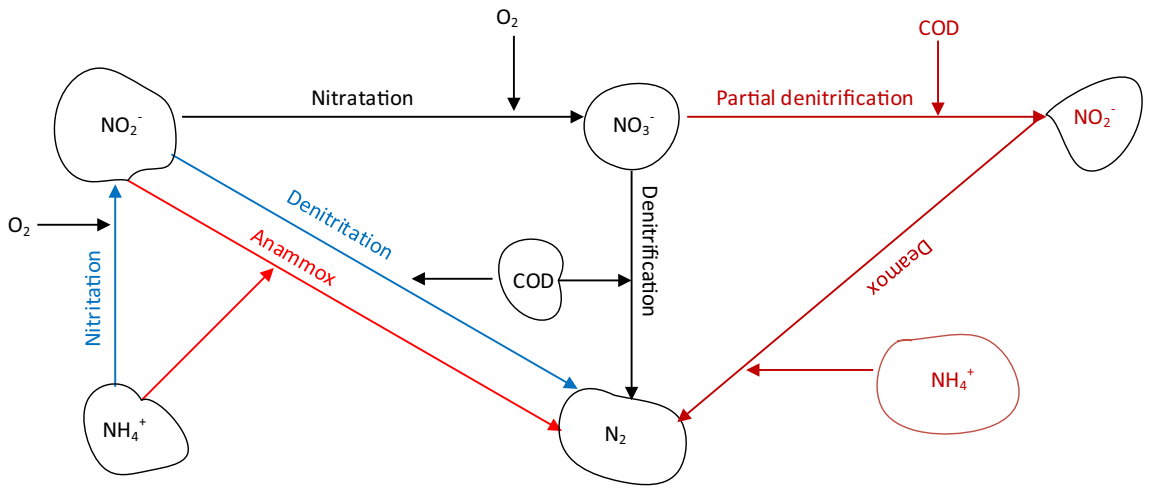

FIGURE 1
Schematic diagram of nitrogen removal processes.

single technology without the inclusion of other low-carbon processes in the discussion, or they did not critically review these technologies with respect to influencing factors. Therefore, these subjects are discussed in this review with reference to experimental data collected from different systems (laboratory-, pilot- or full-scale). The choice of the nitrogen removal processes to be included in this review was informed by process readiness for application at pilot-scale and full-scale installations.

Nitritation-denitritation

Theoretically, 2.86 g of COD would be required to remove 1 g NO_3^--N (Hellinga et al., 1999; Daigger, 2014). However, considering that substantial amount of COD would be oxidized during aeration phase, the actual required C/N ratios for complete nitrogen removal is higher (5–7; (Hellinga et al., 1999; Sahinkaya et al., 2014). On the contrary, 1.94–3\u00B0C/N ratios have been reported to be sufficient for nitrogen removal through the NO_2^- route (nitritation-denitritation) (Hellinga et al., 1999; Van Kempen et al., 2001; Bernat et al., 2016; Table 3). This nitrogen removal option saves approximately 40% COD and 25% aeration costs compared to nitrification/denitrification since NH_4^+ is only oxidized to NO_2^- as opposed to NO_3^- in the case of nitrification/denitrification (Hellinga et al., 1999; Van Kempen et al., 2001; Noutsopoulos et al., 2018; Dobbeleers et al., 2020).

Coupling nitritation with denitritation requires parameter control for successful implementation, including the control of pH, DO, temperature and SRT/HRT. This is done in order to suppress the growth of NOB while promoting the growth of AOB. Generally, temperature (30°C–40°C), pH (7–8), DO (<0.5 mg/L) and HRT/SRT (~1 day) have been reported to suppress NOB growth (Van Kempen et al., 2001). This process, referred to as SHARON (single reactor system for high activity ammonia removal over nitrite), is operated without sludge retention using concentrated wastewaters such as landfill leachate and reject wastewater from anaerobic digestion (Van Kempen et al., 2001; Vilar et al., 2010).

At 5-20°C, NO_2^- oxidizers grow faster than NH_4^+ oxidizers, leading to NO_3^- generation (Hellinga et al., 1998). However, at higher temperatures (30°C–40°C), the reverse is true. This difference in growth rates informs the design of SHARON systems that seek to limit nitratation while favoring nitritation. In the process, a combination of elevated temperatures (30-40°C) and short HRTs (~1 day) lead to NOB washout (Hellinga et al., 1998; Fux et al., 2006). In essence, the high growth rates of AOB compensate for the biomass washed out from the system. Furthermore, the high temperatures and high concentrations of

TABLE 3 Nitrogen removal in laboratory-, pilot- and full-scale nitritation-denitritation systems.

	Influent NH_4^+ conc. (mg-N/L)	C/N ratio	Operational temperature (°C)	HRT (days)	NH_4^+ conversion rates (%)	NRR (kg-N/m^3-day)	NRE (%)	Remarks	References
1	4,559 ± 201	-	36 ± 1	-	60	-	-	250 l system	Ganigué et al. (2010)
2	>1,000	2.4	30–40		>90	-	65-95[a]	Full-scale system	Mulder et al. (2001)
3	1,135	2.2	30–32	2.3	80[b]	1.0	67	5.65 l CSTR	Fux et al. (2006)
4	1,216	1.94		1.0–1.6	95[c]	3.0–3.6	93	6 l SBR with continuous sludge addition	
5	400–700	-	35	-	1-3[d]	-	95-98	7 l CSTR operated with sequencing of operations	Claros et al. (2012)
6	1750-1900[b]	-	-	1.86-2.71/2.71	79–98	0.63	95	Two-stage SBRs (10 l/6 l)	Zhang et al. (2019)
7	200 ± 18[e]	3	20–22	0.71–3.33	-	-	100	5 l SBR	Bernat et al. (2016)

[a]From Figure 6 in the source file.
[b]Estimated in Figure 2 in the source file.
[c]Estimated from Figure 3 in the source file.
[d]Figure 3a in the source file;
[e]NO_2^-.

NH_4^+ and NO_2^- also limit the activities of NOB as they dissociate to FA (free ammonia) and FNA (free nitrous acid), respectively, both of which are more toxic to NOB compared to AOB (Anthonisen et al., 1976; Duan et al., 2019). Indeed, inhibitory FA and FNA concentrations for NOB are 0.10–1.00 mg/L and 0.011–0.070 mg/L, while that of AOB is 10.00–150.00 mg/L and *ca.* 0.40, respectively (Anthonisen et al., 1976; Chen et al., 2020).

For complete nitrogen removal from wastewater using nitritation-denitritation, supplementation of COD is necessary for low COD wastewaters (Figure 1). The process could be implemented in a continuously stirred system in which a COD source is added during an unaerated phase (Lemaire et al., 2008). Since aeration causes pH to drop and denitritation causes pH to rise, the pH could be used to control aeration and dosing of COD sources. This strategy is beneficial as the pH is adjusted during nitritation and denitritation, eliminating the need for addition of alkali (Hellinga et al., 1998). If the influent wastewater contain high C/N ratios (>2), the same wastewater could be utilized as the COD source by implementing a step-feeding strategy as was demonstrated by Lemaire et al. (2008). Other methods for process control include sequencing of operations in order to set time intervals. ORP (oxidation–reduction potential)-based strategies could also be used to regulate the process, as demonstrated previously (Claros et al., 2012).

Lai et al. (2004) reported 96%–98% removal of influent NH_4^+ in a 6.5 m^3 nitritation-denitritation pilot-scale SBR system which was fed with 1.6–1.9 kg COD-equivalent ethanol per kg N removed. The low HRT (0.88 days), and high temperatures (35 ± 2°C) enhanced NOB suppression in line with Hellinga et al. (1998). However, the reported C/N ratios were lower than those reported by (Van Kempen et al., 2001), possibly because of the sequencing of reactor operations in the SBR leading to lower COD consumption by aerobic heterotrophic bacteria compared to continuous dosing in the CSTR. Similar findings were reported in a comparative study of nitritation-denitritation by Fux et al. (2006) in a CSTR and SBR, in which better nitrogen removal in SBR compared to CSTR was observed (Table 3). In addition, lower HRTs were achieved (1–1.6 days) in SBR mode compared to CSTR mode of operation (2.3 days). As a result, operating reactors in CSTR mode would require the application of larger reactors in order to achieve the same performance as SBRs (Fux et al., 2006). Notwithstanding this finding, CSTRs have been applied in full-scale SHARON systems for nitrogen removal (Mulder et al., 2001). Therefore, comparative studies of full-scale nitritation-denitritation systems based on COD consumption/nitrogen removal could be necessary for a better understanding of the impact of reactor configuration.

Autotrophic denitritation could be advantageous to heterotrophic denitritation due to less sludge production ("Autotrophic denitrification"). Co-occurrence of NH_4^+ and inorganic electron donors in some industrial wastewaters (Table 2) presents an opportunity for nitrogen removal through autotrophic denitritation. Indeed, Qian et al. (2016) demonstrated the feasibility of nitritation-denitritation in an autotrophic system. However, low process kinetics and production of SO_4^{2-} and other chemicals ("Autotrophic denitrification") could limit the application of autotrophic denitrification.

ANAMMOX-mediated nitrogen removal

ANAMMOX process has mainly been applied to treat high-strength NH_4^+-containing wastewater (Lackner et al., 2014a). This include reject wastewater, landfill leachate and industrial wastewater (Azari et al., 2017; Yao et al., 2022). Meanwhile, research on the development of mainstream anammox is ongoing. In general, the design of a treatment process depends on a number of variables, including the characteristics of the influent, the concentration of active biomass, and the flow rates. In PN/A

systems, the functions of AOB and anammox bacteria (AMX) are coupled together ("Partial nitritation-ANAMMOX"), while in DEAMOX systems, the activities of nitrate-reducing denitrifying microorganisms are coupled with AMX ("Denitrifying ammonium oxidation").

Partial nitritation-ANAMMOX

In PN/A systems, AOB and AMX sequentially work together to oxidize NH_4^+ to nitrogen gas (N_2) without the consumption of COD (Equations 1–3; (Daverey et al., 2013). However, during this process, approximately 11% of the influent NH_4^+ is converted to NO_3^- (Equation 3), which can be removed downstream of the treatment process by mixing with COD containing wastewater if the effluent limits are exceeded (Mulder et al., 2012), otherwise PN/A alone has been reported to be adequate in many plants (Lackner et al., 2014a). In case of NO_3^- and NH_4^+ presence in the influent such as in, industrial wastewaters (Table 2), activities of AMX could be coupled with that of partially denitrifying microorganisms that could generate NO_2^- for the AMX in a process called DEAMOX (DEnitrifying AMmonium OXidation; "Denitrifying ammonium oxidation"; Le et al., 2019a,b).

$$NH_3 + 1.5O_2 \rightarrow NO_2^- + H_2O + H^+ \quad (1)$$

$$NH_3 + 1.3NO_2^- + H^+ \rightarrow 1.02N_2 + 0.26NO_3^- + 2H_2O \quad (2)$$

$$NH_3 + 0.85O_2 + H^+ \rightarrow 0.44N_2 + 0.11NO_3^- + 1.43H_2O + 0.14H^+ \quad (3)$$

As of 2014, over 100 full-scale PN/A systems had been developed, majority of which were based on SBR configuration (Lackner et al., 2014a). However, despite the progress, this excellent technology is still facing numerous challenges including occasional plant failures, foaming, biomass washout, NOB/heterotrophic bacterial competition for oxygen with AOB and NO_2^- with AMX, etc. (Lackner et al., 2014a). Therefore, further improvements of this technology is imperative for sustainable and efficient nitrogen removal.

The NOB and aerobic heterotrophic bacteria could compete for oxygen with AOB in PN/A systems. In addition, NOB and denitrifying heterotrophic bacteria compete for NO_2^- with AMX (Li et al., 2018a). Successful implementation of PN/A systems thus requires strict control of conditions in order to limit the growth of organisms competing with AOB and AMX. Heterotrophic bacterial growth is generally limited through regulation of influent C/N ratios to $\leq$1 (Li et al., 2018a,b). As a result, sidestream (high-strength: >100-mg-N/L) wastewater is suitable for treatment in PN/A system unlike mainstream wastewaters which are associated with high C/N ratios (Li et al., 2018a).

Selective retention of biomass rich in the desired microorganisms (biofilms) could also be implemented, while that rich in undesired microorganisms (flocs) is wasted (Park et al., 2015). This could be achieved by limiting HRT and SRT in the respective reactors to certain set limits that would allow the growth of the desired microorganisms (AOB/AMX; Han et al., 2016). However, implementation of this strategy varies depending on the reactor configuration. For instance, SRT in SHARON reactors which are usually of CSTRs configuration is basically equal to HRT, while in carrier-based systems, SRTs are indefinite and biomass detachment from the carriers could only be induced through increased shear forces (Syron and Casey, 2008). It is noteworthy that although inducing biomass detachment from the carriers could achieve the intended aim of removing the biomass, the rate of detachment is challenging to control and could lead to unprecedented influence on process performance.

Among the developed reactor configurations, SBR is the most popular because of its simplicity and flexibility (Lackner et al., 2014a). However, the NRRs of this configuration is lower than that of continuous systems such as MBBRs (moving bed biofilm reactors; Lackner et al., 2014a; Table 4). Other systems such as MABRs (membrane aerated biofilm reactors) are complex in nature as the membrane lumens need to be pressurized with air which then diffuse into the bulk liquid, and MBRs (membrane bioreactors) are associated with high energy costs and fouling (Reij et al., 1995; Van Der Star et al., 2008).

Community analyses of ANAMMOX-mediated systems have shown the co-existence of bacteria, viruses, archaea and protozoans in these systems (Suarez et al., 2015). The relationship between these microorganisms is complex, and many things are not yet clearly understood. Some organisms complement each other in terms of sub-division of metabolic activities and generation of essential compounds for growth, while others are predatory in nature (Suarez et al., 2015; Lawson et al., 2017). In ANAMMOX-mediated systems, the presence of all these microbes is dependent on many factors, such as the operating conditions and mode of biomass growth, and as a result could change over time (Park et al., 2015; Suarez et al., 2015).

Within the AMX community, dominance of *Candidatus Brocadia* spp. has been associated with the presence of organic carbon and high substrate concentrations because of their high growth rates and mixotrophic lifestyles (Park et al., 2017a). On the other hand, *Candidatus Kuenenia* spp. have been suggested to dominate in systems with limited substrate concentrations because of their higher affinity for NO_2^- (*K*-strategists) compared to the other species within the AMX community (Van Der Star et al., 2008). The factors influencing the growth dynamics of other bacteria within the AMX community such as *Candidatus Jettenia* spp. and *Candidatus Anammoxoglobus* spp. are yet to be established. *Candidatus* Scalindua spp. are marine in nature (Wei et al., 2016), but its detection in PN/A systems with low salinity as well as in soil has been reported (Wang and Gu, 2013).

Operating conditions have also been reported to influence the growth of AOB and NOB within the ANAMMOX-mediated

TABLE 4 Nitrogen removal in full-scale PN/A systems.

	Influent NH_4^+ conc. (mg-N/L)	Influent NO_2^-/NH_4^+	NRR (kg-N/m^3-day)	NRE (%)	Effluent NO_3^-/NH_4^+ (%)	Remarks	References
1	1,000-2700[a]	1.4 ± 0.6	0.32	86 ± 9	5	Two-stage system consisting of SBRs	Magrí et al. (2021)
2	750-1500[b]	1.31	7.1	-	25	Two-stage SHARON-ANAMMOX	van der Star et al. (2007)
3	960 ± 110	Single stage PN/A	0.18	72-85[c]	8-34	550 m^3 SBR	Lackner et al. (2014b)
4	890 ± 89		-	>85	5-13[d]	393 m^3 MBBR	Klaus et al. (2017)
5	1,043		0.63	90	2–8	350 m^3	Christensson et al. (2013)
6	855		1.2	88	8–22	50×4 m^3	
7	690	1.7-2[d]	3.0	80	3[d]	415 m^3 5-stage system with gel-encapsulated biomass	Isaka et al. (2017)
8	580 ± 90	Single stage	1.8[e]	>80	~12[f]	256 m^3 full-scale PN/A MBBR	Dimitrova et al. (2020)

[a]Feed to nitritation reactor.
[b]Estimated from Figure 4 in the source file.
[c]Ammonium removal.
[d]Estimated from Figure 7 in the source file.
[e]g-N/m^2-day.
[f]Estimated from Figure 2 in the source file.

systems. The growth of AOB-affiliated *Nitrosomonas* spp. which are regarded as *r*-strategists because of their high growth rates have been associated with high substrate concentrations, while *Nitrosospira* spp. which are regarded as *K*-strategists because of their high affinity for substrate have been associated with low substrate concentrations (Awolusi et al., 2015). The factors driving the growth of other AOB-affiliated bacteria such as *Nitrosococcus* spp., *Nitrosovibrio* spp. and *Candidatus Nitrosoglobus* spp. is not well elucidated in the currently available literature and could be investigated in future studies. On the other hand, *Nitrospira* spp. are regarded as *r*-strategists within the NOB community, while *Nitrobacter* spp. are regarded as *K*-strategists. *Nitrolancea hollandica*, which also belong to NOB community, have been detected in ANAMMOX-mediated systems but their dominance has not been reported (Gu et al., 2018).

Denitrifying ammonium oxidation

Treatment of NO_3^--containing wastewater theoretically requires 2.86 g-COD/g-N for complete denitrification (Daigger, 2014). Systems receiving wastewaters with low COD would thus require supplementation of COD from external sources. This would increase the cost of treatment and complicate the treatment process. Therefore, partial denitrification (PD) which consumes less theoretical COD (1.14 g-COD/g-N), could be economically viable when combined with other processes such as ANAMMOX (DEAMOX; Cao and Zhou, 2019).

The success of DEAMOX process, however, relies on the success of PD. The PD process, in turn, depends on many factors including pH, NO_3^- concentration, active microorganisms, nature of carbon sources, etc. (Glass and Silverstein, 1998; Xie et al., 2017; Le et al., 2019a,b). In some studies, it has been reported that the pH influences the accumulation of NO_2^- (Cao and Zhou, 2019). For instance, at pH values of 7.5, 8.5 and 9.0, NO_2^- concentrations of 250, 500 and 900 mg-N/L, respectively, were reported in a denitrification system fed with 2,700 mg-N/L (Glass and Silverstein, 1998). In some other studies, it has been suggested that C/N ratios influence the accumulation of NO_2^- (Ma et al., 2020), while in others, contrary findings relating to C/N ratios have been made (Le et al., 2019a). According to Le et al. (2019a) and Le et al. (2019b), C/N ratios have no influence on the efficiencies of PD, which is in agreement with Sijbesma et al. (1996).

Some microorganisms can only partially reduce NO_3^- to NO_2^-, while others can reduce both compounds to N_2, and others can only reduce NO_2^- to N_2 (Xie et al., 2017). Therefore, it is possible to manipulate the operating conditions in order to enhance the growth of the required microorganisms that contribute to accumulation of NO_2^- (Table 5). In addition, it could also entail the supply of a suitable carbon source preferred by the microorganisms of interest.

Accumulation of NO_2^- (PD) by *Paracoccus denitrificans* was reported by Blaszczyk (1993) in a system fed with a media containing NO_3^- and different carbon sources. However, the amount of NO_2^- accumulation varied with the carbon sources, in agreement with Du et al. (2017) who reported higher efficiencies of PD with acetate compared to ethanol. In addition, Blaszczyk (1993) reported that the NO_2^- was consumed once the NO_3^- was depleted, possibly because: (i) slow induction of NO_2^- reductase in comparison to NO_3^- reductase; (ii) inhibition of NO reductase by NO_3^-; (iii) unbalanced reduction of NO_3^- and NO_2^-; and (iv) inhibition of NO_2^- reductase by NO_3^-. On the other hand, Martienssen and Schöps (1999) reported that species such as *Staphylococcus* could only reduce NO_3^- to NO_2^-, while others such as *Bacillus niacini* could reduce NO_3^- with transient NO_2^- accumulation, and *Pseudomonas pseudoalcaligenes* could reduce NO_3^- to N_2 without NO_2^- accumulation. Denitrifying anaerobic methane oxidizing (DAMO) archaea within the family of *ANME-2D* have also been reported to possess ability to reduce NO_3^- to NO_2^- (Equation 4; Xie et al., 2017). Therefore, with proper selection of carbon source and

TABLE 5 Nitrogen removal in laboratory- and pilot-scale DEAMOX systems.

	Influent NH_4^+ conc. (mg-N/L)	Influent NO_3^- conc. (mg-N/L)	PD eff. (%)	NRR (kg-N/m^3-day)	NRE (%)	C/N ratio	Key microorganisms	Remarks	References
1	60	-	-	-	80 ± 4	2.6	Biofilm: *Ca. Jettenia* spp. (17.83%), *Ca. Kuenenia* spp. (2.62%) and *Thauera* (5.27%)	Two-stage denitratation/ ANAMMOX-nitrification system	Ma et al. (2017)
2	500	530[a]	-	0.98	99.9	-	*Ca. Brocadia* spp. (57%), *Ca. Kuenenia* spp. (43%)	Abundance at family level: ANMED-2D (39%); uc_*Phycisphaerales* (15%); *Rhodocyclaceae* (10%); *Fimbriimonadaceae* (7%); *Brocadiaceae* (5%); uc_*envOPS12* (4%); *Methylomirabiliaceae* (3%)	Xie et al. (2017)
3	30–43	107-137	-	-	>90	2.02[b]	*Ca. Brocadia* spp. (~68%)[c]; *Ca. Jettenia* spp. (~0.5%)[c]; *Denitratisoma* (2.3–2.7%); *Thauera* (4.8–5.4%).	Two-stage PdN-ANAMMOX (5l SBR coupled with 3.2l up-flow anaerobic sludge blanket reactor)	Du et al. (2019)
4	50	50	96	-	82–93	2.6	*Ca. Brocadia* spp. (0.33%); *Ca. Kuenenia* spp. (0.23%); *Thauera* (61.53%);	Acetate-fed laboratory-scale 6l system	Du et al. (2017)
5	50	50	67-87	-	85–90	3	*Ca. Kuenenia* spp. (1.01%); *Thauera* (45.17%); *Denitratisoma* (0.65%);	Ethanol-fed laboratory-scale 6l SBR	
6	50–78	51–104	-	-	41–82	2–4	*Thauera* (43.6%-biofilm and 57.5%-suspension); *Ca. Brocadia* spp. (1.6%-biofilm and 0.1%-suspension)	Sodium acetate-fed laboratory-scale system	Zhang et al. (2022)
7	31–33	-	38	1.2 ± 0.7[d]	>77	2-3[e]	-	Fermentate-fed	Ladipo-Obasa et al. (2022)
8	0	40	64.4 ± 14.5	0.11–0.13	-	4.3–6.1[f]	*Comamonadaceae* (39.2%), *Hyphomicrobiaceae* (14.7%), *Flavobacterium* (12.3%), *Ignavibacteriaceae* (11.1%)	Hydrogenotrophic PD MBBR	Kamei et al. (2022)
9	29±4[g]	-	80-97	-	22-75[h]	2.2-13	-	360l multi-stage system	Le et al. (2019b)

[a]NO_2^-.
[b]Calculated based on data in Table 2 in the source file.
[c]Calculated from Figure 4b in the source file.
[d]g-N/m^2-d.
[e]Influent COD excluding the added COD.
[f]H2/N ratio.
[g]Total inorganic nitrogen.
[h]Estimated from Table 1 in the source file.

strains of desired microorganisms, it is possible to treat wastewaters such as industrial wastewaters rich in both NO_3^- and NH_4^+ (Table 5) by coupling ANAMMOX with denitrification (DEAMOX). Indeed, Xie et al. (2017) reported complete removal of NO_2^- and NH_4^+ in a MABR whose membrane lumens were pressurized with methane. In their study, following metagenomic analyses, it was concluded that DAMO archaea within *ANME-2D* family used methane as carbon source to reduce the NO_3^- produced by AMX to NO_2^-, which was subsequently re-utilized in the ANAMMOX process. Xie et al. (2017) estimated that DAMO bacteria removed 10% of the nitrogen fed into the system, while DAMO archaea and AMX bacteria removed the remainder (90%). Within the ANAMMOX community, *Ca. Brocadia* spp. and *Ca. Kuenenia* spp. were detected at 57 and 43%, respectively (Table 5).

$$CH_4 + 4NO_3^- \rightarrow 4NO_2^- + 2H_2O + CO_2 \quad (4)$$

Ma et al. (2017) reported approximately 80% nitrogen removal in a two-stage denitratation/ANAMMOX-nitrification (anoxic/

oxic) system fed with media containing both NH_4^+ and sodium acetate. In their setup, nitrification process occurred in the second stage in which NO_3^- was generated-and-recycled back to the first stage where denitratation and ANAMMOX processes occurred. Based on the performance, it was reported that a C/N ratio of about 2.6 led to 80% NRE. However, the observed COD requirements were higher than the theoretical 1.14, highlighting the challenges with minimization of COD losses during aeration. In addition, metagenomic analysis revealed higher hits for nitrate reductase compared to nitrite reductase, an indication of faster rate of NO_2^- production from NO_3^- reduction compared to its depletion. Furthermore, it was reported that the dominant microorganisms in the anoxic biofilms were *Ca. Jettenia* spp. (17.83%), *Ca. Kuenenia* spp. (2.62%), and *Thauera* (5.27%).

In another study, Kamei et al. (2022) reported approximately 64% accumulation of NO_2^- in a system supplied with H_2 and NO_3^- (Table 5). However, some of the supplied NO_3^- was not converted to NO_2^- and could not be accounted for in the effluent, an indication that some of the NO_2^- was oxidized further leading to its removal. In addition, dominance of bacteria within the unidentified genus of *Comamonadaceae* was reported (Kamei et al., 2022). Furthermore, an optimal H_2 supply rate of 0.7 (7 min on/3 min off at 15 ml/min flow rate) was reported, while higher and lower rates lead to a decrease in NO_2^- accumulation.

Studies have reported different C/N ratios in systems incorporating PD and ANAMMOX (Table 5). In all the reported studies, the C/N ratios are higher than the theoretical 1.14 g-COD/g-N, an indication of losses through aerobic oxidation. However, the observed values are still lower than that for full denitrification whose C/N ratios are >5. Furthermore, the efficiencies of PD vary in different systems, possibly due to the variation of the microorganisms based on the available carbon sources as previously suggested by Du et al. (2017), or due to some other unknown factors.

Nitrogen removal in DEAMOX systems is comparable to that of PN/A systems (Tables 4, 5). In both systems, process performance has been shown to be influenced by many factors, among which are the reactor configuration and the efficiencies of PD and nitritation (Lackner et al., 2014a; Le et al., 2019b). NREs ranging from 41% to 99.9% were reported in the reviewed articles in DEAMOX systems and NRR was only reported from a single study (Table 5). The factors influencing performance of this process are discussed in "Discussion" together with the factors affecting the other processes.

Biological degradation of cyanide

Some wastewater streams contain cyanide in high concentrations (Table 2). Its removal through biological degradation is favored to physico-chemical processes since this process does not generate harmful chemicals (Akcil et al., 2003; Barakat et al., 2004). Indeed, some bacterial species have been reported to be able to degrade complexed and free cyanide as well as thiocyanide (SCN^-) to ammonia (NH_3) and carbonate (Equations 5 and 6). *Pseudomonas spp.* and *Burkholderia cepacia* are some of the identified microorganisms with this capability (Akcil et al., 2003; Gurbuz et al., 2009).

$$2CN^- + 4H_2O + O_2 \rightarrow 2HCO_3^- + 2NH_3 \quad (5)$$

$$SCN^- + 2H_2O + \frac{5}{2}O_2 \rightarrow SO_4^{2-} + NH_3 + HCO_3^- \quad (6)$$

Some fungi including *Fusarium solani* can also degrade cyanide in a two-step process under alkaline conditions (Dumestre et al., 1997; Equations 7 and 8). However, the degradation rate of cyanide is reportedly slow (*ca.* 1 mmol/h-mg dry cells), possibly due to slow hydrolysis of cyanide at pH > 9. *Cyanide hydratase* and *Rhodanese enzymes* isolated from *Trichoderma* spp. can catabolize cyanide leading to formation of $HCONH_2$ and SCN^-, respectively (Ezzi and Lynch, 2002). On the other hand, *Pseudomonas fluorescens* and *Pseudomonas putida* can aerobically oxidize cyanide to CO_2 and NH_3 using *cyanide oxidase* enzyme (Suh et al., 1994; Chapatwala et al., 1998).

$$HCN + H_2O \rightarrow HCONH_2 \quad (7)$$

$$HCONH_2 + H_2O \rightarrow HCOOH + NH_3 \quad (8)$$

Plants also possess enzymes for cyanide detoxification (*betacyanoalanine synthase*) which can convert cyanide to non-toxic asparagine ($C_4H_8N_2O_3$; Trapp et al., 2003). However, there exists threshold concentrations beyond which cyanide is toxic to plants. For instance, willows can only survive for a few days at 20 mg-CN/L in a hydroponic system, and at 50 mg-CN/L in a sand irrigated system. On the contrary, algal species *Scenedesmus obliquus* have been reported to degrade cyanide concentrations as high as 400 mg/L even without prior adaptation, while *Chlorella* sp. were reported to be able to degrade *ca.* 86% of 100 mg/L solution in a 25-h period (Gurbuz et al., 2004). Aggregation of *Scenedesmus obliquus* cells was observed at 400 mg/L cyanide concentration, possibly as a means of minimizing the impact of cyanide on the cells. However, the mechanisms of algal degradation of cyanide still needs further investigations for better understanding.

Enzymatic degradation of cyanide to NH_4^+ and formate ($HCOO^-$) in a single step has also been demonstrated (Equation 9; Basheer et al., 1992). These enzymes are developed from particular fungi and bacteria such as *Fusarium lateritium, Bacillus pumilus C1* and *Alcaligenes denitrificans*, respectively (Ingvorsen et al., 1991; Basheer et al., 1992; Meyers et al., 1993). Ingvorsen et al. (1991) reported near complete removal of cyanide by *Alcaligenes xylosoxidans* subsp. *denitrificans* in a medium

TABLE 6 Biodegradation of cyanide by fungi, bacteria and enzyme-based catalysts.

	Microorganism/Enzyme	CN^- conc. (mg/L)	Temperature (°C)	pH	Cyanide removal	References
1	*Bacillus pumilus* C1		37	7.8–8[a]		Meyers et al. (1993)
2	*Trichoderma* spp.	40	25	8	-	Ezzi and Lynch (2002)
3	*Arthrospira maxima*	50–100	N/A[b]	N/A[b]	inhibited	Gurbuz et al. (2004)
4	*Chlorella* sp.		N/A[b]	N/A[b]	86%	
5	*Scenedesmus obliquus*		30	10	99%	
6	*Pseudomonas putida*	100	25[a]	7.5[a]	20%–94%	Chapatwala et al. (1998)
7	*Klebsiella oxytoca*	26–156	30	7	12–91	Chen et al. (2008)

[a]Optimal.
[b]Not applicable (not investigated).

containing approximately 25 ppm (parts per million) cyanide. Basheer et al. (1992) also reported near complete removal of cyanide by enzyme developed from *Alcaligenes denitrificans*. Other microorganisms including *Thiobacillus thioparus*. *Pseudomonas stutzeri*, etc. possess degrading abilities for CN^- or its derivatives (Katayama et al., 1992; Meyers et al., 1993; Watanabe et al., 1998).

$$HCN + 2H_2O \rightarrow HCOO^- + NH_4^+ \quad (9)$$

Chen et al. (2008) reported that immobilized cells of *Klebsiella oxytoca* could tolerate wider range of pH compared to suspended cells. In addition, immobilized cells were found to be less affected at higher CN^- concentrations (≥3 mM) compared to suspended cells. Indeed, the removal rates by suspended cells decreased from 49 to 12% when KCN concentration increased from 3 to 6 mM, while that of the cells immobilized in alginate and cellulose triacetate decreased from 59 to 20% and 60 to 26%, respectively (Chen et al., 2008). It is possible that the morphological changes and adsorption in the biofilms softened the impact of high CN^- concentrations on immobilized cells. Similar findings were reported by Babu et al. (1992) in an experimental set up containing 400 mg/L NaCN and a culture of *Pseudomonas putida* immobilized in calcium alginate beads. Overall, biological degradation of CN^- at large scale is feasible (Table 6). However, its degradation systems need to be combined with other NH_4^+-oxidizing processes process such as PN/A, DEAMOX or nitritation-denitritation for complete nitrogen removal.

Bioelectrochemical processes

Coupling of biotic and abiotic processes for nitrogen removal has been previously investigated and documented (Nguyen et al., 2015; Deng et al., 2016; Sander et al., 2017). In most bioelectrochemical systems (BESs), anode and cathode chambers are separated by a proton exchange membrane, and the electrodes therein are connected by an electrical conductor (Nguyen et al., 2015). During operation, the electrons flowing from the anode are used to reduce oxidized nitrogen compounds such as NO_3^- and NO_2^- in the cathode (Sander et al., 2017). The electrons could be generated through biological activity in the anode such as oxidation of organic carbon material, or through the supply of electrical energy (Nguyen et al., 2015; Sander et al., 2017).

Nguyen et al. (2015) found that increasing the supplied voltage from 0.7 to 0.9 V led to an increase in NRE from approximately 18% to 43%, but beyond 0.9 V, there was no improvement in nitrogen removal. Similar findings were made by Clauwaert et al. (2007) in a MFC (microbial fuel cell) with biotic anode and cathode. A comparison of two BESs by Nguyen et al. (2015) in which one had a biotic anode and another one with abiotic anode found that the one with abiotic anode led to lower nitrogen removal (43%) compared to the one with biotic anode (75.4 ± 2.9%). The high NRE with biotic anode as reported by Nguyen et al. (2015) was achieved despite C/N ratio = 3 mg-COD/mg-NO_3^--N), which is lower than for the conventional heterotrophic denitrification, highlighting the potential of this technology for treatment of low carbon (C/N ≤ 3) wastewater. Community analysis revealed that the bacterial consortia in biocathodes of BES with biotic anode differed from those with abiotic anode: species affiliated to *Shinella* sp., *Nitratireductor* sp. and *Dyella* sp. were dominated in BES with abiotic anode, while *Aeromonas* sp., *Pseudomonas* sp. and *Curtobacterium* sp. dominated in BES with biotic anode Nguyen et al. (2015). The observed variation in bacterial communities on biocathodes with the type of anode used still require further investigation to unravel the potential reasons behind these findings.

Transient accumulation of NO_2^- is normally observed in BES, possibly due to slower NO_2^--reduction compared to NO_3^- in line with several previous reports (see "Denitrifying ammonium oxidation "; Park et al., 2006; Nguyen et al., 2015). In addition, accumulation of NH_4^+ has also been reported in these systems, an indication that dissimilatory nitrate reduction (DNR) could be occurring in BESs (Nguyen et al., 2015).

Most of the NRRs for BESs are low (<0.1 kg-N/m^3-day), except for those reported by Sander et al. (2017), Feleke et al. (1998) and Isabel San-Martín et al. (2018) (Table 7). The systems reported by Sander et al. (2017) and Feleke et al. (1998) were up-flow columns, an indication that the motion of wastewater within the cells might have played a role in enhancing process kinetics, while nitrogen removal in the system reported by Isabel San-Martín et al. (2018) was

TABLE 7 Performance of bioelectrochemical processes.

	Process description	Influent N concentrations (mg-N/L)	NRE (%)	NRR (kg-N/m^3-day)	Remarks	References
1	BES (Abiotic anode—biocathode)	4.4–6.8	54–100	0.018–0.121	2l up-flow column with recirculation units	Sander et al. (2017)
1	Abiotic anode—biocathode	50	18–43	0.00063–0.00156	Applied voltage: 0.7–1.1 V; 25°C	Nguyen et al. (2015)
2	Biotic anode—biocathode	50	75.4 ± 2.9	0.0024 ± 0.00035	Cell voltage variation between 0.1 V and 1 V; 25°C; C/N ratio = 3; 150 mg-COD/L CH_3COONa	
3	Microbial fuel cell (MFC): biotic anode and cathode	2,615	-	0.08	1 g/L CH_3COONa in the anodic section and KNO_3 in cathodic section	Clauwaert et al. (2007)
4	Microbial electrolysis cell (biotic anode and cathode)	30.5	90–95[a]	0.01	Applied voltages were 0.4 V, 0.6 V and 0.8 V	Liang et al. (2021)
5	Electrochemical denitrification cell (abiotic anode and cathode)	30.5	57–62 [a]	-	Abiotic conditions were applied	
6	H_2	20	0–100	0.12[b]	Current supplied: −2 to 10 mA	Feleke et al. (1998)
7	biotic anode and cathode with S^{2-} addition in cathode chamber	100	100	-	400 ml system	Jianping et al. (2022)
8	Microbial electrolysis cell	30–1,400[c]	70	0.98[c]	150l MFC; 1 V between anode and anode	Isabel San-Martín et al. (2018)

[a]For both Ti mesh and stainless steel mesh cathodes.
[b]Estimated from Figure 2 in the source file.
[c]Estimated from Figure 4 in the source file.

suggested to have been undertaken by AMX because of the nature of its design. According to Sander et al. (2017), wastewater recirculation could have enhanced the transport of ions and gases from the surface of electrodes leading to the exposure of the surfaces once again.

Conductivity of wastewater could also influence process performance (Sander et al., 2017; Liang et al., 2021). Since increased flow of wastewater could move the ions within the BESs, this could improve conductivity and lower its ohmic resistance (Sander et al., 2017). As reported by Sander et al. (2017), wastewater recirculation decreased the total resistance by approximately 13.6%, an indication that the transport of ions therein had an influence.

Energy consumption in BES was approximated by Sander et al. (2017) to be 0.027 ± 0.001 kWh/m^3, which translated to 12.7–72.5 kWh/kg-N, which is over 5 times higher than for conventional activated sludge process. A huge part of the energy consumption was reported in the gap between the electrodes (*ca.* 13.5%). Therefore, the gap between the electrodes could thus be reduced to a minimum in order to minimize energy losses. However, precautions should be taken when reducing the gap so that oxygen does not diffuse into the cathode region as this would affect the bacterial activities, and promote the growth of aerobic microorganisms (Sander et al., 2017).

Addition of electron donors to the cathode chambers of BESs were demonstrated by Jianping et al. (2022) to enhance nitrogen removal. In addition, it was also reported that the system could generate an average output voltage of 450 mV lasting about 35 h. This thus indicates that BESs could also be utilized in power generation as a way of recovering the resources, and drive the wastewater treatment toward energy autarky.

Autotrophic denitrification

Electron donors such as S, H_2, sulfide (S^{2-}), SCN^-, thiosulfate ($S_2O_3^{2-}$), sulfite (SO_3^{2-}), metallic elements and ions can be used by autotrophic denitrifiers (Cardoso et al., 2006; Di Capua et al., 2019; Statiris et al., 2021). The biomass yield of autotrophic denitrifiers is generally lower than for heterotrophic denitrifiers (Cui et al., 2019), which is advantageous because of less work (cost) in sludge handling. However, metallic elements and ions as well as S and its compounds generate harmful chemicals (Di Capua et al., 2019).

S^{2-} can exist in water as molecular hydrogen sulfide (H_2S) or ionic hydrosulfide (HS^-)/sulfide (S^{2-}) depending on the prevailing conditions (Wiemann et al., 1998; Di Capua et al., 2019). S^{2-} presents serious environmental challenges because of its toxicity, corrosiveness and odor (Di Capua et al., 2019). In addition, S^{2-} is inhibitory to many microorganisms at elevated concentrations including to its consumers (autotrophic denitrifiers; Cardoso et al., 2006).

Stoichiometric reactions for autotrophic denitrification with complete and partial S^{2-} oxidation from NO_3^- and NO_2^- are presented in Equations 10 and 11 (Moraes et al., 2012). The extent of S^{2-} reduction is reportedly influenced by its concentration, with excess concentration leading to production of S according to Equation 17 (Cardoso et al., 2006). Although in some reports, S^{2-} oxidation to sulfate (SO_4^{2-}) has been suggested to be a two-step process in which S^{2-} is first oxidized to S, followed by S oxidation to SO_4^{2-} (Cardoso et al., 2006), in others, it has been suggested that some bacteria oxidize S^{2-} to SO_4^{2-} in a single step without S generation (Cui et al., 2019). According to Moraes et al. (2012),

TABLE 8 Performance of autotrophic denitrification systems.

	Electron donor	Influent N concentrations (mg-N/L)	NRE (%)	NRR (kg-N/m^3-day)	Remarks	References
1	S^{2-}	20	25–98	-	NO_3^-—fed; N/S = 0.9&1.7	Moraes et al. (2012)
2		20	95–100	0.009	NO_2^-—fed; N/S = 1.5&2.8	
3	$S_2O_3^{2-}$	56	-	0.47	415 mgSO_4^{2-}-produced	Cardoso et al. (2006)
4	S^{2-}		-	0.10	87 mgSO_4^{2-}-produced	
5	S		-	0.050	16 mgSO_4^{2-}-produced	
6	S	30–60	30–100[b]	0.30	Sulphur/limestone (v/v) = 1–3	Sahinkaya et al. (2014)
7		25 ± 3	100	0.15	Sulphur/limestone (v/v) = 1	
8	H_2	20–40	92–96	2.7–5.3[c]	Microporous membrane bioreactor	Mansell and Schroeder (2002)
9	S	29–31	79–98	0.05–0.36	10 L sulfoxidizing MBBR	Cui et al. (2019)
10	FeS_2	27	57	0.080[d]	25–50 μm and 50–100 μm pyrite particles	Torrentó et al. (2010)
11	$S_2O_3^{2-}$	60–80	-	0.058[e]	$S_2O_3^{2-}$-driven denitritation	Qian et al. (2016)
12	H_2	25–400	97	1.9–5.8	16.8 l pressurized reactor	Keisar et al. (2021)

[a]Approximated from Figure 4a in the source file.
[b]Estimated from Figure 4 in the source file.
[c]g-NO_3^--N/m^2-day.
[d]g-NO_3^--N/kg-pyrite-day.
[e]Estimated from Figure 3c in the source file.

the two-step process is the preferred pathway for autotrophic S-utilizing denitrifiers, possibly because of lower electron requirements compared to its direct oxidation from S^{2-} to SO_4^{2-}. The formation of S as an intermediate product could lead to formation of white/yellowish color which subsides when S is subsequently consumed. In addition, intermediate production and subsequent consumption of S lead to fluctuation in alkalinity since S generation from S^{2-} lead to alkalinity production (Equation 17), while S oxidation to SO_4^{2-} lead to alkalinity removal (Equation 12) (Doğan et al., 2012; Moraes et al., 2012; Di Capua et al., 2019). In comparison, NO_2^- is reportedly consumed at a higher rate compared to NO_3^-, possibly because of its higher reactivity (Moraes et al., 2012).

$$HS^- + 1.23NO_3^- + 0.438HCO_3^- + 0.027CO_2 + 0.093NH_4^+ + 0.573H^+ \rightarrow 0.093C_5H_7O_2N + SO_4^{2-} + 0.614N_2 + 0.866H_2O \quad (10)$$

$$S^{2-} + 2.26NO_2^- + 0.06HCO_3^- + 0.24CO_2 + 0.06NH_4^+ + 2.26H^+ \rightarrow 0.06C_5H_7O_2N + SO_4^{2-} + 1.13N_2 + 1.07H_2O \quad (11)$$

$$1.10S + NO_3^- + 0.76H_2O + 0.4CO_2 + 0.08NH_4^+ \rightarrow 0.08C_5H_7O_2N + 0.5N_2 + 1.1SO_4^{2-} + 1.28H^+ \quad (12)$$

Among the S compounds, $S_2O_3^{2-}$ is consumed at a higher rate compared to S and S^{2-}, possibly because it is readily available and non-toxic compared to S^{2-} which is toxic, and S which cannot be readily accessed by microorganisms because of mass transfer-related challenges (Cardoso et al., 2006). Notwithstanding the findings, S and S^{2-} have been successfully utilized as electron donors in denitrifying systems (Table 8). Indeed, pilot- and full-scale S-based autotrophic removal of NO_3^- in wastewater was reported by Sahinkaya et al. (2014) in column bioreactors, as well as by Woo et al. (2022) in a A_2O pilot-scale system. It is noteworthy that NO_3^- reduction to N_2 gas is a multi-step process that involves its reduction to NO_2^-, followed by further NO_2^- reduction to N_2 (Chung et al., 2014). In those steps, counter changes in the pH would occur, as NO_3^- reduction would consume alkalinity, while NO_2^- reduction consumes acidity (Chung et al., 2014 [Equations 13 and 14]). However, despite the counter changes, Chung et al. (2014) found that starting at a pH of approximately 8 in a batch experiment, the final pH was 7.8, an indication that not all the alkalinity was recovered in the final step. In addition, process operation at pH of 8 was reported to be optimal by Chung et al. (2014), in agreement with Pan et al. (2018).

$$S_2O_3^{2-} + 3.1NO_3^- + 0.73H_2O + 0.45HCO_3^- + 0.09NH_4^+ \rightarrow 0.09C_5H_7O_2N + 3.1NO_2^- + 2SO_4^{2-} + 1.64H^+ \quad (13)$$

$$S_2O_3^{2-} + 2.07NO_2^- + 0.43H^+ + 0.45HCO_3^- + 0.09NH_4^+ \rightarrow 0.09C_5H_7O_2N + 2SO_4^{2-} + 1.03N_2 + 0.3H_2O \quad (14)$$

SCN^-, which is present in considerable concentrations in gold mining and coking wastewaters, can be utilized as an electron donor in denitrifying systems (Equation 15; Pan et al., 2018). However, SCN^- leads to NH_4^+ production during its oxidation (Equation 15), which would require further nitritation ("Nitritation-denitritation"). Pan et al. (2018) suggested that

SCN^- oxidation takes place in three steps leading to the formation of S as an intermediate product, which is subsequently removed in the final step (Equations 16–18).

$$SCN^- + 2NO_2^- + 1.9H^+ + 1.2H_2O \rightarrow 0.10C_5H_7O_2N + SO_4^{2-} + N_2 + 0.5CO_2 + 0.90NH_4^+ \quad (15)$$

$$5SCN^- + H_2O \rightarrow S^{2-} + CO_2 + CO_2 \quad (16)$$

$$NO_2^- + 1.5S^{2-} + 4H^+ \rightarrow 1.5S + 0.5N_2 + 2H_2O \quad (17)$$

$$2NO_2^- + S \rightarrow SO_4^{2-} + N_2 \quad (18)$$

Some of the known sulfoxidizing denitrifiers include *Thiobacillus denitrificans, Paracoccus pantotropha, Paracoccus denitrificans, Paracoccus versutus*, *Thioploca* spp. and *Beggiatoa* spp. (Cardoso et al., 2006). Other reported sulfoxidisers include *Sulfurimonas denitrificans, Thiobacillus denitrificans* and *Thiohalobacter denitrificans* (Liang et al., 2021). Although some of these denitrifiers are strict chemolithoautotrophic, others are facultative. These denitrifiers are distributed across α-, β-, ε- and γ-*Proteobacteria* (Di Capua et al., 2019).

Feasibility of hydrogen-based autotrophic denitrification has also been demonstrated (Feleke et al., 1998; Mansell and Schroeder, 2002; Lee et al., 2010; Liang et al., 2021). In this process, denitrifiers use H_2 as electron donor according to Equation 19 to reduce NO_3^- to N_2. H_2, in turn, could be generated from purely chemical processes such as electrochemistry ("Biological degradation of cyanide"), or from biological sources (Liang et al., 2021).

$$0.33NO_3^- + H_2 + 0.08CO_2 + 0.34H^+ \rightarrow 0.015C_5H_7NO_2 + 1.11H_2O + 0.16N_2 \quad (19)$$

In a system supplied with H_2 and fed with 22.5 mg-NO_3^--N/L, Szekeres et al. (2002) found that *Ochrobactrum anthropi, Pseudomonas stutzeri, Paracoccus panthotrophus* and *Paracoccus denitrificans* were dominant, an indication that these bacteria were responsible for hydrogenotrophic denitrification. Other previously reported hydrogenotrophic denitrifiers include *Azospirillum brasilence, Rhizobium japonicum, Hydrogenophaga flava, Hydrogenophaga pseudopflava, Hydrogenophaga taeniospiralis and Ralstonia eutropha* (Mansell and Schroeder, 2002). Liang et al. (2021) also reported the dominance of Rhodocyclaceae, *Paracoccus* spp. and *Dethilobacter* spp. in a bioelectrochemical system in which the cathode chamber received H_2 from the anode chamber.

Torrentó et al. (2010) demonstrated the reduction of NO_3^- using pyrite (FeS_2) as an electron donor in batch and flow-through experiments conducted using *Thiobacillus denitrificans*-dominated cultures. Although complete NO_3^- removal was observed, low NRRs were reported (<0.080 g-NO_3^--N/kg-pyrite-day). In addition, it was reported that process kinetics were influenced by grain sizes of pyrite with complete nitrogen removal in experiments with 25–50 μm particles being observed after 14 days, while longer (>14 days) periods were needed in experiments with 50–100 μm particles, probably due to mass transfer challenges. Despite the low NRRs, pyrite-driven process produces less SO_4^{2-} compared to S-driven denitratation. Both iron (II) ions (Fe^{2+}) and S anions donate electrons for NO_3^- reduction to N_2 and/or NO_2^- according to Equations 20–22 (Torrentó et al., 2010):

$$5FeS_2 + 14NO_3^- + 4H^+ \rightarrow 5Fe^{2+} + 2H_2O + 7N_2 + 10SO_4^{2-} \quad (20)$$

$$10Fe^{2+} + 2NO_3^- + 12H^+ \rightarrow 10Fe^{3+} + 6H_2O + N_2 \quad (21)$$

$$2FeS_2 + 15NO_3^- + 7H_2O \rightarrow 2Fe(OH)_3 + 15NO_2^- + 4SO_4^{2-} + 8H^+ \quad (22)$$

Nitrogen removal *via* NO_2^- as opposed to NO_3^- could be implemented as a way of minimizing electron donor demand as denitritation requires only 2.5 S/N (sulfur to nitrogen ratio), while denitratation requires approximately 5.1 S/N (Chung et al., 2014). Therefore, nitrogen removal *via* NO_2^- would provide approximately 50% savings on electron donors. Approximately 40% savings on hydrogen would also be expected on removing nitrogen *via* NO_2^- as opposed to NO_3^- (Rezania et al., 2005).

The reported NRRs in autotrophic denitrification systems driven by S and its compounds range between 0.009–0.47 kg-N/m^3-day (Table 8). These rates are small and it would be challenging to apply in high-strength systems that require higher denitrification rates in order to avoid handling challenges, particularly in relation to the equipment. Therefore, further improvements could be made in order to emerge as a robust process that can treat high-strength wastewaters. On the contrary, hydrogenotrophic denitrification conducted in pressurized vessels have been reported to have high NRRs (>1 kg-N/m^3-day; Table 8). These rates are comparable to those of PN/A and nitritation-denitritation (Tables 3–5), an indication that these technology can be utilized at full-scale level provided that challenges with H_2 handling can be overcome.

Discussion

Several low carbon nitrogen removal processes have been developed and applied at pilot- and full-scale level (Supplementary Table S1 supplementary information). However,

each of these processes is restricted by a number of factors influencing the NREs and NRRs. In addition, efficient generation and utilization of electron donors and acceptors by different microorganisms is always a challenge, as regulatory measures need to be put in place to limit the activities of competing microorganisms that would otherwise present competition. Furthermore, operating conditions such as pH/alkalinity, temperature, DO, ionic strength, etc. impact on the performance of the BNR systems and would require regulation.

Nitritation-denitritation requires theoretical C/N ratios of 1.71 g-COD/g-N, which is higher than that of DEAMOX that requires 1.14 g-COD/g-N. Since DEAMOX requires only about half of influent NH_4^+ to be oxidized to NO_3^- with subsequent reduction to NO_2^- through PD, the actual demand for oxygen in this process is much less than that of partial nitritation-denitritation. Based on these facts, DEAMOX would thus be cheaper than nitritation-denitritation. However, comparisons of the actual COD requirements in the two processes in different studies have revealed that there has been comparable COD consumption in both processes (Tables 3 and 5). This highlights the inefficiencies in COD consumption, with poorer utilization in DEAMOX systems compared to nitritation-denitritation systems. It is possible that the COD is lost through oxidation by aerobic heterotrophic bacteria when the systems are aerated. Therefore, proper process control units need to be put in place to enhance COD utilization in these systems. This could include sequencing of operations to allow dosing of COD during anaerobic periods in order to limit losses through aerobic oxidation. It could also be possible to have a multi-stage system that could allow COD dosing in anaerobic/anoxic tanks only, and aeration in the respective tanks as was demonstrated by Le et al. (2019b). Despite the limitations, nitritation-denitritation has been applied at pilot- and full-scale systems (Supplementary Table S1) since the process kinetics are favorable (>0.5 kg-N/m^3-day; Table 3).

Bioelectrochemical processes (in BESs) are complex in nature and would require personnel with technical skills to operate. The reported NRRs in most of the studies presented in Table 7 are low (≤0.12 kg-N/m^3-day), except those reported by Isabel San-Martín et al. (2018) in a 150 l pilot-scale system in which AMX was suggested to have co-existed with other bacteria. Therefore, further discussion of the findings from this study within the framework of BESs will not be made as it would lead to misrepresentation.

Performance of BESs are limited by low water conductivities, which increase internal resistance, in turn, leading to limitation in the rates of denitrification, and an increase in energy losses (Sander et al., 2017; Liang et al., 2021). The operation of bioelectrochemical systems thus require electron donor and acceptor sites to be in close proximities in order to reduce energy wastage (Sander et al., 2017), which limit their application in full-scale systems (Liang et al., 2021). In addition, the overall construction of the bioelectrochemical cells is complex as it requires the integration of electrochemistry with biological activities. Furthermore, NH_4^+ generation (possibly through dissimilatory NO_3^- reduction) reduce the NRE of bioelectrochemical processes. Further research could thus provide solutions to the challenges still limiting BES to pilot-scale and laboratory-scale applications in its current state of development (Supplementary Table S1).

BESs could be advantageous for hydrogenotrophic denitrification since H_2 is generated *in situ* which enhances its delivery to denitrifiers (Sander et al., 2017). Alternatively, microorganisms might utilize electrons direction without the need for H_2 generation, which could improve process efficiency and kinetics. Generation and utilization of H_2 at the cathode could also improve efficiency of utilization by the microorganisms, unlike in systems where H_2 is supplied from external sources as its poor solubility in wastewater could lead to low utilization efficiencies (Sander et al., 2017).

Autotrophic denitrification appears to have higher NRRs compared to bioelectrochemical processes (Tables 7 and 8). However, the NRRs for S-based processes are still low (<0.47 kg-N/m^3-day), and its application would require huge reactors in large municipal systems. This notwithstanding, full-scale autotrophic denitrification driven by S and its compounds have been developed (Sahinkaya et al., 2014; Supplementary Table S1). Moreover, S compounds are present in different forms in anaerobic wastewater treatment systems as well as in many other streams including tannery wastewater (Wiemann et al., 1998), and its utilization for nitrogen removal is thus necessary as a cost-saving measure instead of sourcing external carbon supply. For instance, Wiemann et al. (1998) reported S^{2-}, organic S and NH_4^+ concentrations of 360 mg/L, 270 mg/L and 385 mg-N/L in tannery wastewater, respectively, meaning that complete removal of nitrogen would require approximately 1101.1 mg-COD/L (based on 2.86*385) that could be obtained from the S^{2-} and organic S (~1,125 mg-COD/L), assuming efficient utilization. Therefore, autotrophic denitrification driven by elemental S and its compounds present viable alternative to the currently applied heterotrophic denitrification and anammox-mediated processes, and could be further optimized for a widespread application. However, generation of SO_4^{2-} in these processes could limit their widespread application as they have inhibitory effects on several biological processes including desulfoxidization (Chung et al., 2014). S^{2-} has been associated with bad odor and corrosiveness (Di Capua et al., 2019), and this could influence its selection as an electron donor in denitrification systems. However, since S^{2-} is present in biogas scrubbing columns (Vu et al., 2022), denitrifying systems could be engineered to utilize the electron donors therein as a cost-cutting measure.

Hydrogenotrophic denitrification was demonstrated by Keisar et al. (2021) and Mansell and Schroeder (2002) in membrane and pressurized bioreactors, respectively, to have high NRRs (1.9–5.8 kg-N/m^3-day). The reported NRRs are comparable to those previously reported for anammox-mediated processes and nitritation-denitritation (Tables 3–5). However, pressurization of vessels and membrane lumens consume extra electrical energy besides that which is

consumed in the operation of pumps and other devices, and could increase the cost of treatment process to unsustainably high levels. Handling H_2 requires care, and its usage could thus be further limited by the challenges faced in its handling. Nonetheless, despite these challenges, hydrogenotrophic denitrification completely remove nitrogen unlike PN/A which generate about 11% NO_3^- per NH_4^+ consumed. Compared to denitrification driven by metallic ions, elemental S and its compounds, hydrogenotrophic denitrification does not generate any environmentally harmful chemicals.

Different microorganisms and plants have been shown to possess varying capacities for CN^- removal ("Biological degradation of cyanide"). Some specific enzymes, in particular, have been demonstrated to degrade CN^- (and SCN^-), leading to NH_3 generation. However, the NH_3 generated in the degradation would require removal in downstream systems in order to avert its negative impact on the environment. Therefore, coupling CN^- degradation with NH_4^+ removal processes such as nitritation-denitritation and ANAMMOX-mediated processes would be imperative for successful nitrogen removal. Alternatively, SCN^--containing wastewater could be treated with NO_3^--containing wastewater so as to allow autotrophic denitrifiers to utilize SCN^- as electron donor in the reduction of nitrate ("Autotrophic denitrification"). This approach would eliminate the need for separate treatment of SCN^- and NO_3^- in the respective streams. On the other hand, the growth of fungi in wastewater treatment systems is limited, and their impact on nitrogen removal might be insignificant. Similarly, the nitrogen removal kinetics of plants and microalgae might be lacking behind those of bacteria, and their use might need further analyses.

Inhibition of bacterial activities by CN^- at concentrations 0.2–1.0 mg/L has been reported in several studies, and its fate in wastewater treatment systems has been adequately addressed (Wild et al., 1994; Dash et al., 2009; Kim et al., 2011; Kapoor et al., 2016). The report by Landkamer et al. (2015) demonstrated co-removal of CN^-, NO_3^- and NH_4^+, in a system containing mixed bacterial culture collected from heap leach sediment and water. From the study, it was suggested that CN^- was hydrolysed according to Equation 8 by native bacteria that were present in the heap leach sediments and water. Formate produced in such a reaction would have likely been utilized as electron donor in partial reduction of NO_3^- to NO_2^-. The NO_2^-, in turn, would have then been used as electron acceptor in the anammox process, leading to NH_4^+ oxidation to nitrogen gas. The growth of AMX in an environment containing *ca.* 15 mg/L CN^- as suggested by Landkamer et al. (2015) contradicts the findings of Huang and Hogsett (2011) who found that anammox specific activities dropped by 50% at CN^- concentrations of just 0.05 mg/L during the first 2 days of incubation, although 80% of the performance was recovered thereafter. This suggests that AMX present in the culture used by Landkamer et al. (2015) could have adapted to the presence of high (15 mg/L) CN^- concentrations prior to the study as the culture was obtained from an environment containing high CN^- concentrations. Adaptation of AOB to high (≥ 10 mg/L) CN^- concentrations has also been demonstrated previously (Do et al., 2008). however, the findings by Do et al. (2008) contradicts Kapoor et al. (2016) who concluded that concentrations higher than 0.2 mg/L could inhibit AOB activities. In another study, Kim et al. (2011) reported that denitrifying bacteria could tolerate CN^- concentrations >40 mg/L, and that NOB are more sensitive to CN^- than AOB, which indicate that the impact of CN^- on different microorganisms could be different, and the inhibitory concentrations could vary with cultures. Further studies using advanced molecular techniques would thus be desirable in order to get a better understanding of the response by different microbial consortia to CN^-. Nitrogen labeling could also assist in understanding the nitrogen transformation pathways in biological systems. Similarly, inhibition by SCN^- could also be further explored as varying concentrations have been reported for different cultures (Kim et al., 2011; Oshiki et al., 2018; Yu et al., 2020).

Low-cost and high efficiencies associated with PN/A has led to increasing interest in the technology (Lackner et al., 2014a). The benefits stem from reduced requirements for oxygen, low-sludge production, and elimination of COD requirements. With this process, it is possible to remove >80% of influent nitrogen (Table 4). However, since about 11% of influent NH_4^+ is converted to NO_3^- in PN/A process, coupling this process with NO_3^--reducing processes such as denitrification could still be necessary for complete nitrogen removal as was demonstrated by Xie et al. (2017). In such a case, the COD requirements would be *ca.* 0.3 g-COD/g-NH_4^+-N. In municipal systems, however, the PN/A effluent can be pumped to mainstream systems that contain high levels of COD, eliminating the need for external carbon (Abma et al., 2010; Wett et al., 2015). Compared to denitrification driven by metallic ions and compounds of S, PN/A does not generate any harmful chemicals. Moreover, in many full-scale systems, PN/A process has been applied to treat mainly landfill leachate and sidestream wastewaters with satisfactory performance without the need for complicated process configurations similar to that of hydrogenotrophic denitrification that require pressurized vessels. Wastewater treatment without external carbon supply minimizes operational costs and simplifies process configuration. Lower sludge production in PN/A process compared to nitritation-denitritation because PN/A process is carried out by autotrophic bacteria could further reduce the operational costs of the process.

The challenges affecting widespread application of PN/A include the sensitivity of the AMX to operating and environmental conditions, as well as the slow growth rates (doubling time: 2.1–11 days) (Van Der Star et al., 2007; Fernández et al., 2008; Zhang et al., 2017). As a result, other bacteria such as NOB and

NO_2^--reducing heterotrophic bacteria could easily out-compete AMX if proper control strategies are not installed. Regulation of C/N ratios is normally applied in order to control the growth of NO_2^--reducing heterotrophic bacteria, while maintenance of low DO concentration, intermittent aeration, SRT/HRT control, FA and FNA inhibition is applied to control NOB growth in PNA systems (see "Nitritation-denitritation"). However, control of *Nitrospira*-affiliated NOB is challenging because they can grow under limited substrate and DO conditions such as in the biofilms (Constantine et al., 2016; Park et al., 2017b). According to Wett et al. (2013), NOB have longer enzymatic lag-phase compared to NOB. Therefore, application of intermittent aeration in PN/A systems could limit their growth as was demonstrated by Regmi et al. (2014). FA and FNA inhibition of NOB could also be exploited in PN/A systems compared to their higher sensitivity compared to AOB and AMX (see "Nitritation-denitritation") (Anthonisen et al., 1976; Dapena-Mora et al., 2007; Fernández et al., 2012; Jaroszynski et al., 2012). Based on the data presented by Lackner et al. (2014a) and Bowden et al. (2015), PN/A has received wide acceptance as an alternative to nitrification/denitrification.

The application of DEAMOX under mainstream conditions has been demonstrated previously (Table 5). However, its application under sidestream conditions might not be attractive, as COD would have to be supplied from external sources. Therefore, in this regard, PN/A would be preferable to DEAMOX in sidestream processes. Compared to nitritation-denitritation, the COD requirements in DEAMOX is less since only approximately half of NH_4^+ would need to be oxidized to NO_3^- before its PD to NO_2^-. The oxidation of only approximately half of NH_4^+ would also translate to about half of aeration costs in DEAMOX compared to nitritation-denitritation. The theoretical COD requirements for DEAMOX is approximately 0.57 g-COD/g-NH_4^+-N (assuming half of NH_4^+ is nitrified), which is lower than for nitritation-denitritation (*ca.* 1.71 g-COD/g-NH_4^+-N). Despite the huge potential of this technology, its highest level of application is at pilot-scale level (Le et al. 2019a,b; Supplementary Table S1).

Recommendations for future studies

The following recommendations are made for future studies:

1. Investigate the factors triggering DNR in BES
2. Study and develop processes for improving H_2 utilization and solubility in hydrogenotrophic denitrification systems
3. Investigate the methods for enhancing conductivity in BESs in order to minimize energy losses and enhance process performance
4. Couple autotrophic denitrification with heterotrophic denitrification as a way of minimizing generation of harmful chemicals
5. Optimize nitritation-denitritation and DEAMOX to enhance COD consumption efficiency

Conclusion

Several low-carbon (C/N ≤ 3) nitrogen removal processes have been developed, including nitritation-denitritation, anammox-mediated processes, bioelectrochemical processes and autotrophic denitrification. Bioelectrochemical processes are limited by low conductivities of wastewater and are characterized by low NRRs, which limit their application in large-scale systems. There is inefficient consumption of COD in DEAMOX and nitritation-denitritation processes. Autotrophic denitrification driven by S and its compounds has moderate NRRs (<0.47 kg-N/m^3-day) and thus requires further improvements in order to emerge as a viable alternative to anammox-mediated processes and nitritation-denitritation. Incorporation of NO_3^--removal processes such as DEAMOX and autotrophic denitrification in PN/A systems could lead to complete nitrogen removal. It is necessary to couple enzymatic degradation of CN^- and SCN^- with NH_4^+-oxidation processes such as PN/A and nitritation-denitritation for a successful nitrogen removal. H_2-deriven autotrophic denitrification has high NRRs (>1 kg-N/m^3-day) and could substitute anammox-mediated processes and nitritation-denitritation. However, its application requires incorporation of pressurized vessels in process lines. Autotrophic denitrification driven by metallic ions as well as S and its compounds generate harmful chemicals which necessitate downstream removal to avert negative impact on the environment. Overall, anammox-mediated nitrogen removal processes present the best alternatives to nitrification/denitrification in terms of COD demand, simplicity and process performance.

Author contributions

KK: conceptualization, investigation, formal analysis, writing—original draft. PZ: investigation, writing—original draft. FB: resources, supervision, funding acquisition. SK: conceptualization, resources, writing—review and editing, supervision, funding acquisition. All authors contributed to the article and approved the submitted version.

Funding

The project is funded by the Water Research Commission of South Africa (grant C2019/2020-00103).

Acknowledgments

The financial support by Water Research Commission (South Africa), National research foundation (South Africa) and Durban University of Technology is hereby acknowledged.

Conflict of interest

The authors declare that the research was conducted in the absence of any commercial or financial relationships that could be construed as a potential conflict of interest.

Publisher's note

All claims expressed in this article are solely those of the authors and do not necessarily represent those of their affiliated organizations, or those of the publisher, the editors and the reviewers. Any product that may be evaluated in this article, or claim that may be made by its manufacturer, is not guaranteed or endorsed by the publisher.

Supplementary material

The Supplementary material for this article can be found online at: https://www.frontiersin.org/articles/10.3389/fmicb.2022.968812/full#supplementary-material

References

Abeysiriwardana-Arachchige, I. S. A., Munasinghe-Arachchige, S. P., Delanka-Pedige, H. M. K., and Nirmalakhandan, N. (2020). Removal and recovery of nutrients from municipal sewage: algal vs. conventional approaches. *Water Res.* 175:115709. doi: 10.1016/j.watres.2020.115709

Abma, W. R., Driessen, W., Haarhuis, R., and Van Loosdrecht, M. C. M. (2010). Upgrading of sewage treatment plant by sustainable and cost-effective separate treatment of industrial wastewater. *Water Sci. Technol.* 61, 1715–1722. doi: 10.2166/wst.2010.977

Adams, M., Xie, J., Kabore, A. W. J., Chang, Y., Xie, J., Guo, M., et al. (2022). Research advances in anammox granular sludge: a review. *Crit. Rev. Environ. Sci. Technol.* 52, 631–674. doi: 10.1080/10643389.2020.1831358

Akcil, A., Karahan, A. G., Ciftci, H., and Sagdic, O. (2003). Biological treatment of cyanide by natural isolated bacteria (pseudomonas sp.). *Miner. Eng.* 16, 643–649. doi: 10.1016/S0892-6875(03)00101-8

Albina, P., Durban, N., Bertron, A., Albrecht, A., Robinet, J.-C., and Erable, B. (2019). Influence of hydrogen electron donor, alkaline pH, and high nitrate concentrations on microbial denitrification: a review. *Int. J. Mol. Sci.* 20:5163. doi: 10.3390/ijms20205163

Anthonisen, A. C., Loehr, R. C., Prakasam, T., and Srinath, E. (1976). Inhibition of nitrification by ammonia and nitrous acid. *J. Water Pollut. Control Fed.* 48, 835–852.

Awolusi, O. O., Enitan, A. M., Kumari, A., and Bux, F. (2015). Nitrification efficiency and community structure of municipal activated sewage sludge. *Int. J. Environ. Chem. Ecol. Geol. Geophys. Eng.* 9, 996–1003.

Azari, M., Walter, U., Rekers, V., Gu, J.-D., and Denecke, M. (2017). More than a decade of experience of landfill leachate treatment with a full-scale anammox plant combining activated sludge and activated carbon biofilm. *Chemosphere* 174, 117–126. doi: 10.1016/j.chemosphere.2017.01.123

Babu, G. R. V., Wolfram, J. H., and Chapatwala, K. D. (1992). Conversion of sodium cyanide to carbon dioxide and ammonia by immobilized cells of pseudomonas putida. *J. Ind. Microbiol.* 9, 235–238. doi: 10.1007/BF01569629

Barakat, M. A., Chen, Y. T., and Huang, C. P. (2004). Removal of toxic cyanide and cu(II) ions from water by illuminated TiO2 catalyst. *Appl. Catal. B Environ.* 53, 13–20. doi: 10.1016/j.apcatb.2004.05.003

Basheer, S., Kut, Ö. M., Prenosil, J. E., and Bourne, J. R. (1992). Kinetics of enzymatic degradation of cyanide. *Biotechnol. Bioeng.* 39, 629–634. doi: 10.1002/bit.260390607

Bernat, K., Kulikowska, D., and Godlewski, M. (2016). Crude glycerol as a carbon source at a low COD/N ratio provides efficient and stable denitritation. *Desalin. Water Treat.* 57, 19632–19641. doi: 10.1080/19443994.2015.1109555

Blaszczyk, M. (1993). Effect of medium composition on the Denitrification of nitrate by Paracoccus denitrificans. *Appl. Environ. Microbiol.* 59, 3951–3953. doi: 10.1128/aem.59.11.3951-3953.1993

Bowden, G., Stensel, H. D., and Tsuchihashi, R. (2015). Technologies for Sidestream nitrogen removal. *Water Intell.* 15:9781780407890. doi: 10.2166/9781780407890

Cao, S., and Zhou, Y. (2019). New direction in biological nitrogen removal from industrial nitrate wastewater via anammox. *Appl. Microbiol. Biotechnol.* 103, 7459–7466.doi: 10.1007/s00253-019-10070-3

Cardoso, R. B., Sierra-Alvarez, R., Rowlette, P., Flores, E. R., Gómez, J., and Field, J. A. (2006). Sulfide oxidation under chemolithoautotrophic denitrifying conditions. *Biotechnol. Bioeng.* 95, 1148–1157. doi: 10.1002/bit.21084

Cecconet, D., Sabba, F., Devecseri, M., Callegari, A., and Capodaglio, A. G. (2020). In situ groundwater remediation with bioelectrochemical systems: a critical review and future perspectives. *Environ. Int.* 137:105550. doi: 10.1016/j.envint.2020.105550

Chapatwala, K. D., Babu, G. R. V., Vijaya, O. K., Kumar, K. P., and Wolfram, J. H. (1998). Biodegradation of cyanides, cyanates and thiocyanates to ammonia and carbon dioxide by immobilized cells of pseudomonas putida. *J. Ind. Microbiol. Biotechnol.* 20, 28–33. doi: 10.1038/sj.jim.2900469

Chen, C. Y., Kao, C. M., and Chen, S. C. (2008). Application of Klebsiella oxytoca immobilized cells on the treatment of cyanide wastewater. *Chemosphere* 71, 133–139. doi: 10.1016/j.chemosphere.2007.10.058

Chen, Z., Zheng, X., Chen, Y., Wang, X., Zhang, L., and Chen, H. (2020). Nitrite accumulation stability evaluation for low-strength ammonium wastewater by adsorption and biological desorption of zeolite under different operational temperature. *Sci. Total Environ.* 704:135260. doi: 10.1016/j.scitotenv.2019.135260

Christensson, M., Ekstrom, S., Andersson Chan, A., Le Vaillant, E., and Lemaire, R. (2013). Experience from start-ups of the first ANITA Mox plants. *Water Sci. Technol.* 67, 2677–2684. doi: 10.2166/wst.2013.156

Chung, J., Amin, K., Kim, S., Yoon, S., Kwon, K., and Bae, W. (2014). Autotrophic denitrification of nitrate and nitrite using thiosulfate as an electron donor. *Water Res.* 58, 169–178. doi: 10.1016/j.watres.2014.03.071

Claros, J., Serralta, J., Seco, A., Ferrer, J., and Aguado, D. (2012). Real-time control strategy for nitrogen removal via nitrite in a SHARON reactor using pH and ORP sensors. *Process Biochem.* 47, 1510–1515. doi: 10.1016/j.procbio.2012.05.020

Clauwaert, P., Rabaey, K., Aelterman, P., De Schamphelaire, L., Pham, T. H., Boeckx, P., et al. (2007). Biological Denitrification in Microbial Fuel Cells. *Environ. Sci. Technol.* 41, 3354–3360. doi: 10.1021/es062580r

Constantine, T., Sandino, J., Houweling, D., Stephan, S., Yin, H., and Nielsen, P. (2016). Incorporating leading edge mainstream Deammonification into full-scale advanced BNR facilities. *Proc. Water Environ. Fed.* 2016, 1007–1018. doi: 10.2175/193864716819714735

Cui, Y.-X., Biswal, B. K., Van Loosdrecht, M. C. M., Chen, G.-H., and Wu, D. (2019). Long term performance and dynamics of microbial biofilm communities performing sulfur-oxidizing autotrophic denitrification in a moving-bed biofilm reactor. *Water Res.* 166:115038. doi: 10.1016/j.watres.2019.115038

Daigger, G. T. (2014). Oxygen and carbon requirements for biological nitrogen removal processes accomplishing nitrification, Nitritation, and Anammox. *Water Environ. Res.* 86, 204–209. doi: 10.2175/106143013X13807328849459

Dapena-Mora, A., Fernández, I., Campos, J. L., Mosquera-Corral, A., Méndez, R., and Jetten, M. S. M. (2007). Evaluation of activity and inhibition effects on Anammox process by batch tests based on the nitrogen gas production. *Enzym. Microb. Technol.* 40, 859–865. doi: 10.1016/j.enzmictec.2006.06.018

Dash, R. R., Gaur, A., and Balomajumder, C. (2009). Cyanide in industrial wastewaters and its removal: a review on biotreatment. *J. Hazard. Mater.* 163, 1–11. doi: 10.1016/j.jhazmat.2008.06.051

Daverey, A., Su, S.-H., Huang, Y.-T., Chen, S.-S., Sung, S., and Lin, J.-G. (2013). Partial nitrification and anammox process: a method for high strength optoelectronic industrial wastewater treatment. *Water Res.* 47, 2929–2937. doi: 10.1016/j.watres.2013.01.028

Deng, S., Li, D., Yang, X., Zhu, S., and Xing, W. (2016). Advanced low carbon-to-nitrogen ratio wastewater treatment by electrochemical and biological coupling process. *Environ. Sci. Pollut. Res.* 23, 5361–5373. doi: 10.1007/s11356-015-5711-0

Di Capua, F., Pirozzi, F., Lens, P. N. L., and Esposito, G. (2019). Electron donors for autotrophic denitrification. *Chem. Eng. J.* 362, 922–937.doi: 10.1016/j.cej.2019.01.069

Dimitrova, I., Dabrowska, A., and Ekström, S. (2020). Start-up of a full-scale partial nitritation-anammox MBBR without inoculum at Klagshamn WWTP. *Water Sci. Technol.* 81, 2033–2042. doi: 10.2166/wst.2020.271

Do, H., Lim, J., Shin, S. G., Wu, Y.-J., Ahn, J.-H., and Hwang, S. (2008). Simultaneous effect of temperature, cyanide and ammonia-oxidizing bacteria concentrations on ammonia oxidation. *J. Ind. Microbiol. Biotechnol.* 35, 1331–1338. doi: 10.1007/s10295-008-0415-9

Dobbeleers, T., Caluwé, M., Dockx, L., Daens, D., D'aes, J., and Dries, J. (2020). Biological nutrient removal from slaughterhouse wastewater via nitritation/denitritation using granular sludge: an onsite pilot demonstration. *J. Chem. Technol. Biotechnol.* 95, 111–122. doi: 10.1002/jctb.6212

Doğan, E. C., Türker, M., Dağaşan, L., and Arslan, A. (2012). Simultaneous sulfide and nitrite removal from industrial wastewaters under denitrifying conditions. *Biotechnol. Bioprocess Eng.* 17, 661–668. doi: 10.1007/s12257-011-0677-3

Du, R., Cao, S., Li, B., Niu, M., Wang, S., and Peng, Y. (2017). Performance and microbial community analysis of a novel DEAMOX based on partial-denitrification and anammox treating ammonia and nitrate wastewaters. *Water Res.* 108, 46–56. doi: 10.1016/j.watres.2016.10.051

Du, R., Cao, S., Peng, Y., Zhang, H., and Wang, S. (2019). Combined partial Denitrification (PD)-Anammox: a method for high nitrate wastewater treatment. *Environ. Int.* 126, 707–716. doi: 10.1016/j.envint.2019.03.007

Duan, H., Ye, L., Lu, X., and Yuan, Z. (2019). Overcoming nitrite oxidizing bacteria adaptation through alternating sludge treatment with free nitrous acid and free ammonia. *Environ. Sci. Technol.* 53, 1937–1946. doi: 10.1021/acs.est.8b06148

Dumestre, A., Chone, T., Portal, J., Gerard, M., and Berthelin, J. (1997). Cyanide degradation under alkaline conditions by a strain of Fusarium solani isolated from contaminated soils. *Appl. Environ. Microbiol.* 63, 2729–2734. doi: 10.1128/aem.63.7.2729-2734.1997

Ezzi, M. I., and Lynch, J. M. (2002). Cyanide catabolizing enzymes in Trichoderma spp. *Enzym. Microb. Technol.* 31, 1042–1047. doi: 10.1016/S0141-0229(02)00238-7

Feleke, Z., Araki, K., Sakakibara, Y., Watanabe, T., and Kuroda, M. (1998). Selective reduction of nitrate to nitrogen gas in a biofilm-electrode reactor. *Water Res.* 32, 2728–2734. doi: 10.1016/S0043-1354(98)00018-9

Fernández, I., Dosta, J., Fajardo, C., Campos, J. L., Mosquera-Corral, A., and Méndez, R. (2012). Short- and long-term effects of ammonium and nitrite on the Anammox process. *J. Environ. Manag.* 95, S170–S174. doi: 10.1016/j.jenvman.2010.10.044

Fernández, I., Vázquez-Padín, J. R., Mosquera-Corral, A., Campos, J. L., and Méndez, R. (2008). Biofilm and granular systems to improve Anammox biomass retention. *Biochem. Eng. J.* 42, 308–313. doi: 10.1016/j.bej.2008.07.011

Fux, C., Velten, S., Carozzi, V., Solley, D., and Keller, J. (2006). Efficient and stable nitritation and denitritation of ammonium-rich sludge dewatering liquor using an SBR with continuous loading. *Water Res.* 40, 2765–2775. doi: 10.1016/j.watres.2006.05.003

Ganigué, R., Gabarró, J., López, H., Ruscalleda, M., Balaguer, M. D., and Colprim, J. (2010). Combining partial nitritation and heterotrophic denitritation for the treatment of landfill leachate previous to an anammox reactor. *Water Sci. Technol.* 61, 1949–1955. doi: 10.2166/wst.2010.968

Glass, C., and Silverstein, J. (1998). Denitrification kinetics of high nitrate concentration water: pH effect on inhibition and nitrite accumulation. *Water Res.* 32, 831–839. doi: 10.1016/S0043-1354(97)00260-1

Grady, Jr C.L., Daigger, G. T., Love, N. G., and Filipe, C. D. (2011). *Biological Wastewater Treatment*, Boca Raton, FL: CRC Press.

Gu, J., Yang, Q., and Liu, Y. (2018). Mainstream anammox in a novel A-2B process for energy-efficient municipal wastewater treatment with minimized sludge production. *Water Res.* 138, 1–6. doi: 10.1016/j.watres.2018.02.051

Gurbuz, F., Ciftci, H., and Akcil, A. (2009). Biodegradation of cyanide containing effluents by Scenedesmus obliquus. *J. Hazard. Mater.* 162, 74–79. doi: 10.1016/j.jhazmat.2008.05.008

Gurbuz, F., Ciftci, H., Akcil, A., and Karahan, A. G. (2004). Microbial detoxification of cyanide solutions: a new biotechnological approach using algae. *Hydrometallurgy* 72, 167–176. doi: 10.1016/j.hydromet.2003.10.004

Han, M., Vlaeminck, S. E., AL-Omari, A., Wett, B., Bott, C., Murthy, S., et al. (2016). Uncoupling the solids retention times of flocs and granules in mainstream deammonification: a screen as effective out-selection tool for nitrite oxidizing bacteria. *Bioresour. Technol.* 221, 195–204. doi: 10.1016/j.biortech.2016.08.115

Hellinga, C., Schellen, A. A. J. C., Mulder, J. W., Van Loosdrecht, M. C. M., and Heijnen, J. J. (1998). The sharon process: an innovative method for nitrogen removal from ammonium-rich waste water. *Water Sci. Technol.* 37, 135–142. doi: 10.2166/wst.1998.0350

Hellinga, C., Van Loosdrecht, M. C. M., and Heijnen, J. J. (1999). Model based Design of a Novel Process for nitrogen removal from concentrated flows. *Math. Comput. Model. Dyn. Syst.* 5, 351–371. doi: 10.1076/mcmd.5.4.351.3678

Huang, P., and Hogsett, M. (2011). The robustness of ANAMMOX communities treating full-scale sidestream municipal anaerobic digester filtrate. *Proc. Water Environ. Fed.* 2011, 3147–3155. doi: 10.2175/193864711802721730

Ingvorsen, K., Højer-Pedersen, B., and Godtfredsen, S. E. (1991). Novel cyanide-hydrolyzing enzyme from Alcaligenes xylosoxidans subsp. denitrificans. *Appl. Environ. Microbiol.* 57, 1783–1789. doi: 10.1128/aem.57.6.1783-1789.1991

Isabel San-Martín, M., Mateos, R., Carracedo, B., Escapa, A., and Morán, A. (2018). Pilot-scale bioelectrochemical system for simultaneous nitrogen and carbon removal in urban wastewater treatment plants. *J. Biosci. Bioeng.* 126, 758–763. doi: 10.1016/j.jbiosc.2018.06.008

Isaka, K., Kimura, Y., Matsuura, M., Osaka, T., and Tsuneda, S. (2017). First full-scale nitritation-anammox plant using gel entrapment technology for ammonia plant effluent. *Biochem. Eng. J.* 122, 115–122. doi: 10.1016/j.bej.2017.03.005

Jaroszynski, L. W., Cicek, N., Sparling, R., and Oleszkiewicz, J. A. (2012). Impact of free ammonia on anammox rates (anoxic ammonium oxidation) in a moving bed biofilm reactor. *Chemosphere* 88, 188–195. doi: 10.1016/j.chemosphere.2012.02.085

Jianping, C., Tang, D., Tang, Z., and Guo, J. (2022). A novel sulfur-driven autotrophic denitrification coupled with bio-cathode system for bioelectricity generation and groundwater remediation. *Water Sci. Technol.* 86, 979–991 doi: 10.2166/wst.2022.216

Jung, S., Lee, J., Park, Y.-K., and Kwon, E. E. (2020). Bioelectrochemical systems for a circular bioeconomy. *Bioresour. Technol.* 300:122748. doi: 10.1016/j.biortech.2020.122748

Kamei, T., Rujakom, S., Nakano, M., Maharjan, A. K., and Kazama, F. (2022). Investigation of nitrite accumulation by hydrogenotrophic denitrification in a moving bed biofilm reactor for partial denitrification and anammox process. *Water Sci. Technol.* 85, 3396–3407. doi: 10.2166/wst.2022.187

Kapoor, V., Elk, M., Li, X., and Santo Domingo, J. W. (2016). Inhibitory effect of cyanide on wastewater nitrification determined using SOUR and RNA-based gene-specific assays. *Lett. Appl. Microbiol.* 63, 155–161. doi: 10.1111/lam.12603

Kartal, B., De Almeida, N. M., Maalcke, W. J., OP Den Camp, H. J., Jetten, M. S. M., and Keltjens, J. T. (2013). How to make a living from anaerobic ammonium oxidation. *FEMS Microbiol. Rev.* 37, 428–461. doi: 10.1111/1574-6976.12014

Katayama, Y., Narahara, Y., Inoue, Y., Amano, F., Kanagawa, T., and Kuraishi, H. (1992). A thiocyanate hydrolase of Thiobacillus thioparus. A novel enzyme catalyzing the formation of carbonyl sulfide from thiocyanate. *J. Biol. Chem.* 267, 9170–9175. doi: 10.1016/S0021-9258(19)50404-5

Keisar, I., Desitti, C., Beliavski, M., Epsztein, R., Tarre, S., and Green, M. (2021). A pressurized hydrogenotrophic denitrification reactor system for removal of nitrates at high concentrations. *J. Water Process Eng.* 42:102140. doi: 10.1016/j.jwpe.2021.102140

Kim, Y. M., Lee, D. S., Park, C., Park, D., and Park, J. M. (2011). Effects of free cyanide on microbial communities and biological carbon and nitrogen removal performance in the industrial activated sludge process. *Water Res.* 45, 1267–1279. doi: 10.1016/j.watres.2010.10.003

Kjeldsen, P. (1999). Behaviour of cyanides in soil and groundwater: a review. *Water Air Soil Pollut.* 115, 279–308. doi: 10.1023/A:1005145324157

Klaus, S., Baumler, R., Rutherford, B., Thesing, G., Zhao, H., and Bott, C. (2017). Startup of a partial Nitritation-Anammox MBBR and the implementation of pH-based aeration control. *Water Environ. Res.* 89, 500–508. doi: 10.2175/106143017X14902968254476

Lackner, S., Gilbert, E. M., Vlaeminck, S. E., Joss, A., Horn, H., and Van Loosdrecht, M. C. M. (2014a). Full-scale partial nitritation/anammox experiences – An application survey. *Water Res.* 55, 292–303. doi: 10.1016/j.watres.2014.02.032

Lackner, S., Thoma, K., Gilbert, E. M., Gander, W., Schreff, D., and Horn, H. (2014b). Start-up of a full-scale deammonification SBR-treating effluent from digested sludge dewatering. *Water Sci. Technol.* 71, 553–559. doi: 10.2166/wst.2014.421

Ladipo-Obasa, M., Forney, N., Riffat, R., Bott, C., Debarbadillo, C., and De Clippeleir, H. (2022). Partial denitrification–anammox (PdNA) application in mainstream IFAS configuration using raw fermentate as carbon source. *Water Environ. Res.* 94:e10711 doi: 10.1002/wer.10711

Lai, E., Senkpiel, S., Solley, D., and Keller, J. (2004). Nitrogen removal of high strength wastewater via nitritation/denitritation using a sequencing batch reactor. *Water Sci. Technol.* 50, 27–33. doi: 10.2166/wst.2004.0601

Landkamer, L. L., Bucknam, C. H., and Figueroa, L. A. (2015). Anaerobic nitrogen transformations in a gold-cyanide leach residue. *Environ. Sci. Technol. Lett.* 2, 357–361. doi: 10.1021/acs.estlett.5b00279

Lawson, C. E., Wu, S., Bhattacharjee, A. S., Hamilton, J. J., Mcmahon, K. D., Goel, R., et al. (2017). Metabolic network analysis reveals microbial community

interactions in anammox granules. *Nat. Commun.* 8:15416. doi: 10.1038/ncomms15416

Le, T., Peng, B., Su, C., Massoudieh, A., Torrents, A., Al-Omari, A., et al. (2019a). Impact of carbon source and COD/N on the concurrent operation of partial denitrification and anammox. *Water Environ. Res.* 91, 185–197. doi: 10.1002/wer.1016

Le, T., Peng, B., Su, C., Massoudieh, A., Torrents, A., Al-Omari, A., et al. (2019b). Nitrate residual as a key parameter to efficiently control partial denitrification coupling with anammox. *Water Environ. Res.* 91, 1455–1465. doi: 10.1002/wer.1140

Leaković, S., Mijatović, I., Cerjan-Stefanović, Š., and Hodžić, E. (2000). Nitrogen removal from fertilizer wastewater by ion exchange. *Water Res.* 34, 185–190. doi: 10.1016/S0043-1354(99)00122-0

Lee, J. W., Lee, K. H., Park, K. Y., and Maeng, S. K. (2010). Hydrogenotrophic denitrification in a packed bed reactor: effects of hydrogen-to-water flow rate ratio. *Bioresour. Technol.* 101, 3940–3946. doi: 10.1016/j.biortech.2010.01.022

Lemaire, R., Marcelino, M., and Yuan, Z. (2008). Achieving the nitrite pathway using aeration phase length control and step-feed in an SBR removing nutrients from abattoir wastewater. *Biotechnol. Bioeng.* 100, 1228–1236. doi: 10.1002/bit.21844

Li, X., Klaus, S., Bott, C., and He, Z. (2018a). Status, challenges, and perspectives of mainstream Nitritation–Anammox for wastewater treatment. *Water Environ. Res.* 90, 634–649. doi: 10.2175/106143017X15131012153112

Li, X., Klaus, S., Bott, C., and He, Z. (2018b). Status, challenges, and perspectives of mainstream Nitritation‐Anammox for wastewater treatment. *Water Environ. Res.* 90, 634–649. doi: 10.2175/106143017X15131012153112

Li, X., Shi, M., Zhang, M., Li, W., Xu, P.-L., Wang, Y., et al. (2022). Progresses and challenges in sulfur autotrophic denitrification-enhanced Anammox for low carbon and efficient nitrogen removal. *Crit. Rev. Environ. Sci. Technol.* 52, 1–16. doi: 10.1080/10643389.2022.2037967

Liang, D., He, W., Li, C., Wang, F., Crittenden, J. C., and Feng, Y. (2021). Remediation of nitrate contamination by membrane hydrogenotrophic denitrifying biofilm integrated in microbial electrolysis cell. *Water Res.* 188:116498. doi: 10.1016/j.watres.2020.116498

Ma, B., Qian, W., Yuan, C., Yuan, Z., and Peng, Y. (2017). Achieving mainstream nitrogen removal through coupling Anammox with Denitratation. *Environ. Sci. Technol.* 51, 8405–8413. doi: 10.1021/acs.est.7b01866

Ma, B., Xu, X., Wei, Y., Ge, C., and Peng, Y. (2020). Recent advances in controlling denitritation for achieving denitratation/anammox in mainstream wastewater treatment plants. *Bioresour. Technol.* 299:122697. doi: 10.1016/j.biortech.2019.122697

Magrí, A., Ruscalleda, M., Vilà, A., Akaboci, T. R. V., Balaguer, M. D., Llenas, J. M., et al. (2021). Scaling-up and long-term operation of a full-scale two-stage partial Nitritation-Anammox system treating landfill leachate. *PRO* 9:800. doi: 10.3390/pr9050800

Mansell, B. O., and Schroeder, E. D. (2002). Hydrogenotrophic denitrification in a microporous membrane bioreactor. *Water Res.* 36, 4683–4690. doi: 10.1016/S0043-1354(02)00197-5

Martienssen, M., and Schöps, R. (1999). Population dynamics of denitrifying bacteria in a model biocommunity. *Water Res.* 33, 639–646. doi: 10.1016/S0043-1354(98)00222-X

Meyers, P. R., Rawlings, D. E., Woods, D. R., and Lindsey, G. G. (1993). Isolation and characterization of a cyanide dihydratase from Bacillus pumilus C1. *J. Bacteriol.* 175, 6105–6112. doi: 10.1128/jb.175.19.6105-6112.1993

Mohsenpour, S. F., Hennige, S., Willoughby, N., Adeloye, A., and Gutierrez, T. (2021). Integrating micro-algae into wastewater treatment: a review. *Sci. Total Environ.* 752:142168. doi: 10.1016/j.scitotenv.2020.142168

Moraes, B. S., Souza, T. S. O., and Foresti, E. (2012). Effect of sulfide concentration on autotrophic denitrification from nitrate and nitrite in vertical fixed-bed reactors. *Process Biochem.* 47, 1395–1401. doi: 10.1016/j.procbio.2012.05.008

Mousazadeh, M., Niaragh, E. K., Usman, M., Khan, S. U., Sandoval, M. A., Al-Qodah, Z., et al. (2021). A critical review of state-of-the-art electrocoagulation technique applied to COD-rich industrial wastewaters. *Environ. Sci. Pollut. Res.* 28, 43143–43172. doi: 10.1007/s11356-021-14631-w

Mulder, A., Versprille, A. I., and Van Braak, D. (2012). Sustainable nitrogen removal by denitrifying anammox applied for anaerobic pre-treated potato wastewater. *Water Sci. Technol.* 66, 2630–2637. doi: 10.2166/wst.2012.466

Mulder, J. W., Van Loosdrecht, M. C. M., Hellinga, C., and Van Kempen, R. (2001). Full-scale application of the SHARON process for treatment of rejection water of digested sludge dewatering. *Water Sci. Technol.* 43, 127–134. doi: 10.2166/wst.2001.0675

Nguyen, V. K., Hong, S., Park, Y., Jo, K., and Lee, T. (2015). Autotrophic denitrification performance and bacterial community at biocathodes of bioelectrochemical systems with either abiotic or biotic anodes. *J. Biosci. Bioeng.* 119, 180–187. doi: 10.1016/j.jbiosc.2014.06.016

Noutsopoulos, C., Mamais, D., Statiris, E., Lerias, E., Malamis, S., and Andreadakis, A. (2018). Reject water characterization and treatment through short-cut nitrification/denitrification: assessing the effect of temperature and type of substrate. *J. Chem. Technol. Biotechnol.* 93, 3638–3647. doi: 10.1002/jctb.5745

Oshiki, M., Masuda, Y., Yamaguchi, T., and Araki, N. (2018). Synergistic inhibition of anaerobic ammonium oxidation (anammox) activity by phenol and thiocyanate. *Chemosphere* 213, 498–506. doi: 10.1016/j.chemosphere.2018.09.055

Pan, J., Ma, J., Wu, H., Ren, Y., Fu, B., He, M., et al. (2018). Simultaneous removal of thiocyanate and nitrogen from wastewater by autotrophic denitritation process. *Bioresour. Technol.* 267, 30–37. doi: 10.1016/j.biortech.2018.07.014

Park, H., Brotto, A. C., Van Loosdrecht, M. C. M., and Chandran, K. (2017a). Discovery and metagenomic analysis of an anammox bacterial enrichment related to Candidatus "Brocadia caroliniensis" in a full-scale glycerol-fed nitritation-denitritation separate centrate treatment process. *Water Res.* 111, 265–273. doi: 10.1016/j.watres.2017.01.011

Park, H., Sundar, S., Ma, Y., and Chandran, K. (2015). Differentiation in the microbial ecology and activity of suspended and attached bacteria in a nitritation-anammox process. *Biotechnol. Bioeng.* 112, 272–279. doi: 10.1002/bit.25354

Park, H. I., Kim, J. S., Kim, D. K., Choi, Y.-J., and Pak, D. (2006). Nitrate-reducing bacterial community in a biofilm-electrode reactor. *Enzym. Microb. Technol.* 39, 453–458. doi: 10.1016/j.enzmictec.2005.11.028

Park, M.-R., Park, H., and Chandran, K. (2017b). Molecular and kinetic characterization of planktonic Nitrospira spp. selectively enriched from activated sludge. *Environ. Sci. Technol.* 51, 2720–2728. doi: 10.1021/acs.est.6b05184

Pu, J., Feng, C., Liu, Y., Li, R., Kong, Z., Chen, N., et al. (2014). Pyrite-based autotrophic denitrification for remediation of nitrate contaminated groundwater. *Bioresour. Technol.* 173, 117–123. doi: 10.1016/j.biortech.2014.09.092

Qian, J., Zhou, J., Zhang, Z., Liu, R., and Wang, Q. (2016). Biological nitrogen removal through nitritation coupled with thiosulfate-driven denitritation. *Sci. Rep.* 6:27502. doi: 10.1038/srep27502

Qin, J.-J., Oo, M. H., Tao, G., and Kekre, K. A. (2007). Feasibility study on petrochemical wastewater treatment and reuse using submerged MBR. *J. Membr. Sci.* 293, 161–166. doi: 10.1016/j.memsci.2007.02.012

Regmi, P., Miller, M. W., Holgate, B., Bunce, R., Park, H., Chandran, K., et al. (2014). Control of aeration, aerobic SRT and COD input for mainstream nitritation/denitritation. *Water Res.* 57, 162–171. doi: 10.1016/j.watres.2014.03.035

Reij, M. W., De Bont, J. A. M., Hartmans, S., and De Gooijer, K. D. (1995). Membrane bioreactor with a porous hydrophobic membrane as a gas–liquid contactor for waste gas treatment. *Biotechnol. Bioeng.* 45, 107–115. doi: 10.1002/bit.260450203

Rezania, B., Cicek, N., and Oleszkiewicz, J. A. (2005). Kinetics of hydrogen-dependent denitrification under varying pH and temperature conditions. *Biotechnol. Bioeng.* 92, 900–906. doi: 10.1002/bit.20664

Sahinkaya, E., Kilic, A., and Duygulu, B. (2014). Pilot and full scale applications of sulfur-based autotrophic denitrification process for nitrate removal from activated sludge process effluent. *Water Res.* 60, 210–217. doi: 10.1016/j.watres.2014.04.052

Sander, E. M., Virdis, B., and Freguia, S. (2017). Bioelectrochemical nitrogen removal as a polishing mechanism for domestic wastewater treated effluents. *Water Sci. Technol.* 76, 3150–3159. doi: 10.2166/wst.2017.462

Sijbesma, W. F. H., Almeida, J. S., Reis, M. A. M., and Santos, H. (1996). Uncoupling effect of nitrite during denitrification by *Pseudomonas fluorescens*: an in vivo 31P-NMR study. *Biotechnol. Bioeng.* 52, 176–182. doi: 10.1002/(SICI)1097-0290(19961005)52:1<176::AID-BIT18>3.0.CO;2-M

Song, Y., Li, Y., He, X., Zhang, H., Zhou, M., and Liu, G. (2021). Recycling of residual valuable metals in cyanide-leached gold wastewater using the N263-TBP system. *J. Environ. Chem. Eng.* 9:106774. doi: 10.1016/j.jece.2021.106774

Statiris, E., Hadjimitsis, E., Noutsopoulos, C., and Malamis, S. (2021). Thiosulphate driven autotrophic denitrification via nitrite using synthetic wastewater. *J. Chem. Technol. Biotechnol.* 96, 1675–1681. doi: 10.1002/jctb.6692

Suarez, C., Persson, F., and Hermansson, M. (2015). Predation of nitritation–anammox biofilms used for nitrogen removal from wastewater. *FEMS Microbiol. Ecol.* 91:fix124. doi: 10.1093/femsec/fiv124

Suh, Y.-J., Park, J. M., and Yang, J.-W. (1994). Biodegradation of cyanide compounds by Pseudomonas fluorescens immobilized on zeolite. *Enzym. Microb. Technol.* 16, 529–533. doi: 10.1016/0141-0229(94)90025-6

Syron, E., and Casey, E. (2008). Membrane-aerated biofilms for high rate biotreatment: performance appraisal, engineering principles, scale-up, and development requirements. *Environ. Sci. Technol.* 42, 1833–1844. doi: 10.1021/es0719428

Szekeres, S., Kiss, I., Kalman, M., and Soares, M. I. M. (2002). Microbial population in a hydrogen-dependent denitrification reactor. *Water Res.* 36, 4088–4094. doi: 10.1016/S0043-1354(02)00130-6

Torrentó, C., Cama, J., Urmeneta, J., Otero, N., and Soler, A. (2010). Denitrification of groundwater with pyrite and Thiobacillus denitrificans. *Chem. Geol.* 278, 80–91. doi: 10.1016/j.chemgeo.2010.09.003

Trapp, S., Larsen, M., Pirandello, A., and Danquah-Boakye, J. (2003). Feasibility of cyanide elimination using plants. *Eur. J. Mineral Process. Environ. Prot.* 3, 128–137.

Van Der Star, W. R., Miclea, A. I., Van Dongen, U. G., Muyzer, G., Picioreanu, C., and Van Loosdrecht, M. C. (2008). The membrane bioreactor: a novel tool to grow anammox bacteria as free cells. *Biotechnol. Bioeng.* 101, 286–294. doi: 10.1002/bit.21891

Van Der Star, W. R. L., Abma, W. R., Blommers, D., Mulder, J.-W., Tokutomi, T., Strous, M., et al. (2007). Startup of reactors for anoxic ammonium oxidation: experiences from the first full-scale anammox reactor in Rotterdam. *Water Res.* 41, 4149–4163. doi: 10.1016/j.watres.2007.03.044

Van Kempen, R., Mulder, J. W., Uijterlinde, C. A., and Loosdrecht, M. C. M. (2001). Overview: full scale experience of the SHARON® process for treatment of rejection water of digested sludge dewatering. *Water Sci. Technol.* 44, 145–152. doi: 10.2166/wst.2001.0035

Vilar, A., Eiroa, M., Kennes, C., and Veiga, M. C. (2010). The SHARON process in the treatment of landfill leachate. *Water Sci. Technol.* 61, 47–52. doi: 10.2166/wst.2010.786

Vu, H. P., Nguyen, L. N., Wang, Q., Ngo, H. H., Liu, Q., Zhang, X., et al. (2022). Hydrogen sulphide management in anaerobic digestion: a critical review on input control, process regulation, and post-treatment. *Bioresour. Technol.* 346:126634. doi: 10.1016/j.biortech.2021.126634

Wang, J., and Gu, J.-D. (2013). Dominance of Candidatus Scalindua species in anammox community revealed in soils with different duration of rice paddy cultivation in Northeast China. *Appl. Microbiol. Biotechnol.* 97, 1785–1798. doi: 10.1007/s00253-012-4036-x

Wang, Z., Xu, X., Gong, Z., and Yang, F. (2012). Removal of COD, phenols and ammonium from Lurgi coal gasification wastewater using A2O-MBR system. *J. Hazard. Mater.* 235-236, 78–84. doi: 10.1016/j.jhazmat.2012.07.012

Watanabe, A., Yano, K., Ikebukuro, K., and Karube, I. (1998). Cyanide hydrolysis in a cyanide-degrading bacterium, *Pseudomonas stutzeri* AK61, by cyanidase. *Microbiology* 144, 1677–1682. doi: 10.1099/00221287-144-6-1677

Wei, Q., Kawagoshi, Y., Huang, X., Hong, N., Van Duc, L., Yamashita, Y., et al. (2016). Nitrogen removal properties in a continuous marine anammox bacteria reactor under rapid and extensive salinity changes. *Chemosphere* 148, 444–451. doi: 10.1016/j.chemosphere.2016.01.041

Wett, B., Omari, A., Podmirseg, S., Han, M., Akintayo, O., Gómez Brandón, M., et al. (2013). Going for mainstream deammonification from bench to full scale for maximized resource efficiency. *Water Sci. Technol.* 68, 283–289. doi: 10.2166/wst.2013.150

Wett, B., Podmirseg, S. M., Gomez-Brandon, M., Hell, M., Nyhuis, G., Bott, C., et al. (2015). Expanding DEMON Sidestream Deammonification technology towards mainstream application. *Water Environ. Res.* 87, 2084–2089. doi: 10.2175/106143015X14362865227319

Wiemann, M., Schenk, H., and Hegemann, W. (1998). Anaerobic treatment of tannery wastewater with simultaneous sulphide elimination. *Water Res.* 32, 774–780. doi: 10.1016/S0043-1354(97)00309-6

Wiesmann, U. (1994). "Biological nitrogen removal from wastewater," in *Biotechnics/wastewater* ed. A. Fiechter. (Berlin, Heidelberg: Springer Berlin Heidelberg).

Wild, S. R., Rudd, T., and Neller, A. (1994). Fate and effects of cyanide during wastewater treatment processes. *Sci. Total Environ.* 156, 93–107. doi: 10.1016/0048-9697(94)90346-8

Winkler, M. K. H., and Straka, L. (2019). New directions in biological nitrogen removal and recovery from wastewater. *Curr. Opin. Biotechnol.* 57, 50–55. doi: 10.1016/j.copbio.2018.12.007

Woo, Y. C., Lee, J. J., and Kim, H.-S. (2022). Removal of nitrogen from municipal wastewater by denitrification using a sulfur-based carrier: a pilot-scale study. *Chemosphere* 296:133969. doi: 10.1016/j.chemosphere.2022.133969

Xie, G.-J., Cai, C., Hu, S., and Yuan, Z. (2017). Complete nitrogen removal from synthetic anaerobic sludge digestion liquor through integrating Anammox and denitrifying anaerobic methane oxidation in a membrane biofilm reactor. *Environ. Sci. Technol.* 51, 819–827. doi: 10.1021/acs.est.6b04500

Yao, H., Zhao, X., Fan, L., Jia, F., Chen, Y., Cai, W., et al. (2022). Pilot-scale demonstration of one-stage partial nitritation/anammox process to treat wastewater from a coal to ethylene glycol (CtEG) plant. *Environ. Res.* 208:112540. doi: 10.1016/j.envres.2021.112540

Yu, X., Nishimura, F., and Hidaka, T. (2020). Anammox reactor exposure to thiocyanate: long-term performance and microbial community dynamics. *Bioresour. Technol.* 317:123960. doi: 10.1016/j.biortech.2020.123960

Zhang, F., Peng, Y., Wang, Z., and Jiang, H. (2019). High-efficient nitrogen removal from mature landfill leachate and waste activated sludge (WAS) reduction via partial nitrification and integrated fermentation-denitritation process (PNIFD). *Water Res.* 160, 394–404. doi: 10.1016/j.watres.2019.05.032

Zhang, J., Peng, Y., Li, X., and Du, R. (2022). Feasibility of partial-denitrification/anammox for pharmaceutical wastewater treatment in a hybrid biofilm reactor. *Water Res.* 208:117856. doi: 10.1016/j.watres.2021.117856

Zhang, L., Narita, Y., Gao, L., Ali, M., Oshiki, M., and Okabe, S. (2017). Maximum specific growth rate of anammox bacteria revisited. *Water Res.* 116, 296–303. doi: 10.1016/j.watres.2017.03.027

Frontiers in Microbiology

Explores the habitable world and the potential of microbial life

The largest and most cited microbiology journal which advances our understanding of the role microbes play in addressing global challenges such as healthcare, food security, and climate change.

Discover the latest Research Topics

See more →

Frontiers

Avenue du Tribunal-Fédéral 34
1005 Lausanne, Switzerland
frontiersin.org

Contact us

+41 (0)21 510 17 00
frontiersin.org/about/contact